Spectral studies and crystal structures of some transition metal complexes of N⁴-substituted semicarbazones

Thesis submitted to

Cochin University of Science and Technology

in partial fulfillment of the requirements

for the award of the degree of

Doctor of Philosophy

in

Chemistry

by

REENA T. A.

Department of Applied Chemistry
Cochin University of Science and Technology
Kochi - 682 022

March 2011

Spectral studies and crystal structures of some transition metal complexes of N^4-substituted semicarbazones

Ph. D. Thesis under the Faculty of Science

Author:

Reena T. A.
Research Fellow, Department of Applied Chemistry
Cochin University of Science and Technology
Kochi, India 682 022
E mail: reenafaisal@cusat.ac.in

Research Advisor:

Dr. M. R. Prathapachandra Kurup
Professor
Department of Applied Chemistry
Cochin University of Science and Technology
Kochi, India 682 022
Email: mrp@cusat.ac.in

Department of Applied Chemistry
Cochin University of Science and Technology
Kochi, India 682 022

March 2011

Front cover: Crystal structure of **[Cd(HL^2)Br$_2$]·DMF**

. . . . to my inspiring stars

Munnas, Chinnas & Ponnoose. . . .

DEPARTMENT OF APPLIED CHEMISTRY
COCHIN UNIVERSITY OF SCIENCE AND TECHNOLOGY
KOCHI - 682 022, INDIA

Phone Off. :	0484-2862423
Phone Res. :	0484-2576904
Telex :	885-5019 CUIN
Fax :	0484-2575804
Email :	mrp@cusat.ac.in
	mrp_k@yahoo.com

Dr. M.R. Prathapachandra Kurup
Professor

Certificate

This is to certify that the thesis entitled "**Spectral studies and crystal structures of some transition metal complexes of N^4-substituted semicarbazones**" submitted by Ms. Reena T.A., in partial fulfillment of the requirements for the degree of Doctor of Philosophy, to the Cochin University of Science and Technology, Kochi-22, is an authentic record of the original research work carried out by her under my guidance and supervision. The results embodied in this thesis, in full or in part, have not been submitted for the award of any other degree.

M. R. Prathapachandra Kurup
(Supervisor)

PREFACE

Coordination chemistry enjoys a prominent place in inorganic chemistry. Werner's coordination theory was the first attempt to explain the bonding in coordination complexes, and he concluded that in complexes the metal shows two different types of valencies, primary and secondary valencies. In the quest of exploring the chelating behavior of some ONS and NNS donor semicarbazones in several metal complexes, we could get more information about their nature of coordination and related structural, spectral and biological properties.

The work embodied in the thesis was carried out by the author in the Department of Applied Chemistry during the period 2006-2010. The work presented in this thesis describes the synthesis, structural and spectral characterization of two novel N^4-substituted semicarbazones of di-2-pyridyl ketone and quinoline-2-carboxaldehyde and their metal complexes. Chapter 1 includes a brief prologue on semicarbazones and their transition metal complexes with an extensive literature survey relating the history, applications and recent developments. Chapter 2 deals with the syntheses and characterization of two NNO donor semicarbazones. The semicarbazones synthesized are di-2-pyridyl ketone-N^4-phenyl-3-semicarbazone (HL^1) and quinoline-2-carboxaldehyde-N^4-phenylsemicarbazone (HL^2). Chapter 3 describes the syntheses and characterization of eight zinc(II) complexes of N^4-substituted semicarbazones, HL^1 and HL^2. Chapter 4 comprises of the syntheses and characterization of six cadmium complexes of N^4-substituted semicarbazones using CHN analysis, infrared, electronic spectra and X-ray diffraction studies. Chapter 5 deals with the syntheses and characterization of mononuclear and binuclear copper(II) complexes with potential NNO donor ligands. Chapter 6 explains the syntheses and characterization of nickel(II), cobalt(II) and manganese(II) complexes.

Acknowledgement

    This thesis would not have been possible without the motivation of a number of hands. I am indebted to many individuals who supported me through out the period of my research studies. It is a pleasure to thank them all who have helped and inspired me.

    I owe my deepest gratitude to my supervising guide Prof. M.R. Prathapachandra Kurup for showering enthusiasm and immense knowledge. His encouragement, guidance and support from the initial to the final level, enabled me to develop an understanding of the subject. I am heartily thankful to Dr. P.V. Mohanan for his encouragement and support as my doctoral committee member. I am grateful to Prof. K. Sreekumar, Head, Department of Applied Chemistry, CUSAT for the support and help during the period of this work. I am thankful for the support received from all the teaching and non-teaching staff of the Department of Applied Chemistry, CUSAT.

    I would like to extend my gratitude to Cochin University of Science and Technology for the financial support offered. I thank heads of the institutions of SAIF Kochi, IISc Bangalore, IIT Bombay and School of Chemistry, University of Hyderabad for services and help they had given during my research studies. I greatly acknowledge the timely assistance rendered by Dr. Shibu, SAIF, Cochin. I appreciate the help offered by Dr. Alex Punnoose for doing the EPR studies of some of my complexes.

    I owe much to Dr. E.B. Seena, Dr. Leji Latheef, Dr. Suni, Dr. P.F. Rapheal, Dr. Mini Kuriakose, Dr. Bessy Raj, Dr. Sreesha Sasi, Dr. E. Manoj, Dr. Binu Varghese, Dr. U.L. Kala and Dr. Suja Krishnan. I use this opportunity to express my special thanks to my friends Nancy Mathew, Sheeja S.R., Renjusha, Roji sir, Neema, Priya, Bibitha , Anju and Jinsa. Always I get highly motivating words from these friends. My friend, technology expert of Inorganic lab II, Easen sir, without your help I am pretty much sure I would not be able to complete this thesis. I cannot count by words how much inspiration I got from you, strong ladies, Manju and Launa. I am thankful to my labmates, Annie miss, Laly miss, Jayakumar sir, Ashokan sir, Jessy

miss for their sisterly consideration towards me. Digna, Leeju and Varsha I cannot avoid you, thank you for your support.

I appreciate the strength you had given me, Mr. Terrel Hill, The Principal, High school, Inc., USA, I am fortunate to work with you.

My parents, Prof. T.S. Abdul Rahman and Anisa Beegum, they deserve a special thanks for the encouragement they had given. My in-laws Msthafa Rawther and Safiya Beevi, you also need a handful of thanks for the support given. My younger sister Rajeena T. A., if she would not have been helping me I cannot imagine about the fulfillment of my dream.

I am extremely fortunate in having husband like Mr. Faisal. I appreciate the mental strength, support, prayers and encouragement he had showered at me throughout my research studies. My kids, Munna and Chinna again I am extremely fortunate of having blossoms like you dear. I appreciate the sacrifice you rendered.

Finally, I would like to thank everybody who was behind the fulfillment of my thesis. Above all, I stoop before God Almighty for having given me His Strength and blessings to carry this work to conclusion.

Reena T. A.

CONTENTS

*Chapter***-3**

SYNTHESIS, SPECTRAL AND STRUCTURAL STUDIES ON Zn(II) COMPLEXES OF *N*[4]-SUBSTITUTED SEMICARBAZONES

*Chapter***-4**

SYNTHESIS, SPECTRAL STUDIES AND STRUCTURES OF Cd(II) COMPLEXES OF *N*[4]-SUBSTITUTED SEMICARBAZONES

CURRICULUM VITAE
RESEARCH PAPER PUBLICATIONS

…..✿….

A BRIEF PROLOGUE ON SEMICARBAZONES AND THEIR TRANSITION METAL COMPLEXES

1.1. General introduction

Coordination compounds have been a challenge to the inorganic chemist since they were identified in the nineteenth century. After the profound studies done by Alfred Werner, inorganic chemistry witnessed a great outflow of coordination compounds, with unique structural characteristics and diverse applications. The stereochemistry of coordination compounds is one of the major interests of the coordination chemist. The development of instrumental techniques provides methods of investigating thermal, spectral and magnetic properties of metal complexes. Coordination compounds can have a wide variety of structures depending on the metal ion, coordination number and denticity of the ligands used. The presence of more electronegative nitrogen, oxygen or sulfur atoms on the ligand structure is established to enhance the coordination possibilities of ligands.

Coordination compounds are widely used as potential drugs, in the field of catalysis and in biological fields. This includes a number of important biological materials such as vitamin B_{12} and haemoglobin. The chemistry of transition metal complexes of semicarbazones and thiosemicarbazones has been receiving considerable attention primarily because of their bioinorganic relevance.

Semicarbazones are the Schiff bases, usually obtained by the condenzation of semicarbazide with suitable aldehydes and ketones (Scheme 1.1).
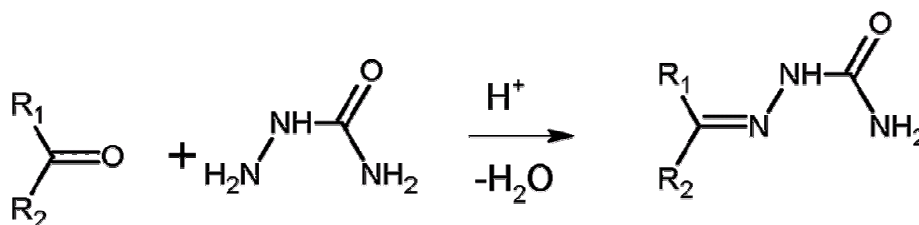
Scheme 1.1. Method of synthesis of the semicarbazone.

According to IUPAC recommendations, semicarbazones may be named by adding the class name 'semicarbazone' after the name of the condensed aldehyde or ketone. It is usual also to include in this class derivatives with substituents on the amide nitrogen. The numbering scheme shown in the Figure 1.1 is in accordance with IUPAC system.
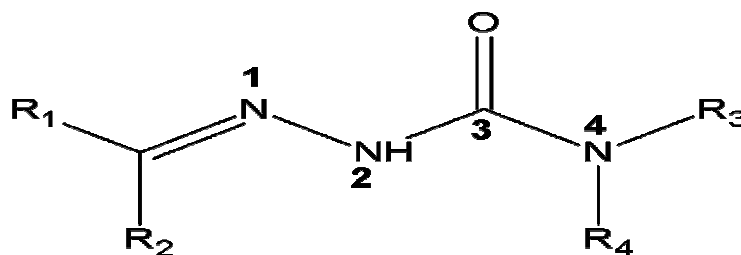
Figure 1.1. Numbering scheme of the semicarbazone.

An interesting attribute of the semicarbazones is that in the solid state, they predominantly exist in the keto form, whereas in solution state, they exhibit a keto-enol tautomerism (Figure 1.2). Keto form acts as a neutral bidentate ligand and the enol form can deprotonate and serve as monoanionic bidentate ligand in metal complexes. Thus semicarbazones are versatile ligands in both neutral and anionic forms.

keto (A)   **enol (B)**
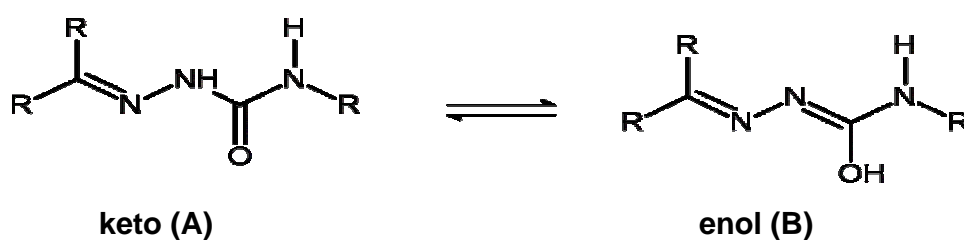
Figure 1.2. Keto-enol tautomerism of semicarbazones.

Both tautomeric forms have an efficient electron delocalization along the semicarbazone moiety. Aromatic substituents on the semicarbazone skeleton can further enhance the delocalization of electron charge density. These classes of compounds usually react with metallic cations giving complexes in which the semicarbazones behave as chelating ligands. Upon coordination to a metal center, the delocalization is further increased through the metal chelate rings. The coordination possibilities are further increased if the substituent has additional donor atoms.

1.2. Stereochemistry, bonding and nature of coordination of semicarbazones

A review of semicarbazones and thiosemicarbazones [1] showed that in free unsubstituted semicarbazones in the solid state, the C=N–NH–CO–NH$_2$ backbone is usually planar, with O atom trans to the azomethine N atom (Scheme 1.2). Few semicarbazones are exceptions to this rule. Although there are several electronic and steric factors that may contribute to the adoption of

this rearrangement, the most important is probably that the trans arrangement places the amine and azomethine nitrogen atoms in relative positions suitable for intramolecular hydrogen bonding [2].
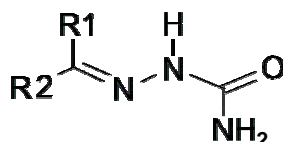
Scheme 1.2

Interestingly, semicarbazones show a variety of coordination modes with transition metals. The coordination mode is influenced by the number and type of substituents. This is because the active donor sites of the ligand vary depending upon the substituents. According to the reports, the coordination mode of the semicarbazone is very sensitive towards minor variations in the experimental conditions, the nature of the substituents on the carbonyl compound and the metal salt [3]. The presence of di-2-pyridyl ketone/ quinoline-2-carboxaldehyde at the carbonyl part attributes many interesting coordinating possibilities for the ligand systems under study. In most of the metal complexes we synthesized semicarbazones act as tridentate ligand and in some cases, semicarbazones exhibit as potential quadridentate when the second pyridyl nitrogen involves in coordination process. The coordination mode of the N^4-substituted semicarbazones [4] is given below.
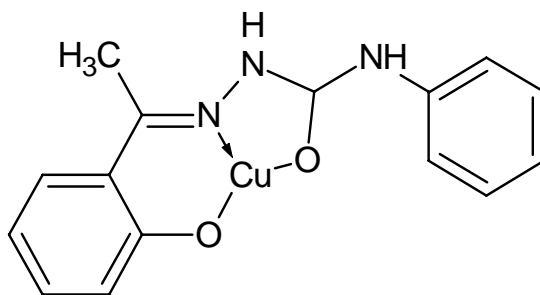
O, N, O-tricoordination.

The different coordination modes of the substituted benzaldehyde semicarbazone are given below [5].
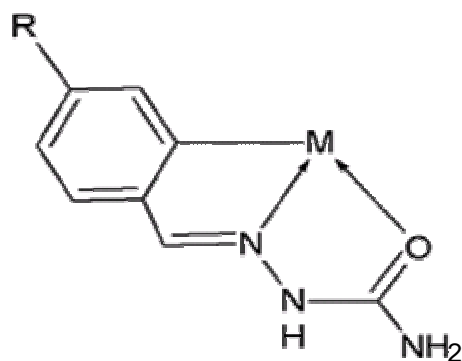
C,N,O-tricoordination.
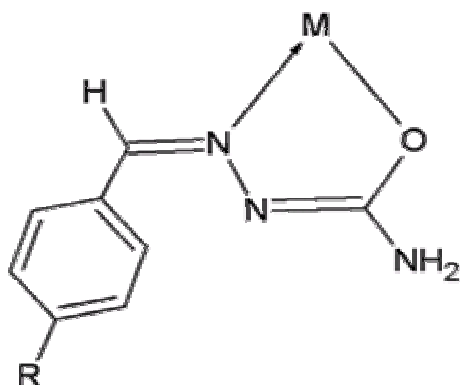
N,O-coordination forming a stable five membered chelate.
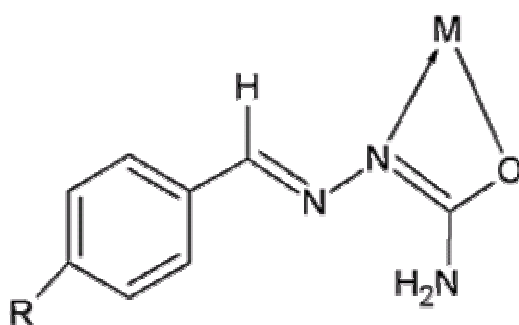
An unusual four membered chelate formation as an N,O donor.

1.3. Applications of semicarbazones and their complexes

Semicarbazones present a wide range of bioactivities, and their chemistry and pharmacological applications have been extensively investigated. The biological properties of semicarbazones are often related to metal ion coordination. Firstly, lipophilicity, which controls the rate of entry in to the cell, is modified by coordination [6]. Also, the metal complex can be more active than the free ligand. The mechanism of action can involve binding to a metal *in vivo* or the metal complex may be a vehicle for activation of the ligand as the cytotoxic agent. Moreover, coordination may lead to significant reduction of drug-resistance [7].

A variety of 5-nitrofuryl semicarbazone derivatives have been developed for the therapy of Chagas disease, a major problem in the Central and the South America [8]. 4-Bromobenzaldehyde semicarbazone has been used as anticonvulsant. Recently, a review reported on the anticonvulsant activity of thiosemicarbazones, semicarbazones and hydrazones derived from aromatic and unsaturated carbonyl compounds as well as from other precursors [9]. In contrast to thiosemicarbazones, literature records fewer examples of semicarbazones presenting significant anticancer and cytotoxic activity but some nitroso, naphtopyran, and fluorine derivatives showed anti-leukemia effect in mice [10]. Several N^4-substituted semicarbazone derivatives of o- and p- chlorobenzaldehyde and 2,6-dichlorobenzaldehyde exhibit potent anti-hypertensive effects [11]. The orally administered drug naftazone (1,2-naphtoquinone semicarbazone) protects the vascular system through an inhibitory effect on nitric oxide synthesis [12].

Many other bioactivities of semicarbazones have been reported, such as their antimicrobial [13], pesticide [14], herbicide [15], and hypnotic [16] properties or the ability of some of their Cu(II) complexes to mimic superoxide

dismutase activity [17]. Semicarbazones are widely used as spectrophotometric agents for the analysis of metal ions [18]. Semicarbazones are frequently used in the qualitative organic analysis of carbonyl compounds [19].

1.4. Objectives and scope of the present work

There has been considerable interest in the studies of semicarbazones due to their unusual coordination modes when bound to metals [20]. The wide applications and structural diversity of metal complexes of semicarbazones prompted us to synthesize the tridentate NNO-donor semicarbazones and their metal complexes. Due to good chelating ability, the present work is mainly concerned with the studies on complexes of N^4-substituted semicarbazones. By emphasizing this point the objectives of the present work are as follows:

The present work is concentrated on the studies of two novel semicarbazones, di-2-pyridyl ketone-N^4-phenyl-3-semicarbazone (HL^1) and quinoline-2-carboxaldehyde-N^4-phenyl-3-semicarbazone (HL^2). The compositions of these semicarbazones were determined by the CHN analyses. For the characterization of these compounds we have used IR, UV and NMR spectral studies. The molecular structure of quinoline-2-carboxaldehyde-N^4-phenyl-3-semicarbazone (HL^2) was obtained by single crystal X-ray diffraction studies. Also, we have synthesized Zn(II), Cd(II), Cu(II), Ni(II), Co(II) and Mn(II) complexes of these semicarbazones, HL^1 and HL^2. These complexes were characterized by various spectroscopic techniques, magnetic and conductivity studies. We could isolate single crystals of some Zn(II) and Cd(II) compounds suitable for X-ray diffraction studies. For other complexes we could not isolate single crystals of good quality for single crystal X-ray diffraction studies. This thesis is divided into six chapters.

Chapter 1 gives an introduction of semicarbazones and their metal complexes with an extensive literature survey relating the history, applications

and recent developments. This gives a detailed idea about bonding and stereochemistry of the semicarbazones.

Chapter 2 explains syntheses and characterization of two NNO donor semicarbazones.

Chapters 3, 4, 5 and 6 describe the syntheses and characterization of Zn(II), Cd(II), Cu(II), Ni(II), Co(II) and Mn(II) complexes of these semicarbazones.

1.5. Introduction to the relevant analytical techniques

The physicochemical methods adopted during the present investigation are discussed below:

1.5.1. Elemental analysis

CHN analyses were carried out using Vario EL III CHNS analyzer at the SAIF, Kochi, India.

1.5.2. Conductivity measurements

The molar conductivities of the complexes in DMF/DMSO solutions (10^{-3} M) at room temperature were measured using a direct reading conductivity meter at the Department of Applied Chemistry, CUSAT, Kochi, India.

1.5.3. Magnetic susceptibility measurements

Magnetic susceptibility measurements of Cu(II) complexes were carried out on a Vibrating Sample Magnetometer using $Hg[Co(SCN)_4]$ as a calibrant at the SAIF, Indian Institute of Technology, Madras. The magnetic moments for Ni(II), Co(II) and Mn(II) complexes were found out using Gouy Balance at the Department of Applied Chemistry, CUSAT, Kochi, India.

1.5.4. Infrared spectroscopy

Infrared spectra of some of the complexes were recorded on a JASCO FT-IR-5300 Spectrometer in the range 4000-400 cm^{-1} using KBr pellets at the

Department of Applied Chemistry, CUSAT, Kochi, India, whereas for some other complexes IR spectra were recorded on a Thermo Nicolet AVATAR 370 DTGS model FT-IR Spectrophotometer with KBr pellets at the SAIF, Kochi, India.

1.5.5. Electronic spectroscopy

Electronic spectra in the range 200-500 nm were recorded on a Cary 5000 version 1.09 UV-VIS- NIR Spectrophotometer using solutions in DMF/DMSO at the SAIF, Kochi, India. The spectra in the range 500-900 nm were recorded on a Spectro UV-vis Double Beam UVD-3500 spectrometer at the Department of Applied Chemistry, CUSAT, Kochi, India.

1.5.6. NMR spectroscopy

The ^{1}H and ^{13}C NMR spectra were recorded using Bruker DRX 500 Spectrometer, with CDCl$_3$ as solvent and TMS as standard at the Sophisticated Instruments Facility, Indian Institute of Science, Bangalore, India.

1.5.7. EPR spectroscopy

EPR spectra were recorded in a Varian E-112 X-band EPR Spectrometer using TCNE as a standard at SAIF, IIT, Bombay, India. *g* factors were quoted relative to the standard marker TCNE (*g*=2.00277). EPR simulation of manganese(II) complexes were done using Easy spin program [21].

1.5.8. X-ray crystallography

X-ray diffraction measurements were carried out on a CrysAlis CCD diffractometer with graphite-monochromated Mo Kα (λ = 0.71073 Å) radiation at National Single Crystal X-ray Facility, IIT Bombay, Mumbai, India and University of Hyderabad, Hyderabad, India. The program CrysAlis RED was used for data reduction and cell refinement. The structure was solved by direct methods using SHELXS and refined by full-matrix least-squares refinement on F^2 using SHELXL.

References

[1]   J.S. Casas, M.S. Garcia-Tasende, J. Sordo, Coord. Chem. Rev. 209 (2000) 197.

[2]   J.N. Brown, K.C. Agarwal, Acta Crystallogr., Sect. B 34 (1978) 2038.

[3]   F. Basuli, S.M. Peng, S. Bhattacharya, Inorg. Chem. 40 (2001) 1126.

[4]   A. Sreekanth, U.L. Kala, C.R. Nayar, M.R.P. Kurup, Polyhedron 23 (2004) 41.

[5]   F. Basuli, S.M. Peng, S. Bhattacharya, Inorg. Chem. 36 (1997) 5645.

[6]   N. Farrell, Coord. Chem. Rev. 1 (2002) 232.

[7]   D.X. West, S.B. Padhye, P.B. Sonawane, Structure and Bonding Springer-Verlag: New York 76 (1991) 1.

[8]   H. Cerecetto, M. Gonzalez, M. Curr. Topics Med. Chem. 2 (2002) 1185.

[9]   H. Beraldo, D. Gambino, Mini reviews in Med. Chem. 4 (2004) 159.

[10]   S.N. Pandeya, J.R. Dimmock, Pharmazie 48 (1993) 659.

[11]   J.D. Warren, D.L. Woodward, J. Med. Chem. 29 (1977) 1520.

[12]   P. Sogni, S. Yang, C. Pilette, R. Moreau, A. Gadano, G. Avenard, C. Bloy, D. Lebrec, Eur. J. Pharmacol. 344 (1998) 37.

[13]   A. Singh, R. Dharkarey, G.C. Saxena, J. Indian Chem. Soc. 73 (1996) 339.

[14]   R.J. Anderson, I.S. Cloudsdale, R.J. Lamoreaux, K. Schaefer, J. Harr, US Patent 6 110 (2000) 869.

[15]   L.G. Copping, J.C. Kerry, T.I. Watkins, R.J. Wllis, H. Bryan, US Patent 4 394 (1983) 387.

[16]   S.N. Pandeya, N. Aggarwal, J.S. Jain, Pharmazie 54 (1999) 4.

[17]   J. Patole, S. Dutta, S. Padhye, E. Sinn, Inorg. Chim. Acta 318 (2001) 207.

[18]   T. Atalay, E.G. Akgemci, Tr. J. Chem. 22 (1998) 123.

[19]   V.M. Kolb, J.W. Stupar, T.E. Janota, W.L. Duax, J. Org. Chem. 54 (1989) 2341.

[20]   F. Basuli, M. Ruff, C.G. Pierpont, S. Bhattacharya, Inorg. Chem. 37 (1998) 6113.

[21]   S. Stoll, A. Schweiger, J. Magn. Reson. 178 (2006) 42.

…..ಇಂ…..

SYNTHESIS, SPECTRAL AND STRUCTURAL CHARACTERIZATION OF SEMICARBAZONE LIGANDS

Contents	**2.1 Introduction**
	2.2 Experimental
	2.3 Results and discussion

2.1. Introduction

Semicarbazones are the condenzation products of semicarbazides with aldehyde or ketone. These compounds are having the formula $R_2C=N–NH–CO–NH_2$. Semicarbazones are compounds with versatile structural features and can coordinate to the metal in both neutral and anionic forms. These classes of compounds usually react with metallic cations giving complexes in which semicarbazones behave as chelating ligands. The coordination possibilities of the semicarbazones are increased if the substituents of the aldehyde or ketone include additional donor atoms. These compounds are associated with diverse pharmacological activities such as antibacterial, antifungal, antihypertensive, hypolipidemic, antineoplastic, hypnotic and anticonvulsant. The biological activities are due to the ability to form terdentate chelates with transition metal ions bonding through oxygen, pyridyl and azomethine nitrogen atoms [1]. Lipophilicity can be modified by coordination and the metal complex can be more active than the free ligand. It was reported that aryl semicarbazones were devoid of sedative hypnotic activity and exhibited anticonvulsant activity with less neurotoxicity [2]. Semicarbazones are also used as protected carbonyl compounds

in synthesis [3]. Several semicarbazones and its metal complexes have been the subject of chemical and structural studies [4]. Semicarbazones have been known as anticancer and antiviral agents for many years [5]. Due to their good complexing properties, biological activities and analytical application, semi-/thiosemi-/isothiosemicarbazides and their Schiff bases of different denticity, as well as their metal complexes, have been the subject of many studies.

We have synthesized two N^4-phenyl substituted semicarbazones using di-2-pyridyl ketone and quinoline-2-carboxaldehyde.

(i)   Di-2-pyridyl ketone-N^4-phenyl-3-semicarbazone (HL^1)
(ii)   Quinoline-2-carboxaldehyde-N^4-phenyl-3-semicarbazone (HL^2)

This chapter deals with the synthesis, spectral and structural characterization of semicarbazones, HL^1 and HL^2. The structural formulae and numbering scheme of the two semicarbazones are given in Figure 2.1. However it should be noted that the numbering scheme in the crystal structures are based on the types of different atoms present.

Molecular formula: $C_{18}H_{15}N_5O$
Formula weight: 317.34
Melting point : 160 ^{o}C

Di-2-pyridyl ketone-N^4-phenyl-3-semicarbazone (HL^1)

Molecular formula: $C_{17}H_{14}N_4O$
Formula weight: 290.32
Melting point : 188 ^{o}C

Quinoline-2-carboxaldehyde-N^4-phenyl-3-semicarbazone (HL^2)
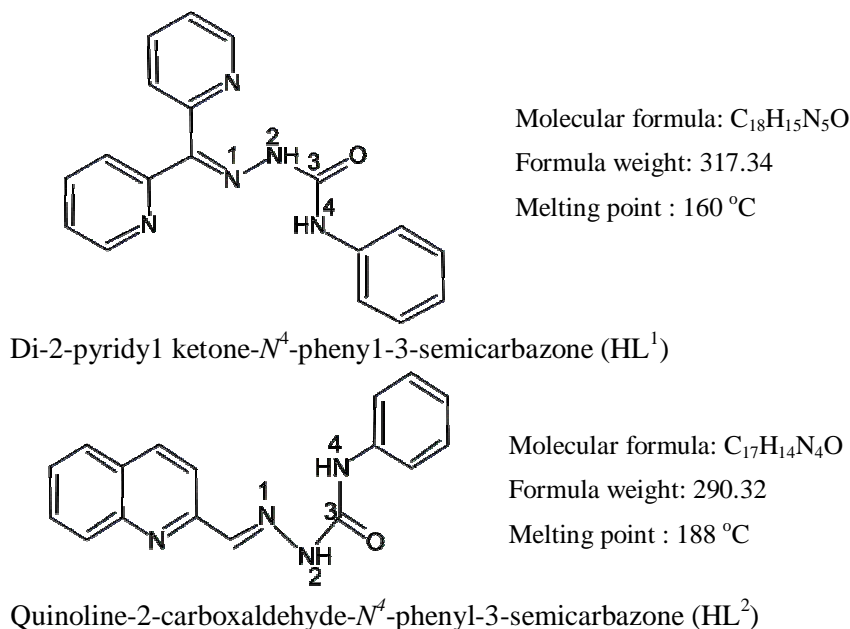
Figure 2.1. Structures and numbering schemes of the semicarbazones.

2.2. Experimental
2.2.1. Materials

Di-2-pyridyl ketone (Aldrich), N^4-phenylsemicarbazide (Aldrich), quinoline-2-carboxaldehyde (Aldrich) and methanol were used as received. The solvents were purified according to standard procedures.

2.2.2. Synthesis of semicarbazones

(i) Di-2-pyridyl ketone-N^4-phenyl-3-semicarbazone (HL^1)

A methanolic solution of di-2-pyridyl ketone (0.184 g, 1 mmol) was mixed with N^4-phenylsemicarbazide (0.151 g, 1 mmol) in methanol and to this mixture 3 drops of glacial acetic acid was added. The reaction mixture was refluxed for 2 hrs. On slow evaporation, colorless crystalline compound formed was filtered, washed with ether and recrystallized from ethanol and dried over P_4O_{10} *in vacuo* (Scheme 2.1).

Melting point = 160 °C; yield: 85%.
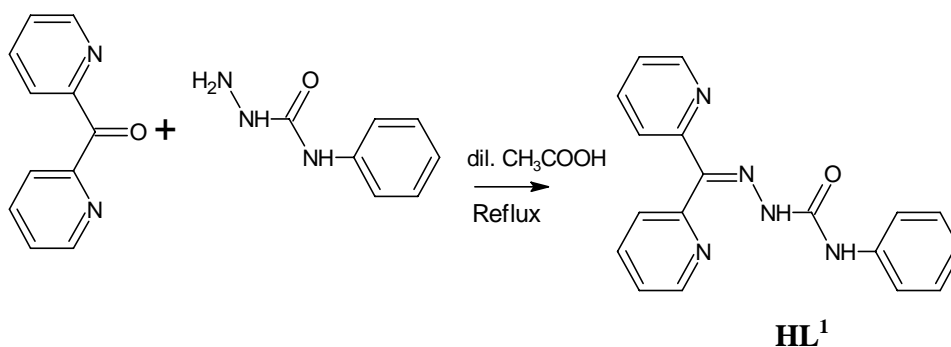
Scheme 2.1

(ii) Quinoline-2-carboxaldehyde-N^4-phenyl-3-semicarbazone (HL^2)

A solution of quinoline-2-carboxaldehyde (0.157 g, 1 mmol) in methanol was mixed with a methanolic solution of N^4-phenylsemicarbazide (0.151 g, 1 mmol) and 3 drops of glacial acetic acid was added to this. The

reaction mixture was refluxed for 2 hrs. On slow evaporation, colorless crystalline compound was filtered, washed with ether and recrystallized from ethanol and dried over P_4O_{10} *in vacuo* (Scheme 2.2).

Melting point =188 $^\circ$C; yield: 75%

HL^2
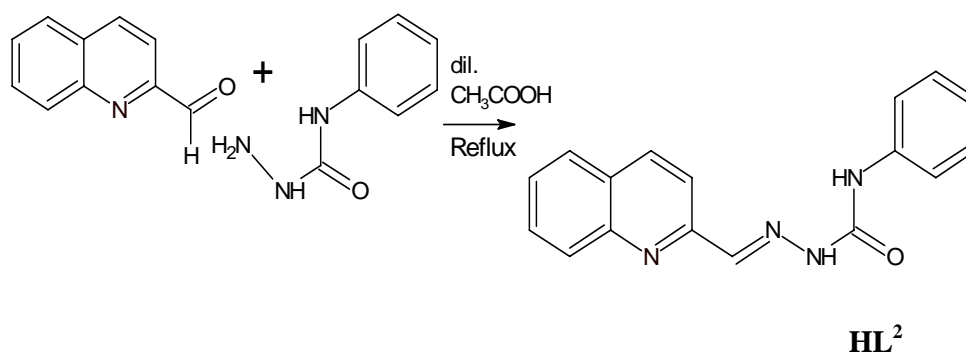
Scheme 2.2

2.2.3. Characterization of semicarbazones

The semicarbazones were characterized by using ^{1}H and ^{13}C NMR spectra, IR spectra, electronic spectra and partial elemental analyses. One of the semicarbazones, quinoline-2-carboxaldehyde-N^4-phenyl-3-semicarbazone (HL^2) was characterized by single crystal X-ray diffraction studies also. Elemental analyses were carried out using a Vario EL III CHNS analyzer at the SAIF, Kochi, India. Infrared spectra were recorded on a JASCO FT-IR-5300 Spectrometer in the range 4000-400 cm^{-1} using KBr pellets. Electronic spectra were recorded on a Cary 5000 version 1.09 UV-VIS-NIR Spectrophotometer using solutions in DMF. The ^{1}H and ^{13}C NMR spectra were recorded using Bruker DRX 500 Spectrometer, with CDCl$_3$ as solvent and TMS as standard at the Sophisticated Instruments Facility, Indian Institute of Science, Bangalore, India.

2.2.4. X-ray crystallography

Single crystals of HL^2 suitable for X-ray analysis were obtained from its solution in 1:1 (v/v) mixture of methanol and DMF. A crystal with approximate dimensions 0.36 x 0.23 x 0.21 mm^3 was selected for collecting the data. The crystallographic data and structure refinement parameters of compound HL^2 are given in Table 2.1. X-ray crystallographic data were collected at 150(2) K on a Crys Alis CCD diffractometer with graphite-monochromated Mo Kα (λ = 0.71073 Å) radiation. The program Crys Alis RED was used for data reduction and cell refinement. The structure was solved by direct methods and refined by least-square on F_o^2 using SHELXL-97 [6]. All non-hydrogen atoms were refined anisotropically. All hydrogen atoms except those attached to nitrogens were geometrically fixed at calculated positions. Those on nitrogen atoms were refined from Fourier maps. Refinement of F^2 was done against all reflections. All esds, except the esd in the dihedral angle between two least square planes, are estimated using the full covariance matrix. Flack x parameter is 0(2). As this value is 0, with small standard uncertainty, the absolute structure given by the structure refinement is likely correct [7]. The molecular graphics employed were DIAMOND version 3.1d [8] and PLATON [9]. A total of 12679 reflections were collected. The final refinement cycle was based on all 2488 independent reflections and 207 variables with R_1= 0.0628 and wR_2= 0.0834.

Table 2.1. Crystal data and structure refinement parameters of HL^2

Empirical formula	$C_{17}H_{14}N_4O$
Formula weight	290.32
Temperature	150(2) K
Wavelength	0.71073 Å
Crystal system	Orthorhombic
Space group	$P2_12_12_1$
Unit cell dimensions	a = 6.4662(3) Å
	b = 10.3994(5) Å
	c = 21.0315(11) Å
	$\alpha = 90°$
	$\beta = 90°$
	$\gamma = 90°$
Volume	1414.25(12) $Å^3$
Z	4
Density (calculated)	1.364 Mg/m^3
Absorption coefficient	0.089 mm^{-1}
F(000)	608
Crystal size	0.36 x 0.23 x 0.21 mm^3
θ range for data collection	3.30 to 25.00°.
Reflections collected	12679
Index ranges	$-7 \leq h \leq 7$, $-12 \leq k \leq 12$, $-25 \leq l \leq 21$
Independent reflections	2488
Refinement method	Full-matrix least-squares on F^2
Data / restraints / parameters	2488 / 0 / 207
Goodness-of-fit on F^2	1.019
Final R indices [I>2σ(I)]	$R_1 = 0.0427$, $wR_2 = 0.0754$
R indices (all data)	$R_1 = 0.0628$, $wR_2 = 0.0834$
Largest diff. peak and hole	0.148 and -0.135e.$Å^{-3}$

$R_1 = \Sigma||F_o| - |F_c|| / \Sigma|F_o|$ $wR_2 = [\Sigma w(F_o^2 - F_c^2)^2 / \Sigma w(F_o^2)^2]^{1/2}$

2.3. Results and discussion

Semicarbazone is the condenzation product of semicarbazide and aldehyde or ketone. The compound HL[1] is formed by the condenzation of N^4-phenylsemicarbazide and di-2-pyridyl ketone in the molar ratio 1:1 and HL[2] is formed from N^4-phenylsemicarbazide and quinoline-2-carboxaldehyde in the same molar ratio. The condenzation reaction is catalyzed by an acid. Methanol is used as the solvent. The elemental analysis data obtained are in good agreement with the stoichiometry of di-2-pyridyl ketone-N^4-phenyl-3-semicarbazone (HL[1]) and quinoline-2-carboxaldehyde-N^4-phenylsemicarbazone (HL[2]). The semicarbazones HL[1] and HL[2] can exist in keto or enol form or an equilibrium mixture of two tautomers since it has an amide, –NH–C=O function. However crystal study and spectral studies indicate the existence of keto form in the solid state. The analytical data of the semicarbazones are presented in Table 2.2.

Table 2.2. Analytical data

Compound	Empirical formula	Found (Calcd) %		
		C	H	N
HL[1]	$C_{18}H_{15}N_5O$	67.44 (68.13)	4.80 (4.76)	22.14 (22.07)
HL[2]	$C_{17}N_{14}N_4O$	70.13 (70.33)	4.99 (4.86)	19.22 (19.30)

2.3.1. Crystal structure of HL[2]

The molecular structure of HL[2] along with the atom numbering scheme is given in Figure 2.2. Selected bond lengths and angles are given in Table 2.3. The compound crystallizes into an orthorhombic space group $P2_12_12_1$. The molecule is almost planar and exists in the E configuration with respect to C10=N2 bond. [10]. A torsion angle value of 179.5(2)° corresponding to

O(1)–C(11)–N(3)–N(2) moiety confirms the trans configuration of the O(1) atom with respect to hydrazine nitrogen atom N(2). As a result, atom N(2) lies cis to N(4), with an N(4)–C(11)–N(3)–N(2) torsion angle of -1.9(3). This arrangement favors the hydrogen bond interaction of N(2) and H–N(4). The C(10)–N(2) bond distance [1.282(3) Å] is appreciably close to that of C=N double bond [1.28 Å], confirming the azomethine bond formation. The existence of semicarbazone in the keto form in the solid state is evidenced by the C(11)–O(1) bond distance of 1.222(3) Å, which is very close to a formal C=O bond length [1.21 Å]. However, the N(2)–N(3) [1.379(3) Å] and N(3)–C(11) [1.376(3) Å] bond distances are intermediate between the ideal values of corresponding single [N–N; 1.45 Å and C–N; 1.47 Å] and double bonds [N=N; 1.25 Å and C=N; 1.28 Å], which is in support of an extended π delocalization along the semicarbazone chain [11]. Out of two C(11)–N bonds, C(11)–N(4) bond is significantly shorter than C(11)–N(3), suggesting greater double bond character for the former bond and indicating increased electron localization at this substituted end [12].

Figure 2.2. Molecular structure of HL^2.

Table 2.3. Selected bond lengths (Å) and bond angles (°) of HL^2

Bond lengths		Bond angles	
C(12)–N(4)	1.422(3)	O(1)–C(11)–N(4)	125.4(2)
C(11)–O(1)	1.222(3)	O(1)–C(11)–N(3)	119.5(2)
C(11)–N(4)	1.353(3)	N(4)–C(11)–N(3)	115.0(2)
C(11)–N(3)	1.376(3)	N(2)–C(10)–C(9)	121.1(2)
C(10)–N(2)	1.282(3)	C(11)–N(3)–N(2)	121.2(2)
C(10)–C(9)	1.469(3)	C(10)–N(2)–N(3)	114.3(2)
N(3)–N(2)	1.378(3)	C(9)–N(1)–C(1)	118.1(2)

Figures 2.3 and 2.4 show unit cell packing of HL^2. The assemblage of molecules in the respective manner in the unit cell is resulted by the π–π, C–H⋯π and hydrogen bonding interactions. The centroid Cg(1) is involved in π–π interaction with Cg(3) of the neighboring molecule at a distance of 4.5426 Å and a C–H⋯π interaction, C(4)–H(4)⋯Cg(2) at a distance of 2.67 Å contribute stability to the unit cell packing. The unit cell comprises of four molecules.

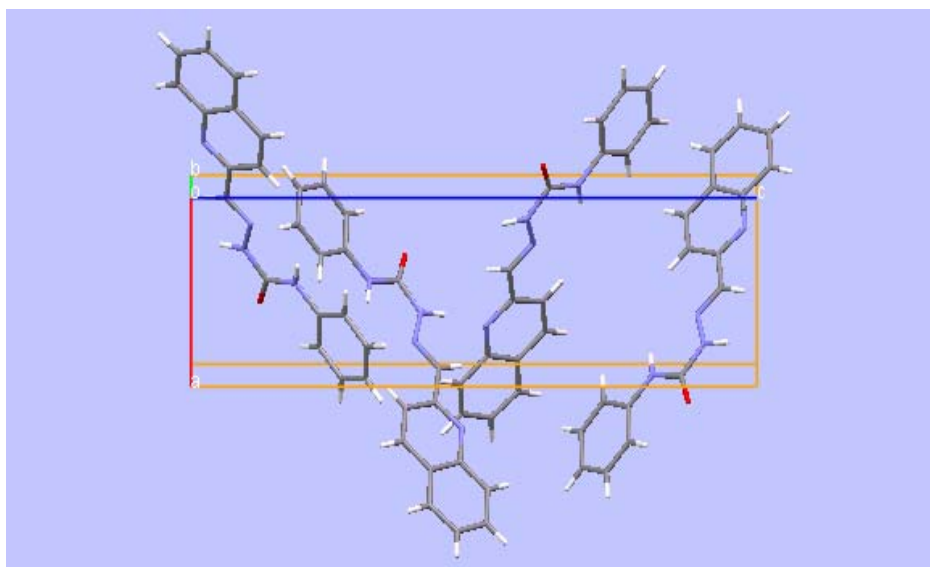**Figure 2.3.** Unit cell packing diagram of HL^2 along *b* axis.
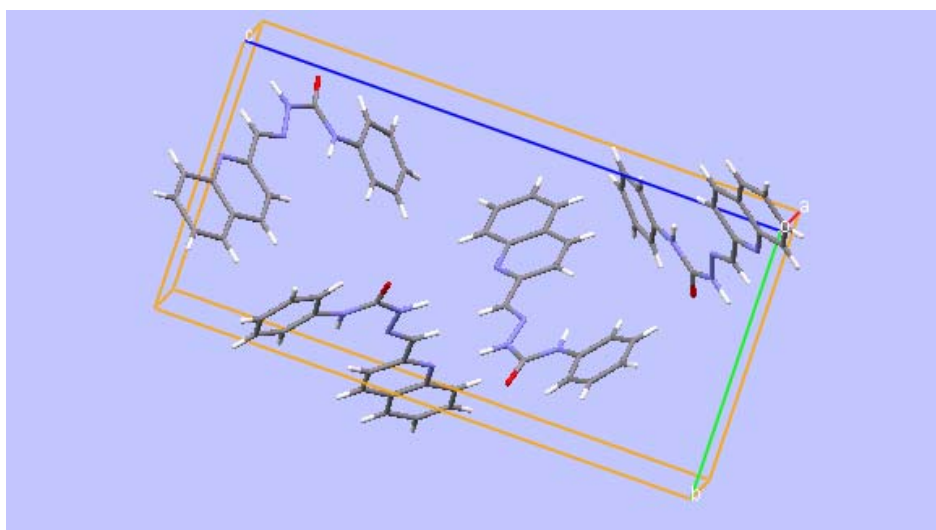
Figure 2.4. Unit cell packing diagram of HL^2 along *c* axis.

There are two prominent intramolecular and one intermolecular hydrogen-bonding interactions (Table 2.4 and Figure 2.5). The crystal structure is stabilized by intra- and intermolecular hydrogen bonding and the molecules are arranged in opposite manner. Two prominent intramolecular hydrogen bonding interactions, *viz.* N(4)–H(4)···N(2) and C(17)–H(17)···O(1) led to the formation of one five membered ring and one six membered ring comprising of atoms N(2), N(3), C(11), N(4), H(4)N and O(1), C(11), N(4), C(12), C(17), H(17)C respectively [13,14]. An intermolecular hydrogen bonding, N(3)–H(3)···N(1) at a N(3)–N(1) distance of 3.028(3) Å also supports the present conformation of the semicarbazone.

Table 2.4. Hydrogen-bond geometry (Å, º)

D–H···A	D···H (Å)	H···A (Å)	D···A (Å)	D–H···A (°)
N(4)–H(4)···N(2)	0.860(3)	2.280(3)	2.662(3)	107(2)
C(17)–H(17)···O(1)	0.950	2.230	2.848(3)	122
N(3)–H(3)···N(1)[a]	1.04(3)	1.99(3)	3.028(3)	173(2)

A=acceptor, D=donor, Equivalent position code: a= -1/2+x,3/2-y, 1-z

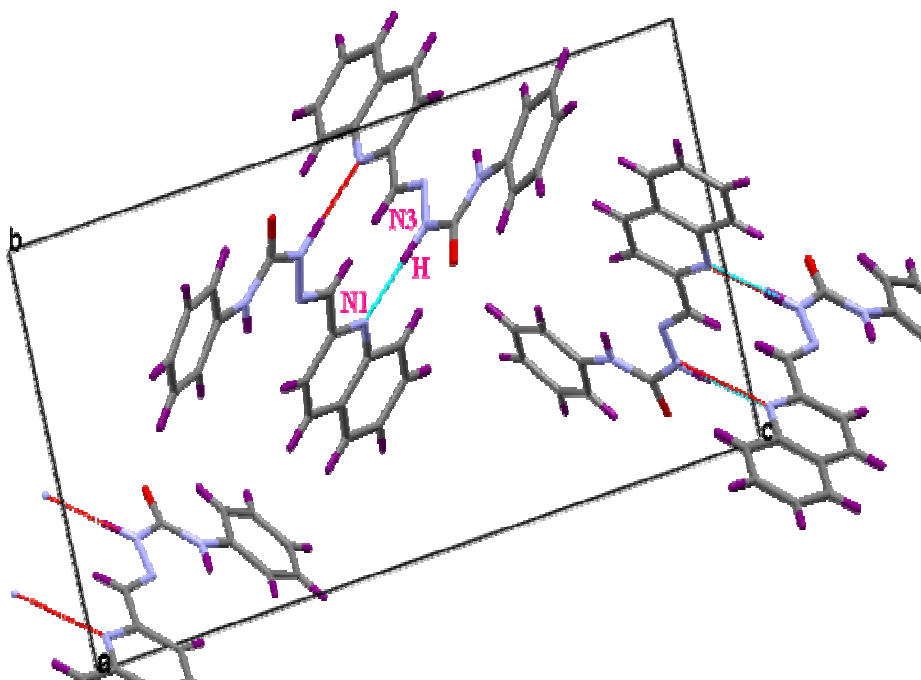**Figure 2.5.** Intermolecular hydrogen bonding interactions.

The phenyl ring Cg(3) and quinoline ring Cg(4) make a dihedral angle of 14.62(10)° between each other. The quinoline ring Cg(4) and semicarbazone moiety make a dihedral angle of 3.96(6)°. Least deviation is between Cg(2) and Cg(4) at a dihedral angle of 0.39(9)°. The largest deviation is observed between the planes of the phenyl ring Cg(3) and Cg(2) positioned at a dihedral angle of 14.75(12)° between each other. Some weak π–π and C–H···π interactions, *viz.* Cg(1)···Cg(3)[b]; [Cg(1): N(1), C(9), C(8), C(7), C(6), C(1) and Cg(3): C(12), C(13), C(14), C(15), C(16), C(17); Cg···Cg=4.5426(14) Å; b=1+x,y,z], Cg(3)···Cg(1)[c]; [Cg···Cg=4.5426(14) Å; c= -1+x,y,z] and C(4)–H(4)···Cg(2)[d]; [Cg(2): C(6), C(5), C(4), C(3), C(2),C(1); C(4)···Cg=2.67Å; d=½+x, $\frac{5}{2}$ -y,1-z], are the shortest interactions observed of their type in the lattice of the present compound (Table 2.5).

Table 2.5. $\pi \cdots \pi$ interactions

Cg(I)$\cdots$Cg(J)	Cg–Cg (Å)	$\alpha°$	$\beta°$
Cg(1)$\cdots$Cg(3)[b]	4.5426 (14)	14.60 (11)	51.04
Cg(3)$\cdots$Cg(1)[c]	4.5426 (14)	14.60 (11)	37.25

Equivalent position code:

b=1+x, y, z; c= -1+x, y, z

Cg(1) = N(1), C(9), C(8), C(7), C(6), C(1)

Cg(3) = C(12), C(13), C(14), C(15), C(16), C(17)

α = Dihedral angle between planes 1 and 3 (Deg)

β = Angle between Cg–Cg and Cg(J) perp.

C–H$\cdots\pi$ interactions

X–H$\cdots$Cg(J)	H$\cdots$Cg (Å)	X–H$\cdots$Cg (°)	X$\cdots$Cg (Å)
C(4)–H(4)$\cdots$Cg(2)[d]	2.67	146	3.498

Equivalent position code:

d= ½+x, $\frac{5}{2}$ -y, 1-z

Cg(2)= C(6),C(5),C(4),C(3),C(2),C(1)

2.3.2. Infrared spectra

Infrared spectra were recorded on a JASCO FT-IR-5300 spectrometer in the range 4000-400 cm^{-1} using KBr pellets. The characteristic IR bands observed for the semicarbazones, HL^1 and HL^2 along with their relative assignments are presented in the Table 2.6.

The characteristic IR bands of the semicarbazones provide significant information regarding the various functional groups present in them. The IR

frequencies of the carbonyl group of the semicarbazones drew interest rather early. It was observed that the IR frequency of the carbonyl of the semicarbazones is normally found at *ca*.1690 cm^{-1} (in KBr), which appeared abnormally high as compared to those of amides and urea [15]. This shift of IR frequency can be explained by the combined inductive effect of nitrogen atoms, which would pull the π cloud of carbonyl closer to the carbon, diminishing the polar character of the C=O. This would cause a rise in the IR frequency of the C=O [16]. The presence of bands at 1718 and 1702 cm^{-1} of HL^1 and HL^2 respectively assigned to v(C=O) stretching vibrations which reveal the presence of keto form in the solid state. Medium bands observed at 3369 and 3380 cm^{-1} are assigned to the v_a(NH) of the imino group of semicarbazones, HL^1 and HL^2 respectively and this also suggest that HL^1 and HL^2 exist in keto form in the solid state. The azomethine stretching vibrations are observed at 1591 and 1592 cm^{-1} for HL^1 and HL^2 respectively which are in agreement with earlier reports of N^4-substituted semicarbazones [17]. The IR spectral bands of HL^1 and HL^2 observed at 1129 and 1153 cm^{-1} correspond to v(N–N) [18,19]. Presence of bands at 1535 and 1526 cm^{-1} for the ligands HL^1 and HL^2 respectively are due to the interactions between N–H bending and C–N stretching vibrations of the C–N–H group of the amide function. Weak bands at 1265 and 1269 cm^{-1} also result from the N–H bending and C–N stretching interactions.

Table 2.6. IR spectral assignments (cm^{-1}) of the semicarbazones

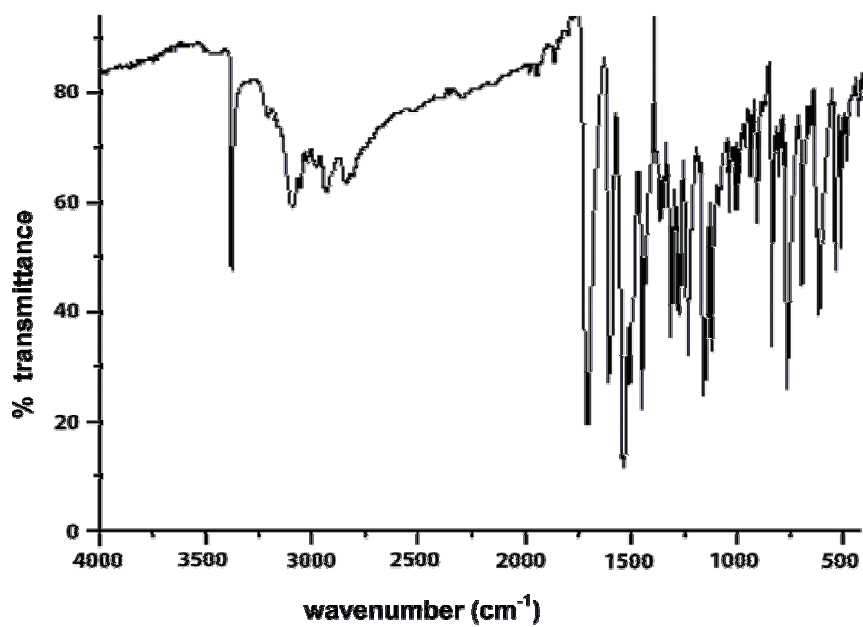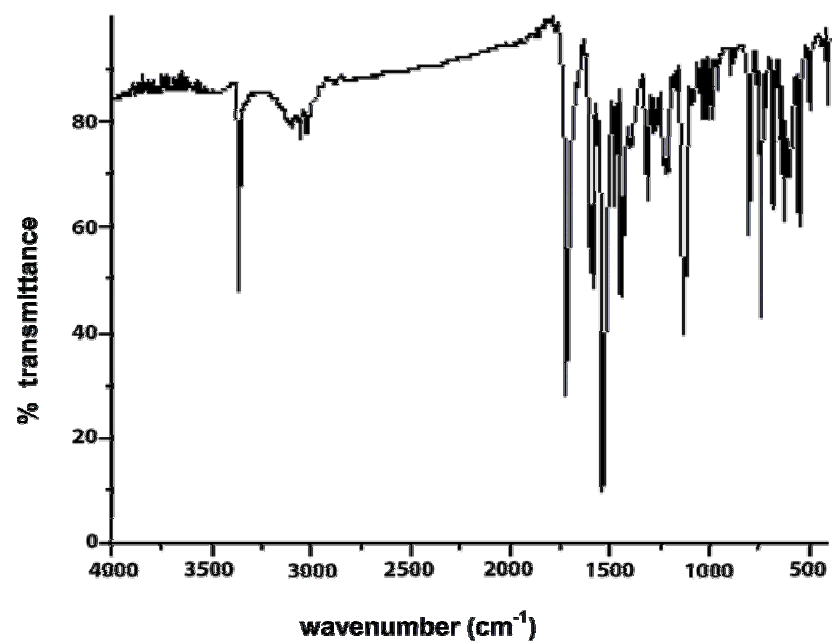| Compound	v(NH)	v(C=N)	v(CO)	v(N–N)
HL^1	3369	1591	1718	1129
HL^2	3380	1592	1702	1153

Figure 2.6. IR spectra of HL^1 and HL^2.

The bands at 1216 and 1034 cm^{-1} for HL[1] and 1225 and 1113 cm^{-1} for HL[2] correspond to the in-plane vibrations of the pyridyl and quinoline rings respectively while the out-of-plane vibrations are observed at 601 and 689 cm^{-1} for HL[1] and HL[2] respectively [20-22]. IR spectra of the semicarbazones HL[1] and HL[2] are presented in Figure 2.6.

2.3.3. Electronic spectra

In contrast to the infrared spectrum, the electronic spectrum is not used primarily for the identification of individual functional groups, but rather to show the relationship between functional groups, chiefly conjugation [23]. The UV-visible spectra of organic compounds are associated with the electronic transition between energy levels, and at wavelengths above 200 nm, excitation of electrons from the π-orbitals usually giving rise to informative spectra [24]. The tentative assignments of the significant electronic spectral bands of semicarbazones are presented in Table 2.7. Electronic spectra were recorded on a Cary 5000 version 1.09 UV-VIS- NIR Spectrophotometer using solutions in DMF. Electronic spectrum of semicarbazone HL[1] shows absorption maxima at 36300 and 31160 cm^{-1} respectively, which are attributed to π→π* transition of the pyridyl ring and imine function of the semicarbazone moiety and n→π* transition of azomethine and carbonyl groups respectively. For HL[2], π→π* transition is observed at 36940 whereas n→π* transitions are observed in the range 32200-28770 cm^{-1}. Electronic spectra of the semicarbazones are presented in Figure 2.7.

Table 2.7. Electronic spectral assignments of semicarbazones

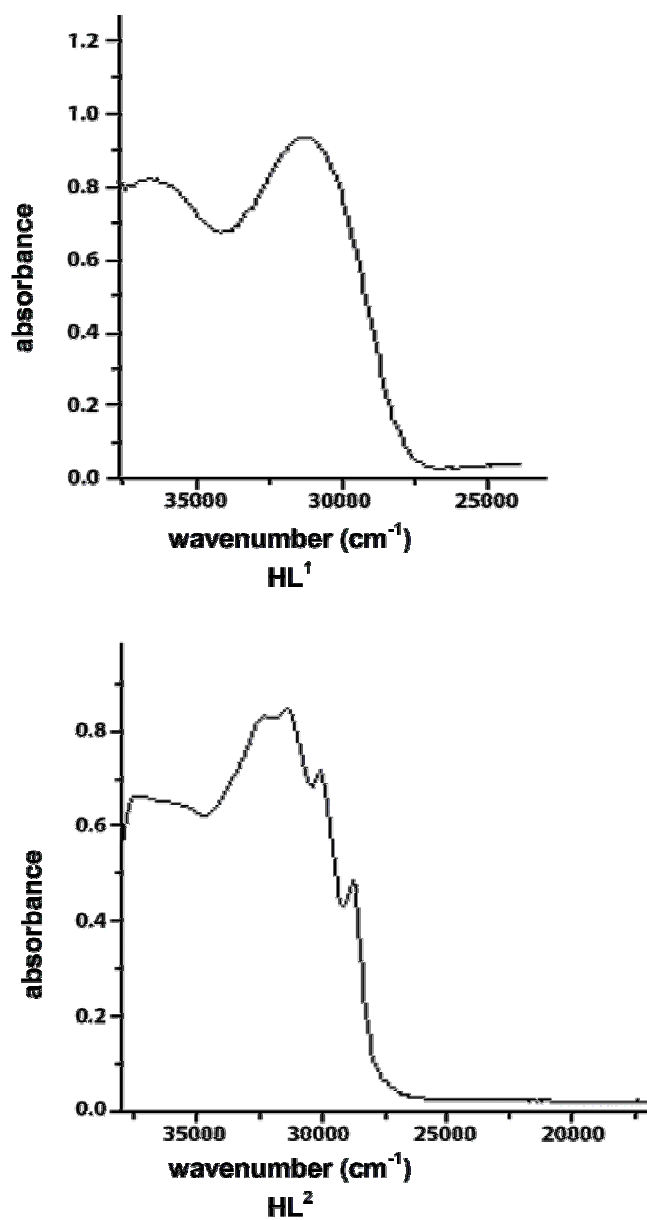| Compound	π–π*	n–π*
HL[1]	36300	31160
HL[2]	36940	32200, 31300, 29900, 28770

Figure 2.7. Electronic spectra of semicarbazones.

2.3.4. ^{1}H NMR spectra

The ^{1}H NMR spectra were recorded using Bruker DRX 500 Spectrometer, with $CDCl_3$ as solvent and TMS as standard at the Sophisticated Instruments Facility, Indian Institute of Science, Bangalore, India. Proton

magnetic resonance spectroscopy is a helpful tool for the identification of organic compounds in conjunction with other spectrometric informations. The assignments are done on the basis of chemical shifts, multiplicities and coupling constants. These give insight into the average effective magnetic fields present, interaction of nuclear spin with the adjacent atoms and the number of equivalent protons.

The ^{1}H NMR spectrum of HL^1 along with the assignments is given in Figure 2.8. For HL^1, a sharp singlet, which integrate as one hydrogen at δ=13.37 ppm is assigned to the proton attached to the nitrogen atom N(4). The downfield shift of this proton is assigned to its hydrogen bonding interaction with adjacent nitrogen atom N(1). Another singlet at δ=8.37 ppm is assigned to the N(5) proton. This downfield also explained with the hydrogen bonding interaction with nitrogen atom N(3). Hydrogen bonding decreases the electron density around the proton and thus moves the proton absorption to a lower field. Absence of any coupling interactions by N(4)H and N(5)H protons due to the lack of availibity of protons on neighboring atoms render singlet peaks for the imine protons. So the downfield shift of N(4) and N(5) protons can be explained by the hydrogen bonding interaction and the decoupling by the electric quadrupole effects.

Two doublets at δ=8.78 and 8.66 ppm are assigned to the C(1)H and C(11)H protons respectively. These signals are shifted to lower field due to electronic effect of the adjacent electronegative pyridyl nitrogens and the more downfield shift of C(1)H can be attributed to the increased charge density on N(1) resulted by its hydrogen bonding to N(4)H. The proton resonances of the two pyridyl rings also appear separately in the NMR spectrum, due to the intramolecular hydrogen bonding. There are two triplets at δ=7.87 and 7.79 ppm corresponding to similar protons on C(3) and C(9) of the two pyridyl rings, while the C(2) and C(10) protons resonances appear overlapped in the multiplet 7.34 ppm. Another two doublets at δ=7.56 and 7.51 ppm are assigned to C(4) and C(8)

protons. The resonances for the C_6H_5-group appear as triplet at 7.04 ppm for para proton and as multiplets at 7.34 ppm for ortho and meta phenyl protons [25].
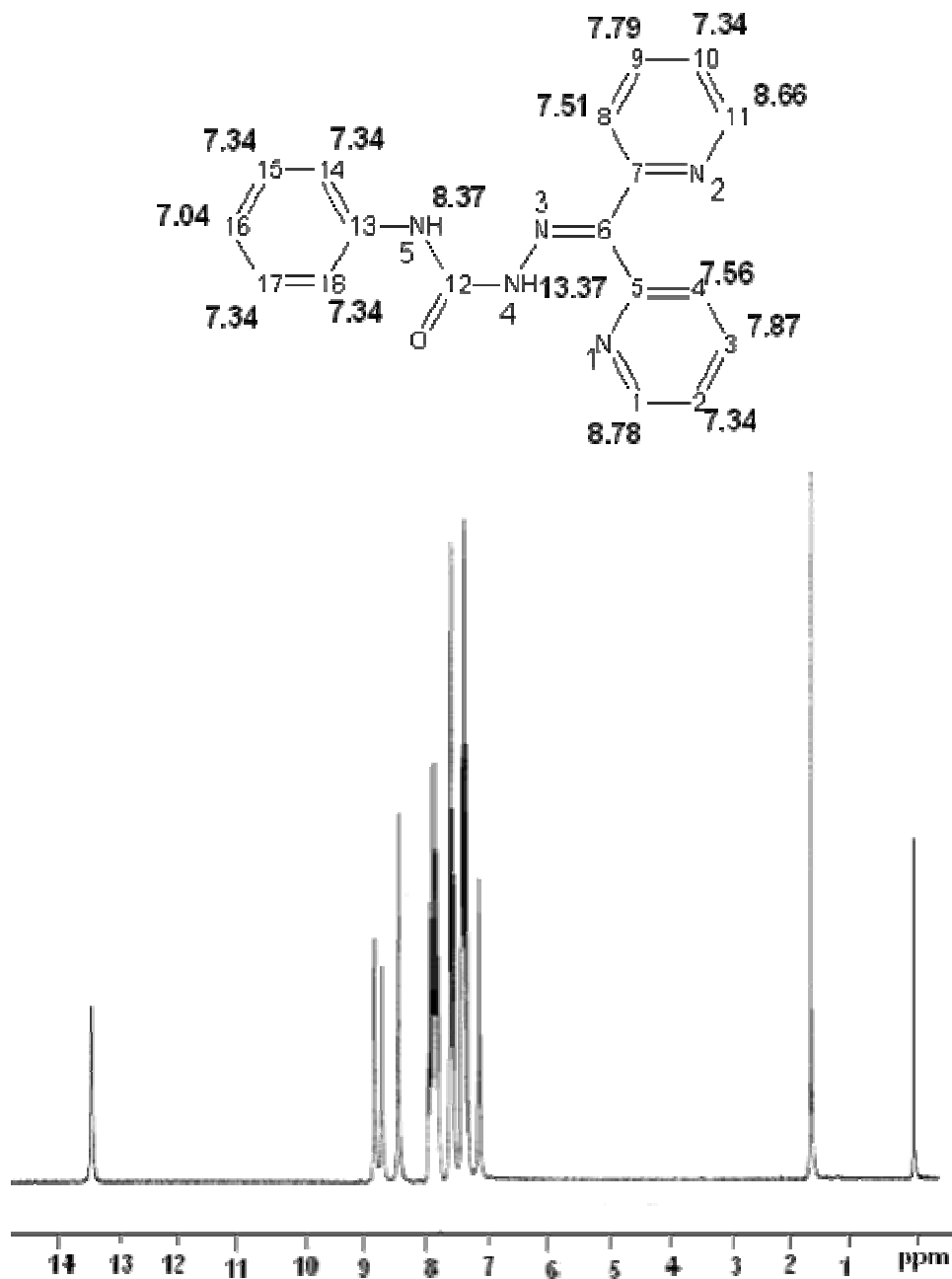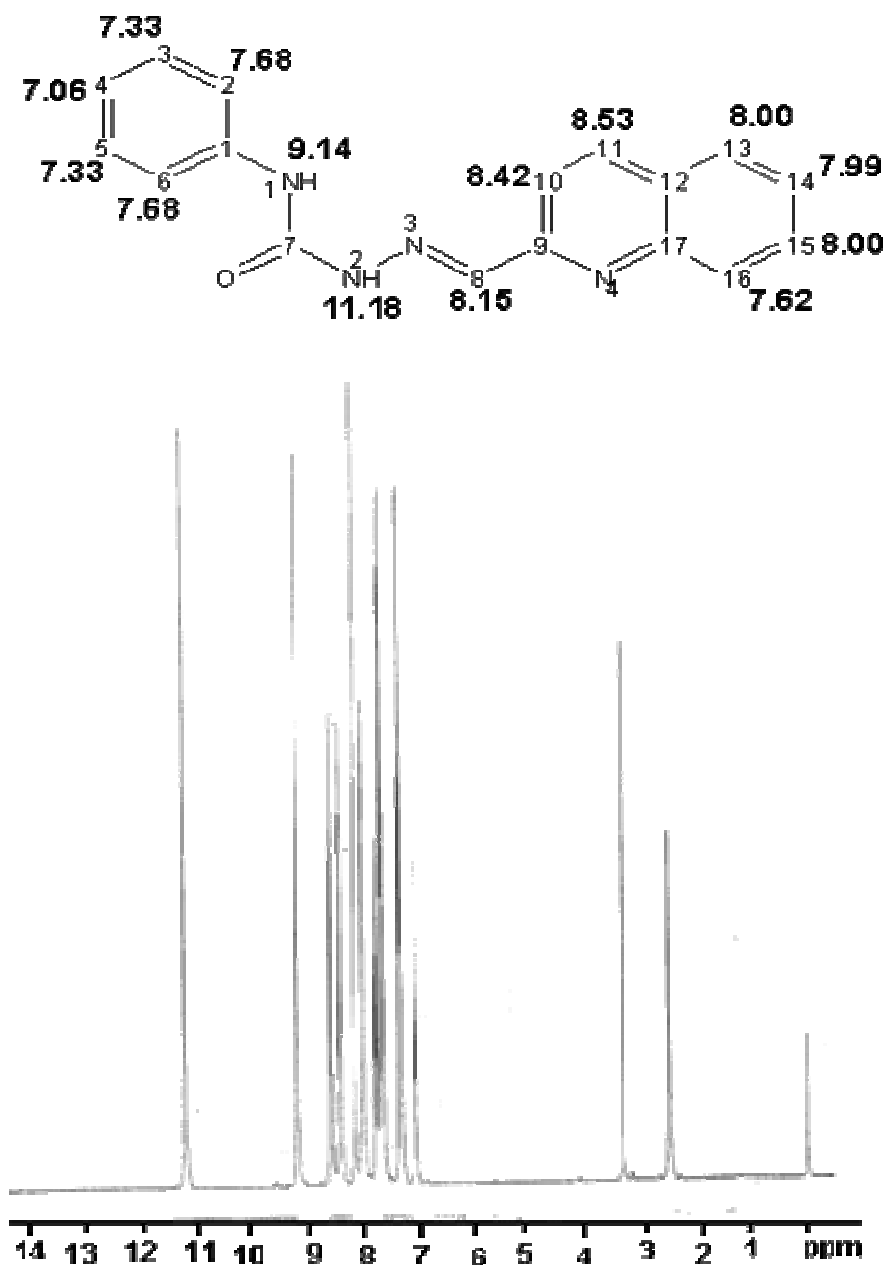

Figure 2.8. ^{1}H NMR spectrum of HL^1.

The ^{1}H NMR spectrum of the semicarbazone, HL^2 along with the spectral assignments is given in Figure 2.9. The signals at δ=11.18 and 9.14 ppm are assigned to N(2)H and N(1)H protons respectively.

Figure 2.9. ^{1}H NMR spectrum of HL^2.

These protons are shifted downfield because they are attached to hetero atoms and so are easily subjected to hydrogen bonding and are decoupled by the electrical quadrupole effects. The protons attached to N(2) and N(1) appear as singlets as expected since these NH protons are decoupled from the nitrogen atoms and the protons from the adjacent atoms. Absence of any coupling interactions by C(8)H proton due to the non-availability of protons on neighboring atoms render singlet peak at δ=8.15 ppm. Two doublets at δ=8.53 and 8.42 ppm are assigned to the C(11)H and C(10)H protons respectively. At δ=8.00, we got a quartet which is assigned to be a merged form of one triplet and a doublet corresponding to C(15)H and C(13)H protons. Another triplet at δ=7.99 ppm is assigned to C(14)H proton. The resonances for the C_6H_5-group appear as a doublet at δ=7.68 ppm (ortho) and as triplets at δ=7.33 and 7.06 ppm corresponding to meta and para phenyl protons. All the assignments made above are in good agreement with previous reports [26,27].

2.3.5. ^{13}C NMR spectra

^{13}C NMR spectra of semicarbazones, HL^1 and HL^2 were recorded in $CDCl_3$. The ^{13}C NMR spectrum provides direct information about the carbon skeleton of compounds. The carbon atoms were assigned on the basis of proton decoupled ^{13}C NMR spectrum. The signals from ^{13}C spectrum are much weaker than that of the corresponding proton NMR spectrum. Assignment of different resonant peaks to respective carbon atoms of HL^1 is presented in Figure 2.10. Considering the two pyridyl rings non-equivalent, resulting from the hydrogen bonding interaction, there are 15 unique carbon atoms in the molecule, which give a total of 15 different peaks in the ^{13}C NMR spectrum. In both the pyridyl rings, the C(1) and C(11) carbon atoms adjacent to the more electronegative nitrogen

atoms N(1) and N(2) are shifted farther downfield when compared to the neighboring carbon atoms.
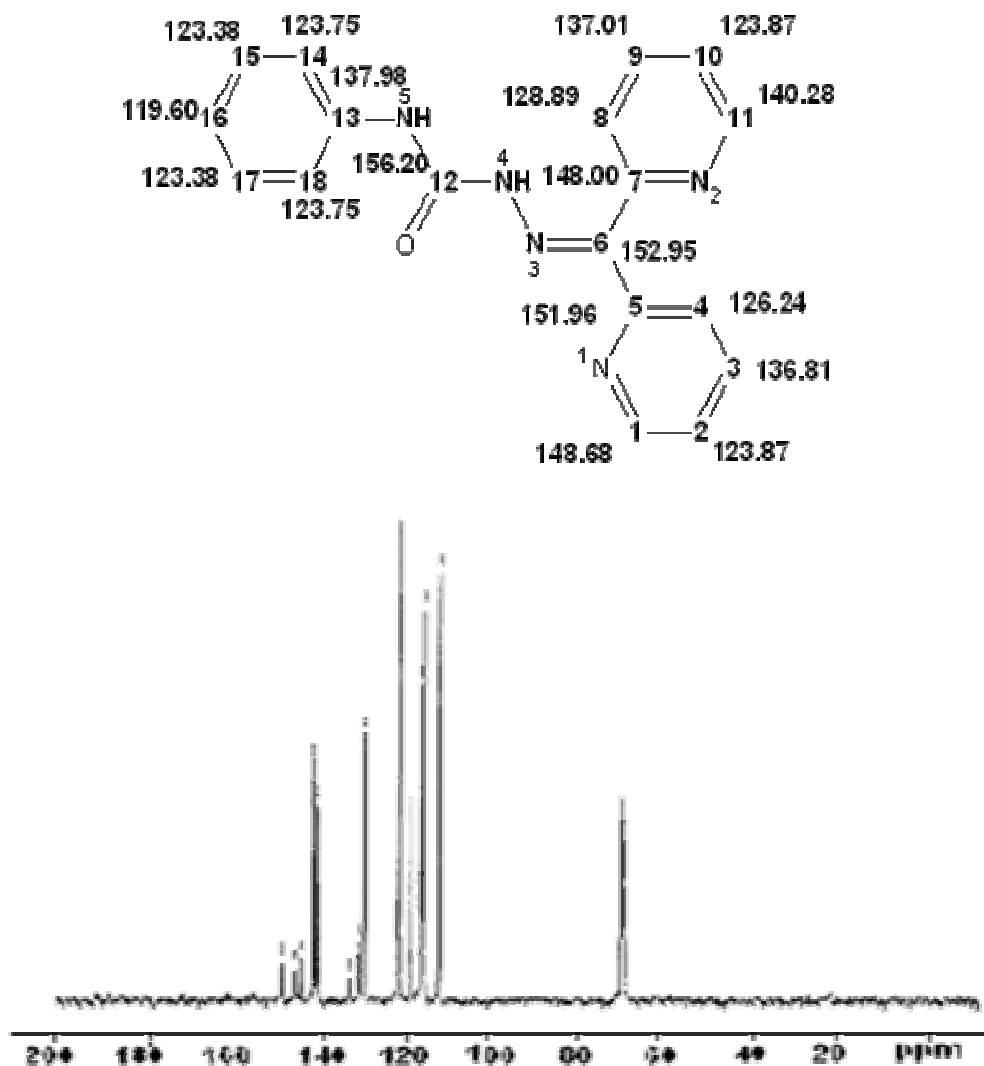

Figure 2.10. ^{13}C NMR spectrum of HL^1.

Also the carbon atoms at para position to the hetero atoms *viz.* C(3) and C(9) resonate at lower field values when compared to the meta positioned carbons C(2), C(4), C(8) and C(10). The ^{13}C peaks are assigned as follows :

C(1), 148.68 ppm ; C(2), 123.87 ppm; C(3), 136.81 ppm; C(4), 126.24 ppm; C(5), 151.96 ppm; C(6), 152.95 ppm; C(7), 148.00 ppm; C(8), 128.89 ppm; C(9), 137.01 ppm; C(10), 123.87 ppm; C(11), 140.28 ppm; C(12), 156.20 ppm; C(13), 137.98 ppm; C(14), 123.75 ppm; C(15), 123.38 ppm; C(16), 119.60 ppm; C(17), 123.38 ppm; C(18), 123.75 ppm. The non- protonated carbon atom at C(6) is shifted farthest downfield in the spectrum (δ= 152.95 ppm), effected by the magnetic interaction of two bulky pyridyl rings and π electron delocalization on the C(6)=N(3) bond. Similarly, the C(12) carbon atom resonance is also observed at a lower field of 156.20 ppm resultant of the conjugative effect of the –N(3)–N(4)–C(O)–N(5)– semicarbazone skeleton.

The proton decoupled ^{13}C spectrum of the semicarbazone, HL^2 contains 15 peaks corresponding to the fifteen magnetically unique carbon atoms. Assignment of different resonant peaks to respective carbon atoms is presented in Figure 2.11. The peaks at 152.86, 147.31 and 141.42 ppm correspond to the C(8), C(9) and C(17) carbon atoms respectively. The carbon atom at para position to the heteroatom viz. C(11) resonate at lower field value when compared to the meta positioned carbon atom C(10). The non-protonated carbon C(7) is showing more downfield shift due to increased electron density resulting from the presence of electronegative oxygen and conjugative effect of the –N(3)–N(2)–C(O)–N(1)– semicarbazone skeleton. The ^{13}C peaks are assigned as follows. C(1), 138.85 ppm; C(2), 122.81 ppm; C(3), 120.32 ppm; C(4), 118.20 ppm; C(5), 120.32 ppm; C(6), 122.81 ppm; C(7), 153.90 ppm; C(8), 152.86 ppm; C(9), 147.31 ppm; C(10), 129.89 ppm; C(11), 136.24 ppm; C(12), 128.75 ppm; C(13), 127.76 ppm; C(14), 126.98 ppm; C(15), 128.45 ppm; C(16), 127.92 ppm; C(17), 141.42 ppm. The downfield shift of C(8) carbon is due to the π electron delocalization on the C(8)=N(3) bond [28].
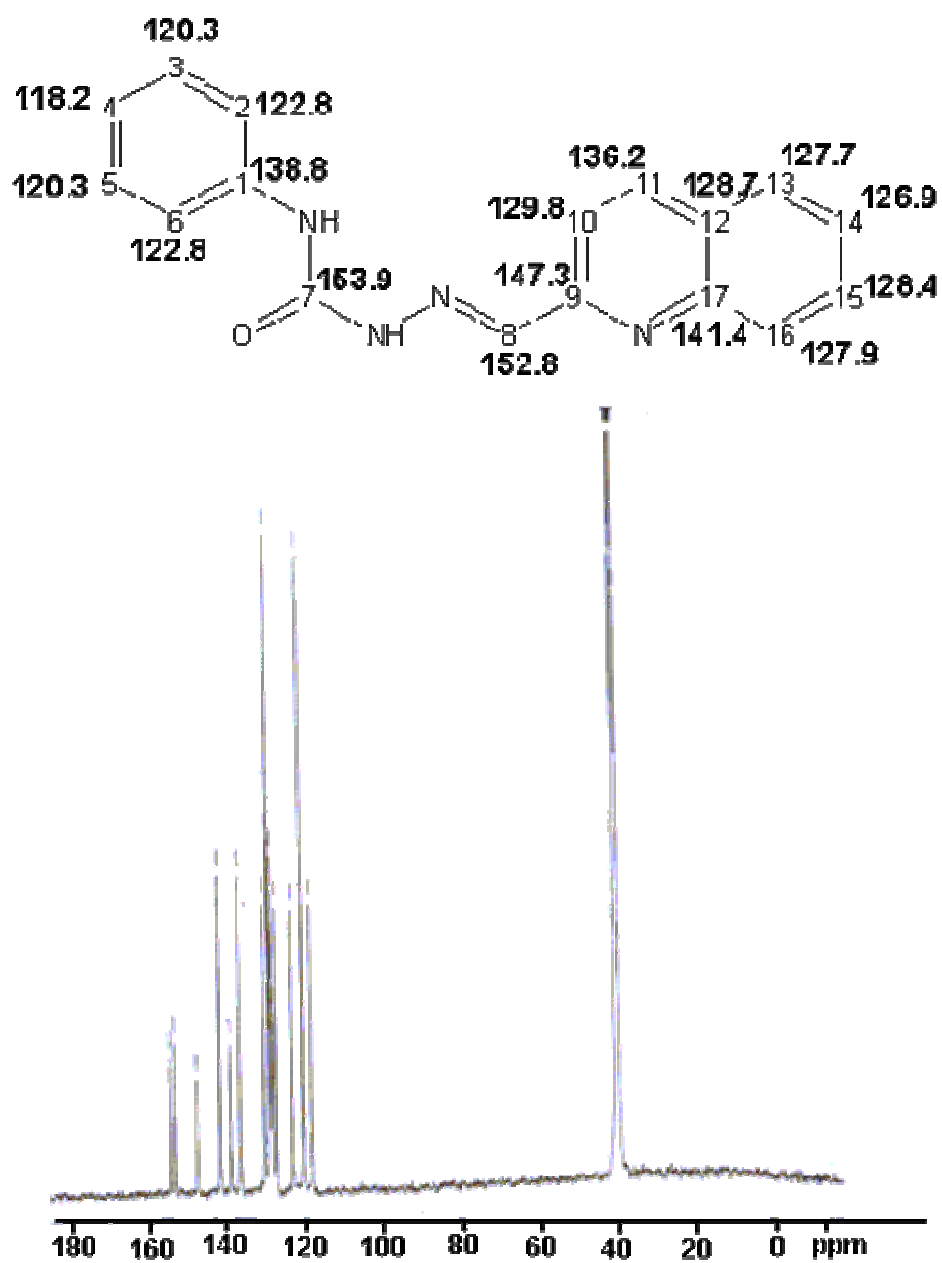
Figure 2.11. ^{13}C NMR spectrum of HL^2.

References

[1]   S.N. Pandeya, J.P. Dimmock, Pharmazie 48 (1993) 659.

[2]   M. Shalini, P.Yogeeswari, D. Sriram, J.P. Stables, Biomedicine and Pharmacotherapy 8 (2007) 1.

[3]   E.J. Eisenbraun, R.P. Wesley, R.S. Budhram, B. DewPrasad, Chem-Ind.(London) 15 (1989) 459.

[4]   H.G. Petering, G.J. VanGiessen, Biochem. Copper Proc.Symp., New York, Harriman 197 (1965).

[5]   D.X. West, P.B. Sonawane, A.S. Kumbhar, R.G.Yerande, Coord.Chem.Rev. 123 (1993) 49.

[6]   G.M. Sheldrick, SHELXL-97 and SHELXS-97 Program for the solution of Crystal Structures, University of Göttingen, Germany, 1997.

[7]   H.D. Flack, G. Bernardinelli, J. Appl. Cryst. 33 (2000) 114.

[8]   K. Brandenburg, Diamond Version 3.1d, Crystal Impact GbR, Bonn, Germany 2006.

[9]   A.L. Spek, J. Appl. Cryst. 36 (2003) 7.

[10]   J. March, Advanced Organic Chemistry, Reactions, Mechanisms and Structure, fourth ed., Wiley, New York, 1992.

[11]   T.A. Reena, E.B. Seena, M.R.P. Kurup, Polyhedron 27 (2008) 1825.

[12]   U.L. Kala, S. Suma, M.R.P Kurup, Suja Krishnan, R.P. John, Polyhedron 26 (2007) 1427.

[13]   E.B. Seena, M.R.P. Kurup, E. Suresh, J. Chem. Cryst. 38 (2008) 93.

[14]   E. Manoj, M.R.P. Kurup, H.-K. Fun, J. Chem. Cryst. 38 (2008) 157.

[15]   T.S. Wang, Appl. Spectrosc. 22 (1968) 167.

[16]   V.M. Kolb, J.W. Stupar, T.E. Janota, W.L. Duax, J. Org. Chem. 54 (1989) 2341.

[17] A.K. El-Sawaf, D.X. West, F.A. El-Saied, R.M. El-Bahnasawy, Trans. Met. Chem. 23 (1998) 649.

[18] D.X. West, A.M. Stark, G.A. Bain, A.E. Liberta, Trans. Met. Chem. 21 (1996) 289.

[19] H. Beraldo, A.M. Barreto, R.P. Vieira, A.P. Rebolledo, N.L. Speziali, C.B. Pinheiro, G. Chapuis, J. Mol. Struct. 645 (2003) 213.

[20] M. Joseph, V. Suni, Chandini R. Nayar, M.R.P. Kurup, H.-K. Fun, J. Mol. Struct. 705 (2004) 63.

[21] R. Mayer, in: M. Jansen (Ed.), Organosulfur Chemistry, Inter-science, New York 1967.

[22] V. Philip, V. Suni, M.R.P. Kurup, M. Nethaji, Polyhedron 24 (2005) 1133.

[23] R.T. Morrison, R.N. Boyd, Organic Chemistry, fourth ed., Allyn and Bacon Inc., London, 1990.

[24] D.H. Williams, I. Fleming, Spectroscopic methods in Organic Chemistry, fourth ed., Mcgraw-Hill, London, 1989.

[25] S.R. Breeze, S. Wang, J.E. Greedan, N.P. Raju, Inorg. Chem. 35 (1996) 6945.

[26] J.K. Swearingen, W. Kaminsky, D.X. West, Trans. Met. Chem. 27 (2002) 724.

[27] V. Suni, M. Nethaji, M.R.P. Kurup, J. Mol. Struct. 749 (2005) 177.

[28] V. Suni, M.R.P. Kurup, M. Nethaji, Spectrochim. Acta 63A (2006) 17.

…..ဆဂ…..

SYNTHESIS, SPECTRAL AND STRUCTURAL STUDIES ON Zn(II) COMPLEXES OF N^4-SUBSTITUTED SEMICARBAZONES

Contents	3.1 **Introduction**
	3.2 **Experimental**
	3.3 **Results and discussion**

3.1. Introduction

Centuries before zinc was discovered in the metallic form, its ores were used for making brass and zinc compounds were used for healing wounds and sore eyes. Ores containing zinc are widespread geologically and geographically and many ore bodies are still awaiting development when sufficient demand occurs. The abundance of zinc in the earth's crust is approximately 132 ppm by weight. Usually zinc ores are found in association with those of lead, copper, gold, silver as well as other metals. Rarely is the ore, as mined, rich enough to be used directly by smelters; it needs to be concentrated. Typically zinc ores contain 3% to more than 10% zinc and zinc concentrates will contain 55% zinc.

Zinc is an essential trace element in the human body, where it is found in high concentration in the red blood cells as an essential part of enzyme carbonic anhydrase, which promotes many reactions relating to carbon dioxide metabolism. It is vital for many biological functions such as disease

resistance, wound healing, digestion, reproduction, physical growth, diabetes control, taste and smell [1]. Every cell in the human body requires zinc to multiply and more than 300 enzymes need zinc for proper functioning. The World Health Organization's "World Health Report 2002" estimated that one-third (33%) of the world's population is at risk of inadequate zinc intakes. The effects of zinc deficiency may be severe, ranging from impaired neuropsychological functions, growth retardation and stunting, impaired reproduction, immune disorders, dermatitis, impaired wound healing, lethargy, loss of appetite and loss of hair [2].

Zinc element has a $d^{10}s^2$ electronic arrangement and they typically form M^{2+} ions. However, many of their compounds are appreciably covalent. In view of the stability of the filled d sublevel, the element shows a few of the characteristics of transition metals despite its position in the d-block of the periodic table. It resembles other transition metals in the formation of stable complexes with O, N and S-donor ligands and with ions like cyanide, halide etc. This means high flexibility in the structure, coordination mode and coordination number of the complexes produced. Among these complexes, some have attracted special attention as model compounds for the active sites of zinc-containing enzymes [3] and their functions strongly depend upon the coordination environment around the zinc ion. Therefore, for understanding or creating functional zinc complexes, it is important to consider the relationship of the coordination characteristics peculiar to zinc ion. Biological activity of thiosemicarbazones and semicarbazones are found to increase on complexation with transition metals [4], higher activity being incorporated with substitution at N^4-position [5]. Tetrahedral as well as octahedral Zn(II) complexes of thiosemicarbazide and thiosemicarbazone, in which the ligands are known to be bidentate, have been reported [6]. On the other hand, ligands, such as ethylacetoacetate

semicarbazone and thiosemicarbazone are found to be tridentate in their zinc complexes [7], in which the third coordinating center is provided by the carbonyl group. This chapter describes the synthesis and characterization of eight zinc(II) complexes of N^4-substituted semicarbazones, HL^1 and HL^2.

3.2. Experimental

3.2.1. Materials

The syntheses of the semicarbazones, HL^1 and HL^2 have been described already in Chapter 2. Zinc(II) bromide, zinc(II) chloride, zinc(II) acetate dihydrate and sodium azide were commercial products of higher grade (Aldrich) and reagents used were of Analar grade and used without further purification.

3.2.2. Synthesis of complexes

[Zn(HL^1)Br$_2$] (1)

A solution of semicarbazone, HL^1 (0.317 g, 1 mmol) in 20 ml of methanol was treated with a methanolic solution of zinc(II) bromide (0.225 g, 1 mmol). The solution was heated under reflux for 4 h. The resulting solution was allowed to stand at room temperature and after slow evaporation yellow crystals separated out, which were collected, washed with ether and dried over P_4O_{10} *in vacuo.*

Yield ~0.35 g.

[Zn(HL^1)Cl$_2$] (2)

A solution of semicarbazone, HL^1 (0.317 g, 1 mmol) in 20 ml of methanol was treated with a methanolic solution of zinc(II) chloride (0.136 g, 1 mmol). The solution was heated under reflux for 4 h. The resulting solution was allowed to stand at room temperature and after slow evaporation yellow crystals separated out, which were collected, washed with ether and dried over P_4O_{10} *in vacuo.*

Yield ~0.28 g.

[ZnL^1(OAc)] (3)

A solution of semicarbazone, HL^1 (0.317 g, 1 mmol) in 20 ml of methanol was treated with a methanolic solution of zinc(II) acetate dihydrate (0.219 g, 1 mmol). The solution was heated under reflux for 3 h. The resulting solution was allowed to stand at room temperature and after slow evaporation yellow crystals separated out, which were collected, washed with ether and dried over P$_4$O$_{10}$ *in vacuo.*

Yield ~0.32 g.

[ZnL^{1}N$_3$] (4)

A solution of the semicarbazone, HL^1 (0.317 g, 1 mmol) in methanol was treated with a methanolic solution of zinc(II) acetate dihydrate (0.219 g, 1 mmol). The solution was heated under reflux and sodium azide (0.130 g, 2 mmol) was added in portions to the solution and further refluxed for 4 h. The resulting solution was allowed to stand at room temperature and upon slow evaporation gave yellow crystals. The crystals separated out were collected, washed with ether and dried over P$_4$O$_{10}$ *in vacuo*.

Yield ~0.25 g.

[ZnL^1$_2$] (5)

A solution of the semicarbazone, HL^1 (0.317 g, 1 mmol) in 20 ml of methanol was treated with a methanolic solution of zinc(II) acetate dihydrate (0.109 g, 0.5 mmol). The solution was heated under reflux for 2 h. The resulting solution was allowed to stand at room temperature and after slow evaporation yellow crystals were separated out, which were collected, washed with ether and dried over P$_4$O$_{10}$ *in vacuo*.

Yield ~0.20 g.

[ZnL$^1_2$]·0.3H$_2$O (6)

A solution of the semicarbazone, HL^1 (0.317 g, 1 mmol) in methanol was treated with a methanolic solution of zinc(II) acetate dihydrate (0.219 g, 1 mmol). The solution was heated under reflux and sodium azide (0.065 g, 1 mmol) was added in portions to the solution and further refluxed for 4 h. The resulting solution was allowed to stand at room temperature and upon slow evaporation gave yellow crystals. The crystals separated out were collected, washed with ether and dried over P$_4$O$_{10}$ *in vacuo.*

Yield ~0.16 g.

[ZnL^2(OAc)]·5H$_2$O (7)

A solution of the semicarbazone, HL^2 (0.290 g, 1 mmol) in DMF is mixed with methanolic solution of zinc(II) acetate dihydrate (0.219 g, 1 mmol) and the mixture was heated under reflux for 3 h and cooled. The complex separated was filtered, washed thoroughly with ether and dried over P$_4$O$_{10}$ *in vacuo.*

Yield ~0.20 g.

[ZnL^{2}N$_3$]·2H$_2$O (8)

A solution of the semicarbazone, HL^2 (0.290 g, 1 mmol) in DMF is mixed with methanolic solution of zinc(II) acetate dihydrate (0.219 g, 1 mmol) and the mixture was heated under reflux for 4 h and sodium azide (0.130 g, 2 mmol) was added in portions to the solution and further refluxed for 3 h. The resulting solution was allowed to stand at room temperature and upon slow evaporation gave yellow crystals. The crystals separated out were collected, washed with ether and dried over P$_4$O$_{10}$ *in vacuo.*

Yield ~0.25 g.

3.2.3. Analytical methods

Carbon, hydrogen and nitrogen analyses were carried out using a Vario EL III CHNS analyzer at the SAIF, Kochi, India. Infrared spectra were

recorded on a JASCO FT-IR-5300 Spectrometer in the range 4000-400 cm^{-1} using KBr pellets. Electronic spectra were recorded on a Cary 5000 version 1.09 UV-VIS-NIR Spectrophotometer using solutions in DMF. The ^{1}H and ^{13}C NMR spectra were not recorded due to insolubility of complexes in CHCl$_3$, CH$_2$Cl$_2$ and CH$_3$CN.

3.2.4. X-ray crystallography

Single crystals of compound, [Zn(HL^1)Br$_2$] (**1**) suitable for X- ray diffraction were obtained by slow evaporation of its solution in 1:1:1 mixture of CH$_3$OH, CHCl$_3$ and CH$_2$Cl$_2$. Single crystals of compound, [ZnL$^1_2$] (**5**) were obtained by slow evaporation of its solution in 1:1 mixture of CH$_3$OH and CH$_3$CN and of compound [ZnL$^1_2$]·0.3H$_2$O (**6**) was obtained by slow evaporation of solution of the compound in 1:1:1:1 mixture of DMF, CHCl$_3$, CH$_3$CN and CH$_3$OH. X-ray diffraction measurements were carried out on a CrysAlis CCD diffractometer with graphite-monochromated Mo Kα (λ = 0.71073 Å) radiation. The program CrysAlis RED was used for data reduction and cell refinement [8]. The structure was solved by direct methods using SHELXS [9] and refined by full-matrix least-squares refinement on F^2 using SHELXL [9]. The N–H hydrogen atoms were located from difference Fourier maps and refined isotropically. The remainder of the H-atoms were included in calculated positions and refined as riding atoms using default SHELXL parameters. Compound [ZnL$^1_2$]·0.3H$_2$O (**6**) is non-centrosymmetric and its Flack *x* parameter is 0.001(12). As this value is near to 0, with small standard uncertainty, the absolute structure given by the structure refinement is likely correct [10].

The structures of the compounds were plotted using the program ORTEP [11]. The crystallographic data along with the structural refinements are given in Table 3.1.

Table 3.1. Crystal data and structure refinement parameters of [Zn(HL₁)Br₂] (1), [ZnL₂] (5) and [ZnL₂]·0.3H₂O (6)

	1	5	6
Empirical formula	$C_{18}H_{15}Br_2N_5OZn$	$C_{16}H_{18}N_{10}O_2Zn$	$C_{16}H_{18}N_{10}O_2Zn \cdot 0.3H_2O$
Formula weight	542.54	698.05	702.85
Temperature	120(2) K	120(2) K	120(2) K
Wavelength	0.71073 Å	0.71073 Å	0.71073 Å
Crystal system	Monoclinic	Monoclinic	Orthorhombic
Space group	$P2_1/n$	$P2_1/n$	$P2_12_12_1$
Unit cell dimensions	a = 7.3466(3) Å	a = 11.0982(2) Å	a = 8.5993(4) Å
	b = 14.5893(4) Å	b = 16.6320(3) Å	b = 17.0904(6) Å
	c = 18.5267(5) Å	c = 17.8826(4) Å	c = 22.3002(11) Å
	α = 90°	α = 90°	α = 90°
	β = 98.315(3)°	β = 98.690(2)°	β = 90°
	γ = 90°	γ = 90°	γ = 90°
Volume	1964.85(11) Å³	3262.97(11) Å³	3277.4(3) Å³
Z	4	4	4
Density (calculated)	1.834 Mg/m³	1.421 Mg/m³	1.424 Mg/m³
Absorption coefficient	5.335 mm⁻¹	0.803 mm⁻¹	0.801 mm⁻¹
F(000)	1064	1440	1450
Crystal size	0.32 x 0.28 x 0.26 mm³	0.26 x 0.21 x 0.19 mm³	0.18 x 0.11 x 0.08 mm³
θ range for data collection	3.01 to 25.00°	2.99 to 25.00°	2.99 to 25.00°
Index ranges	-8≤h≤8, -17≤k≤17, -21≤l≤22	-13≤h≤12, -19≤k≤18, -21≤l≤21	-10≤h≤10, -20≤k≤20, -26≤l≤26
Reflections collected	16909	30049	31407
Independent reflections	3445 [R(int) 0.0341]	5729 [R(int) 0.0358]	5772 [R(int) 0.1000]
Refinement method	Full-matrix least-squares on F²	Full-matrix least-squares on F²	Full-matrix least-squares on F²
Data / restraints / parameters	3445 / 0 / 252	5729 / 0 / 450	5772 / 0 / 454
Goodness-of-fit on F²	1.058	1.073	1.010
Final R indices [I>2σ(I)]	R₁ = 0.0273, wR₂ = 0.0532	R₁ = 0.0306, wR₂ = 0.0638	R₁ = 0.0500, wR₂ = 0.0661
R indices (all data)	R₁ = 0.0507, wR₂ = 0.0632	R₁ = 0.0444, wR₂ = 0.0711	R₁ = 0.0741, wR₂ = 0.0734
Largest diff. peak and hole	0.362 and -0.262 e.Å⁻³	0.272 and -0.290 e.Å⁻³	0.608 and -0.415 e.Å⁻³

$R_1 = \Sigma ||F_o| - |F_c|| / \Sigma |F_o|$ $wR_2 = [\Sigma w(F_o^2 - F_c^2)^2 / \Sigma w(F_o^2)^2]^{1/2}$

3.3. Results and discussion

The analytical data of all the complexes are listed in Table 3.2. Di-2-pyridyl ketone-N^4-phenyl-3-semicarbazone, (HL^1) reacts with zinc(II) halides in the molar ratio 1:1 in **1** and **2**, the complexes of the type Zn(HL^1)X$_2$, where X = Br and Cl. The complexes **3**, **4**, **7** and **8** were consistent with the general composition ZnLY where Y = OAc, N$_3$, OAc and N$_3$ respectively and for complexes **5** and **6**, the composition ZnL$^1_2$ was obtained. For the preparation of complexes **3**, **7** and **5**, Zn(OAc)$_2$·2H$_2$O and semicarbazones were taken in 1:1, 1:1 and 1:2 ratio respectively and in complexes **4**, **8** and **6**, Zn(OAc)$_2$·2H$_2$O, semicarbazones and NaN$_3$ were taken in 1:1:2, 1:1:2 and 1:1:1 ratios respectively. In complex **6**, however, the azide added was not coordinated and [ZnL$^1_2$]·0.3H$_2$O was obtained accidentally, though the yield was much lower. Although the molecular formulae of **5** and **6** are slightly different, the crystallographic parameters are totally different. In the complexes **1** and **2**, the semicarbazone coordinates as neutral keto form whereas in all other complexes semicarbazones coordinate in monoanionic enolate form. All the complexes are found to be diamagnetic as expected for a d^{10} Zn(II) system.

Table 3.2. Analytical data

Compound	Color	Found (Calculated) %		
		C	H	N
[Zn(HL^1)Br$_2$] (**1**)	Yellow	39.92 (39.85)	2.63 (2.79)	12.99 (12.91)
[Zn(HL^1)Cl$_2$] (**2**)	Yellow	47.72 (47.66)	3.41 (3.33)	15.57 (15. 44)
[ZnL^1(OAc)] (**3**)	Yellow	53.73 (54.25)	4.30 (4.33)	15.71 (15.82)
[ZnL^{1}N$_3$] (**4**)	Yellow	50.75 (51.02)	3.27 (3.33)	26.56 (26.44)
[ZnL$^1_2$] (**5**)	Yellow	61.53 (61.94)	3.96 (4.04)	20.01 (20.07)
[ZnL$^1_2$]·0.3H$_2$O (**6**)	Yellow	60.87 (61.41)	4.01 (4.10)	19.25 (19.89)
[ZnL^2(OAc)]·5H$_2$O (**7**)	Yellow	45.83 (45.29)	5.38 (5.20)	11.33 (11.12)
[ZnL^{2}N$_3$]·2H$_2$O (**8**)	Yellow	47.07 (47.18)	3.36 (3.96)	22.57 (22.66)

3.3.1. Crystal structures of [Zn(HL^1)Br$_2$] (1), [ZnL$^1_2$] (5) and [ZnL$^1_2$]·0.3H$_2$O (6)

The molecular structure of the complex **1**, along with the atom numbering scheme is presented in Figure 3.1. The compound crystallizes in the monoclinic space group $P2_1$/n. In this compound, Zn atom is coordinated by azomethine nitrogen (N2), pyridyl nitrogen (N1), ketoxy oxygen (O1) and two bromide ions (Br1 and Br2). The bond distances to Zn are in the order Zn–N$_{(azo)}$< Zn–N$_{(py)}$< Zn–O$_{(ketoxy)}$< Zn–Br1< Zn–Br2. The bond lengths, Zn–N$_{(py)}$, 2.154(3) Å and Zn–N$_{(azo)}$, 2.130(3) Å are very similar compared to other Zn complexes of thiosemicarbazones [12-14]. The Zn–Br bond distances are 2.3561(5) and 2.4026(6) Å, but there is a difference of 0.0465 Å between the Zn–Br bonds of [Zn(HL^1)Br$_2$]. The basal plane could involve either Br1 or Br2 with semicarbazone moiety, but because Zn–Br1 is marginally shorter and it can be designated as the apical position. The Zn atom is displaced with a distance of 0.8335 Å above the basal plane and elongated towards Br1. The selected bond lengths and bond angles are given in Table 3.3.
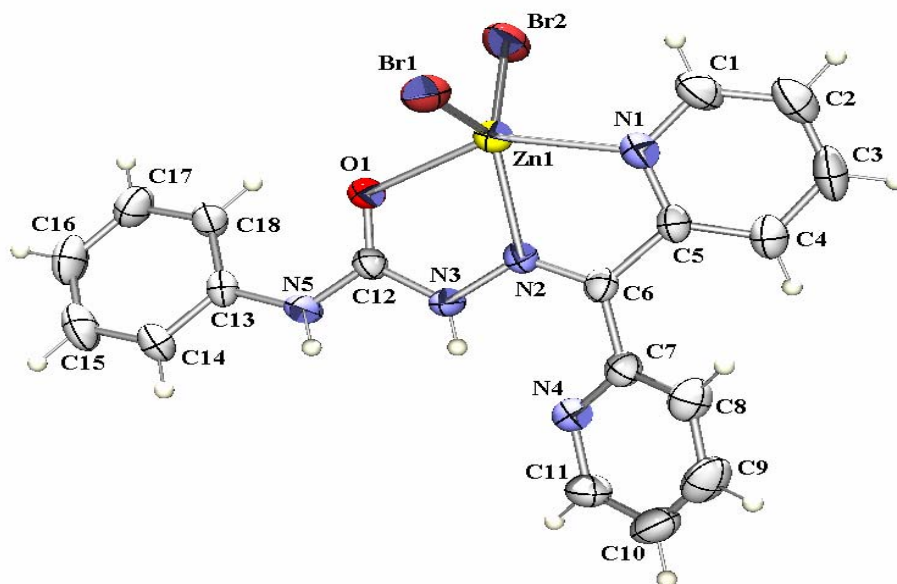
Figure 3.1. Molecular structure of [Zn(HL^1)Br$_2$] (**1**).

According to Addison *et al.* [15], for five coordinated complexes, the angular structural parameter (τ) is used to propose an index of trigonality. The value of τ is defined by an equation represented by $\tau = (\beta - \alpha)/60$, where β is the greatest basal angle and α is the second greatest angle; τ is 0 for square pyramidal forms and 1 for trigonal bipyramidal forms [16]. However, in the case of the five coordinate systems, the structures vary from near regular trigonal bipyramidal (RTB) to near square based pyramidal (SBP). The value of τ for the compound **1** of 0.27 indicates that the coordination geometry around Zn(II) is best described as distorted square based pyramidal geometry [17].

The deviations from the least-square plane through the O1, N1, N2 and Br2 atoms comprising the square plane are 0.3697, 0.5336, -0.6794 and -0.0054 Å, respectively, and the Zn1 atom is deviated by 0.8335 Å in the direction of the Br1 atom. Ring puckering analysis and least square plane calculations show that the rings Cg(1) comprising of atoms Zn1, O1, C12, N3 and N2 and Cg(2) comprising of atoms Zn1, N1, C5, C6 and N2 adopt a twisted conformation Cg(1) on N2–Zn1 and Cg(2) on C5–C6 [18]. In the crystal packing four molecules are present and two of them are complementary to each other (Figure 3.2). In the unit cell π–π, C–H$\cdots\pi$ and hydrogen bonding interactions were observed. The π–π interaction is perceived at 4.0873 Å for Cg(1)–Cg(1)[a] [Cg(1) = Zn1–O1–C12–N3–N2; a = 1–*x*, 1–*y*, 1–*z*]. Only one C–H$\cdots\pi$ interaction is shown in the unit cell and that is between C(8)–H(8)$\cdots$Cg(5)[b] [Cg(5) = C(13)–C(14)–(15)–C(16)–C(17)–C(18); $d_{H\cdots Cg}$ = 2.95 Å; b = 1–*x*, 1–*y*, 1–*z*]. One intra- and one intermolecular hydrogen bonding interactions were observed, *i.e.*, N3(H) and N4 of the same molecule and N5(H) of one with Br2 of the other molecule [N(3)–H(3N)$\cdots$N(4), D–H = 0.80(3) Å, H$\cdots$A = 2.04(3)Å, D$\cdots$A = 2.669(4) Å, D–H$\cdots$A = 135(3)°; N(5)–H(5N) $\cdots$Br(2)[c], D–H=0.70(3)Å, H$\cdots$A = 2.68(3) Å, D$\cdots$A = 3.374(3) Å, D–H$\cdots$A = 170(3)°, c = 1–*x*, 1–*y*, 1–*z*].
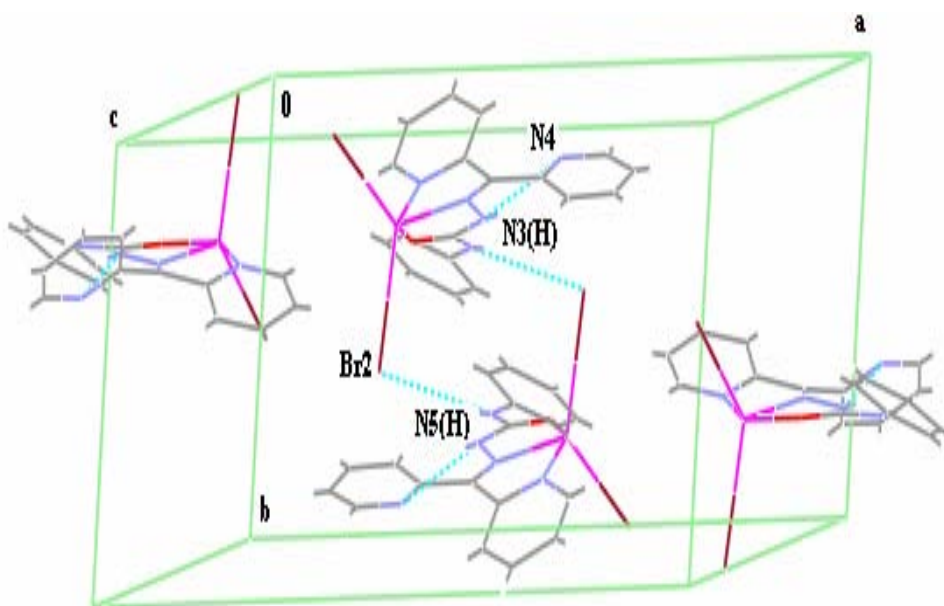
Figure 3.2. Partial unit cell packing diagram for the compound 1 with intra- and intermolecular hydrogen bonding interactions shown as dotted lines.

Figures 3.3 and 3.4 show the molecular structures of compounds **5** and **6** along with the atom numbering schemes. The compound **5** crystallizes in the monoclinic space group $P2_1/n$, while compound **6** in the orthorhombic space group $P2_12_12_1$. In both the compounds, Zn atom is six coordinate in which both ligands are coordinated in their anion forms *via* the pyridine nitrogen, azomethine nitrogen and enolate oxygen atoms. The ligands with their donor atoms are arranged around the zinc ion in a meridional fashion and both compounds are polymorphic. In compound **5**, atoms O1, O2, N1 and N6 lie in the equatorial plane and N2 and N7 occupy the axial positions, while in compound **6**, atoms O1, O2, N1 and N6 lie in the equatorial plane, N2 and N7 occupy the axial positions of the distorted octahedron. In both compounds **5** and **6**, the atoms Zn1, O1, O2, N1, N6 do not deviate significantly from the least square plane [0.0034 Å for **5** and 0.0015 Å for **6**]. Each semicarbazone fragments {(O1 and N1, O2 and

N6 for **5**); (O1 and N1, O2 and N6 for **6**)} are coordinated to the Zn centre with an angle of 150.95(6), 151.03(6)° and 151.17(11), 151.42(11)° respectively, for **5** and **6**, having large distortion from ideal octahedron (180°). The planes containing Zn1, O1, N1, N2, N7 (plane 1) and Zn1, O2, N2, N6, N7 (plane 2) are deviated from the central metal atom (Zn1) by 0.0837 and 0.0248 Å, respectively, in compound **5**, similarly in compound **6**, the planes containing Zn1, O2, N7, N6, N2 (plane 3) and Zn1, O1, N2, N1, N7 (plane 4) are deviated from the central metal atom (Zn1) by 0.0314 and 0.0610 Å, respectively. The dihedral angle formed by the planes 1 and 2 is 85.81 (0.04)° for compound **5** and by the planes 3 and 4 in compound **6** is 85.69 (0.08)°, consistent with a nearly 90° octahedral angle. The selected bond lengths and bond angles are given in Table 3.3.
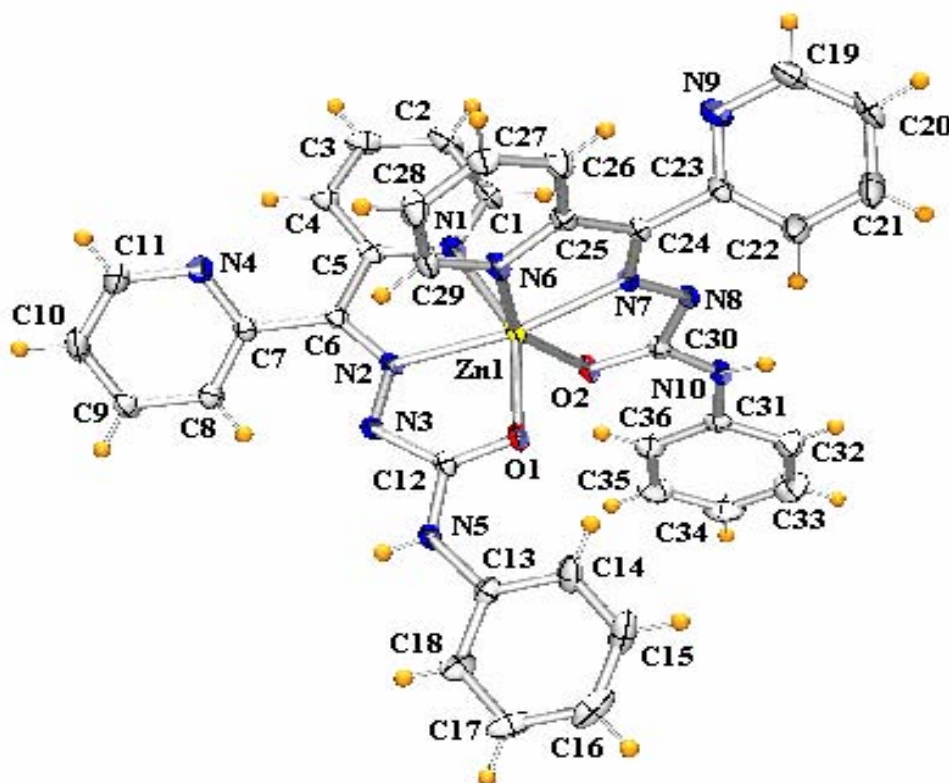
Figure 3.3. Molecular structure of [ZnL$^1_2$] (**5**).
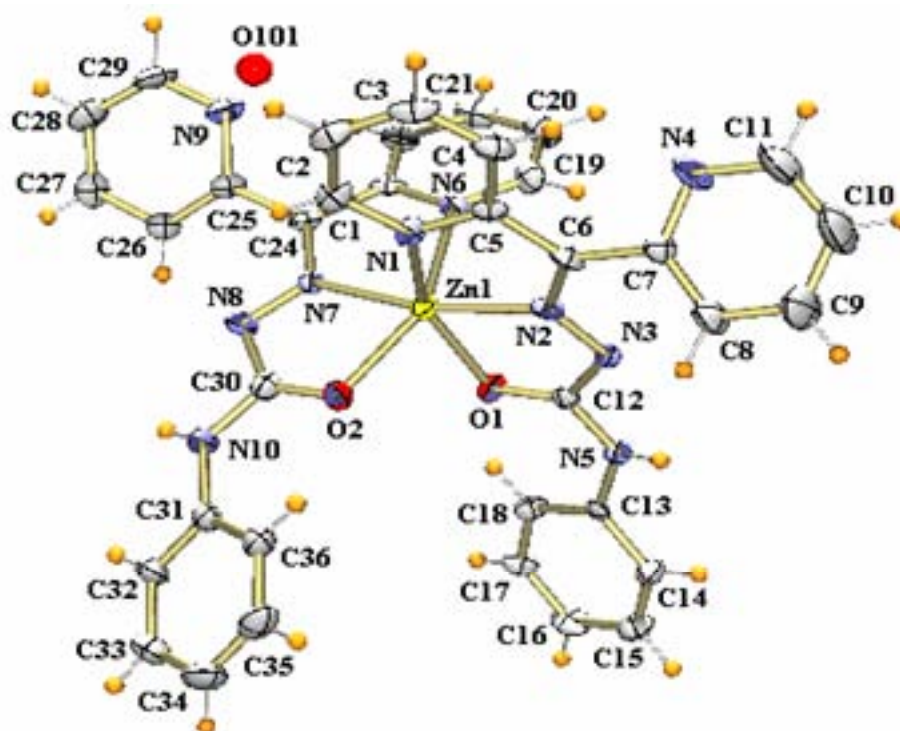
Figure 3.4. Molecular structure of [ZnL$^1_2$]·0.3H$_2$O (**6**).

In compound **5**, when viewed along *a* axis, the molecules are arranged in an opposite manner and are interconnected through N5(H) and N3 of the same molecule with N8 and N10(H) of the nearby molecule, respectively (Figure 3.5) [D–H···A, N(5)–H(5)···N(8)[d]; D–H = 0.84(3) Å; H···A = 2.13(3) Å; D···A = 2.961(2) Å; D–H···A = 170.(2)°; Symmetry code, d = ½-x, ½+y, $^3/_2$-z; D–H···A, N(10)–H(10)···N(3)[e]; D–H = 0.83(2)Å; H···A = 2.21(2) Å; D···A = 3.023(2) Å; D–H···A = 170.(2)°; Symmetry code, e = ½-x, -$^1/_2$+y, $^3/_2$-z]. Intramolecular hydrogen bonding interactions were also observed *i.e.*, C4(H) with N4 and C8(H) with N3 and C14(H) with O1 [D–H···A, C(4)–H(4)···N(4); D–H = 0.93 Å; H···A = 2.42 Å; D···A = 2.984(3) Å; D–H···A = 119°; D–H···A, C(8)–H(8)···N(3); D–H = 0.93 Å; H···A = 2.56 Å; D···A = 2.940(3) Å; D–H···A = 105°; D–H···A, C(14)–H(14)···O(1); D–H = 0.93 Å; H···A = 2.32 Å; D···A = 2.901(3) Å; D–H···A = 120°].

Table 3.3. Selected bond lengths (Å) and bond angles (º) for [Zn(HL^1)Br$_2$] (**1**), [ZnL$^1_2$] (**5**) and [ZnL$^1_2$]·0.3H$_2$O (**6**)

1		**5**		**6**	
Bond lengths					
Zn1–N2	2.130(3)	Zn1–N7	2.0716(17)	Zn1–N2	2.073(3)
Zn1–N1	2.154(3)	Zn1–N2	2.0851(17)	Zn1–N7	2.077(3)
Zn1–O1	2.243(2)	Zn1–O1	2.0950(14)	Zn1–O1	2.097(3)
Zn1–Br1	2.3561(5)	Zn1–O2	2.1234(13)	Zn1–O2	2.099(3)
Zn1–Br2	2.4026(6)	Zn1–N1	2.1499(17)	Zn1–N1	2.155(3)
O1–C12	1.233(3)	Zn1–N6	2.2047(16)	Zn1–N6	2.221(3)
N1–C1	1.328(4)	O1–C12	1.257(2)	O1–C12	1.252(4)
N1–C5	1.345(4)	O2–C30	1.257(2)	O2–C30	1.256(4)
N2–C6	1.287(4)	N5–C12	1.363(3)	N1–C1	1.339(4)
N2–N3	1.355(4)	N5–C13	1.403(3)	N1–C5	1.352(5)
N3–C12	1.369(4)	N3–N2	1.352(2)	N2–C6	1.296(5)
				N2–N3	1.347(4)
Bond angles					
N2–Zn1–N1	73.88(10)	N7–Zn1–N2	165.27(6)	N2–Zn1–N7	167.20(14)
N2–Zn1–O1	72.60(9)	N7–Zn1–O1	109.11(6)	N2–Zn1–O1	76.08(11)
N1–Zn1–O1	146.06(9)	N2–Zn1–O1	76.14(6)	N7–Zn1–O1	109.42(11)
N2–Zn1–Br1	129.81(8)	N7–Zn1–O2	76.17(6)	N2–Zn1–O2	115.77(12)
N1–Zn1–Br1	99.40(7)	N2–Zn1–O2	118.01(6)	N7–Zn1–O2	76.30(12)
O1–Zn1–Br1	97.86(6)	O1–Zn1–O2	91.14(5)	O1–Zn1–O2	90.11(10)
N2–Zn1–Br2	114.29(8)	N7–Zn1–N1	99.93(6)	N2–Zn1–N1	75.84(12)
N1–Zn1–Br2	101.82(8)	N2–Zn1–N1	75.49(6)	N7–Zn1–N1	99.40(12)
O1–Zn1–Br2	96.60(6)	O1–Zn1–N1	150.95(6)	O1–Zn1–N1	151.17(11)
Br1–Zn1–Br2	115.75(2)	O2–Zn1–N1	96.65(6)	O2–Zn1–N1	96.25(11)
C12–O1–Zn1	114.11(19)	N7–Zn1–N6	74.92(6)	N2–Zn1–N6	92.80(13)
		N2–Zn1–N6	90.96(6)	N7–Zn1–N6	75.15(13)
		O1–Zn1–N6	96.57(6)	O1–Zn1–N6	98.13(11)
		O2–Zn1–N6	151.03(6)	O2–Zn1–N6	151.42(11)
		N1–Zn1–N6	90.05(6)	N1–Zn1–N6	89.61(11)
		C12–O1–Zn1	111.16(13)	C12–O1–Zn1	110.7(3)

In compound **6**, two intermolecular hydrogen bonding interactions are observed *i.e.*, N5(H) and N3 of the same molecule with N8 and N10(H) of the next molecule which are arranged in an opposite manner (Figure 3.6) [D–H···A, N(5)–H(5)···N(8)^f; D–H = 0.84(3) Å; H···A = 2.15(3) Å; D···A = 2.992(5) Å; D–H···A = 179(5)° ; Symmetry code, f = 1-x, ½+y, ½-z; D–H···A, N(10)–H(10)···N(3)^g; D–H = 0.84(3) Å; H···A = 2.18(3) Å; D···A = 3.018(5) Å; D–H···A = 176(3)°; Symmetry code, g = 1-x, -$^1/_2$+y, ½-z]. Intramolecular hydrogen bonding interactions were also observed *i.e.*, C4(H) with N4 and C14(H) with O1 and C22(H) with N9 [D–H···A, C(4)–H(4)···N(4); D–H = 0.95 Å; H···A = 2.45 Å; D···A = 3.041(6) Å; D–H···A = 120°; D–H···A, C(14)–H(14)···O(1); D–H = 0.95 Å; H···A = 2.36 Å; D···A = 2.921(5) Å; D–H···A = 118°; D–H···A, C(22)–H(22)···N(9); D–H = 0.95 Å; H···A = 2.61 Å; D···A = 3.026(5) Å; D–H···A = 107°] (Table 3.4).
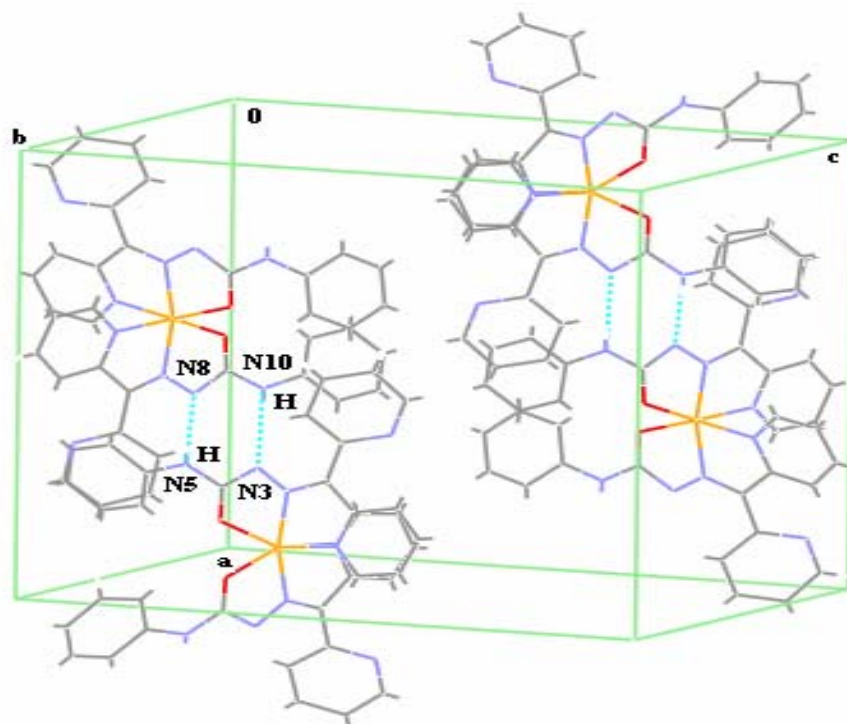
Figure 3.5. Partial unit cell packing diagram for the compound **5** with intermolecular hydrogen bonding interactions shown as dotted lines.
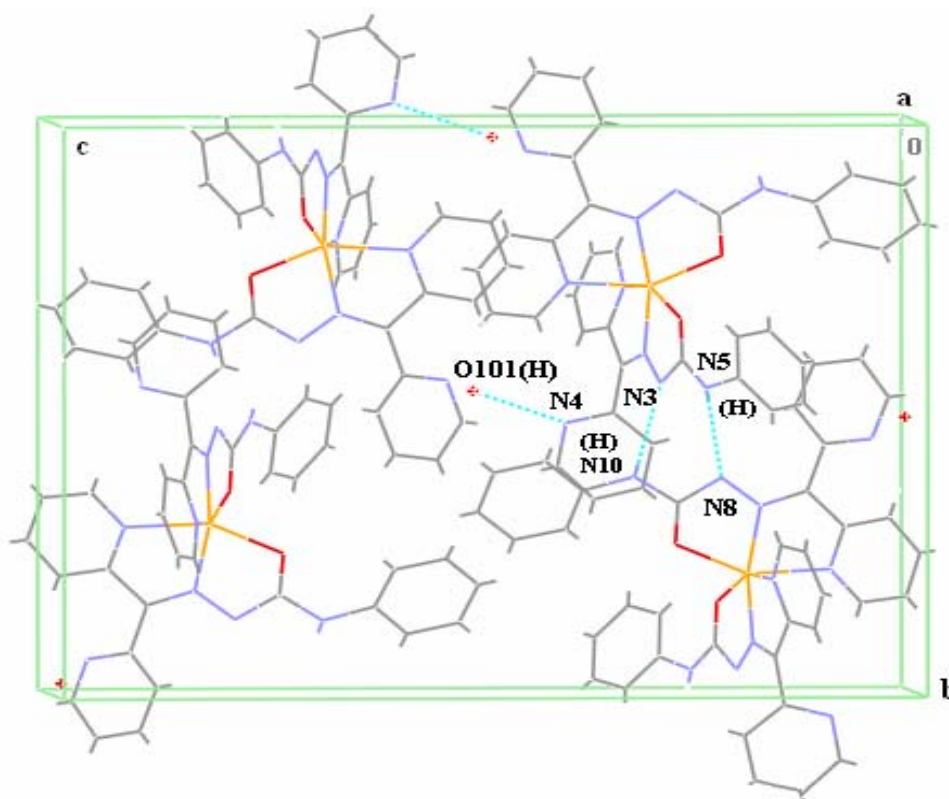
Figure 3.6. Intermolecular hydrogen bonding interactions of compound **6**.

3.3.2. Infrared spectra

The infrared spectra of the free semicarbazones when compared with those of the complexes confirm the coordination of the semicarbazone to the metal. The significant bands observed in the IR spectra of semicarbazones and their complexes with the tentative assignments are presented in Table 3.5. The ν_a(NH) vibrations of the imino group are observed at 3369 cm^{-1} in the IR spectrum of HL^1. The lack of an N–H stretching vibrations in the spectra of the complexes **3**-**6** endorses the ligand coordination to zinc(II) ion in the deprotonated enolate form.

Table 3.4. Interaction parameters of the compounds $[Zn(HL^1)Br_2]$ (**1**), $[Zn(L^1)_2]$ (**5**) and $[Zn(L^1)_2]\cdot 0.3H_2O$ (**6**)

π···π interactions

Cg(I)···Cg(J)	Cg–Cg (Å)	α °	β °
Cg(1)···Cg(1)[a]	4.0874	0.02	31.75

Eqivalent position codes : a=1-x,1-y,1-z

Cg(1)= Zn(1), O(1), C(12), N(3), N(2)

C–H···π interactions

X–H···Cg(J)	H···Cg (Å)	X–H···Cg (°)	X···Cg (Å)
C(8)–H(8)···Cg(5)[b]	2.95	118	3.447(4)

Equivalent position codes : b = 1-x,1-y,1-z

Cg(1)= C(13), C(14), C(15), C(16), C(17), C(18)

H bonding

D–H···A	D–H (Å)	H···A (Å)	D···A (Å)	D–H···A (°)
$[Zn(HL)Br_2]$ (**1**)				
N(3)–H(3N)···N(4)	0.80(3)	2.04(3)	2.669(4)	135(3)
N(5)–H(5N)···Br(2)[c]	0.70(3)	2.68(3)	3.374(3)	170(3)
$[Zn(L)_2]$ (**5**)				
N(5)–H(5N)···N(8)[d]	0.84(3)	2.13(3)	2.961(2)	170(2)
N(10)–H(10N)···N(3)[e]	0.83(2)	2.21(2)	3.023(2)	170(2)
C(4)–H(4)···N(4)	0.93	2.42	2.984(3)	119
C(8)–H(8)···N(3)	0.93	2.56	2.940(3)	105
C(14)–H(14)···O(1)	0.93	2.32	2.901(3)	120
$[Zn(L)_2]\cdot 0.3H_2O$ (**6**)				
N(5)–H(5N)···N(8)[f]	0.84(3)	2.15(3)	2.992(5)	179(5)
N(10)–H(10N)···N(3)[g]	0.84(3)	2.18(3)	3.018(5)	176(3)
C(4)–H(4)···N(4)	0.95	2.45	3.041(6)	120
C(14)–H(14)···O(1)	0.95	2.36	2.921(5)	118
C(22)–H(22)···N(9)	0.95	2.61	3.026(5)	107

Equivalent position codes :c = 1-x,1-y,1-z

d = $^1/_2$-x, $^1/_2$+y, $^3/_2$-z ; e = $^1/_2$-x, -$^1/_2$+y, $^3/_2$-z; f = 1-x, $^1/_2$+y, $^1/_2$-z; g = 1-x, -$^1/_2$+y, $^1/_2$-z

D=Donor, A=acceptor, Cg=Centroid, α=dihedral angles between planes I & J, β= angle between Cg-Cg and Cg(J) perp.

However in the complexes **1** and **2**, the presence of bands at 3239 and 3369 cm^{-1}, corresponding to v(NH) vibrations, indicates that the semicarbazone is coordinated in the neutral form. A strong band at 1591 cm^{-1} in the IR spectrum of HL^1 corresponds to v(C=N) band which suffers shift to 1552-1570 cm^{-1} for the compounds **1-6** upon complexation. In the compounds **3-6**, the appearance of new bands at 1592-1598 cm^{-1} assigned to newly formed C=N bond as a result of enolization. But this band is absent in the complexes **1** and **2** which again confirms the coordination of the semicarbazone in the neutral form in these complexes. Coordination of azomethine nitrogen atom is also consistent with the presence of bands in the region 502-520 cm^{-1}, assignable to v(Zn–N$_{azo}$) for these complexes [19-21]. A band at 1718 cm^{-1} in the semicarbazone has significant contribution from C=O stretching vibration and it is shifted to 1667 cm^{-1} in complexes **1** and 1661 cm^{-1} in **2** confirming keto form of HL^1 in these complexes. In complexes **1-6**, the bands at 404-420 cm^{-1} are assignable to v(Zn–O), consistent with keto/enol oxygen coordination. The spectra of the complexes exhibit a systematic shift in the position of v(N–N) bands in the region 1129-1229 cm^{-1}. A medium band around 601 cm^{-1} indicates out-of-plane pyridyl ring vibration in uncomplexed semicarbazone, shifts to higher frequencies on complexation which confirms the coordination of ligand to metal *via* pyridine nitrogen [22-25]. Compound [ZnL^{1}N$_3$] (**4**) exhibits strong bands at 2076 and 1302 cm^{-1} corresponding to the asymmetric and symmetric stretching of the coordinating azido group. For the complex [ZnL^1(OAc)] (**3**), the asymmetric and symmetric stretching vibrations of the acetate group appear at 1562 and 1433 cm^{-1}. The presence of a band at 3440 cm^{-1} for [ZnL$^1_2$]·0.3H$_2$O (**6**) indicates the presence of the H$_2$O molecule.

In the IR spectrum of the semicarbazone, HL^2 the band at 1702 cm^{-1} is assigned to v(C=O), which is absent in the complexes [ZnL^2(OAc)]·5H$_2$O (**7**) and [ZnL^{2}N$_3$]·2H$_2$O (**8**). This indicates that in these complexes the semicarbazone, HL^2 is coordinated through enolate oxygen atom. This is further corroborated with the absence of v(N–H) bands in the complexes **7** and **8**, which appeared at 3380 cm^{-1} for the semicarbazone, HL^2. The coordination through enolate oxygen atom is again confirmed by the appearance of bands which are assignable to v(Zn–O), at 405 and 408 cm^{-1} respectively for the complexes **7** and **8**. The band at 1592 cm^{-1} due to v(C=N) of the semicarbazone moiety shifts to 1518 cm^{-1} upon complexation. This confirms the coordination *via* azomethine nitrogen. Coordination of azomethine nitrogen is also consistent with the presence of bands at 510 and 504 cm^{-1}, assignable to v(Zn–N$_{azo}$) for the complexes **7** and **8** respectively. In the spectra of the complexes **7** and **8**, the bands corresponding to the newly formed C=N bond due to the enolization of the semicarbazone are observed at 1595 and 1597 cm^{-1} respectively. In these complexes the v(N–N) frequency shifts from 1150 cm^{-1} to 1132 and 1166 cm^{-1} respectively and these bands confirm the enolization and the subsequent deprotonation of the semicarbazone during complexation. For the complex [ZnL^2(OAc)]·5H$_2$O (**7**), the asymmetric and symmetric stretching vibrations of the acetate group appear at 1566 and 1434 cm^{-1}. Compound [ZnL^{2}N$_3$]·2H$_2$O (**8**) exhibits strong bands at 2075 and 1300 cm^{-1} corresponding to the asymmetric and symmetric stretching of the coordinating azido group. IR spectra of complexes are presented in Figures 3.7-3.12.

Table 3.5. IR spectral assignments for semicarbazones and their zinc(II) complexes

Compound	ν(NH)	ν(C=N)	ν(CO)	ν(C=N)[a]	ν(N–N)	ν(Zn–O)	ν(Zn–N$_{azo}$)
HL^1	3369	1591	1718	-	1129	-	-
[Zn(HL^1)Br$_2$](1)	3239	1582	1661	-	1147	407	510
[Zn(HL^1)Cl$_2$](2)	3369	1556	1667	-	1153	404	505
[ZnL^1(OAc)](3)	-	1561	-	1592	1156	414	516
[ZnL^{1}N$_3$](4)	-	1570	-	1595	1148	404	502
[ZnL$^1_2$](5)	-	1562	-	1597	1223	420	518
[ZnL$^1_2$]·0.3H$_2$O (6)	-	1562	-	1598	1229	416	520
HL^2	3380	1592	1702	-	1150	-	-
[ZnL^2(OAc)](7)	-	1518	-	1595	1132	405	510
[ZnL^{2}N$_3$](8)	-	1518	-	1597	1166	408	504

[a] Newly formed C=N
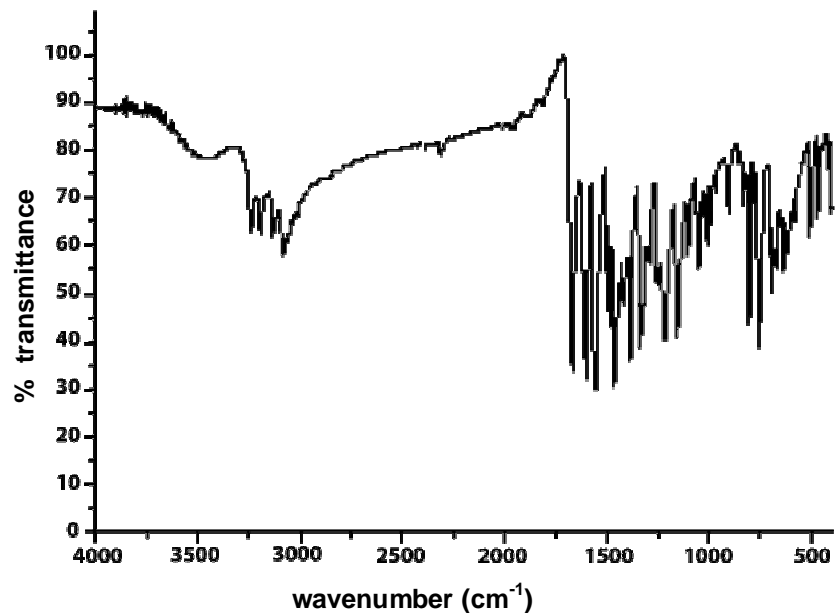
Figure 3.7. IR spectrum of the compound [Zn(HL^1)Br$_2$] (**1**).
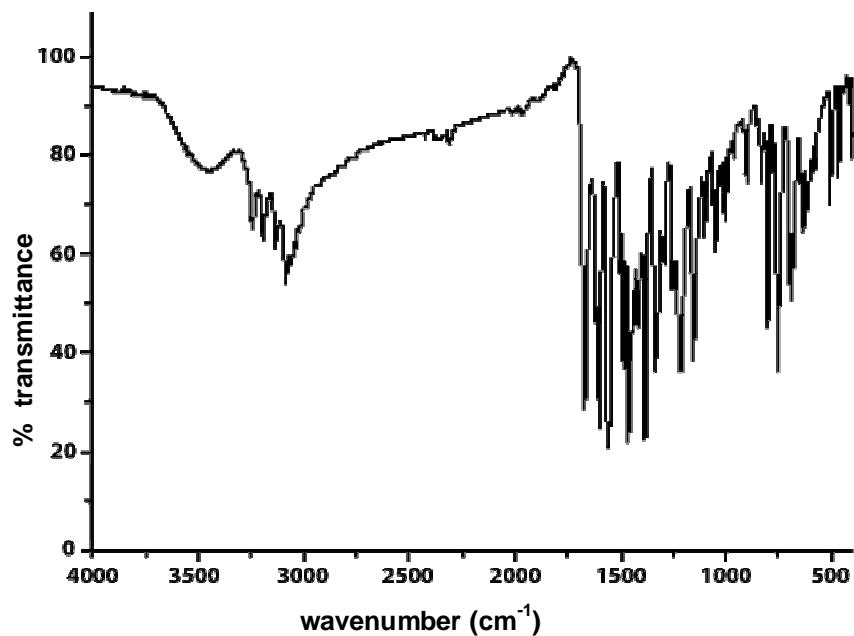
Figure 3.8. IR spectrum of the compound [Zn(HL^1)Cl$_2$] (**2**).
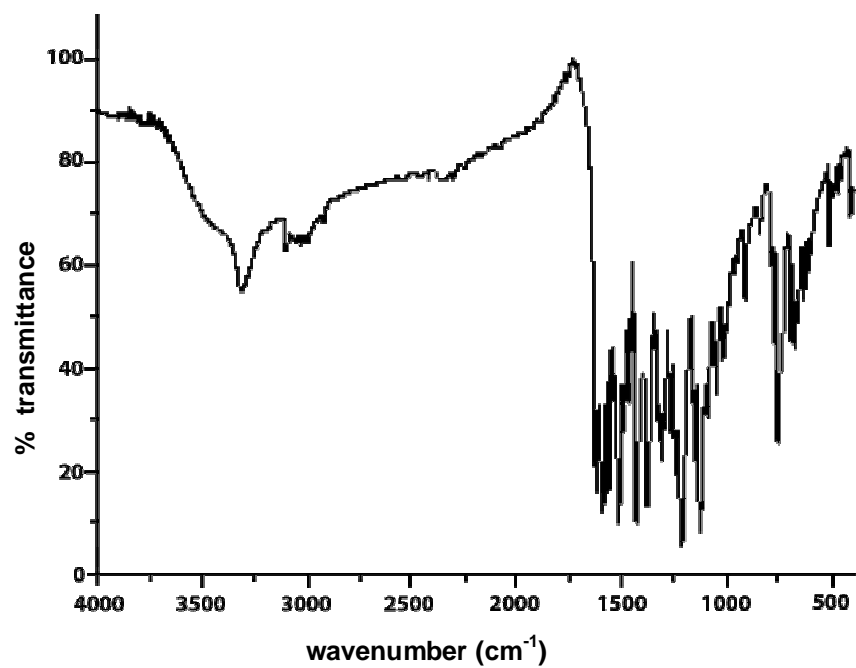
Figure 3.9. IR spectrum of the compound [ZnL^1(OAc)] (**3**).
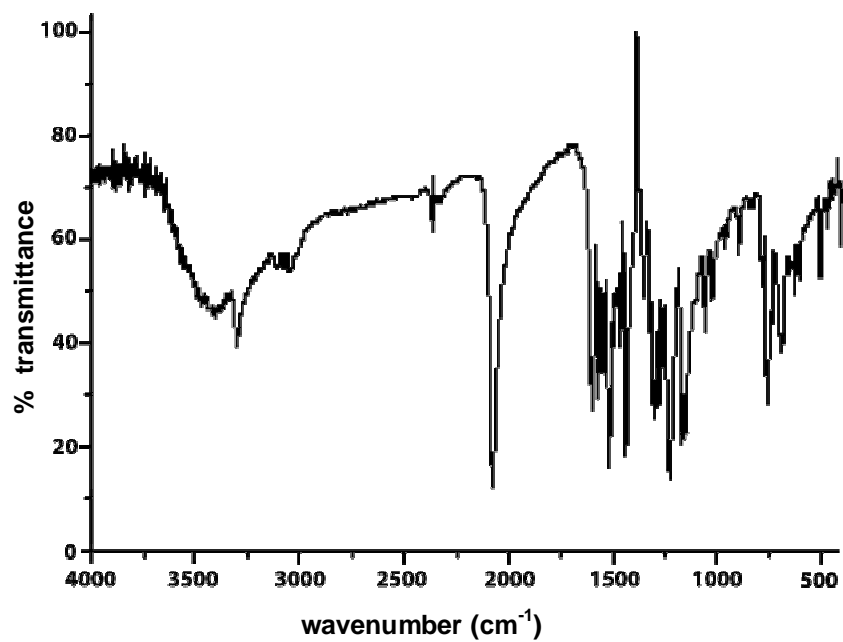
Figure 3.10. IR spectrum of the compound [ZnL^{1}N$_3$] (**4**).
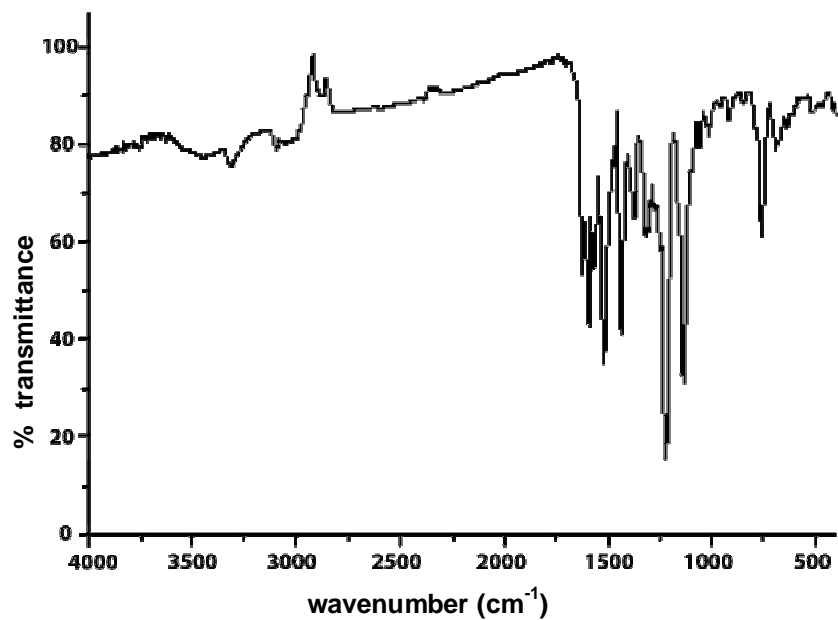
Figure 3.11. IR spectrum of the compound [ZnL^2(OAc)] (**7**).
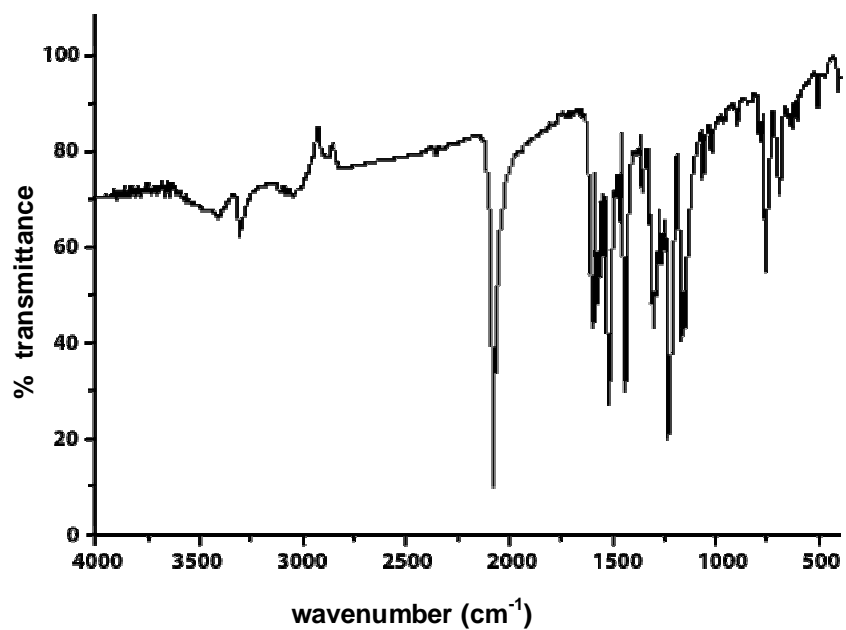
Figure 3.12. IR spectrum of the compound [ZnL^{2}N$_3$] (**8**).

3.3.3. Electronic spectra

The electronic spectral data of zinc(II) complexes are given in Table 3.6 and selected spectra are given in Figures 3.13-3.18. The semicarbazone HL^1, has an absorption at 36300 cm^{-1} due to π-π* transitions of the pyridyl ring and imine function of the semicarbazone moiety. Another band at 31160 cm^{-1} for HL^1 corresponding to n-π* transition of the amide function. These intra-ligand transitions are shifted in the range 31490-31940 cm^{-1} for the complexes **1**-**6** and this shift on complexation indicates coordination *via* the pyridyl nitrogen with a reduction in intensity [26]. The shift of the intra-ligand transitions is also a result of C=O bond being weakened and conjugation system being enhanced after the formation of the complex. In the electronic spectra of complexes **1**-**6**, the metal-ligand CT bands are found in the range 24090-24220 cm^{-1}.

The semicarbazone HL^2 has absorption bands at 36940 and 32200-28770 cm^{-1} attributable to the π-π* and n-π* transitions respectively of the azomethine group. The energy of these bands is shifted on complexation. The shift shows the donation of the lone pair of electrons to the metal by the coordination of azomethine nitrogen. New bands at 25290 and 25130 cm^{-1} are observed in the spectra of the complexes **7** and **8** respectively. These new bands are assigned to Zn(II)→O charge-transfer band. The appearance of Zn(II)→O charge-transfer band in the electronic spectra of Zn(II) complexes is a strong evidence for the coordination of the semicarbazone through keto oxygen atom. No appreciable absorption is observed below 20000 cm^{-1} in DMF solution which is in accordance with the d^{10} electronic configuration of Zn(II) ion.

Table 3.6. Electronic spectral assignments for the semicarbazones and their zinc(II) complexes

Compound	Absorbance, λ_{max} (cm^{-1})
HL^1	36300, 31160
[Zn(HL^1)Br$_2$] (**1**)	31940, 24220
[Zn(HL^1)Cl$_2$] (**2**)	31490, 24190
[ZnL^1(OAc)] (**3**)	31650, 24170
[ZnL^{1}N$_3$] (**4**)	31860, 24090
[ZnL$^1_2$] (**5**)	31880, 24120
[ZnL$^1_2$] ·0.3H$_2$O (**6**)	31880, 24130
HL^2	36940, 32200, 31300, 29900, 28770
[ZnL^2(OAc)] (**7**)	33080, 25290
[ZnL^{2}N$_3$] (**8**)	32510, 25130
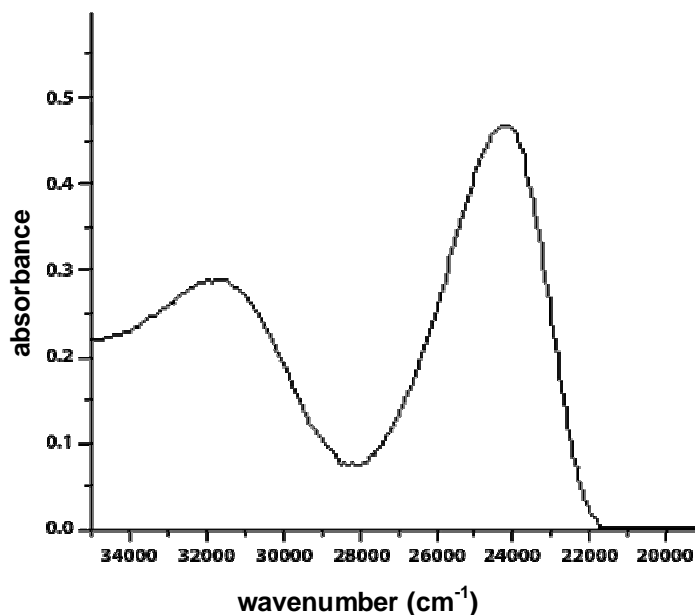
Figure 3.13. Electronic spectrum of the compound [Zn(HL^1)Br$_2$] (**1**).
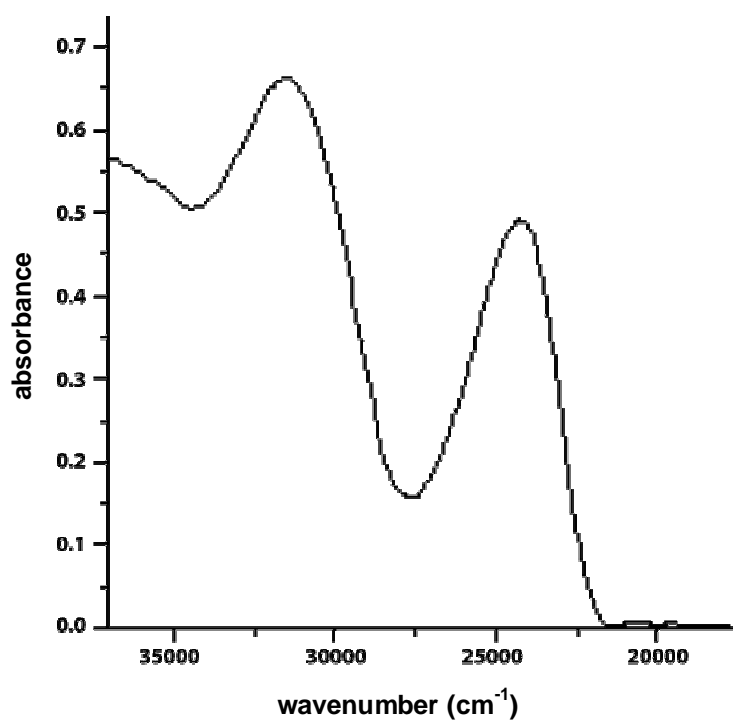
Figure 3.14. Electronic spectrum of the compound [Zn(HL^1)Cl$_2$] (**2**).
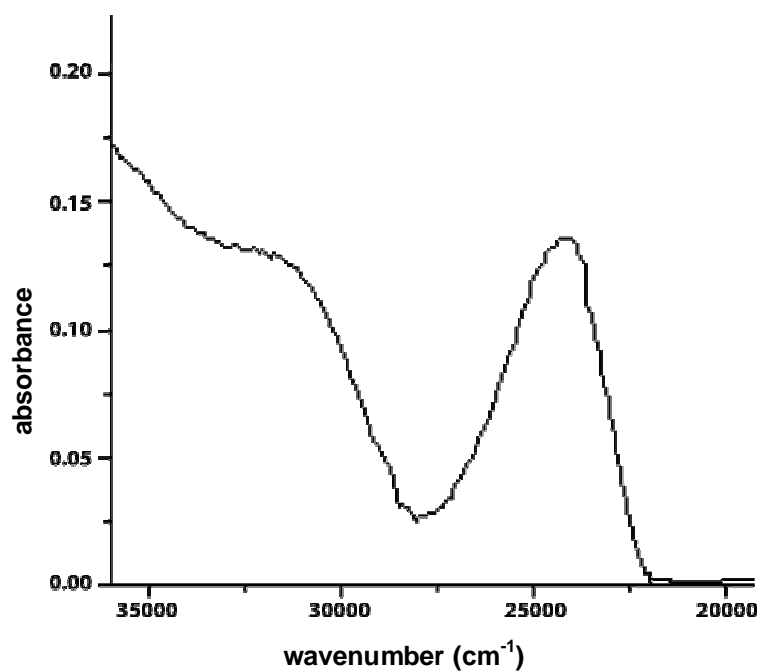
Figure 3.15. Electronic spectrum of the compound [ZnL^1(OAc)] (**3**).
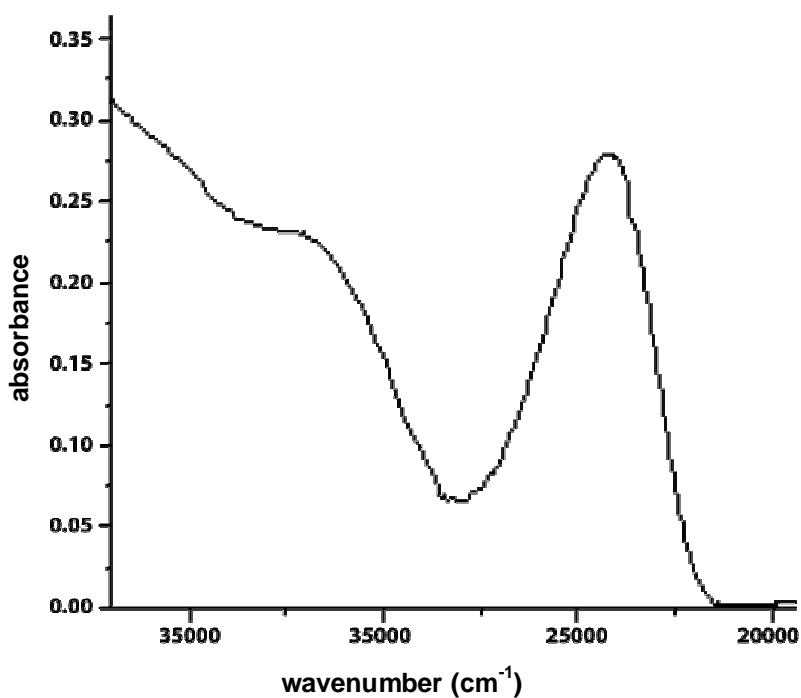
Figure 3.16. Electronic spectrum of the compound [ZnL^{1}N$_3$] (**4**).
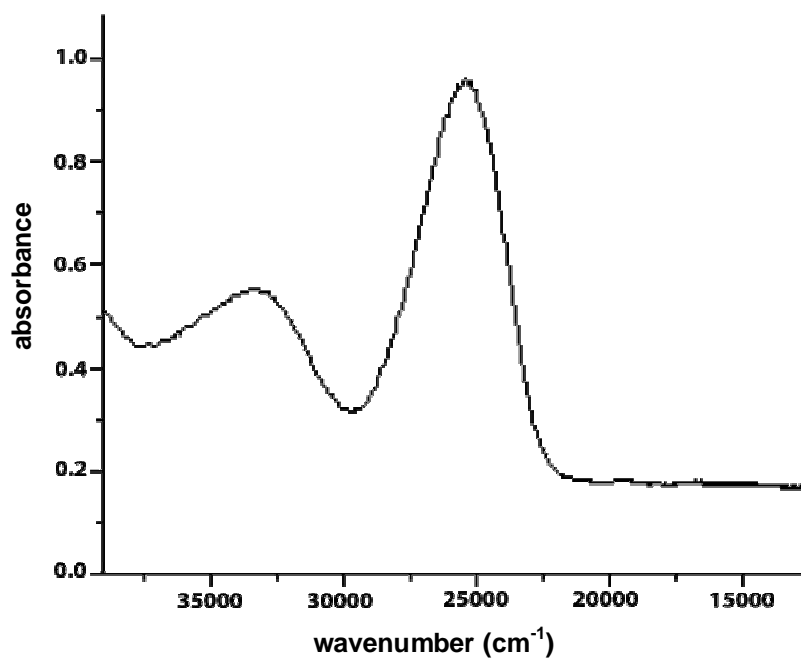
Figure 3.17. Electronic spectrum of the compound [ZnL^2(OAc)] (**7**).
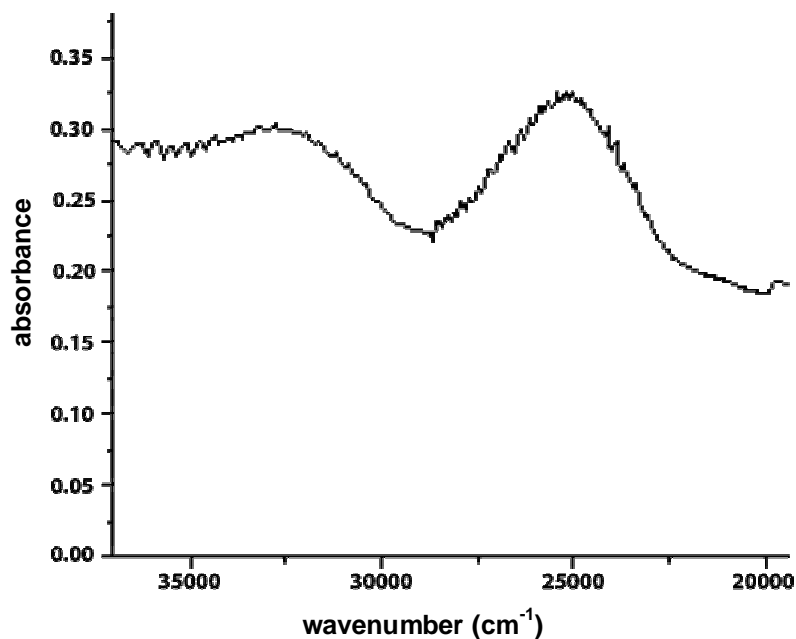
Figure 3.18. Electronic spectrum of the compound [ZnL^{2}N$_3$] (**8**).

References

[1]   L.S. Sarma, J.R. Kumar, K.J. Reddy, T. Thriveni, A.V. Reddy, J. Braz. Chem. Soc. 17 (2006) 463.

[2]   T. Matsukura, H. Tanaka, Biochemistry 65 (2000) 817.

[3]   G. Parkin, Chem. Commun. 1971 (2000).

[4]   D.X. West, A.E. Liberta, S.B. Padhye, R.C. Chikate, P.B. Sonawane, A.S. Kumbhar, R.G. Yerande, Coord. Chem. Rev. 123 (1993) 49.

[5]   D.L. Klayman, J.F. Bartosevich, T.S. Griffin, C.J. Manson, J.P. Scovill, J. Med. Chem. 22 (1979) 885.

[6]   P. Malatesta, G.P. Accinelli, G.P. Quaglia, Ann. Chim. Rome 49 (1959) 397.

[7]   S.B. Padhye, G.B. Kauffman, Coord. Chem. Rev. 63 (1985) 127.

[8]   CrysAlis CCD and CrysAlis RED Versions 1.171.29.2 (CrysAlis171. NET), Oxford Diffraction Ltd, Abingdon, Oxfordshire, England, 2006.

[9]   G.M. Sheldrick, Acta Crystallogr. A 64 (2008) 211.

[10]   H.D. Flack, G. Bernardinelli, Appl. Crystallogr. 33 (2000) 1143.

[11]   L.J. Farrugia, J. Appl. Crystallogr. 30 (1997) 565.

[12]   K.A. Ketcham, J.K. Swearingen, A. Castineiras, I. Garcia, E. Bermejo, D. X.West, Polyhedron 20 (2001) 3265.

[13]   E. Bermejo, A. Castineiras, I. Garcia-Santos, D.X. West, Z. Anorg. Allg. Chem. 630 (2004) 1097.

[14]   I. Garcia, E. Bermejo, A.K. El Sawaf, A. Castineiras, D.X. West, Polyhedron 21 (2002) 729.

[15]   A.W. Addison, T.N. Rao, J. Reedijk, J. Van Rijn, G.C. Verschoor, J. Chem. Soc., Dalton Trans. (1984) 1349.

[16]   G. Murphy, C.O. Sullivan, B. Murphy, B. Hathaway, Inorg. Chem. 37 (1998) 240.

[17]   M. Vaidyanathan, R. Balamurugan, U. Sivagnanam, M. Palaniandavar, J. Chem. Soc., Dalton Trans. (2001) 3498.

[18]   D. Cremer, J.A. Pople, J. Am. Chem. Soc. 97 (1975) 1354.

[19]   K. Nakamoto, Infrared and Raman Spectra of Inorganic and Coordination compounds, fifth ed., Wiley, New York, 1997.

[20]   D.F. Xiang, C.Y. Duan, X.S. Tan, Q.W. Hang, W.X. Tang, J. Chem. Soc., Dalton Trans. 7 (1998) 1201.

[21]   M.J.M. Campbell, Coord. Chem. Rev.17 (1975) 279.

[22]   E. Bayer, C.G. Witte, J. Coord. Chem. 7 (1997) 13.

[23]   D.F. Little, C.J. Long, Inorg. Chem.7 (1968) 3401.

[24]   M. Canadas, E. Lopez-Torres, A. Martinez-Arias, M.A. Mendiola, M.T. Sevilla, Polyhedron 19 (2000) 2059.

[25] R.A. Bailey, S.L. Kozak, T.W. Michelsen, W.N. Mills, Coord. Chem. Rev. 6 (1971) 407.

[26] V. Philip, V. Suni, M.R.P. Kurup, M. Nethaji, Polyhedron 24 (2005) 1133.

…..ഇൻ…..

SYNTHESIS, SPECTRAL STUDIES AND STRUCTURES OF Cd(II) COMPLEXES OF N^4-SUBSTITUTED SEMICARBAZONES

Contents	**4.1** **Introduction**
	4.2 **Experimental**
	4.3 **Results and discussion**

4.1. Introduction

Cadmium is a relatively abundant element. It was discovered in 1817 by Fredrich Stromeyer as an impurity in zinc carbonate. The metal was named after the Latin word for calamine, since the metal was found in this zinc compound. Cadmium containing ores are rare and are found to occur in small quantities. However, traces do naturally occur in phosphate, and have been shown to transmit in food through fertilizer application [1]. Gadreenockite (CdS), the only cadmium mineral of importance, is nearly associated with sphalerite (ZnS). As a consequence, cadmium is produced mainly as a byproduct from mining, smelting and refining sulfide ores of zinc, and, to a lesser degree, lead and copper. Small amounts of cadmium, about 10% of consumption, are produced from secondary sources, mainly from dust generated by recycling iron and steel scrap. Production in the United States began in 1907, but it was not until after World War I that cadmium came into wide use. One place where metallic cadmium can be found is the Vilyuy River basin in Siberia [2].

At one time an important commercial use of cadmium was as an electrodeposited coating on iron and steel for corrosion protection. Nickel-cadmium batteries are the second-largest application, with pigment and chemical uses third. Sizable amounts are used in low-melting-point alloys, similar to Wood's metal, and in automatic fire sprinklers, and relatively smaller uses are in brazing alloys, solders, and bearings. Cadmium compounds are used as stabilizers in plastics and the production of cadmium phosphors. Because of its great neutron-absorbing capacity, especially the isotope 113, cadmium is used in control rods and shielding for nuclear reactors.

Cadmium element has a $d^{10}s^2$ electronic arrangement and it typically forms M^{2+} ions and many of its compounds are appreciably covalent. The most stable form of cadmium is Cd^{2+}. Cadmium(II) complexes have tetrahedral, square pyramidal, trigonal bipyramidal and octahedral geometries. There is substantial interest in the coordination chemistry of cadmium complexes because of the toxic environmental impact of cadmium. The mobilization and immobilization of cadmium in the environment, in organisms, and in some technical processes (such as in ligand exchange chromatography) have been shown to depend significantly on the complexation of the metal center by chelating nitrogen donor ligands [3]. Cadmium is well known to form complexes with acetates and carboxy-ligands to yield both charged and neutral compounds [4]. The possibility of forming structures with higher coordination numbers has resulted in the observation of unusual coordination geometries about the metal atom and the formation of polymeric species [5]. Cd^{2+} forms most stable complexes with soft donor atoms (S>>N >O). Generally the stability of the complexes increases with the number of coordination groups contributed by the ligand. It has also been reported that some cadmium complexes of thiosemicarbazones can show quite large SHG efficiency [6].

This chapter describes the synthesis and characterization of six cadmium complexes of N^4-substituted semicarbazones using infrared, electronic and X-ray diffraction studies.

4.2. Experimental
4.2.1. Materials

The syntheses of the semicarbazones, HL^1 and HL^2 have been described already in Chapter 2. Cadmium(II) bromide tetrahydrate, cadmium(II) acetate dihydrate, cadmium(II) chloride and sodium azide were commercial products of higher grade (Aldrich). The reagents used were of Analar grade and used without further purification.

4.2.2. Synthesis of complexes
[CdL^1(OAc)]$_2$·2CH$_3$OH (9)

A methanolic solution of HL^1 (0.317 g, 1 mmol) and Cd(CH$_3$COO)$_2$·2H$_2$O (0.266 g, 1 mmol) were mixed and heated under reflux for 5 h. On slow evaporation, yellow crystals were obtained, which were separated, washed with ether and dried over P$_4$O$_{10}$ *in vacuo*.
Yield ~0.25 g.

[Cd(HL^1)Br$_2$] (10)

A methanolic solution of HL^1 (0.317 g, 1 mmol) and CdBr$_2$·4H$_2$O (0.344 g, 1 mmol) were mixed and heated under reflux for 5 h. On slow evaporation, yellow colored solid was resulted which was separated, washed with ether and dried over P$_4$O$_{10}$ *in vacuo*.
Yield ~0.49 g.

[Cd$_2$L$^1_2$(N$_3$)$_2$]·H$_2$O (11)

A methanolic solution of HL^1 (0.317 g, 1 mmol) and Cd(CH$_3$COO)$_2$·2H$_2$O (0.266 g, 1 mmol) were mixed and heated under reflux for 2 h and then added methanolic solution of NaN$_3$ (0.065 g, 1 mmol). The resulting mixture was

refluxed for 4 h. On slow evaporation yellow colored solid formed was separated, washed with ether and dried over P_4O_{10} *in vacuo*.

Yield ~0.35 g.

$[Cd(HL^2)(OAc)_2]\cdot^4/_3H_2O$ (12)

A solution of the semicarbazone, HL^2 (0.290 g, 1 mmol) in DMF was mixed with a methanolic solution of cadmium(II) acetate dihydrate (0.266 g, 1 mmol) and the mixture was heated under reflux for 4 h and cooled. The complex separated was filtered, washed thoroughly with ether and dried over P_4O_{10} *in vacuo*.

Yield ~0.30 g.

$[Cd(HL^2)Cl_2]$ (13)

A solution of semicarbazone, HL^2 (0.290 g, 1 mmol) in DMF was treated with a methanolic solution of cadmium(II) chloride (0.183 g, 1 mmol). The solution was heated under reflux for 4 h. The resulting solution was allowed to stand at room temperature and after slow evaporation yellow crystals separated out, which were collected, washed with ether and dried over P_4O_{10} *in vacuo*.

Yield ~0.32 g.

$[Cd(HL^2)Br_2]\cdot DMF$ (14)

A solution of semicarbazone, HL^2 (0.290 g, 1 mmol) in DMF was treated with a methanolic solution of cadmium(II) bromide tetrahydrate (0.344 g, 1 mmol). The solution was heated under reflux for 4 h. The resulting solution was allowed to stand at room temperature and after slow evaporation yellow crystals separated out, which were collected, washed with ether and dried over P_4O_{10} *in vacuo*.

Yield ~0.30 g.

4.2.3. Analytical methods

Elemental analyses were carried out using a Vario EL III CHNS analyzer at the SAIF, Kochi, India. Infrared spectra were recorded on a Thermo Nicolet AVATAR 370 DTGS FTIR Spectrometer in the range 4000-400 cm^{-1} using KBr pellets at SAIF, Cochin University of Science and Technology, Kochi 22, India. Electronic spectra were recorded on a Cary 5000 version 1.09 UV-VIS-NIR Spectrophotometer using solutions in DMF. The ^{1}H and ^{13}C NMR spectra were not recorded due to insolubility of complexes in the solvents.

4.2.4. X-ray crystallography

Single crystals of compound **9** suitable for X-ray analysis were obtained from its methanolic solution and were found to be orthorhombic space group 'p_{bca}'. Single crystals of compounds **13** and **14** were obtained from a solution of mixture of methanol and DMF. The crystals of compounds **13** and **14** were found to be triclinic and monoclinic space groups P1 and $P2_1/c$ respectively. X-ray diffraction measurements were carried out on CrysAlis CCD diffractometer with graphite-monochromated Mo Kα (λ = 0.71073 Å) radiation. The program CrysAlis RED was used for data reduction and cell refinement [7]. The structures were solved by direct methods using SHELXS [8] and refined by full-matrix least-squares refinement on F^2 using SHELXL [9]. The N–H hydrogen atoms were located from difference Fourier maps and refined isotropically. The remainder of the H-atoms were included in calculated positions and refined as riding atoms using default SHELXL parameters. The structures of the compounds **9, 13** and **14** were plotted using the program DIAMOND version 3.1d [10] and PLATON [11]. The crystallographic data along with the structural refinements are given in Table 4.1.

Table 4.1. Crystal data and Structure refinement parameters of [CdL^1(OAc)]$_2$·CH$_3$OH (9), [Cd(HL^2)Cl$_2$] (13) and [Cd(HL^2)Br$_3$]·DMF (14)

	9	13	14
Empirical formula	C$_{42}$H$_{42}$Cd$_2$N$_{10}$O$_8$	C$_{17}$H$_{14}$CdCl$_2$N$_4$O	C$_{20}$H$_{21}$Br$_3$CdN$_5$O$_2$
Formula weight	1039.68	473.62	635.63
Temperature (K)	120(2)	150(2)	293(2)
Wavelength (Å)	0.71073	0.71073	0.71073
Crystal system	Orthorhombic	Triclinic	Monoclinic'
Space group	$Pbca$	P-1	$P2_1/c$
Unit cell dimensions			
a (Å)	13.8648(3)	7.939(2)	7.6560(15)
b (Å)	15.3588(5)	8.149(2)	15.608(3)
c (Å)	19.2468(4)	14.068(4)	18.722(4)
α (°)	90	98.53(2)	90.00
β (°)	90	96.01(2)	93.83(3)
γ (°)	90	94.33(2)	90.00
Volume (Å^3)	4098.54(18)	891.3(4)	2232.1(8)
Z	4	2	4
D$_{calc}$ (g/cm^3)	1.685	1.765	1.891
Absorption coefficient	1.105 mm^{-1}	1.537 mm^{-1}	4.585 mm^{-1}
F(000)	2096	468	1240.0
Crystal size (mm^3)	0.23 x 0.18 x 0.13	0.13 x 0.08 x 0.05	0.40x 0.18 x 0.10
θ range for data collection	2.86-25°	3.13-25.00°	2.54-25.90°
Index ranges	-13 ≤ h ≤ 16, -18 ≤ k ≤ 15, -22 ≤ l ≤ 22	-9≤h≤9, -9≤k≤9,-16≤l≤16	-9≤h≤9, -19≤k≤19, -23≤l≤23
Reflections collected	3610	3132	4404
Independent reflections [R(int)]	290 [0.0361]	2009 [0.0000]	3531 [0.0369]
Refinement method	Full-matrix least-squares on F^2	Full-matrix least-squares on F^2	Full-matrix least-squares on F^2
Data / restraints / parameters	5041 / 0 / 313	3132 / 21 / 228	4398 / 0 / 274
Goodness-of-fit on F^2	1.065	1.164	1.039
Final R indices [I>2σ(I)]	R$_1$ = 0.0301, wR$_2$ = 0.0665	R$_1$ = 0.1357, wR$_2$ = 0.2673	R$_1$ = 0.0286, wR$_2$ = 0.0612
R indices (all data)	R$_1$ = 0.0440, wR$_2$ = 0.0725	R$_1$ = 0.1943, wR$_2$ = 0.2957	R$_1$ = 0.0391, wR$_2$ = 0.0649
Largest diff. peak and hole	0.722 and -0.503 e.Å^3	3.029 and -2.200 e. Å^3	8.080 and -0.762 e.Å^3

$R_1 = \Sigma||F_o| - |F_c|| / \Sigma|F_o|$ $wR_2 = [\Sigma w(F_o^2 - F_c^2)^2 / \Sigma w(F_o^2)^2]^{1/2}$

4.3. Results and discussion

The analytical data of all the complexes are given in Table 4.2. Compounds **9, 10, 12, 13** and **14** were prepared by direct reaction between the semicarbazones and the corresponding cadmium(II) salts, while the compound **11** was prepared by the replacement of the acetate in $Cd(CH_3COO)_2 \cdot 2H_2O$ by the azide ion. Elemental analyses data of all the complexes reveal that metal-ligand are in the ratio 1:1 and in the complexes **10**, **12**, **13** and **14** semicarbazone interacts with Cd(II) ion in neutral keto form. In complexes **9** and **11** the metal, ligand and anion are present in the molar ratio 1:1:1 whereas, in other complexes this molar ratio is 1:1:2.

Table 4.2. Analytical data

Compound	Color	Found (Calcd) %		
		C	H	N
$[CdL^1(CH_3COO)]_2 \cdot 2CH_3OH$ (**9**)	Yellow	48.16 (48.52)	3.97 (4.07)	13.30 (13.47)
$[Cd(HL^1)Br_2]$ (**10**)	Yellow	36.69 (36.67)	2.64 (2.56)	12.45 (11.88)
$[CdL^1N_3]_2$ (**11**)	Yellow	44.46 (45.06)	3.05 (3.15)	23.98 (23.36)
$[Cd(HL^2)(OAc)_2] \cdot {}^4/_3H_2O$ (**12**)	Yellow	46.10 (45.46)	4.06 (3.58)	10.49 (10.52)
$[Cd(HL^2)Cl_2]$ (**13**)	Yellow	42.93 (43.11)	3.39 (2.98)	11.78 (11.83)
$[Cd(HL^2)Br_2] \cdot DMF$ (**14**)	Yellow	37.43 (37.79)	2.94 (3.33)	11.10 (11.02)

4.3.1. Crystal structures of $[CdL^1(OAc)]_2 \cdot 2CH_3OH$ (9), $[Cd(HL^2)Cl_2]$ (13) and $[Cd(HL^2)Br_2] \cdot DMF$ (14)

Figure 4.1 shows the molecular structure of the binuclear centrosymmetric Cd(II) complex with the atom numbering scheme. Both Cd centres being hexacoordinated and the coordination around the Cd(II) ion can

be best described as a distorted octahedron with a CdO$_3$N$_3$ chromophore. Each Cd atom is coordinated by azomethine nitrogen, oxygen atom from the principal ligand, two pyridyl nitrogens and two oxygen atoms from the acetate group. The acetate groups serve as bidentate ligands and the semicarbazones as tetradentate ligands. The two pyridyl nitrogens from the principal ligand are coordinated to two different Cd centres forming cyclic type architecture (Figure 4.2). The coordination of oxygen from the semicarbazone ligand occurs through deprotonation after enolization, confirmed by the partial single and double bond nature of C7–O1 [1.350(4) Å] and N3–C7 [1.368(4) Å] bond lengths [12,13]. The C6–N2 and N2–N3 bond distances are 1.257(4) Å and 1.338(3) Å respectively, which reveal extensive delocalization over the entire binuclear coordination framework. Table 4.3 shows the selected bond lengths and bond angles of the compound **9**.
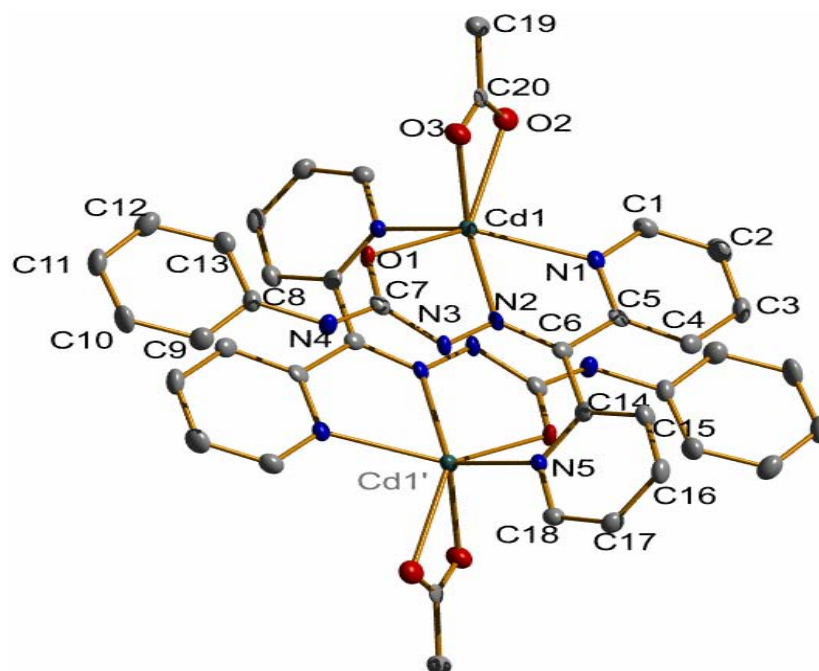
Figure 4.1. Structure and labeling diagram for compound **9** (hydrogen atoms and methanol molecule are omitted for clarity).
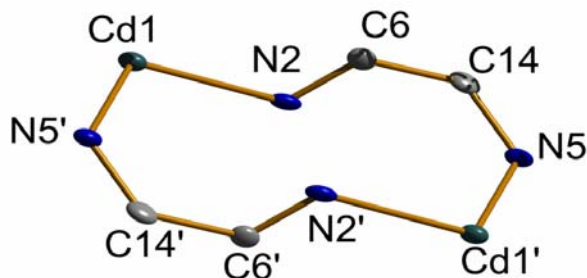
Figure 4.2. Cyclic formation through cadmium centers.

Table 4.3. Selected bond lengths (Å) and bond angles (°) of compound **9**

Bond lengths		Bond angles	
Cd(1)–N(5)	2.155(3)	N(5)–Cd(1)–N(1)	116.23(9)
Cd(1)–N(1)	2.168(3)	N(5)–Cd(1)–O(1)	92.67(9)
Cd(1)–O(1)	2.249(2)	N(1)–Cd(1)–O(1)	132.65(9)
Cd(1)–O(3)	2.434(2)	N(5)–Cd(1)–O(3)	107.15(9)
Cd(1)–N(2)	2.515(3)	N(1)–Cd(1)–O(3)	116.82(9)
O(1)–C(7)	1.350(4)	N(5)–Cd(1)–N(2)	119.45(9)
N(1)–C(1)	1.349(4)	O(3)–Cd(1)–N(2)	123.35(8)
N(1)–C(5)	1.479(4)	C(7)–O(1)–Cd(1)	119.56(18)
N(2)–C(6)	1.257(4)	C(1)–N(1)–C(5)	125.7(3)
N(2)–N(3)	1.338(3)	C(6)–N(2)–N(3)	113.1(3)
N(3)–C(7)	1.368(4)	C(6)–N(2)–Cd(1)	120.7(2)
N(4)–C(8)	1.326(4)	N(3)–N(2)–Cd(1)	126.16(19)
N(4)–C(7)	1.354(4)	N(2)–N(3)–C(7)	100.2(3)
N(4)–H(4N)	0.85(3)	O(1)–C(7)–N(3)	130.7(3)
Cd1···Cd1ʹ	5.4181(4)		

In the case of this Cd-semicarbazone complex, Cd–O bond distances are Cd1–O1, 2.249(2) Å; Cd1–O2, 2.7666 Å; Cd1–O3, 2.434(2) Å and Cd–N bond distances are Cd1–N1, 2.168(3) Å; Cd1–N2, 2.515(3) Å and Cd1–N5, 2.155(3) Å respectively. The Cd1–O1 bond distance is slightly less than the

other Cd–O bond distances reported for other octahedral Cd(II) complexes [14,15]. The Cd1–O2 and Cd1–O3 bond distances lie within the range of Cd–$O_{carboxylate}$ bond distances [2.209(2) – 2.879(2) Å] reported for Cd(II)–$O_{carboxylate}$ coordination polymers [16]. The Cd1–N2 bond distance is slightly larger than the other Cd–N bond distances, which supports the lack of significant out-of-plane π-bonding. The trans angle, O2–Cd1–N2 is 155.84(8)° indicating that the compound **9** has large distortion from octahedral geometry [17]. Other indication of distorted octahedral geometry is the bond angle of O1–Cd1–O3, 85.51(8)°. The Cd1···Cd1 distance is 5.4181(4) Å.

The unit cell packing diagram of the complex **9** viewed along the *b* axis is given in Figure 4.3. It can be observed that the molecules are packed in a zig-zag manner. Ring puckering analysis show that the ring Cg(3) consisting of atoms Cd1–N1–C5–C6–N2 adopts an envelope on Cd1 [Q_T =0.1086(22) Å, ϕ= 358.0622(15702)°] [18]. The diverse π–π stacking and C–H···π interactions give rise to polymeric chains in the unit cell. The shortest π–π interactions (Table 4.5) are perceived at 3.1992 Å for Cg(2)···Cg(3)[a] [Cg(2) = Cd1–O1–C7–N3–N2; a = –x, –y, 2–z]. Two C–H···π interactions are present in the unit cell. They are C(11)–H(11)···Cg(2)[b] [$d_{H···Cg}$ = 2.94 Å; b = –1/2+x, y, 3/2–z] and C(21)–H(21)···Cg(5)[c] [$d_{H···Cg}$ = 2.93 Å; c = x, 1/2–y, –1/2+z]. The π-π, C–H···π and hydrogen bonding interactions contribute stability to the unit cell packing.

The molecules in the unit cell are connected through intermolecular hydrogen bonding interactions involving the oxygen atom of the methanol molecule [O(4)─H(4) ···O(3); O(4)─H(4), 0.81(4) Å; O(4)···O(3), 2.726(4) Å; H(4)···O(3), 1.92(4) Å; O(4)─H(4)···O3, 174(3)° and N(4)─H(4)···O(4)[d] [d = –x, –1/2+y, 3/2–z]; N(4)─H(4), 0.85(3) Å; N(4)···O(4), 3.132(4) Å; H(4)···O(4), 2.30(3) Å; N(4)─H(4)···O(4), 166(3)°] (Figure 4.4).
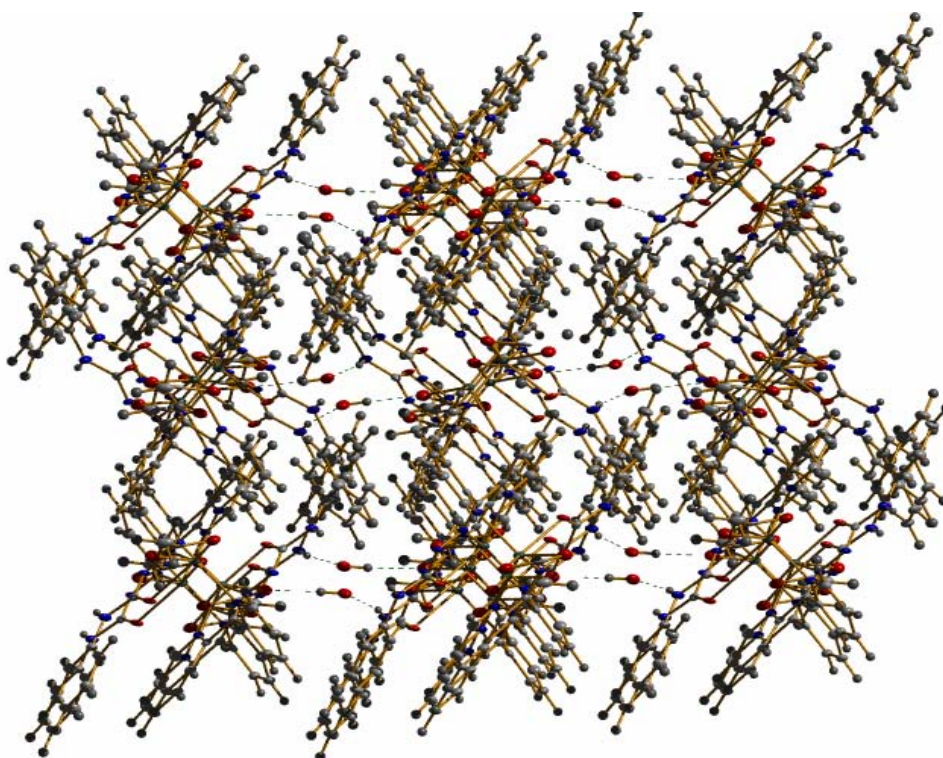
Figure 4.3. Unit cell packing diagram of compound **9**.
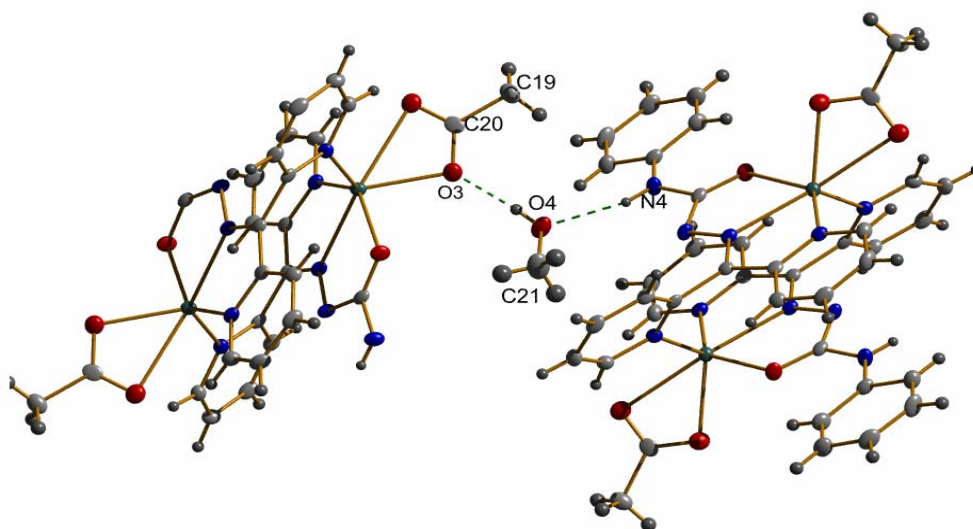
Figure 4.4. Intermolecular hydrogen bonding interactions through methanol molecule of compound **9**.

The compound **13** crystallizes in the triclinic space group *P*1 whereas the compound **14** crystallizes in the monoclinic space group *P*2$_1$/*c*. Figures 4.5 and 4.6 show the molecular structures of the Cd(II) complexes, **13** and **14** with atom numbering scheme. Cd atoms in these compounds are coordinated by azomethine nitrogen (N2), quinolyl nitrogen (N1), ketoxy oxygen (O1) and two anionic ligands. In both compounds, **13** and **14**, the Cd atom is pentacoordinated in which both ligands are coordinated in their neutral keto forms. The chloride/bromide ions serve as bidentate and the semicarbazones as tridentate ligands. In compound **13**, the bond distances to Cd are in the order Cd–N$_{(azo)}$< Cd–N$_{(quinolyl)}$< Cd–Cl1< Cd–O$_{(ketoxy)}$< Cd–Cl2, where as in compound **14**, Cd–N$_{(azo)}$< Cd–N$_{(quinolyl)}$< Cd–O$_{(ketoxy)}$< Cd–Br1< Cd–Br2. The bond length Cd–N$_{(azo)}$ of compound **13** and **14** are 2.295(14) and 2.326(2) Å respectively, which is less than the other Cd–N$_{(azo)}$ bond distances reported earlier whereas, the Cd–O$_{(ketoxy)}$ bond lengths of compounds **13** and **14** are 2.432(11) and 2.461(19) Å respectively, which are larger than the other reported Cd–O$_{(ketoxy)}$ bond distances [19]. This indicates stronger coordination of azomethine nitrogen atom in the compounds **13** and **14** [20]. The Cd–N$_{(azo)}$ bond distance in both compounds is slightly less than the other Cd–N distance, which supports the significant out-of-plane π-bonding. The Cd–Cl bond distances are 2.404(6) and 2.454(6) Å, but there is a difference of 0.05 Å between the Cd–Cl bonds of [Cd(HL^2)Cl$_2$] (**13**). In compound **14** the Cd–Br bond distances are 2.531(7) and 2.548(6) Å, and here the difference is 0.017 Å. Table 4.4 shows selected bond lengths and bond angles of compounds **13** and **14**.
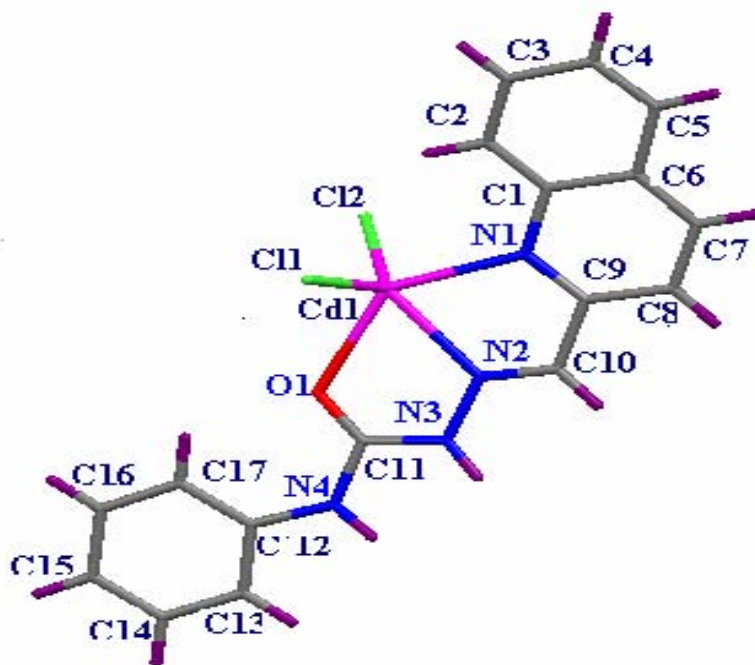
Figure 4.5. Structure and labeling diagram of compound **13**.
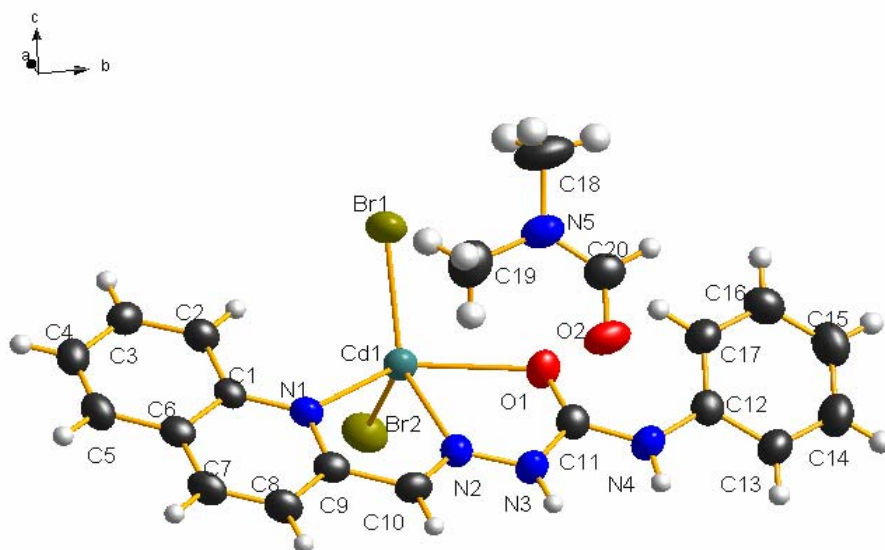
Figure 4.6. Structure and labeling diagram of compound **14**.

Table 4.4. Selected bond lengths (Å) and bond angles (°) for **13** and **14**

	13		**14**	
	Bond lengths		*Bond lengths*	
Cd1–N2	2.295(14)		Cd1–N2	2.326(2)
Cd1–N1	2.370(13)		Cd1–N1	2.420(2)
Cd1–Cl1	2.404(6)		Cd1–O1	2.4612(19)
Cd1–O1	2.432(11)		Cd1–Br1	2.5317(7)
Cd1–Cl2	2.454(6)		Cd1–Br2	2.5481(6)
O1–C11	1.20(2)		O1–C11	1.226(3)
N1–C9	1.30(2)		N1–C9	1.336(3)
N1–C1	1.42(2)		N1–C1	1.361(3)
N2–C10	1.24(2)		N2–C10	1.273(3)
N2–N3	1.398(19)		N3–N2	1.345(3)
N3–C11	1.35(2)		N3–C11	1.372(3)
N4–C11	1.38(2)		N4–C11	1.356(3)
N4–C12	1.40(2)		N4–C12	1.413(3)
	Bond angles		*Bond angles*	
N2–Cd1–N1	69.3(5)		N2–Cd1–N1	68.79(8)
N2–Cd1–O1	67.3(4)		N2–Cd1–O1	66.36(7)
N1–Cd1–O1	136.6(5)		N1–Cd1–O1	33.83(7)
N2–Cd1–Cl2	111.2(4)		N2–Cd1–Br1	137.26(6)
N1–Cd1–Cl2	99.9(4)		N1–Cd1–Br1	108.10(5)
O1–Cd1–Cl2	93.6(4)		O1–Cd1–Br1	97.50(5)
N2–Cd1–Cl1	124.0(4)		N2–Cd1–Br2	105.61(6)
N1–Cd1–Cl1	101.2(4)		N1–Cd1–Br2	102.01(6)
O1–Cd1–Cl1	104.4(4)		O1–Cd1–Br2	99.89(5)
Cl1–Cd1–Cl2	124.81(19)		Br1–Cd1–Br2	116.33(3)
C11–O1–Cd1	116.0(11)		C11–O1–Cd1	114.79(17)
			C9–N1–Cd1	115.03(17)

For the compound **13** the coordination of the semicarbazone to the Cd atom through ketoxy oxygen in neutral form is confirmed by the bond length of C11–O1 [1.20(2) Å] which is very near to the reported values for C=O for zinc complexes of semicarbazones [21]. But this bond distance is slightly different from the reported value for free semicarbazone and this is due to the complexation. Also, C10–N2 bond length [1.24(2) Å] is comparable to the value reported for other semicarbazone complexes [21]. The C11–N3 and N2–N3 bond distances are 1.35(2) and 1.398(19) Å respectively, which reveal extensive delocalization over entire coordination framework. The coordination results in the changes of bond lengths and bond angles of the semicarbazone moiety, as expected. In the compound **14** the bond length of C11–O1 is 1.226(3) Å which supports coordination of the semicarbazone in the keto form. The extensive delocalization over the semicarbazone moiety is evidenced by the bond length of N2–N3 1.345(3) Å, which is in between the single and double bond distance value. This is again confirmed by the bond distance of C11–N3, which is 1.372(3) Å. The basal coordination plane in compound **13** is occupied by the ketoxy oxygen (O1), azomethine nitrogen (N2), quinolyl nitrogen (N1) of the semicarbazone and the chloride ion (Cl1). The apical position is occupied by the second chloride ion (Cl2), at a larger distance [2.454(6) Å]. Also in the complex **14,** ketoxy oxygen (O1), azomethine nitrogen (N2), quinolyl nitrogen (N1) of the semicarbazone and the bromide ion, (Br1) correspond to the basal plane where as the apical position is occupied by bromide ion, Br2.

The angular structural parameter (τ) is calculated by $\tau = (\beta - \alpha)/60$, where β is the greatest basal angle and α is the second greatest angle; τ is 0 for rectangular pyramidal forms and 1 for trigonal bipyramidal forms [22,23]. The value of the τ for the compounds **13** and **14** are 0.145 and 0.057 respectively which indicate that the coordination geometries around Cd(II) are best described as distorted square based pyramid [24].

In compound **13**, the deviations from the least-square plane through the O1, N1, N2, Cl1 and Cd1 atoms comprising the square plane are 0.4345, 0.7593, 1.6978, 0.2064 and 0.0516 Å, respectively, and the N2 atom shows maximum deviation from the plane of 1.6978 Å. The deviations from the least-square plane through the O1, N1, N2, Br1 and Cd1 atoms in compound **14** comprising the square plane are 0.5050, 0.8134, 1.3516, 0.0528 and 0.0907 Å respectively and the N2 atom has maximum deviation from the plane of 1.3516 Å.

In the crystal packing of compound **13** two molecules are present and two of them are parallel to each other. In the case of the compound **14** there are 4 molecules in the unit cell packing and the molecules are complement to one another (Figure 4.7). For the compounds **13** and **14**, in the unit cell π–π and hydrogen bonding interactions were observed. In compound **13**, π–π interaction is perceived at 3.569(11) Å for Cg(3)–Cg(5)^e [Cg(3) = N1–C1–C6–C7–C8–C9; Cg(5) = C12–C13–C14–C15–C16–C17, e = 2-x,– y, 1–z]. Three intermolecular hydrogen bonding interactions were observed, *i.e.*, N3(H) and N4(H) of one molecule with chlorine atom (Cl2) of the another molecule and C10(H) and Cl2 of the other molecule [N(3)–H(3N)···Cl(2)^f, D–H = 0.88 Å, H···A = 2.45 Å, D···A = 3.247(17) Å, D–H···A = 151º; N(4)–H(4N)···Cl(2)^f, D–H = 0.88 Å, H···A = 2.45 Å, D···A = 3.265(16) Å, D–H···A = 155º, f = 2–x, –y, 1–z; C(10)–H(10C)···Cl(2)^g, D–H = 0.95 Å, H···A = 2.69 Å, D···A = 3.575(11) Å, D–H···A = 120º, g = 1+x, y, z]. In compound **14**, the π–π interaction is apparent at 3.7137(18) Å for Cg(3)–Cg(4)^h [Cg(3) = N1–C1–C6–C7–C8–C9; Cg(4) = C1–C2–C3–C4–C5–C6, h = 1-x,1– y, –z]. Two intermolecular hydrogen bonding interactions were observed, *i.e.*, N3(H) and O2 of the other molecule and N4(H) and O2 of other molecule [N(3)–H(3N)···O(2)^i, D–H = 0.86 Å, H···A = 1.91 Å, D···A = 2.705(3) Å, D–H···A = 154º; N(4)–H(4N) ···O(2)^i, D–H = 0.86 Å, H···A = 2.10 Å, D···A = 2.890(3) Å, D–H···A = 152º, i = 1–x, 2–y, –z].
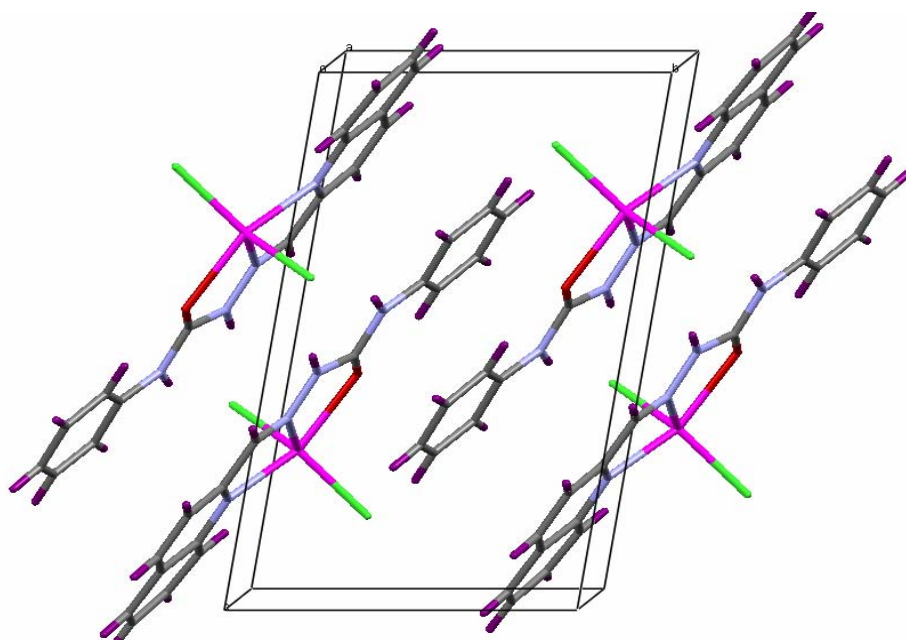
Figure 4.7. Unit cell packing diagram of compound **13**.
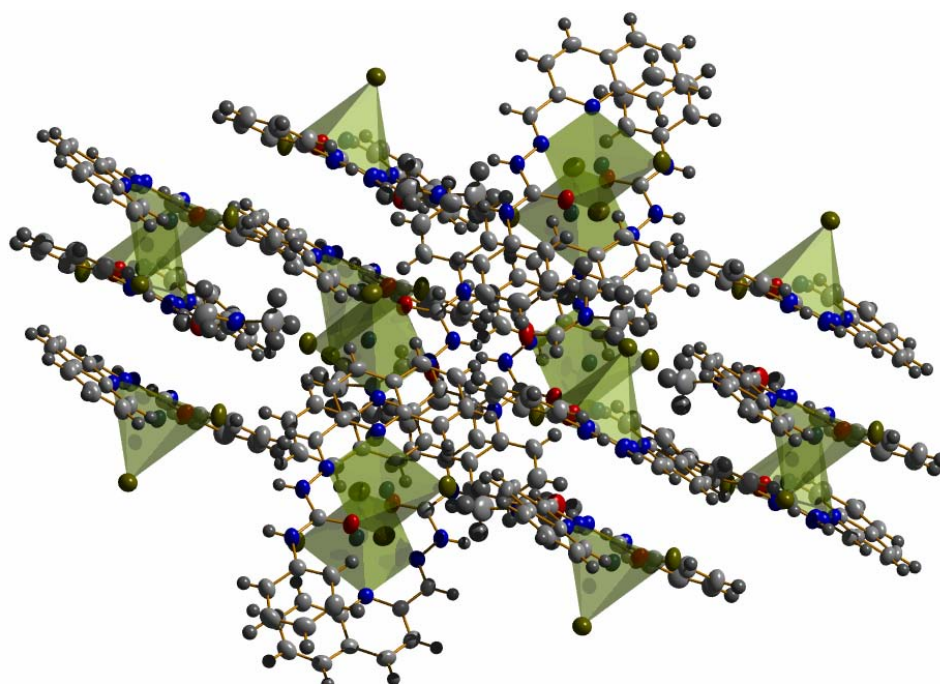
Figure 4.8. Unit cell packing diagram of compound **14**.
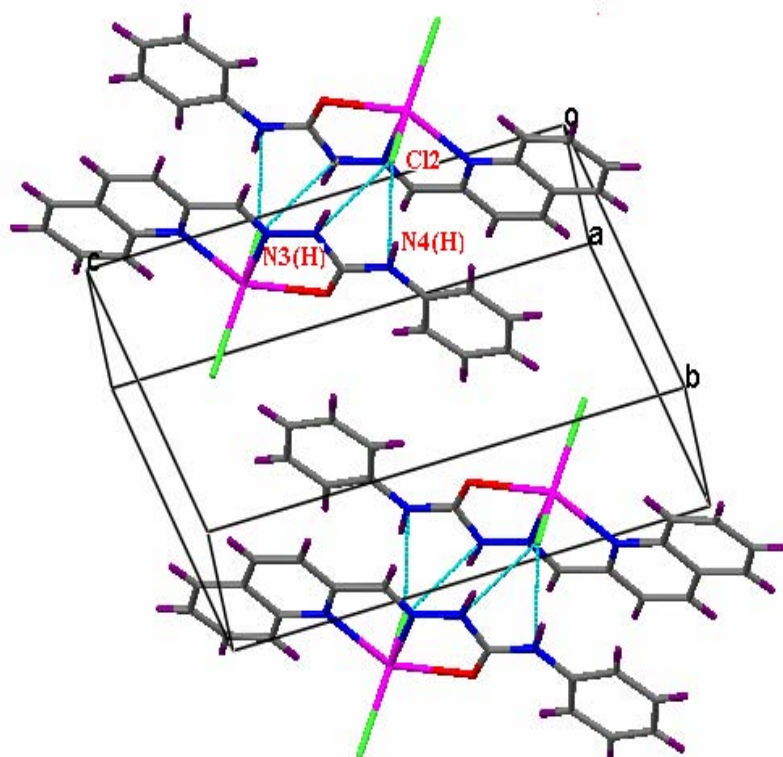
Figure 4.9. Intermolecular hydrogen bonding interactions of **13**.
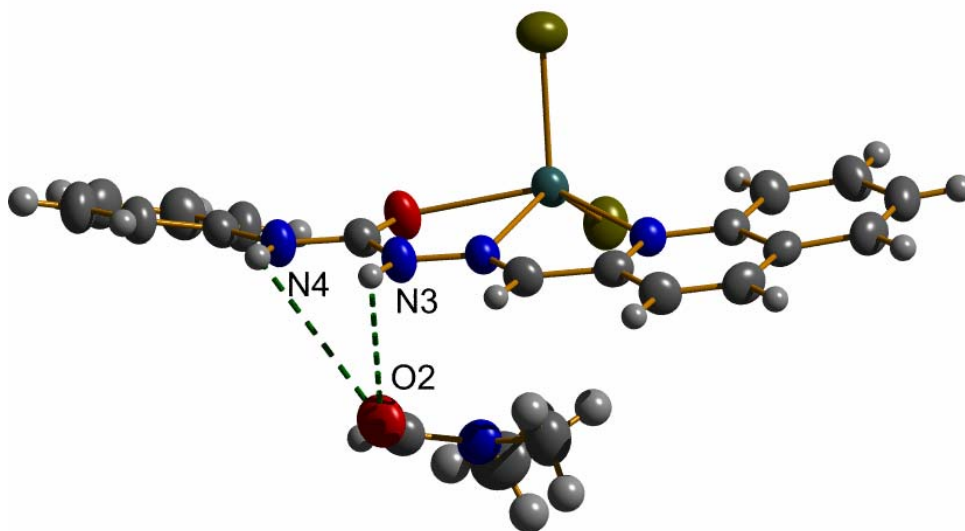
Figure 4.10. Intermolecular hydrogen bonding interactions of **14**.

Table 4.5. Interaction parameters of the compounds **9**, **13** and **14**

π···π interactions			
Cg(I)···Cg(J)	Cg–Cg (Å)	α °	β °
9			
Cg(2)···Cg(3) [a]	3.1992(15)	5.44	18.54
13			
Cg(3)···Cg(5) [e]	3.569(11)	3.8(9)	20.25
14			
Cg(3)···Cg(4) [h]	3.7137(18)	2.21(13)	19.24

Equivalent position codes : a = -x, -y, 2-z; e = 2-x,-y,1-z; h = 1-x, 1-y, -z

For compound **9,** Cg(2) = Cd(1), O(1), C(7), N(3), N(2), Cg(3) = Cd(1), N(1), C(5), C(6), N(2)

For compound **13**, Cg(3) = N(1), C(1), C(6), C(7), C(8), C(9), Cg(5) = C(12), C(13), C(14), C(15), C(16), C(17)

For compound **14**, Cg(3) = N(1), C(1), C(6), C(7), C(8), C(9), Cg(4) = C(1), C(2), C(3), C(4), C(5), C(6)

H bonding				
D–H···A	D–H (Å)	H···A (Å)	D···A (Å)	D–H···A (°)
[CdL^1(OAc)]$_2$·CH$_3$OH (**9**)				
N4−H(4N)···O(4) [d]	0.85(3)	3.132(4)	2.30(3)	166(3)
[Cd(HL^2)Cl$_2$] (**13**)				
N(3)−H(3N)···Cl(2) [f]	0.88	2.45	3.247(17)	151
N(4)−H(4N)···Cl(2) [f]	0.88	2.45	3.265(16)	155
C(10)−H(10C)···Cl(2) [g]	0.95	2.69	3.575(11)	120
[Cd(HL^2)Br$_2$] (**14**)				
N(3)−H(3N)···O(2) [i]	0.86	1.91	2.705(3)	154
N(4)−H(4N)···O(2) [i]	0.86	2.10	2.890(3)	152

Equivalent position codes : d = –*x*, –1/2+*y*, 3/2–*z*; f = 2-x,-y,1-z; g = 1+x,y,z; i = 1-x, 2-y, -z

D=Donor, A=acceptor, Cg=Centroid, α=dihedral angles between planes I & J, β= angle between Cg-Cg and Cg(J) perp.

4.3.2. Infrared spectra

The IR spectral bands most useful for the determination of the mode of coordination are given in Table 4.6. The absence of ν(NH) in the spectra of the complexes **9** and **11** suggests that the semicarbazone, HL^1 loses this proton on complexation, thus acting as uninegative ligand [25]. In complex **10**, the presence of a band at 3251 cm^{-1} corresponding to ν(NH) vibration indicates that the semicarbazone is coordinated in the neutral form. A band at 1718 cm^{-1} in the semicarbazone, HL^1 has significant contribution from C=O stretching vibration and absence of such a band in the complexes **9** and **11** confirming the coordination through enolate oxygen. The presence of a band at 1656 cm^{-1} for the complex **10** supports the keto form of the semicarbazone in this complex.

On coordination of the azomethine nitrogen, the IR stretching frequency ν(C=N) at 1591 cm^{-1} shifts to 1570, 1562 and 1561 cm^{-1} for the complexes **9**, **10** and **11** respectively [26-28]. The spectra of the complexes exhibit a systematic shift in the position of ν(N–N) bands in the region 1148-1141 cm^{-1} and confirms the coordination of the azomethine nitrogen. This shift to higher region is due to the increase in the double bond character off-setting the loss of electron density *via* donation to the metal. The bands appearing in the region 484-501 cm^{-1} which correspond to ν(Cd–N$_{azo}$) for complexes **9-11** again confirm the coordination of the azomethine nitrogen [29]. Coordination of pyridyl nitrogen causes the out-of-plane bending vibrational band to shift from 601 cm^{-1} to higher frequencies 622, 621 and 627 cm^{-1} for complexes **9-11** [30]. Presence of bands at 1600 and 1596 cm^{-1} for the complexes **9** and **11** are assigned to the newly formed ν(C=N) band after enolization [31]. The presence of new peaks in the 457, 451 and 463 cm^{-1} are due to the ν(Cd–O) bands. The asymmetric and symmetric stretching vibrations of the acetate group appear at 1568 and 1437 cm^{-1} respectively for the

complex **9** having the separation value $\Delta v = 131$ cm^{-1} suggests the presence of chelating acetate group linked with the metal center for the complex [32,33]. The azido complex **11** exhibits a strong band at 2052 cm^{-1} corresponding to v_a(N–N–N) stretching vibration of the coordinating azido group.

The IR spectrum of the semicarbazone, HL^2 has a band at 1702 cm^{-1} is assigned to v(C=O), which is shifted to lower wavenumber in complexes **12**-**14**. This indicates that in these complexes, semicarbazone coordinates in keto form. This is further confirmed by the presence of bands in the region 3245-3274 cm^{-1}, attributed to v(NH) vibration for the complexes **12**-**14**. The strong band observed at 1592 cm^{-1} due to v(C=N) of the semicarbazone moiety shifts to 1565, 1565 and 1554 cm^{-1} upon complexation. This lowering of frequencies confirms the coordination *via* azomethine nitrogen. The coordination of azomethine nitrogen is also consistent with presence of a new band in the range 500-510 cm^{-1}, assignable to v(Cd–N$_{azo}$) for these complexes. A shift in the absorption bands due to v(N–N) stretching vibrations from 1150 cm^{-1} to higher region confirms the coordination of semicarbazone through azomethine nitrogen atom. The new peaks observed in the range 470-477 cm^{-1} are due to the v(Cd–O) band [34-37]. The presence of bands at 1503 and 1423 cm^{-1} for the complex **12** are assignable as asymmetric and symmetric stretching vibrations respectively of the acetate group. IR spectra of complexes are presented in Figures 4.11-4.16.

Table 4.6. IR spectral assignments for semicarbazones and their cadmium (II) complexes

Compound	ν(NH)	ν(C=N)	ν(CO)	ν(C=N)[a]	ν(N–N)
HL^1	3369	1591	1718	-	1129
[CdL^1(OAc)]$_2$·2CH$_3$OH (9)	-	1570	-	1600	1148
[Cd(HL^1)Br$_2$] (10)	3251	1562	1656	-	1147
[CdL^{1}N$_3$]$_2$ (11)	-	1561	-	1596	1141
HL^2	3380	1592	1702	-	1150
[Cd(HL^2)(OAc)$_2$]·$^1/_3$H$_2$O (12)	3245	1565	1667	-	1160
[Cd(HL^2)Cl$_2$] (13)	3272	1565	1678	-	1166
[Cd(HL^2)Br$_2$]·DMF (14)	3274	1554	1680	-	1169

[a] Newly formed C=N
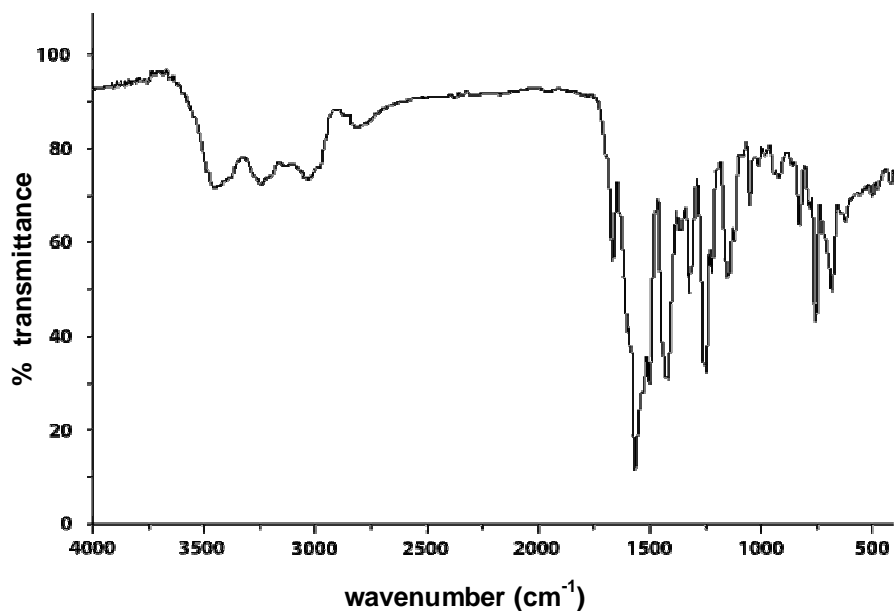
Figure 4.11. IR spectrum of the compound [CdL^1(CH$_3$COO)]$_2$·2CH$_3$OH (**9**).
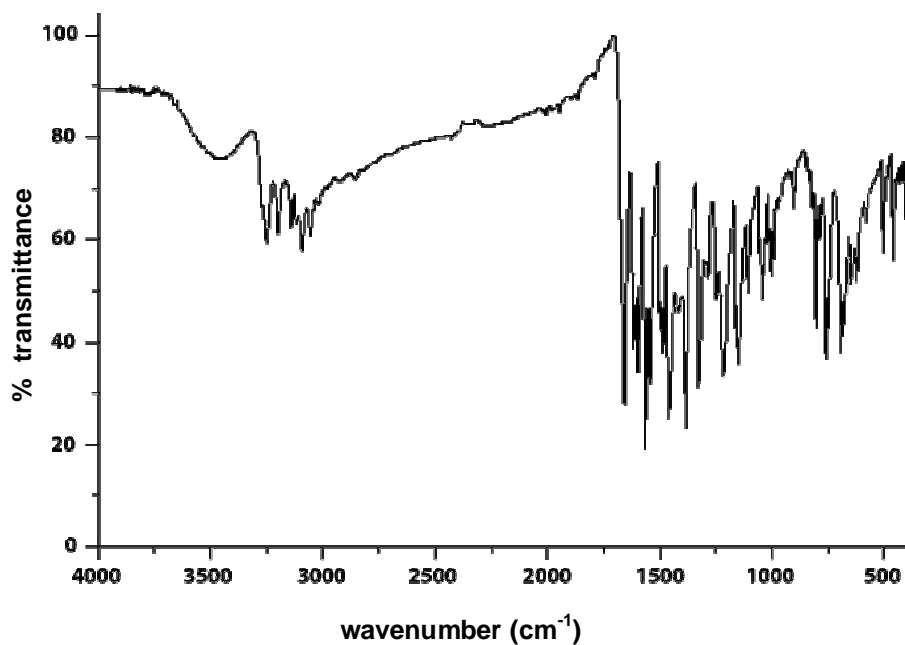
Figure 4.12. IR spectrum of the compound [Cd(HL^1)Br$_2$] (**10**).
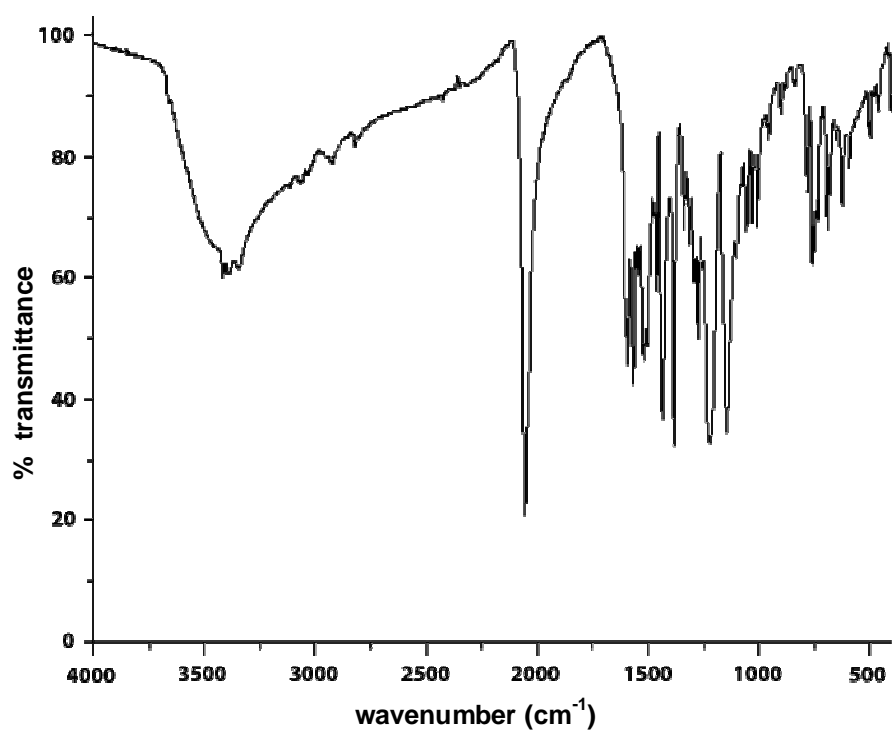
Figure 4.13. IR spectrum of the compound $[CdL^1N_3]_2$ (**11**).
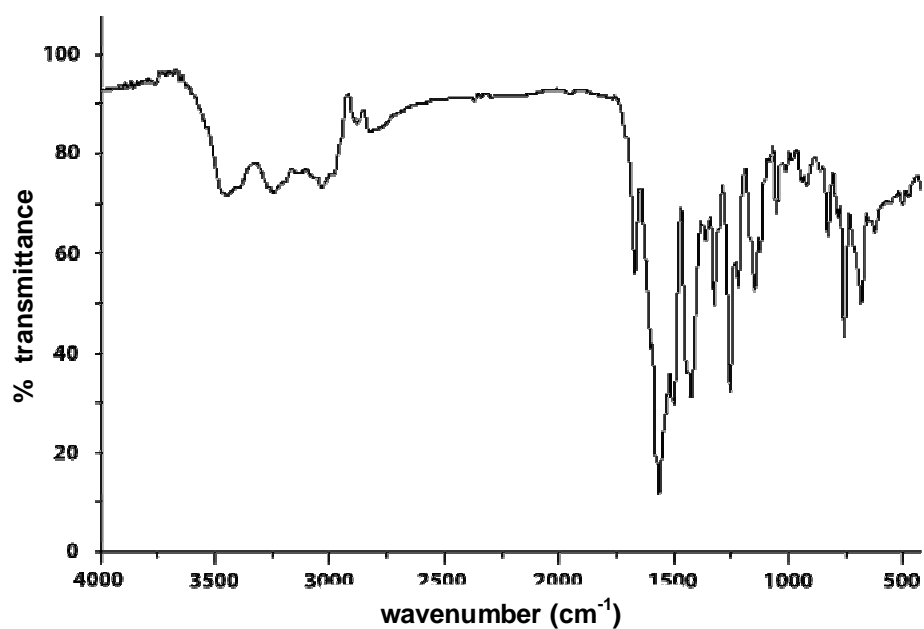
Figure 4.14. IR spectrum of the compound $[Cd(HL^2)(OAc)_2] \cdot {}^4/_3 H_2O$ (**12**).
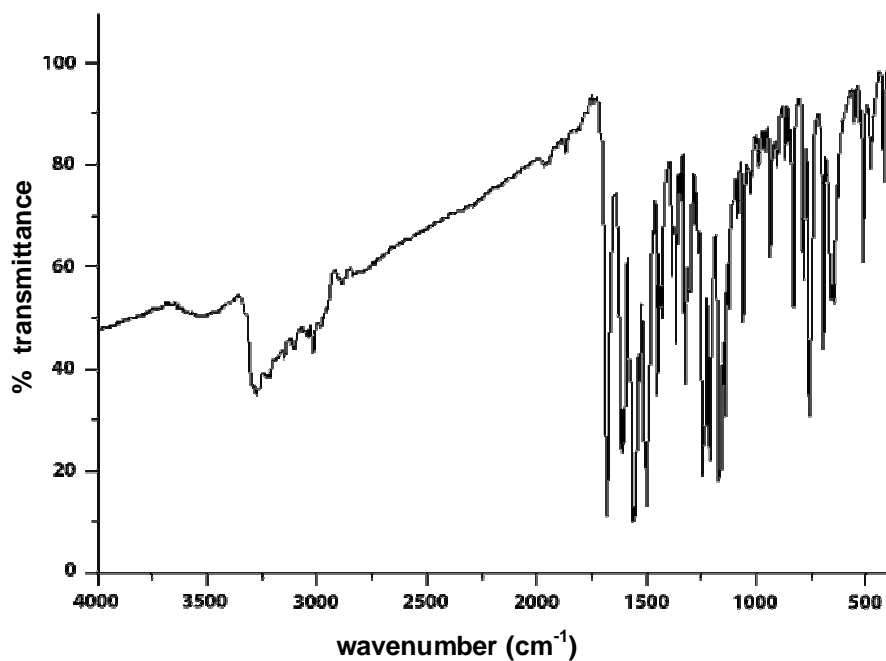
Figure 4.15. IR spectrum of the compound [Cd(HL^2)Cl$_2$]. $^4/_3$H$_2$O (**13**).
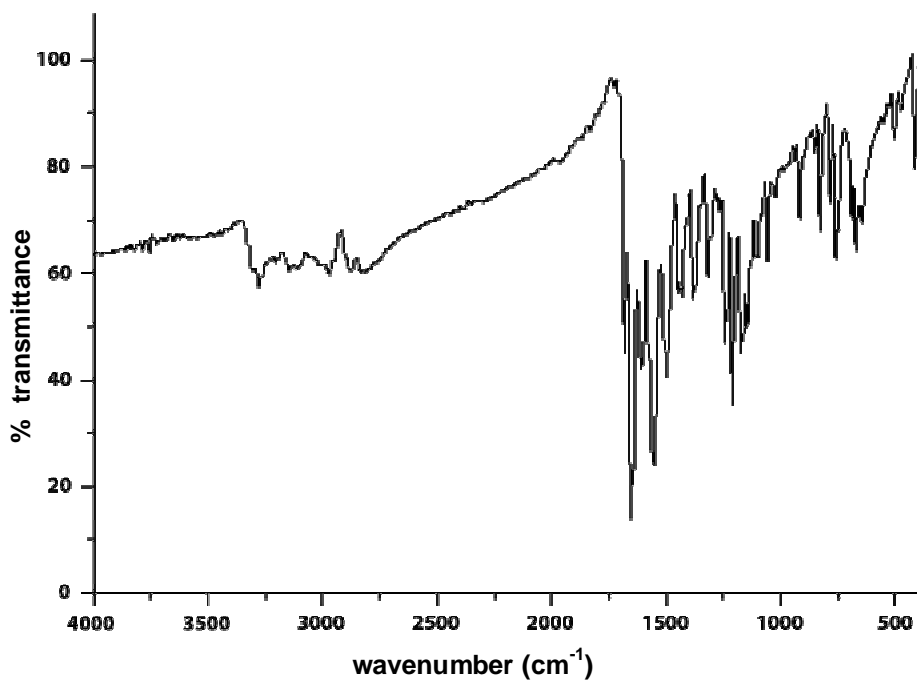
Figure 4.16. IR spectrum of the compound [Cd(HL^2)Br$_2$]·DMF (**14**).

4.3.3. Electronic spectra

The electronic absorption bands of the Cd(II) complexes, recorded in DMF solution, are given in Table 4.7. The energy of intraligand bands slightly changed upon complexation. This is due to the involvement of C=O bond and azomethine nitrogen atom in coordination [28]. The intraligand transitions are observed in the region 31270-31440 cm^{-1} for the compounds **9**-**11** whereas for the complexes **12**-**14** intraligand transitions are in the range 22360-32140 cm^{-1}. The new bands observed for the complexes **9**-**14** in the region 22360-24230 cm^{-1} are assigned to Cd(II) →O transitions. No appreciable absorptions occurred below 20000 cm^{-1} in DMF solution indicating the absence of *d-d* bands which is in accordance with d^{10} configuration of Cd(II) ion. Electronic spectra of complexes are presented in Figures 4.17-4.20.

Table 4.7. Electronic spectral assignments for the semicarbazones and its Cd(II) complexes

Compound	Absorbance, λ_{max} (cm^{-1})
HL^1	36300, 31160
[CdL^1(CH$_3$COO)]$_2$·2CH$_3$OH (**9**)	31440, 24230
[Cd(HL^1)Br$_2$] (**10**)	31270, 24140
[CdL^{1}N$_3$]$_2$ (**11**)	31380, 24090
HL^2	36940, 32200, 31300, 29900, 28770
[Cd(HL^2)(OAc)$_2$]·$^4/_3$H$_2$O (**12**)	32060, 30740, 29500, 23600
[Cd(HL^2)Cl$_2$] (**13**)	31270, 29900, 28720, 22360
[Cd(HL^2)Br$_2$]·DMF (**14**)	32140, 30650, 29330, 23870
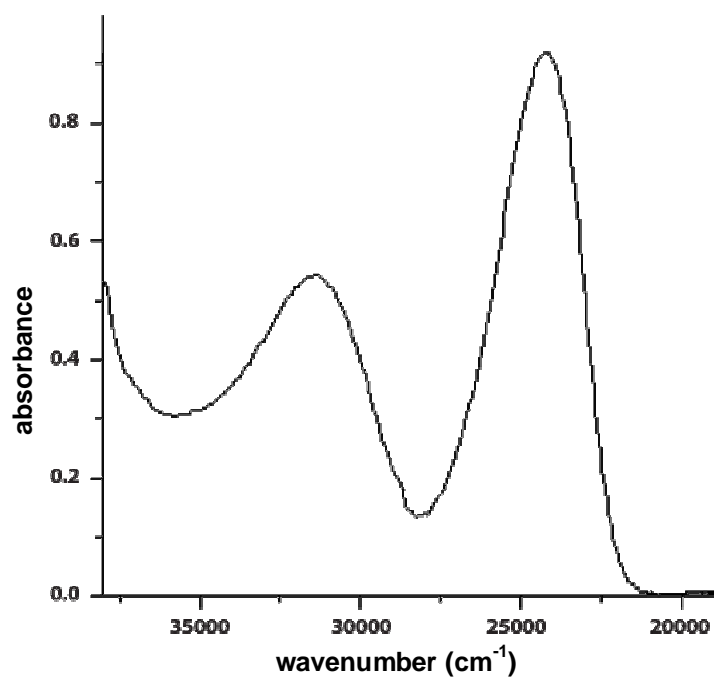
Figure 4.17. Electronic spectrum of the compound [CdL¹(CH₃COO)]₂ ·2CH₃OH (**9**).
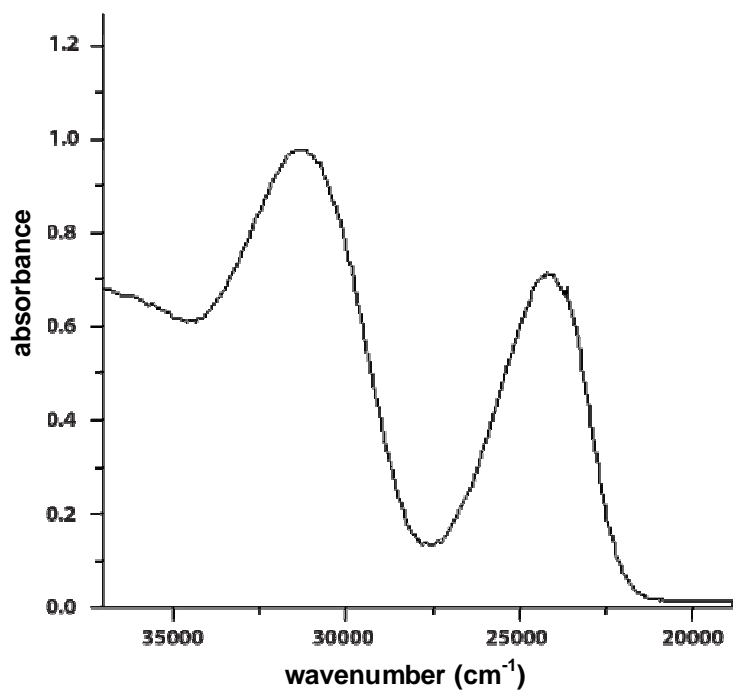
Figure 4.18. Electronic spectrum of the compound [Cd(HL¹)Br₂] (**10**).
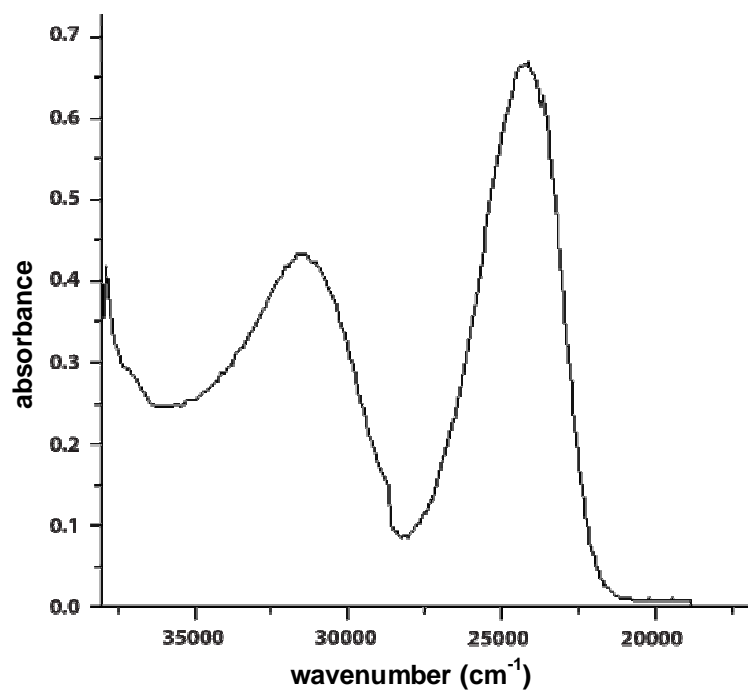
Figure 4.19. Electronic spectrum of the compound $[CdL^1N_3]_2$ (**11**).
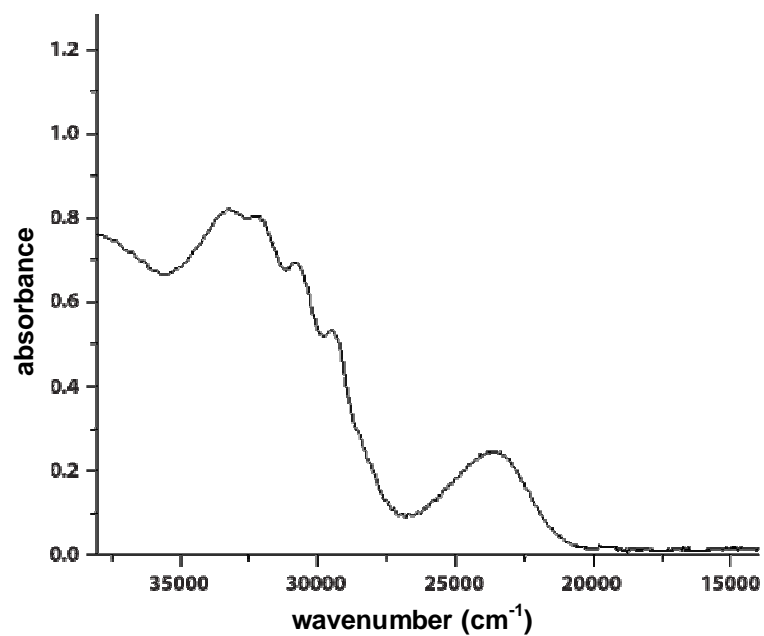
Figure 4.20. Electronic spectrum of the compound $[Cd(HL^2)(OAc)_2] \cdot {}^4/_3 H_2O$ (**12**).

References

[1]   Y. Jiao, G.A. Cynthia, B.D. Loraine, J. of the Science of Food and Agriculture 84 (2004) 777.

[2]   F. Michael, "New Mineral Names" American Mineralogist 65 (1980) 1065.

[3]   L. Pag, J.N. Lindner, G. Davies, D.E. Seitz, B.L Karger, *Anal. Chem.* 51 (1979) 433.

[4]   M.L. Post, J. Trotter, J. Chem. Soc., Dalton Trans. 7 (1974) 674.

[5]   P.A. Prasad, S. Neeraj, S. Natarajan, C.N.R. Rao, Chem. Commun. 14 (2000) 1251.

[6]   C.Y. Duan, Y.P. Tian, C.Y. Zhao, X.Z. You, T.C.W. Mak, Polyhedron 16 (1997) 2857.

[7]   CrysAlis CCD and CrysAlis RED Versions 1.171.29.2 (CrysAlis171. NET), Oxford Diffraction Ltd, Abingdon, Oxfordshire, England, 2006.

[8]   G.M. Sheldrick, Acta Cryst. A46 (1990) 467.

[9]   G.M Sheldrick, SHELXS-97, Program for X-ray Crystal Structure Refinement, University of Göttingen, Germany, 1997.

[10]   K. Brandenburg, Diamond Version 3.1d, Crystal Impact GbR, Bonn, Germany, 2006.

[11]   A.L. Spek, J. Appl. Cryst. 36 (2003) 7.

[12]   U.L. Kala, S. Suma, M.R.P. Kurup, S. Krishnan, R.P. John, Polyhedron 26 (2007) 1427.

[13]   V.M. Kolb, W.S. Joseph, T.E. Janota, W.L. Duax, J. Org. Chem. 54 (1989) 2341.

[14]   S. Sen, M.K. Saha, P. Kundu, S. Mitra, C. Kruger, J. Bruckmann, Inorg. Chim. Acta 288 (1999) 118.

[15]   A.F. Cameron, R.H. Nuttall, D.W. Taylor, J. Chem. Soc., Chem. Commun. 3 (1971) 129.

[16]   W. Clegg, J.T. Cressey, A. McCamley, B.P. Straughan, Acta Crystallogr. C51 (1995) 234.

[17] A.F. Cameron, R.H. Nuttall, D.W. Taylor, J. Chem. Soc., Dalton Trans. 15 (1972) 1608.

[18] D. Cremer, J.A. Pople, J. Am. Chem. Soc. 97 (1975) 1354.

[19] T.A. Reena, E.B. Seena, M.R.P. Kurup, Polyhedron 27 (2008) 1825.

[20] L. Latheef, M.R.P. Kurup, Spectrochim. Acta A 70 (2008) 86.

[21] T.A. Reena, E.B. Seena, M.R.P. Kurup, Polyhedron 27 (2008) 3461.

[22] A.W. Addison, T.N. Rao, J. Reedijk, J. Van Rijn, G.C. Verschoor, J. Chem. Soc., Dalton Trans. 7 (1984) 1349.

[23] G. Murphy, C.O. Sullivan, B. Murphy, B. Hathaway, Inorg. Chem. 37 (1998) 240.

[24] M. Vaidyanathan, R. Balamurugan, U. Sivagnanam, M. Palaniandavar, J. Chem. Soc., Dalton Trans. 23 (2001) 3498.

[25] M.T.H. Tarafder, A. Kasbollah, K.A. Crouse, A.M. Ali, B.M. Yamin, H.-K. Fun, Polyhedron 20 (2001) 2363.

[26] A. Sreekanth, H.-K. Fun, M.R.P. Kurup, Inorg. Chem. Commun. 7 (2004) 324.

[27] V. Philip, V. Suni, M.R.P. Kurup, M. Nethaji, Polyhedron 25 (2006) 1931.

[28] V. Philip, V. Suni, M.R.P. Kurup, M. Nethaji, Polyhedron 24 (2005) 1133.

[29] A. Majumder, G. M. Rosair, A. Mallick, N. Chattopadhyay, S. Mitra, Polyhedron 25 (2006) 1753.

[30] V. Philip, V. Suni, M.R.P. Kurup, M. Nethaji, Spectrochim. Acta A 64 (2006) 171.

[31] K. Nakamoto, Infrared and Raman spectra of Inorganic and Coordination compounds, fifth edition, Wiley, NY, 1997.

[32] R. Kruszynski, A. Turek, J. Coord. Chem. 57 (2004) 1089.

[33] A. Sreekanth, U.L. Kala, C.R. Nayar, M.R.P. Kurup, Polyhedron 23 (2004) 41.

[34] I. Ghassan, M.A. Khan, E. Chebli, G.M. Bouet, Trans. Met. Chem. 24 (1994) 294.

[35] G. Ibrahim, M.A. Khan, P. Richomme, O. Benali-Baitich, G. Bouet, Polyhedron 16 (1997) 3455.

[36] M.P. Swami, D. Gupta, M. Mohan, A.K. Srivastava, Prog. Nat. Acad. Sci. India A 50 (III) (1980) 176.

[37] E.M. Jouad, M. Allain, M.A. Khan, G.M. Bouet, Polyhedron 24 (2005) 327.

…..୧ଓ…..

Cu(II) COMPLEXES OF N^4-SUBSTITUTED SEMICARBAZONES: SYNTHESIS AND SPECTRAL STUDIES

Contents	**5.1 Introduction**
	5.2 Experimental
	5.3 Results and discussion

5.1. Introduction

Copper is one of the most abundant (25th in order of abundance) elements in the earth's crust. It exists in two oxidation states, copper(I) and copper(II). The most common oxidation state of copper is +2 and copper(II) complexes have been extensively studied. These complexes have tetrahedral, octahedral, square planar and trigonal bipyramidal geometries [1]. The role of copper in organic reactions is related to its oxidation states. This metal is used in the electrical industry due to high conductivity and it is also used for water pipes because of its inertness. Copper catalyses redox reactions in biological systems primarily in the reduction of oxygen to water [2]. Due to the presence of unpaired electron, all the copper(II) complexes are paramagnetic.

Considerable interest in Schiff base compounds containing thiosemicarbazones and their transition metal complexes has grown in the areas of biology and chemistry due to biological activities [3-5]. But semicarbazone analogs received much less attention. However, semicarbazones are also reported to possess versatile structural features [6]. Their metal complexes, especially

those containing copper(II) and iron(II) are more active than uncoordinated semicarbazones and this enhanced biological activity of metal semicabazones has been under investigation for some time [7]. Copper(II) complexes are interesting due to their biological roles and medicinal properties.

This chapter deals with the synthesis and characterization of mononuclear and binuclear copper(II) complexes with potential NNO donor ligands, di-2-pyridyl ketone-N^4-phenyl-3-semicarbazone (HL^1) and quinoline-2-carboxaldehyde-N^4-phenyl-3-semicarbazone (HL^2).

5.2. Experimental
5.2.1. Materials
The semicarbazones were synthesized as discussed in Chapter 2. Solvents used were ethanol, methanol and water. Copper(II) acetate monohydrate, copper(II) sulfate pentahydrate, copper(II) nitrate hemipentahydrate, copper(II) chloride dihydrate, sodium azide and potassium thiocyanate (all are BDH, AR grade) were used as received.

5.2.2. Synthesis of complexes
[Cu$_3$L$_2^1$Cl$_4$]·4H$_2$O (15)

A solution of semicarbazone, HL^1 (0.317 g, 1 mmol) in 20 ml of methanol was treated with a methanolic solution of the copper(II) chloride dihydrate (0.170 g, 1 mmol). The solution was heated under reflux for 4 h. The complex formed was filtered, washed with ether and dried over P$_4$O$_{10}$ *in vacuo.*
Yield ~0.48 g

[CuL^{1}OAc] (16)

This complex was synthesized by refluxing methanolic solution of HL^1 (0.317 g, 1 mmol) and solution of copper(II) acetate monohydrate (0.199 g, 1 mmol) in methanol for 4 h. The complex formed was filtered, washed with ether and dried over P$_4$O$_{10}$ *in vacuo.*
Yield ~0.50 g.

[CuL¹NO₃]₂ (17)

This complex was synthesized by refluxing methanolic solution of HL^1 (0.317 g, 1 mmol) and copper(II) nitrate hemipentahydrate (0.120 g, 0.5 mmol). The complex formed was collected, washed with ether and dried over P_4O_{10} *in vacuo.*

Yield ~0.39 g.

[CuL¹N₃] (18)

A solution of HL^1 (0.158 g, 0.5 mmol) in 20 ml of methanol was treated with a methanolic solution of copper(II) acetate monohydrate (0.099 g, 0.5 mmol). The solution was heated under reflux for 1 h and sodium azide (0.032 g, 0.5 mmol) was added in portions to the solution and further refluxed for 2 h. The resulting solution was allowed to stand at room temperature and after slow evaporation complex was separated out, which was collected, washed with ether and dried over P_4O_{10} *in vacuo.*

Yield ~0.55 g.

[CuL¹SCN]·³/₂H₂O (19)

For the synthesis of this complex, methanolic solutions of HL^1 (0.158 g, 0.5 mmol) and copper(II) acetate monohydrate (0.099 g, 0.5 mmol) were refluxed for 1 h and methanolic solution of KCNS (0.048 g, 0.5 mmol) was added and further refluxed for 3 h. The resulting solution was allowed to stand at room temperature and after slow evaporation complex was separated out, which was collected, washed with ether and dried over P_4O_{10} *in vacuo.*

Yield ~0.48 g.

[Cu(HL¹)L¹]₂(ClO₄)₂·6H₂O (20)

A solution of HL^1 (0.317 g, 1 mmol) in 20 ml of methanol was treated with a methanolic solution of the copper(II) perchlorate hexahydrate (0.185 g, 0.5 mmol).

The solution was stirred for 2 h. The complex formed was filtered, washed with ether and dried over P_4O_{10} *in vacuo.*

Yield ~0.52 g.

[Cu(HL^2)Cl$_2$]$_2$·H$_2$O (21)

An aqueous solution of the copper(II) chloride dihydrate (0.170 g, 1 mmol) is mixed with a solution of the semicarbazone, HL^2 (0.290 g, 1 mmol) in DMF. The resulting solution was refluxed for 5 h. The complex formed was filtered, washed with ether and dried over P_4O_{10} *in vacuo.*

Yield ~0.39 g.

[CuL^{2}OAc]·^{6}/$_5$H$_2$O (22)

This complex was synthesized by refluxing a solution of HL^2 (0.290 g, 1 mmol) in DMF and solution of copper(II) acetate monohydrate (0.199 g, 1 mmol) in methanol for 5 h. The complex formed was filtered, washed with ether and dried over P_4O_{10} *in vacuo.*

Yield ~0.35 g.

[CuL^{2}N$_3$]·CH$_3$OH (23)

A solution of HL^2 (0.145 g, 0.5 mmol) in 20 ml of DMF was treated with a methanolic solution of copper(II) acetate monohydrate (0.099 g, 0.5 mmol). The solution was heated under reflux for 2 h and sodium azide (0.032 g, 0.5 mmol) was added in portions to the solution and further refluxed for 2 h. The resulting solution was allowed to stand at room temperature and after slow evaporation complex was separated out, which was collected, washed with ether and dried over P_4O_{10} *in vacuo.*

Yield ~0.51 g.

5.2.3. Analytical methods

The carbon, hydrogen and nitrogen analyses were carried out using a Vario EL III CHNS analyzer at SAIF, Kochi, India. Infrared spectra were recorded on a

JASCO FT-IR-5300 Spectrometer in the range 4000-400 cm^{-1} using KBr pellets. Electronic spectra were recorded on a Cary 5000, version 1.09 UV-VIS-NIR Spectrophotometer using solutions in DMSO. Magnetic susceptibility measurements were carried out on a Vibrating Sample Magnetometer using Hg[Co(SCN)$_4$] as a calibrant. EPR spectra were recorded on a Varian E-112 X-band EPR Spectrometer using TCNE as a standard at SAIF, IIT, Bombay, India. Molar conductivity measurements were made in DMSO solutions.

5.3. Results and discussion

The semicarbazones HL^1 and HL^2 were synthesized by the direct condenzation of N^4-phenylsemicarbazide with di-2-pyridyl ketone and quinoline-2-carboxaldehyde respectively. These semicarbazones can coordinate with metal ions in keto and enol forms.

The complexes, [CuL^{1}NO$_3$]$_2$ (**17**) and [Cu(HL^1)L^1]$_2$(ClO$_4$)$_2$·6H$_2$O (**20**) were formed by the reaction of the semicarbazone, HL^1 with appropriate copper(II) salt in the molar ratio 2:1. The complexes [Cu$_3$L$_2^1$Cl$_4$]·4H$_2$O (**15**), [CuL^{1}OAc] (**16**), [Cu(HL^2)Cl$_2$]$_2$ H$_2$O (**21**) and [CuL^{2}OAc]·^{6}/$_5$H$_2$O (**22**) were formed by the reaction of the semicarbazones with copper(II) salts in 1:1 molar ratio. In complexes [CuL^{1}N$_3$] (**18**), [CuL^{2}N$_3$]·CH$_3$OH (**23**) and [CuL^{1}SCN]·^{3}/$_2$H$_2$O (**19**), acetate anion was metathetically displaced by azide or thiocyanate anion. In the complex **21,** the semicarbazone HL^2 is coordinated as neutral keto form whereas in complex **20**, one of the molecules of the semicarbazone, HL^1 coordinates in keto form and second molecule of semicarbazone undergoes deprotonation. In all other complexes semicarbazones are coordinated in deprotonated enolate form. Complexes **15**, **19, 20, 21** and **22** contain uncoordinated water molecules. Complexes **16** and **18** have general formula MLX where X is OAc and N$_3$ respectively. The stoichiometry we assigned for all copper(II) complexes are in good agreement with CHN analyses data. For compound **15**, a structure with

bridged chlorine atoms is proposed and in this compound third copper atom undergoes covalent bonding with pyridyl nitrogen atoms. The proposed structure of compound **15** is shown in the Figure 5. 1.
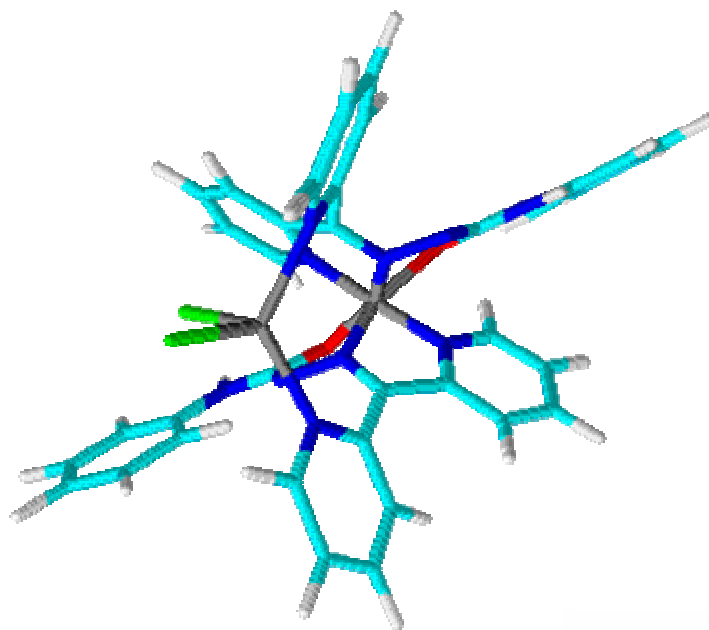
Figure 5.1. Proposed structure of compound **15** (water molecules are omitted).

Magnetic moments of the complexes were calculated from magnetic susceptibility measurements. Present mononuclear copper(II) complexes exhibit magnetic moments in the range 1.51-2.04 B.M., which are close to their spin-only value. Magnetic moments of binuclear copper(II) complexes **17**, **20** and **21** are at 1.40, 1.12 and 1.28 B.M. respectively [8]. Low values of magnetic moments for the binuclear complexes suggest the presence of strong antiferromagnetic spin-spin interactions. The conductivity measurements were carried out in DMSO solutions and all the complexes except **15** and **20** were found to be non-electrolytes [9]. Higher conductivity for the complex **15** may be due to the partial ionization of the complex in DMF solution. Attempts to isolate single crystals suitable for X-ray diffraction studies were unsuccessful. The analytical data of the complexes are presented in Table 5.1.

Table 5.1. Colors, elemental analyses, magnetic susceptibilities and molar conductivities of copper(II) complexes of HL^1 and HL^2

Compound	Color	Found (Calculated) %			μ (B.M.)	Λ_M^a
		C	H	N		
HL^1	Colorless	67.44 (68.13)	4.80 (4.76)	22.14 (22.07)	-	-
$[Cu_3L2^1Cl_4]\cdot4H_2O$ (15)	Green	41.38 (41.69)	3.51 (3.50)	13.46 (13.50)	1.36	91
$[CuL^1OAc]$ (16)	Brown	54.48 (54.73)	3.61 (3.90)	15.82 (15.96)	1.76	2
$[CuL^1NO_3]_2$ (17)	Green	49.86 (48.92)	3.60 (3.19)	19.71 (19.02)	1.40	24
$[CuL^1N_3]$ (18)	Green	51.40 (51.24)	3.10 (3.34)	26.10 (26.56)	2.04	5
$[CuL^1SCN]\cdot^3/_2H_2O$ (19)	Brown	48.43 (49.08)	3.11 (3.69)	18.47 (18.07)	2.01	20
$[Cu(HL^1)L^1]_2(ClO_4)_2\cdot6H_2O$ (20)	Green	50.1 (50.83)	3.7 (4.15)	16.3 (16.46)	1.52	91
HL^2	Colorless	70.13 (70.33)	4.99 (4.86)	19.22 (19.30)	-	-
$[Cu(HL^2)Cl_2]_2\cdot H_2O$ (21)	Brown	46.87 (47.07)	3.30 (3.49)	12.71 (12.92)	1.28	5
$[CuL^2OAc]\cdot6/5H_2O$ (22)	Brown	51.98 (52.64)	3.90 (4.28)	13.59 (12.92)	1.64	6
$[CuL^2N_3]\cdot CH_3OH$ (23)	Green	50.13 (50.64)	3.42 (4.01)	22.15 (22.97)	1.51	5

a = $ohm^{-1}\ cm^2\ mol^{-1}$

5.3.1. Infrared spectra

The IR spectra of compounds were recorded with KBr discs in the range 4000-400 cm^{-1}. The characteristic IR bands of the complexes differ from their semicarbazones, HL^1 and HL^2 and provide significant indications regarding the coordination and bonding sites of semicarbazones. The significant IR bands with the tentative assignments of the copper(II) complexes are presented in Table 5.2.

The presence of a strong band at 1718 cm^{-1} for the semicarbazone, HL^1 is assigned to C=O stretching vibration, which is absent in complexes **15-19**. This indicates that in these complexes, HL^1 has undergone deprotonation and coordinated in enolate form. But in complex **20,** a band at 1679 cm^{-1} is assigned as v(C=O) which has undergone a shift and coordination is through keto oxygen atom [10]. The coordination through keto/enol oxygen atom is further corroborated with the appearance of a band at 413-456 cm^{-1} region due to v(Cu–O) stretch in the spectra of the complexes [11-13]. The v_a(NH) vibrations of the imino group is observed at 3369 cm^{-1} in the IR spectrum of HL^1 and this band disappears in the spectra of the complexes except **20**, providing a strong evidence for the ligand coordination around copper(II) ion in the deprotonated form [14]. The intense band at 1591 cm^{-1} in the spectrum of HL^1 has been assigned to v(C=N) of the semicarbazone moiety. This band is shifted to lower wavenumbers by 23-35 cm^{-1} in the spectra of complexes indicating coordination *via* the azomethine nitrogen [15,16]. Coordination of azomethine nitrogen is consistent with the presence of a band at *ca*. 504-511 cm^{-1}, assignable to v(Cu–N$_{azo}$) for these complexes [17,18]. But with loss of proton from N, another strong band is found in the region 1599-1597 cm^{-1} which may be due to the newly formed C=N bond as a result of enolization of the semicarbazone in complexes **15-20**, again confirms the coordination *via* enolate oxygen. The increase in v(N–N) in the spectra of complexes in the

range 1143-1154 cm^{-1} is due to enhanced double bond character through chelation, thus offsetting the loss of electron density *via* donation to the metal ion, and is supportive of azomethine coordination. Coordination of the pyridyl nitrogen causes the out-of-plane bending vibrational band to shift from 601 cm^{-1} to higher frequencies 625, 615, 634, 621, 621 and 690 cm^{-1} respectively for the complexes **15**-**20** [19].

The asymmetric and symmetric stretching vibrations of the acetate group appear at 1520 and 1384 cm^{-1} respectively for the acetato complex **16** [20,21]. For the nitrato complex **17** three strong bands at 1542, 1384 and 1298 cm^{-1} are observed corresponding to v_1, v_2 and v_4 of the nitrato group indicating the presence of a terminal monodentate coordination of the nitrato group [22]. A combination of $(v_{1+}v_2)$ considered as diagnostic for the monocoordinate nitrato group, has been observed at 1698 cm^{-1} [23]. v_3, v_5 and v_6 couldn't be assigned due to the richness of the spectrum of the complex. The azido complex **18** shows a single strong band at 2054 cm^{-1} due to the asymmetric stretching mode and the band associated with symmetric stretching mode is located at 1387 cm^{-1}. Thiocyanato complex **19** has a very strong band at 2091 cm^{-1}, a medium band at 775 cm^{-1} and a weak band at 493 cm^{-1} corresponding to v(CN), v(CS) and δ(NCS) respectively [24]. The intensity and band position indicates the unidentate coordination of the thiocyanate through nitrogen atom. Perchlorate anion coordinates to the metal only when its complexes are prepared in non-aqueous solvents. The perchlorato complex **20** shows a broad band at 1097 cm^{-1} corresponding to v_3(ClO$_4$) and an unsplit strong band at 621 cm^{-1} assignable to v_4(ClO$_4$) [25]. This along with the absence of a band corresponding to v_1 at 920 cm^{-1}, indicates the presence of an ionic perchlorate group [26]. IR spectra of complexes **15**-**20** are presented in Figures 5.2-5.7.

Table 5.2. Infrared spectral assignments (cm^{-1}) of semicarbazones and copper(II) complexes

Compound	ν(NH)	ν(C=N)	ν(CO)	ν(C=N)[a]	ν(N–N)	ν(Cu–N$_{azo}$)	ν(Cu–O)
HL^1	3369	1591	1718	-	1129	-	-
[Cu$_3$L$_2^1$Cl$_4$]·4H$_2$O(15)	-	1568	-	1599	1154	504	447
[CuL^{1}OAc] (16)	-	1562	-	1598	1146	507	413
[CuL^{1}NO$_3$]$_2$ (17)	-	1568	-	1597	1147	508	456
[CuL^{1}N$_3$] (18)	-	1562	-	1599	1144	504	414
[CuL^{1}SCN]·$^3/_2$H$_2$O (19)	-	1556	-	1598	1143	511	413
[Cu(HL^1)L^1]$_2$(ClO$_4$)$_2$·6H$_2$O (20)	3359	1562	1679	1599	1154	504	414
HL^2	3380	1592	1702	-	1150	-	-
[Cu(HL^2)Cl$_2$]$_2$·H$_2$O (21)	3207	1556	1694	-	1167	551	502
[CuL^{2}OAc]·$^6/_5$ H$_2$O (22)	-	1567	-	1599	1161	560	505
[CuL^{2}N$_3$]·CH$_3$OH (23)	-	1562	-	1586	1160	555	509

[a] Newly formed C=N
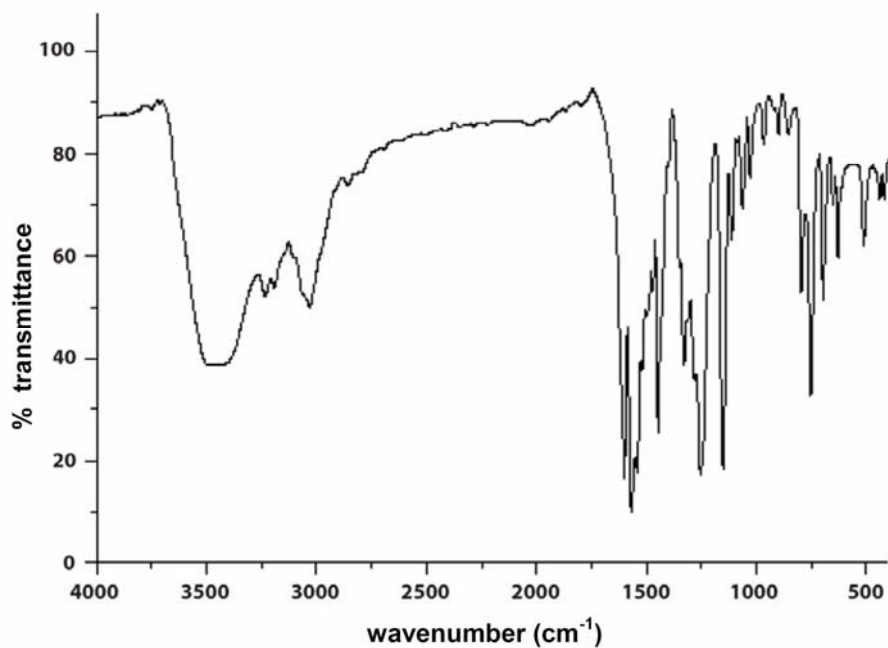
Figure 5.2. IR spectrum of the compound [Cu$_3$L$_2^1$Cl$_4$]·4H$_2$O (**15**).
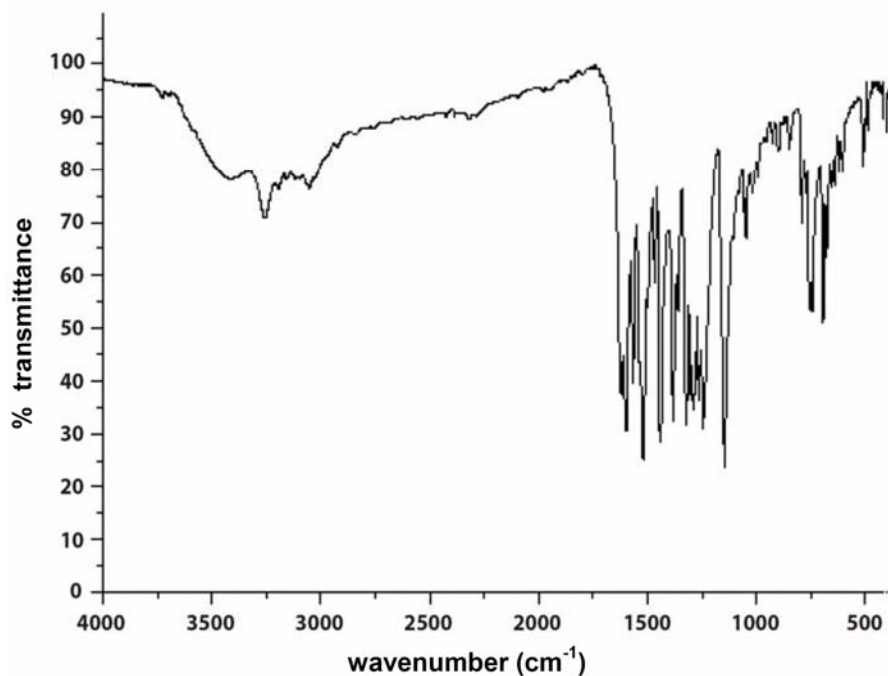
Figure 5.3. IR spectrum of the compound [CuL^{1}OAc] (**16**).
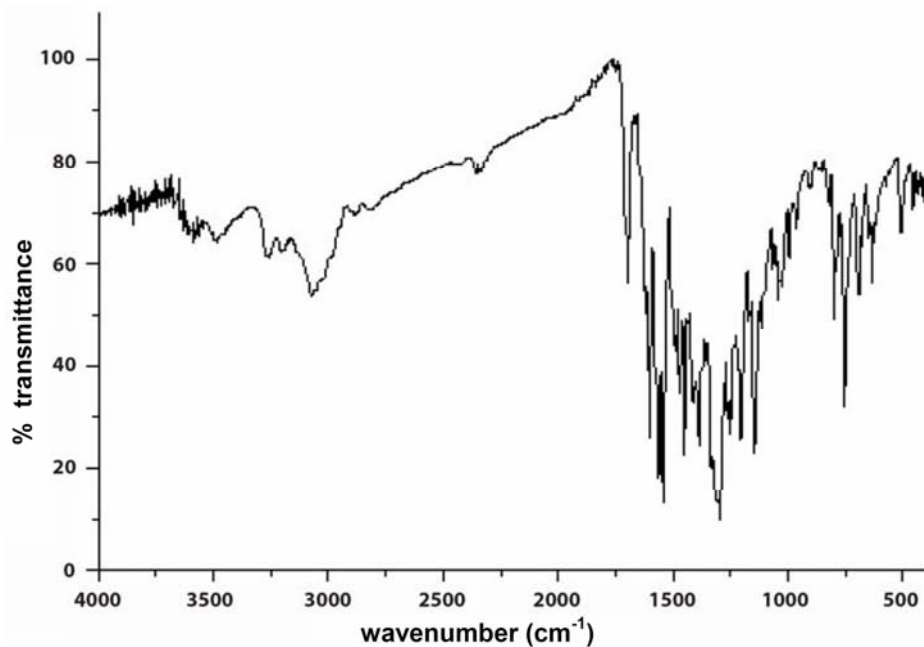
Figure 5.4. IR spectrum of the compound [CuL^{1}NO$_3$]$_2$ (**17**).
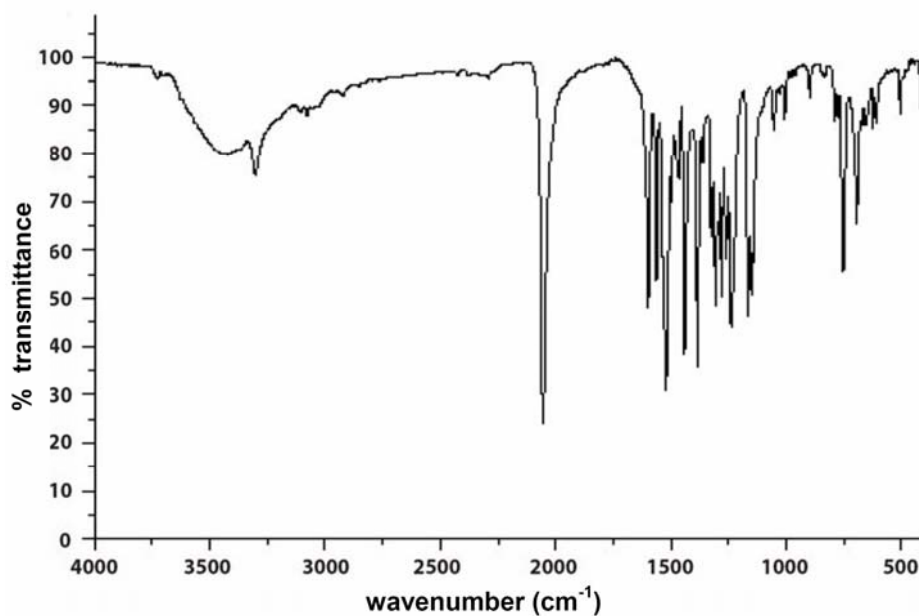
Figure 5.5. IR spectrum of the compound [CuL^{1}N$_3$] (**18**).
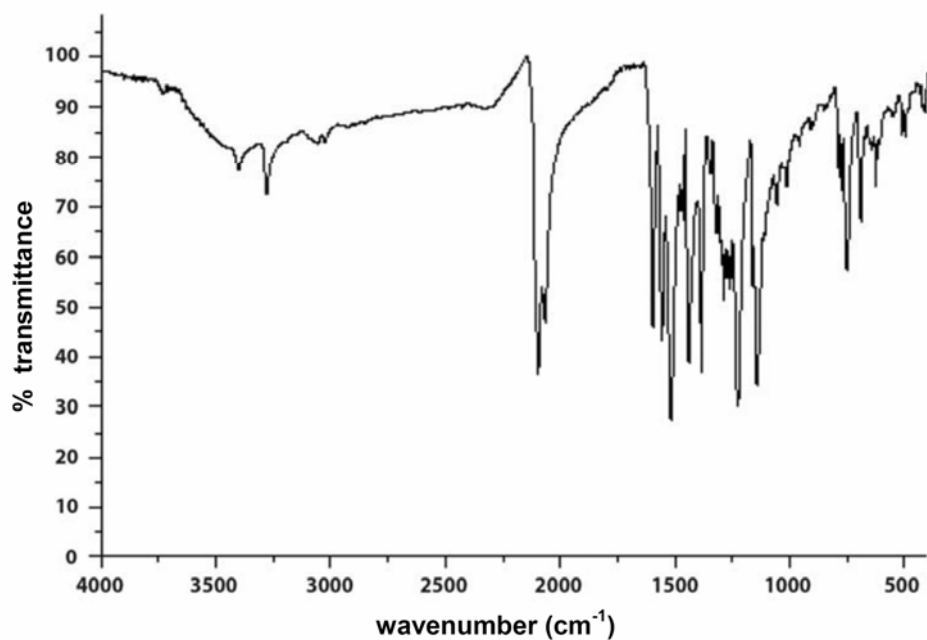
Figure 5.6. IR spectrum of the compound [CuL^{1}SCN]·^{3}/$_2$H$_2$O (**19**).
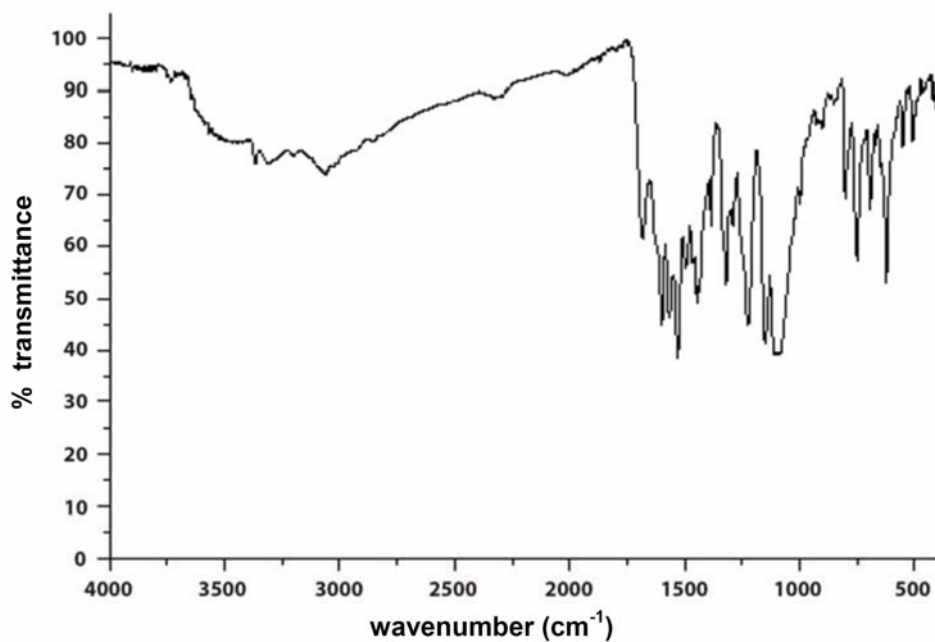
Figure 5.7. IR spectrum of the compound [Cu(HL^1)L^1]$_2$(ClO$_4$)$_2$·6H$_2$O (**20**).

The presence of a band in the spectrum of the semicarbazone, HL^2 at 1702 cm^{-1} is due to $v(C=O)$, which is shifted to 1694 cm^{-1} in the chloro complex **21**. This indicates that in this complex semicarbazone, HL^2 is coordinated in the neutral, keto form. But this band is absent in complexes **22** and **23**, which means that in these complexes HL^2 is coordinated as enol form. This is supported by the fact that in complexes **22** and **23** new bands are observed at 1599 and 1586 cm^{-1}, which are due to newly formed $v(C=N)$ after enolization. However this band is absent in complex **21**. Upon complexation, the azomethine stretching vibration was shifted from 1592 cm^{-1} to lower wavenumbers in the range 1556-1567 cm^{-1}. In the complexes **21**-**23,** there is an increase in $v(N-N)$ in the range 1160-1167 cm^{-1} which confirms the coordination of the semicarbazone through azomethine nitrogen.

For the chloro complex **21**, the bands at 1243 and 1119 cm^{-1} correspond to the in-plane vibrations of the quinoline ring while out-of-plane vibrations are observed at 744 and 686 cm^{-1}. The bands at 551 and 502 cm^{-1} are assigned to $v(Cu-N_{azo})$ and $v(Cu-O)$ respectively. For the acetato complex **22,** the band at 1249 cm^{-1} corresponds to the in-plane vibration of the quinoline ring while out-of-plane vibrations are observed at 753 and 692 cm^{-1}. The bands at 560 and 505 cm^{-1} are assigned to $v(Cu-N_{azo})$ and $v(Cu-O)$ respectively. For this complex, the bands at 1510 and 1469 cm^{-1} correspond to asymmetric and symmetric stretching vibrations of the acetate group respectively. For the azido complex **23,** a sharp band at 2054 cm^{-1} correspond to the asymmetric $v(N_3)$ mode. The band associated with the symmetric $v(N_3)$ mode is observed at 1344 cm^{-1}. The broad band observed at 652 cm^{-1} is assigned to $\partial(N-N-N)$. The bands at 1247 and 1118 cm^{-1} correspond to the in-plane vibrations of the quinoline ring while out-of-plane vibrations are observed at 751 and 692 cm^{-1}. The bands at 555 and 509 cm^{-1} are assigned to $v(Cu-N_{azo})$ and $v(Cu-O)$ respectively. The IR spectra of the complexes are presented in Figures 5.8-5.10.
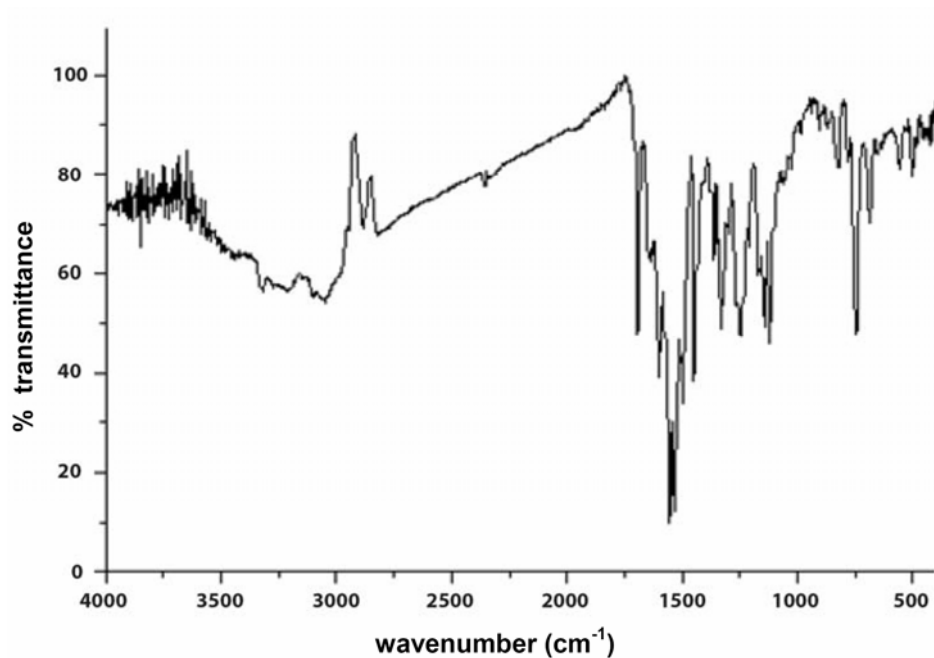
Figure 5.8. IR spectrum of the compound $[Cu(HL^2)Cl_2]_2 \cdot H_2O$ (**21**).
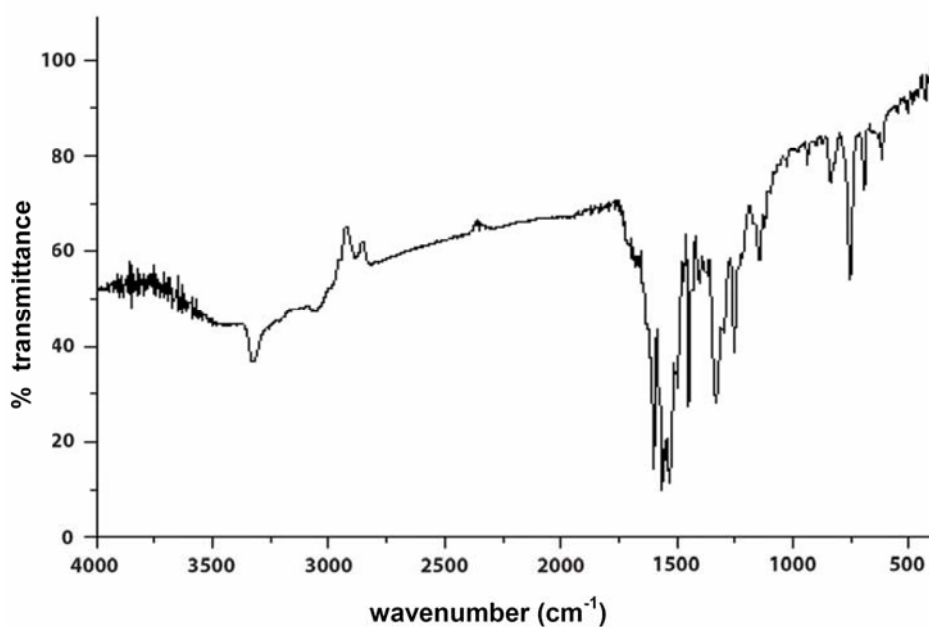
Figure 5.9. IR spectrum of the compound $[CuL^2OAc] \cdot {}^6/_5 H_2O$ (**22**).
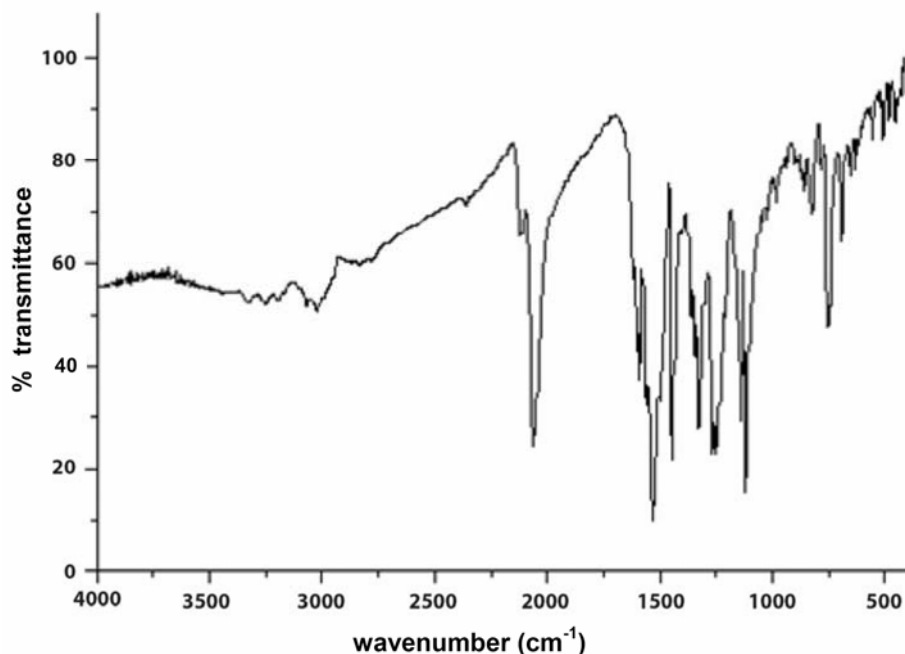
Figure 5.10. IR spectrum of the compound [CuL^{2}N$_3$]·CH$_3$OH (**23**).

5.3.2. Electronic spectra

The electronic spectral data of semicarbazones and copper(II) complexes recorded in DMSO solution are given in Table 5.3 and electronic spectra are shown in the Figures 5.11-5.17. The semicarbazones HL^1 and HL^2 have absorptions at 36300 and 36940 cm^{-1} respectively due to π-π* transitions of the pyridyl ring/quinoline ring and imine function of the semicarbazone moiety. Bands in the region 28770-32200 cm^{-1} correspond to n-π* transitions of the amide function [27] for HL^1 and HL^2. This intraligand transitions are observed in the range 32290-28800 cm^{-1}, which undergoes shift upon complexation. This shift may be due to the weakening of C=O bond and donation of lone pair of electrons to the metal on complexation.

The high intense ligand-to-metal charge transfer (LMCT) transitions are observed at high energy region. The intensity of these transitions reflects the overlap of the ligand and metal orbitals involved in the charge transfer. In all

the complexes 1**5**-**23**, LMCT transitions are observed in the region 22100-24050 cm^{-1} and which are assigned to O→ Cu and N→ Cu LMCT transitions. In the chloro complex **21** shoulder region is observed at 28800 cm^{-1}, which is assigned as Cl→ Cu charge-transfer transition [28]. For a tetragonal field three spin allowed transitions, $^2A_{1g}←^2B_{1g}$, $^2B_{2g}←^2B_{1g}$ and $^2E_{g}←^2B_{1g}$ are possible and square pyramidal complexes have the d_{yz}, $d_{xz}← d_{x^2-y^2}$ and $d_{z^2}←d_{x^2-y^2}$ transitions. But it is difficult to resolve them into separate bands due to the very low energy difference between these bands. All copper(II) complexes **15**-**23** have very broad *d-d* combination bands (Figures 5.18-5.21) in the range 14000-16000 cm^{-1} [29,30].

Table 5.3. Electronic spectral assignments of semicarbazones and their Cu(II) complexes

Compound	Absorbance, λ_{max} (cm^{-1})	LMCT	*d-d*
HL^1	36300, 31160	-	-
[Cu$_3$L$_2^1$Cl$_4$]·4H$_2$O (**15**)	32030	23820	14590
[CuL^{1}OAc] (**16**)	31940	23880	15200
[CuL^{1}NO$_3$]$_2$ (**17**)	31780	24050	14590
[CuL^{1}N$_3$] (**18**)	32110	23940	16000
[CuL^{1}SCN]·$^3/_2$H$_2$O (**19**)	32290	23970	14600
[Cu(HL^1)L^1]$_2$(ClO$_4$)$_2$·6H$_2$O (**20**)	31270	23630	15300
HL^2	36940, 32200, 31300, 29900, 28770	-	-
[Cu(HL^2)Cl$_2$]$_2$·H$_2$O (**21**)	31940, 30160	22100,28800	15380
[CuL^{2}OAc]·$^6/_5$ H$_2$O (**22**)	31780	22780	15620
[CuL^{2}N$_3$]·CH$_3$OH (**23**)	31860	22270	14000
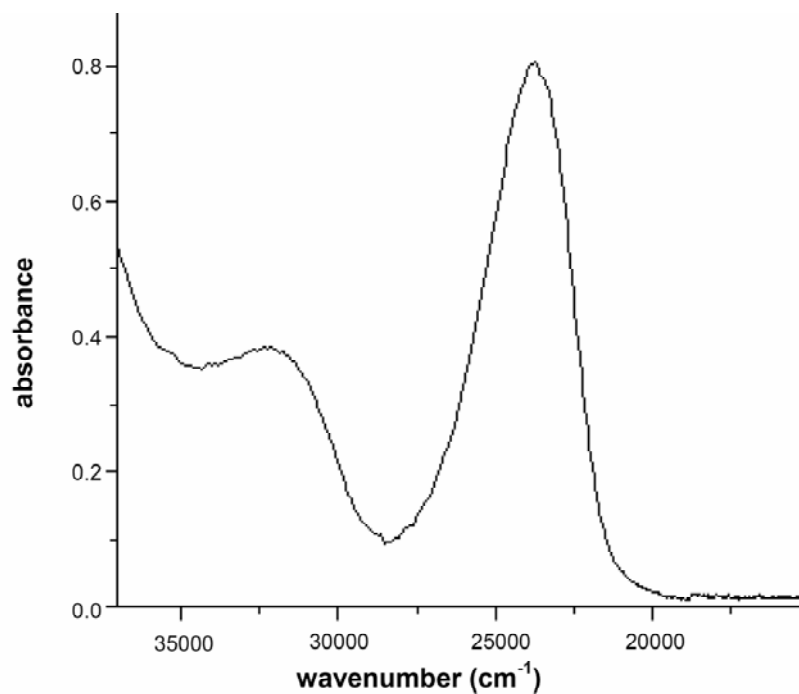
Figure 5.11. Electronic spectrum of the compound $[Cu_3L_2{}^1Cl_4]\cdot 4H_2O$ (**15**).
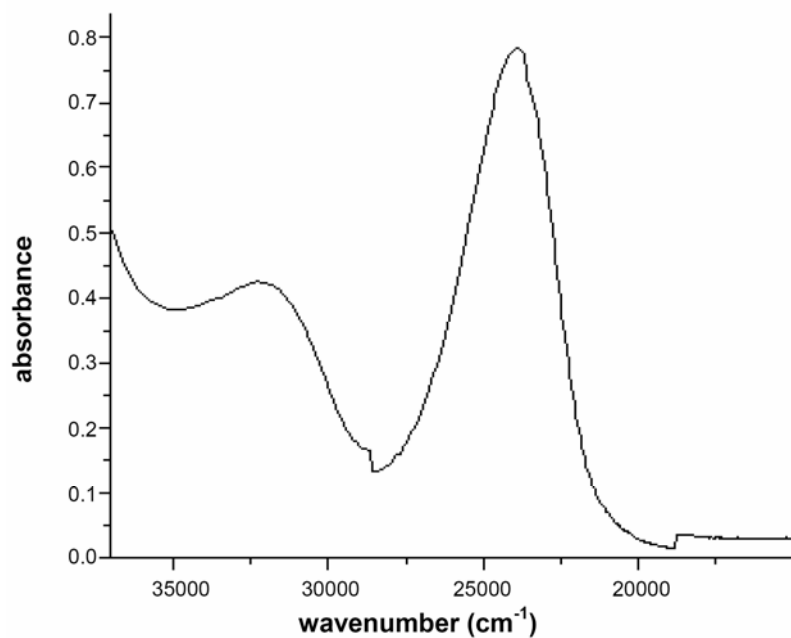
Figure 5.12. Electronic spectrum of the compound $[CuL^1OAc]$ (**16**).
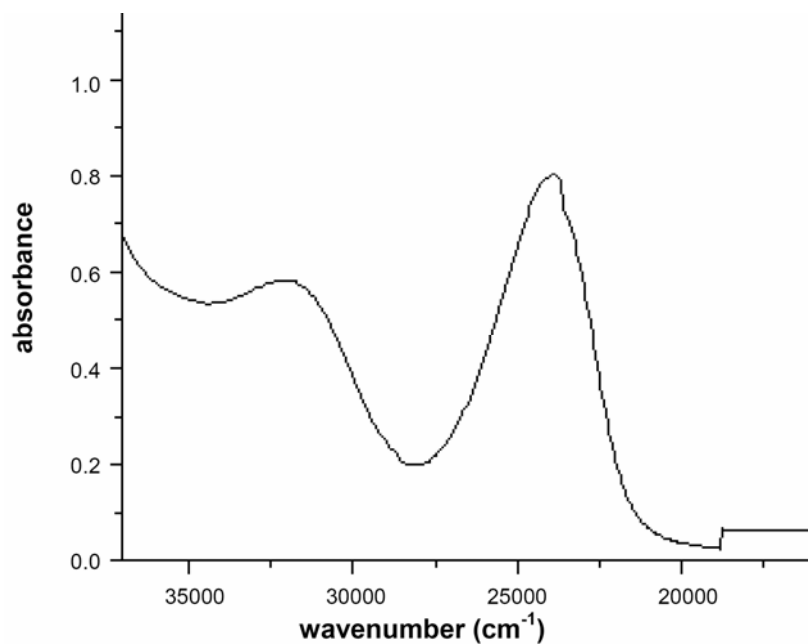
Figure 5.13. Electronic spectrum of the compound $[CuL^1NO_3]_2$ **(17)**.
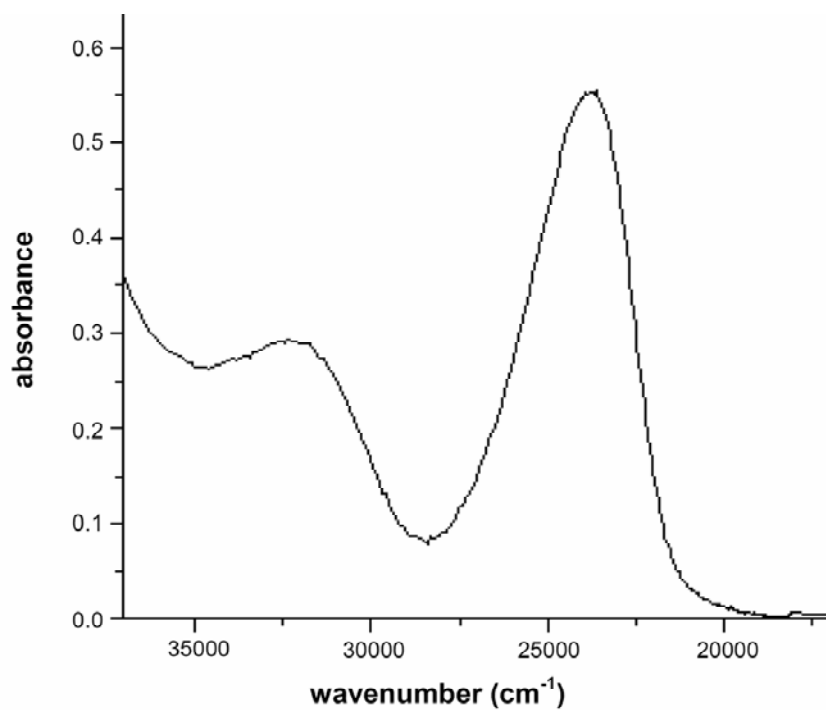
Figure 5.14. Electronic spectrum of the compound $[CuL^1N_3]$ **(18)**.
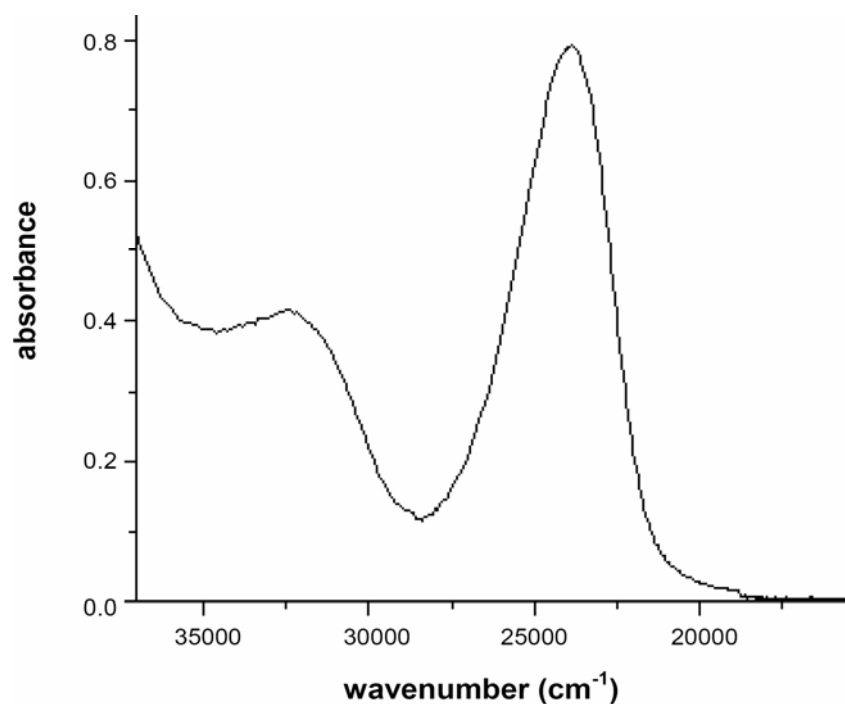
Figure 5.15. Electronic spectrum of the compound $[CuL^1SCN] \cdot {}^3/_2 H_2O$ (**19**).
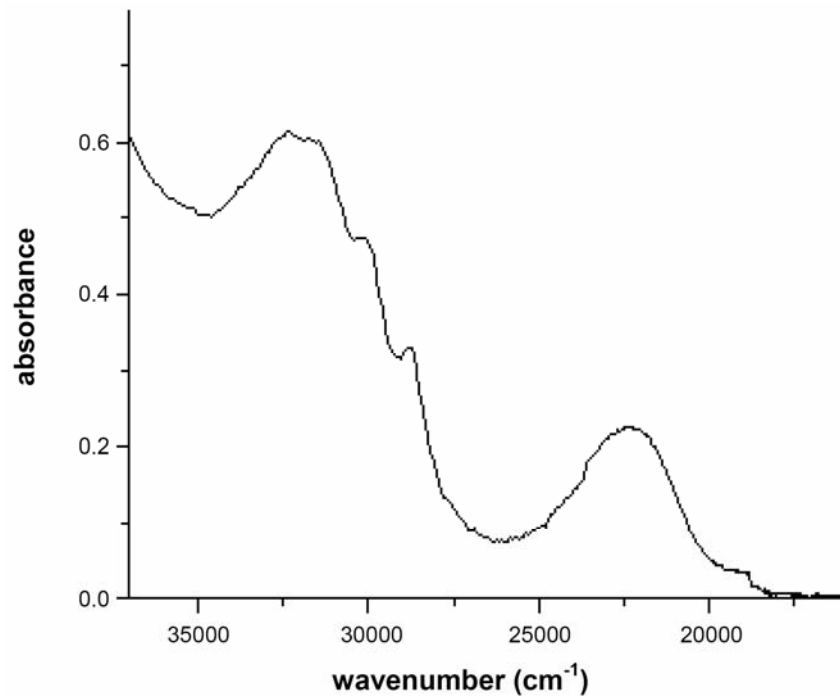
Figure 5.16. Electronic spectrum of the compound $[Cu(HL^2)Cl_2]_2 \cdot H_2O$ (**21**).
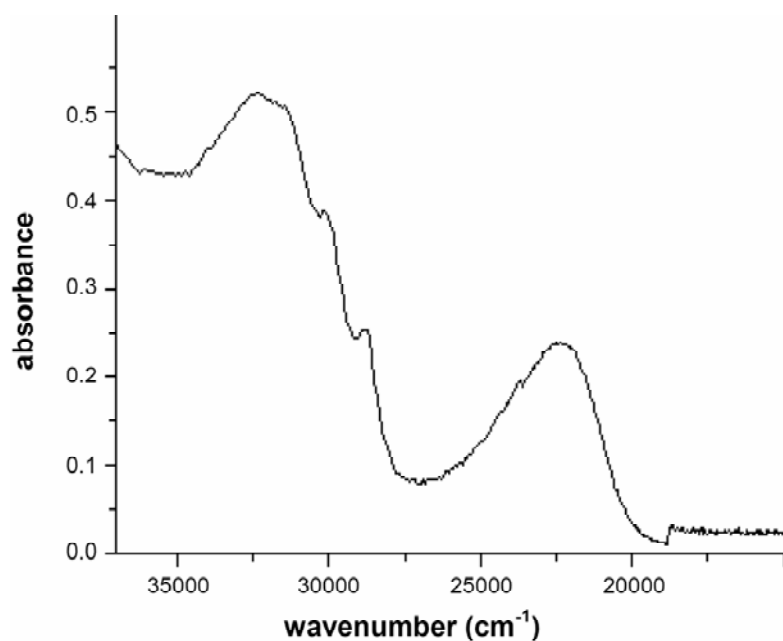
Figure 5.17. Electronic spectrum of the compound [CuL^{2}N$_3$]·CH$_3$OH (**23**).
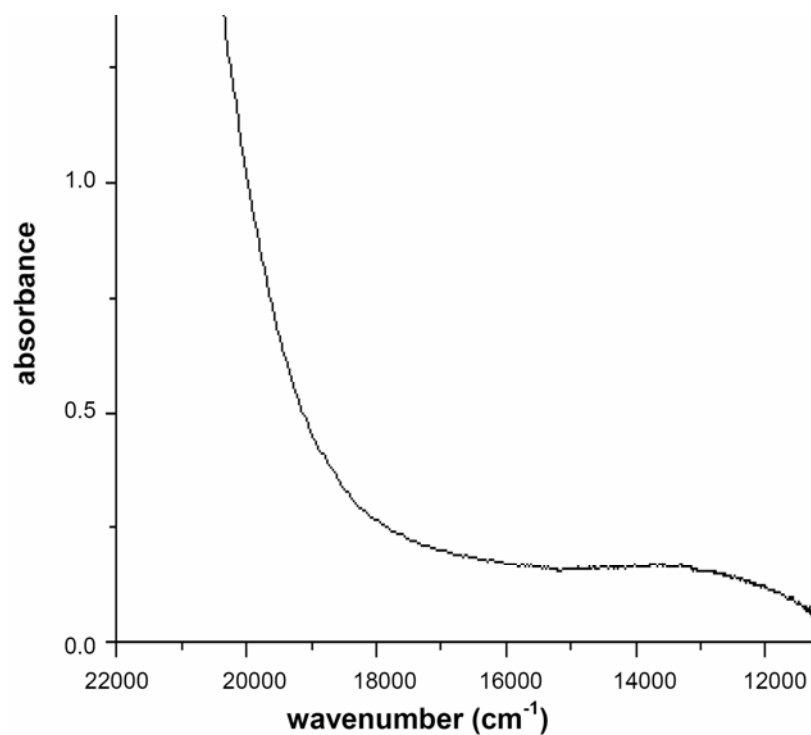
Figure 5.18. Electronic spectrum of the compound [Cu$_3$L$_2$^{1}Cl$_4$]·4H$_2$O (**15**) in the visible region.
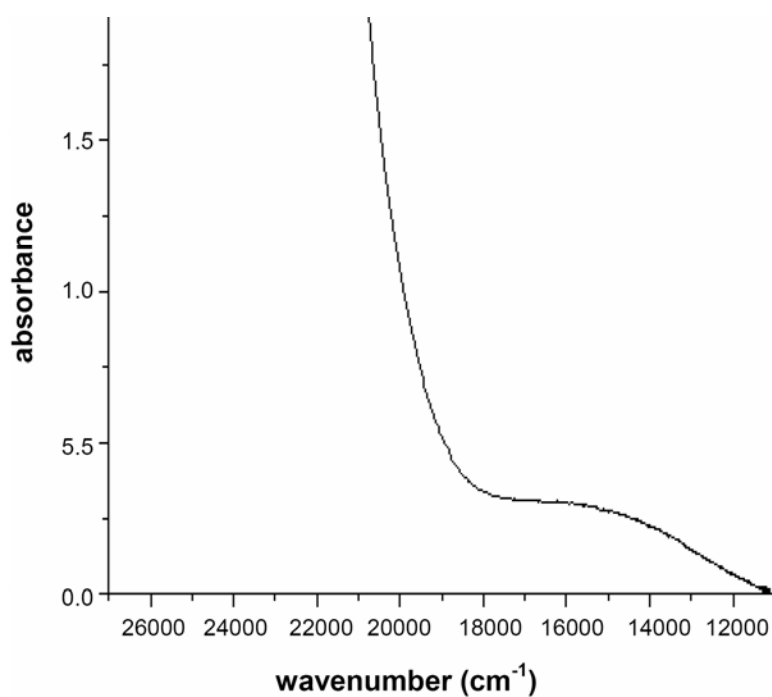
Figure 5.19. Electronic spectrum of the compound [CuL^{1}N$_3$] **(18)** in the visible region.
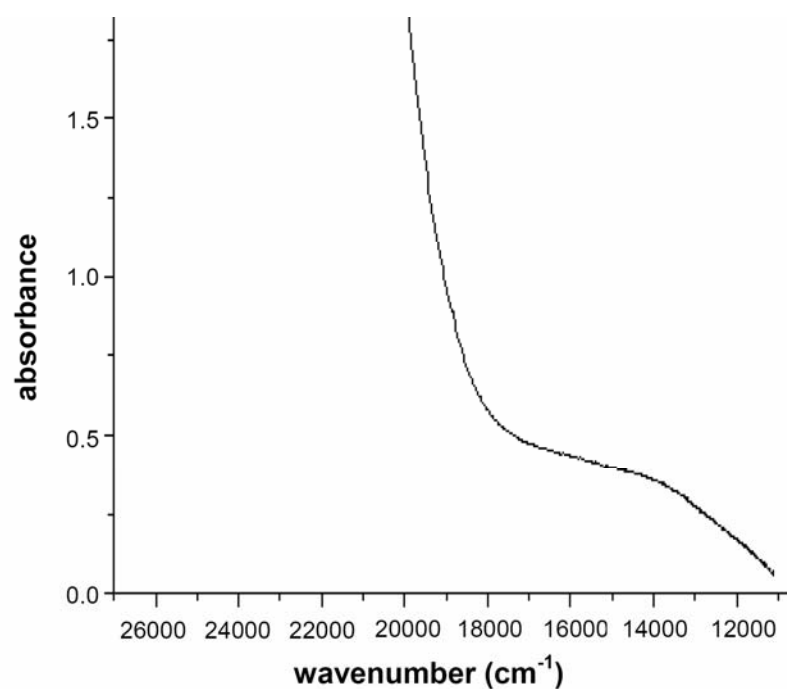
Figure 5.20. Electronic spectrum of the compound [CuL^{1}SCN]·^{3}/$_2$H$_2$O **(19)** in the visible region.
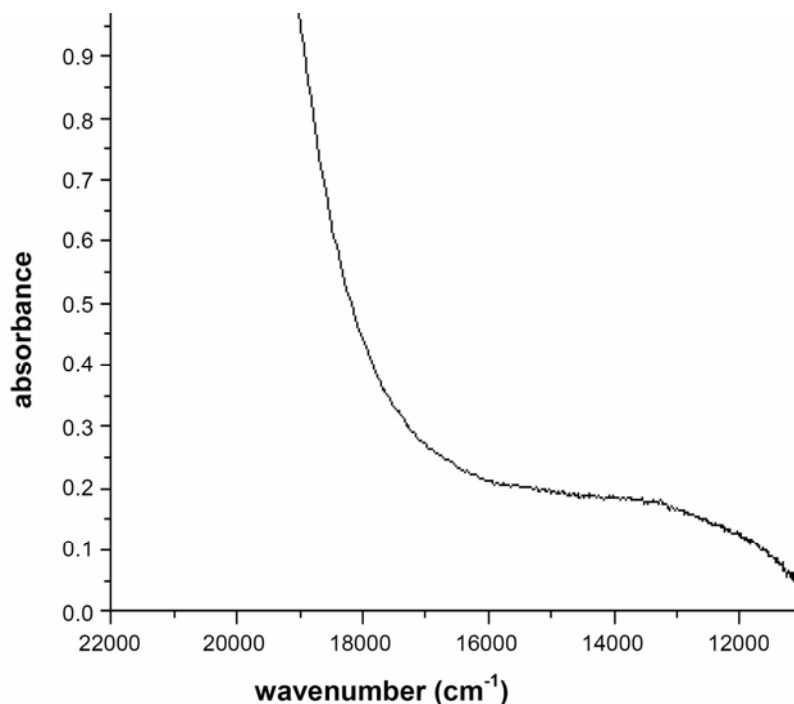
Figure 5.21. Electronic spectrum of the compound [CuL^{2}N$_3$]·CH$_3$OH
(**23**) in the visible region.

5.3.3. Electron paramagnetic resonance spectra

EPR spectroscopy is a powerful tool to infer details about the structure of complexes formed by paramagnetic metal ions. It is the electronic analog of NMR spectroscopy that probes the nuclear spin of molecules. An easy application of EPR spectroscopy uses the Cu(II) ion, a particularly favorable example of a metal ion that exhibits a wide range of stereochemistry with a variety of intermediate situations. For coordination geometries corresponding to an elongated octahedron, a square pyramid or square planar, the ground state is $d_{x^2-y^2}$. When the coordination around Cu(II) ion is a compressed octahedron or a trigonal bipyramid, the ground state is d_z^2. EPR spectroscopy can distinguish the ground states $d_{x^2-y^2}$ and d_z^2 on the basis of the principal values of the *g* tensor in the anisotropic spectra. The value of *g* is the primary

empirical parameter that characterizes the response of a paramagnetic molecule and provides a quantitative measure of the molecule's magnetic moment and is sensitive to the changes in the molecule's electronic structure. The Cu(II) ion has an effective spin of $S=3/2$ and is associated with a spin angular momentum $m_s= \pm 1/2$, leading to a doubly degenerate spin state in the absence of magnetic field. In a magnetic field the degeneracy is lifted between these states and the energy difference between them is given by $E = hv = g\beta B$, where h is the Planck's constant, v is the frequency, g is the Lande's splitting factor equals to 2.0023 (for a free electron), β is the Bohr magneton and B is the magnetic field.

The EPR spectra of polycrystalline sample at 298 K and solution at 77 K were recorded in the X-band with 100 kHz field modulation and g factors were quoted relative to the standard marker TCNE ($g=2.00277$). The EPR spectra of the complexes recorded in polycrystalline state at room temperature provide information about the coordination environment around Cu(II) in these complexes. All these values are in good agreement with earlier reported values of semicarbazones [31].

The EPR spectra of the compounds **15**, **17, 21** and **22** in the polycrystalline state at 298 K show only one broad signal at g_{iso} = 2.089, 2.129, 2.150 and 2.150 respectively (Figures 5.22-5.23). Such isotropic spectra arise from extensive exchange coupling through misalignment of the local molecular axes between different molecules in the unit cell (dipolar broadening) and enhanced spin lattice relaxation. This type of spectra unfortunately give no information about the electronic ground state of the Cu(II) ion present in the complex.
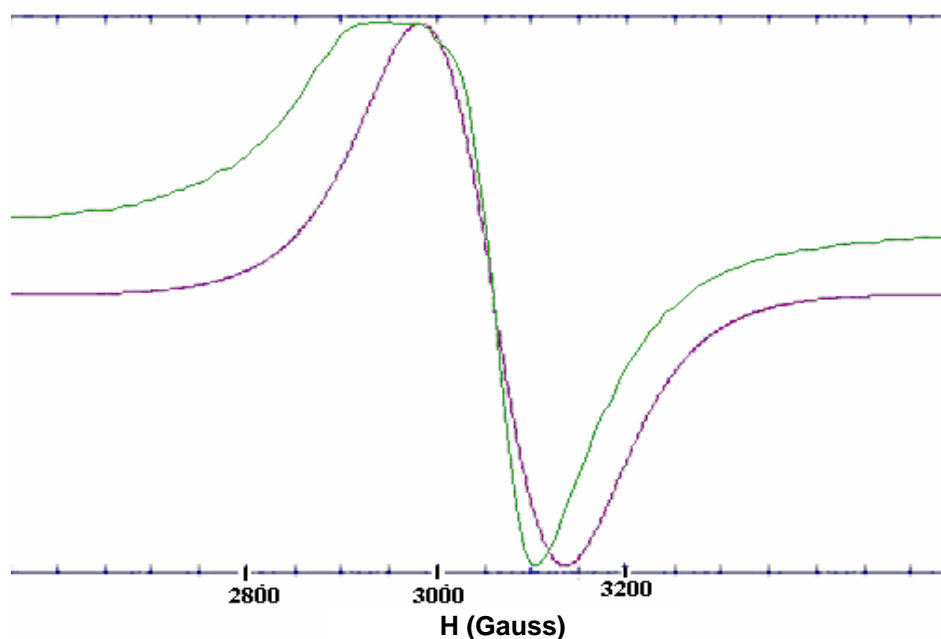
Figure 5.22. EPR spectrum of the compound $[Cu_3L_2{}^1Cl_4]\cdot 4H_2O$ (**15**) in polycrystalline state at 298 K (Experimental (green) and simulated best fit (purple) of the EPR spectra).
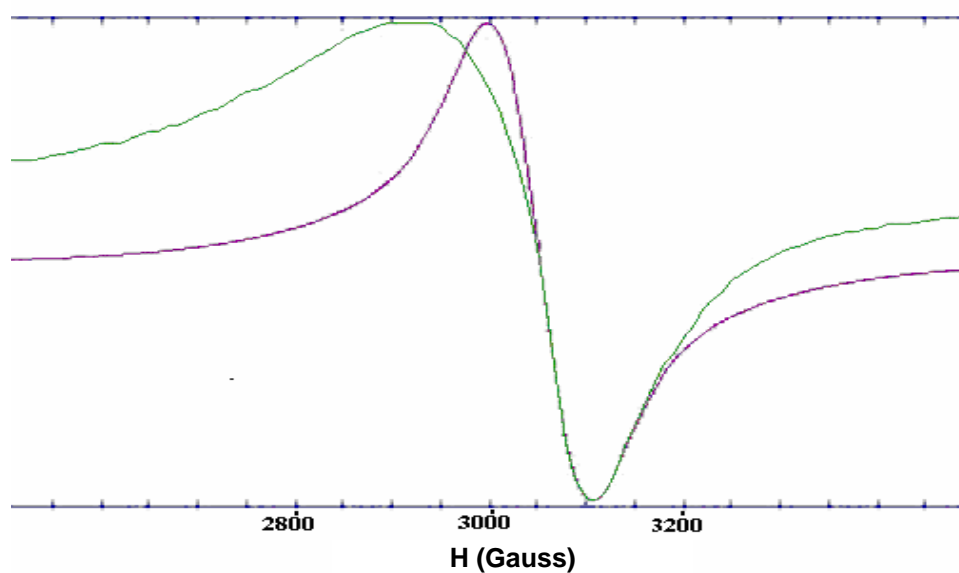

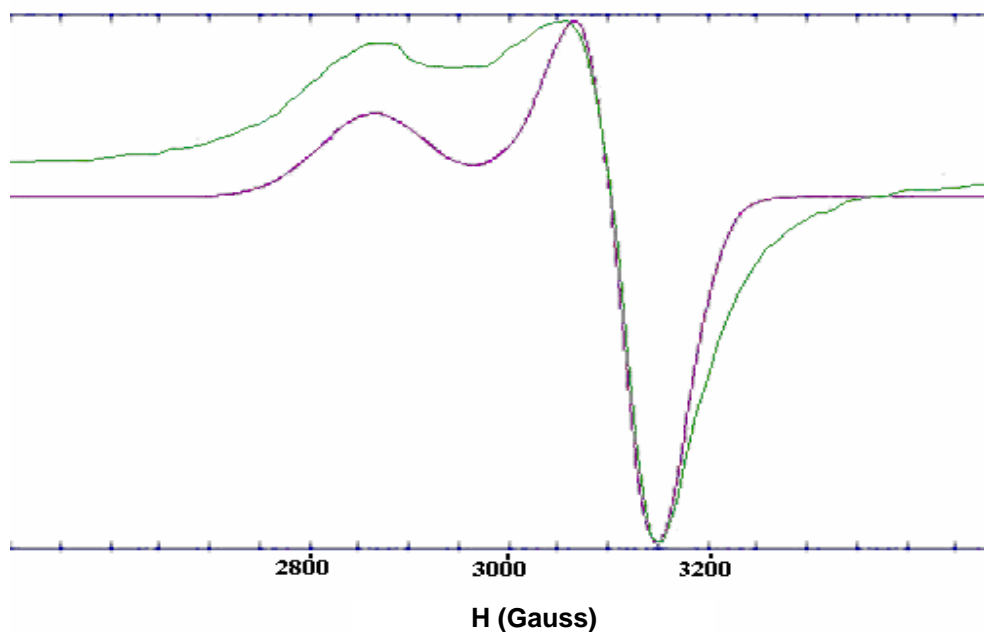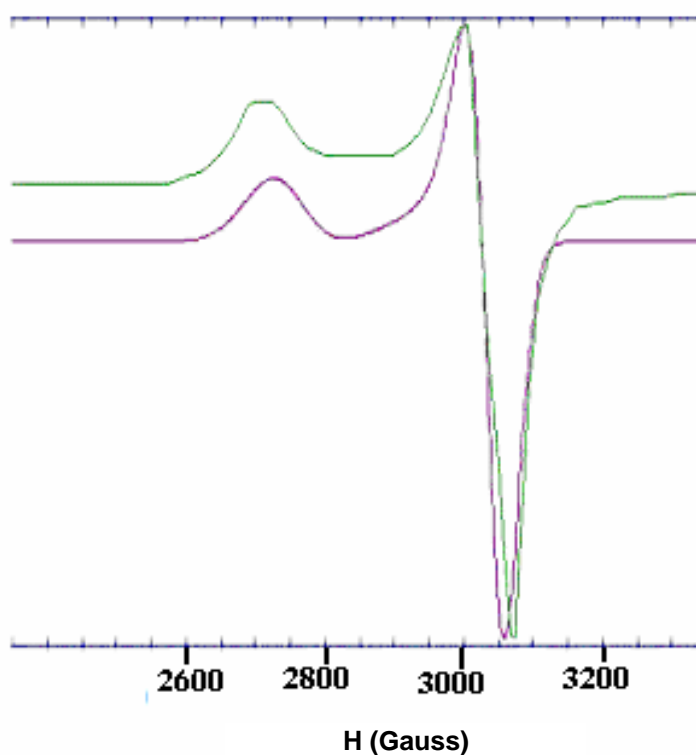**Figure 5.23.** EPR spectrum of the compound $[CuL^1NO_3]_2$ (**17**) in polycrystalline state at 298 K (Experimental (green) and simulated best fit (purple) of the EPR spectra).

For the compounds **16**, **18** and **20** we got axial spectra with well defined $g_\parallel$ and $g_\perp$ features. The variation of $g_\parallel$ and $g_\perp$ values in these complexes indicate the geometry of the compounds in the solid state is affected by the nature of the coordinating gegenions. The geometric parameter G is calculated as $G = g_\parallel{-}2.0023/g_\perp{-}2.0023$ for axial spectra and it is a measure of exchange interaction between copper centers in the polycrystalline compound. If $G > 4.4$, exchange interaction is negligible and if it is less than 4.4, considerable exchange interaction is indicated in the solid complex [32-34]. The geometric parameter G for the compounds **16**, **18** and **20,** are 3.258, 2.448 and 2.441 respectively, which indicate the fact that the unit cells of the compounds contain magnetically equivalent sites. For the complexes **16**, **18** and **20**, $g_\parallel > g_\perp > 2$ and G values falling in the range 2–4 are consistent with a $d_{x^2-y^2}$ ground state.

Figure 5.24. EPR spectrum of the compound [CuL^{1}OAc] (**16**) in polycrystalline state at 298 K (Experimental (green) and simulated best fit (purple) of the EPR spectra).

Figure 5.25. EPR spectrum of the compound [CuL¹N₃] **(18)** in polycrystalline state at 298 K (Experimental (green) and simulated best fit (purple) of the EPR spectra).

For the compound **19,** we got three g values $g_1 = 2.028$, $g_2 = 2.104$ and $g_3 = 2.306$ which indicate rhombic distortion in geometry (Figure 5.26). In the spectra with $g_3 > g_2 > g_1$ rhombic spectral values, $R = g_2 - g_1/ g_3 - g_2$ may be significant. If $R > 1$, a predominant d_z^2 ground state is present and if $R < 1$ a predominant $d_{x^2-y^2}$ state is present and if $R = 1$ then the ground state is approximately an equal mixture of d_z^2 and $d_{x^2-y^2}$. For the complex **19**, $R < 1$ suggesting a $d_{x^2-y^2}$ ground state indicates that the exchange interaction is negligible. The EPR spectrum of the compound [CuL²N₃]·CH₃OH **(23)** is reverse axial (Figure 5.27) with well defined $g_∥$ and $g_⊥$ features. This axially

compressed spectra has $g_\perp > g_\parallel$ with 2.045 and 2.130 as $g_\parallel$ and $g_\perp$ values respectively. As $g_\perp > g_\parallel$ the ground state is d_z^2. Absence of half field signals for compounds reinforce the assumption of superexchange interactions.
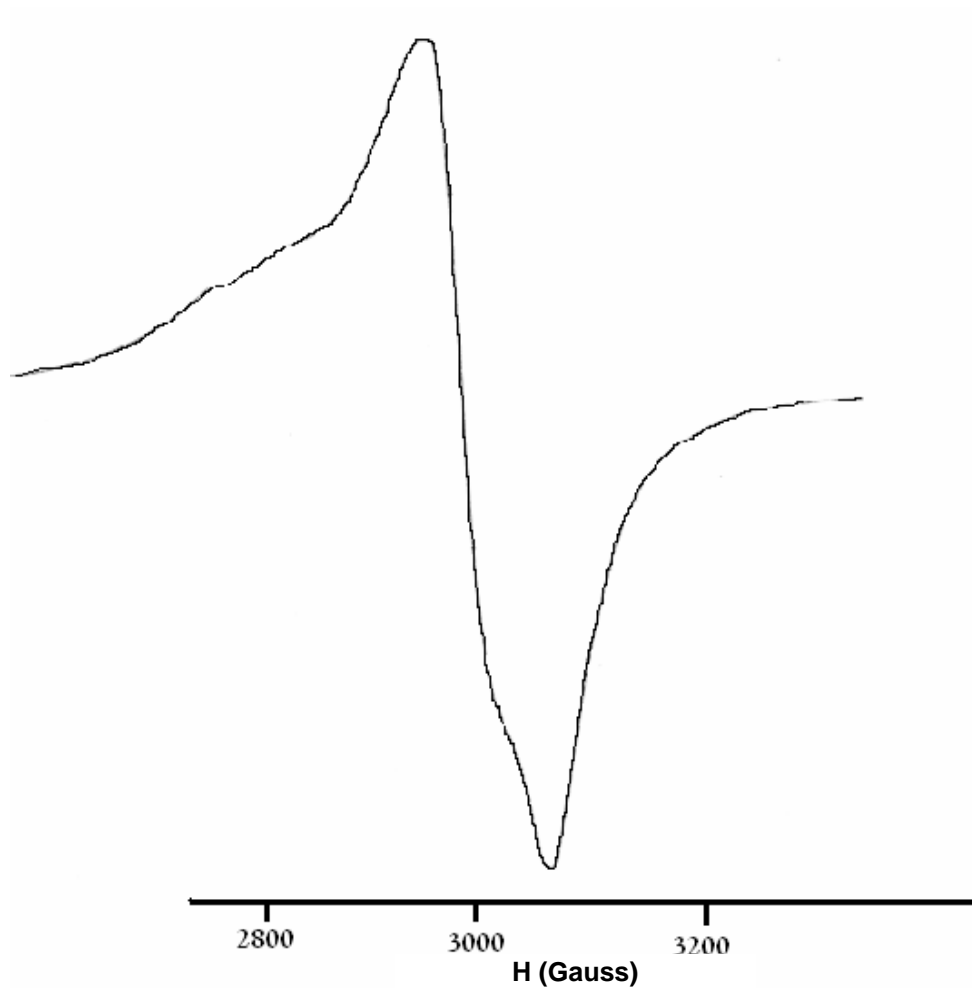

Figure 5.26. EPR spectrum of the compound $[CuL^1SCN]\cdot^3/_2H_2O$ (**19**) in polycrystalline state at 298 K.
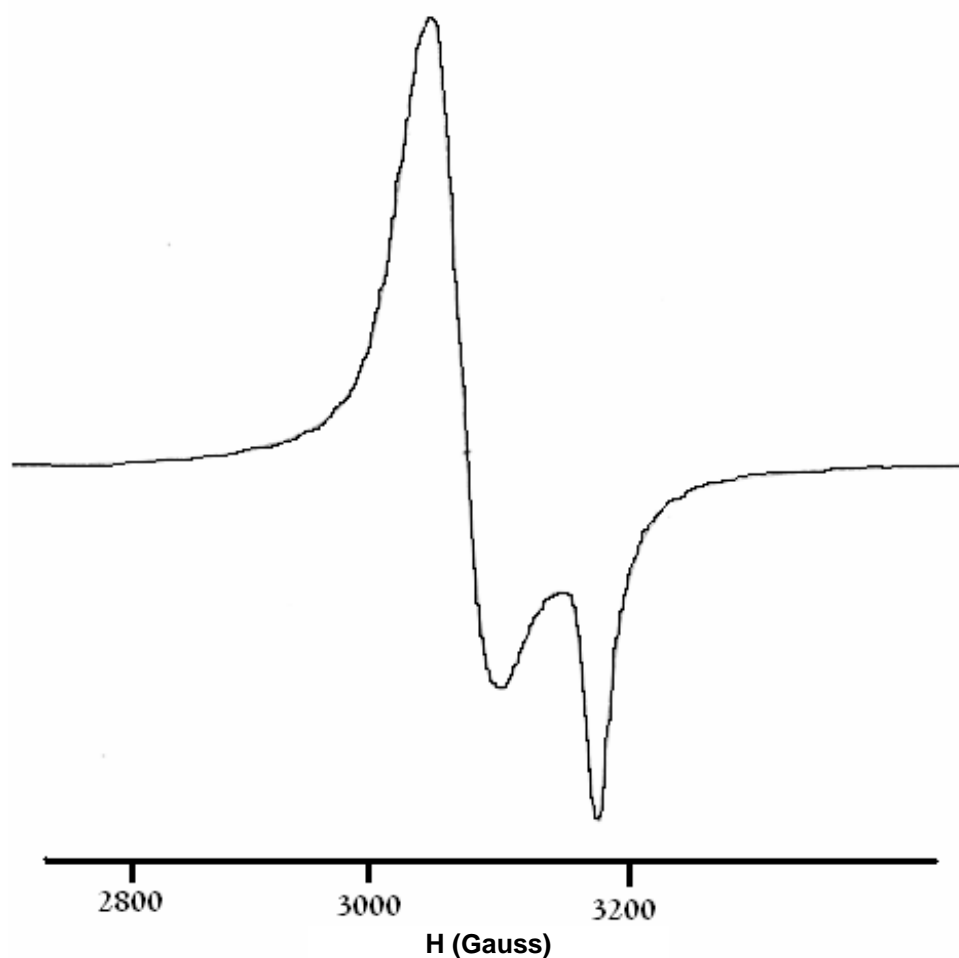
Figure 5.27. EPR spectrum of the compound $[CuL^2N_3] \cdot CH_3OH$ (**23**) polycrystalline state at 298 K.

The solution spectra of all complexes were recorded in DMF at 77 K. An axial spectrum was obtained for compound **15** (Figure 5.28) with 2.250, 2.061 and 178.33 x 10^{-4} cm^{-1} as $g_{\parallel}$, $g_{\perp}$ and $A_{\parallel}$ values. In the low field region, seven hyperfine lines are obtained that are moderately resolved suggesting a dimeric structure with two copper centers. This seven line hyperfine splitting is due to interaction of the electrons with two copper nuclei (^{65,63}Cu, $I = 3/2$), so that electrons are exchanged between two Cu(II)

ions *via* the bridging chlorine atoms at a rate faster than EPR time scale. The binuclear nature was confirmed by the presence of half field signal ($\Delta M_s = \pm 2$) at *ca.* 1570 G with *g* value 4.133. It is observed that *g* values of this complex in the solid state at 298 K and in DMF at 77 K are not much different from each other hence the geometry around the Cu(II) ion is unaffected on cooling the solution to liquid nitrogen temperature. As $g_{\parallel} > g_{\perp}$, the possibility of trigonal bipyramidal geometry has been ruled out and square pyramidal structure is suggested. Thus the coordination polyhedron comprises of one pyridyl nitrogen, azomethine nitrogen, enolate oxygen and chlorine atom and the bridging chlorine atom occupies the axial position.
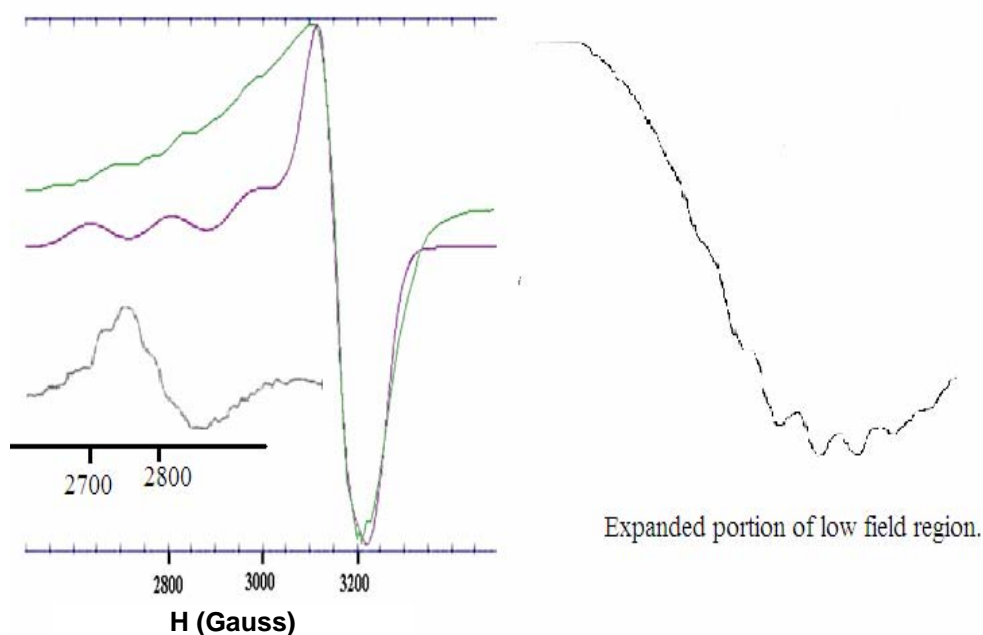

Figure 5.28. EPR spectrum of the compound $[Cu_3L_2{}^1Cl_4]\cdot4H_2O$ (**15**) in DMF at 77 K (Experimental (green) and simulated best fit (purple) of the EPR spectra).

In the compound **16**, an axial spectrum is obtained with $g_\parallel$ 2.250 and $g_\perp$ 2.045 values. Spectrum of this complex (Figure 5.29) has four copper hyperfine lines in both parallel and perpendicular regions. $A_\parallel(Cu)$ and $A_\perp(Cu)$ are calculated to be 150 x10^{-4} and 16 x10^{-4} cm^{-1} respectively. A_{av} is calculated by using the formula $A_{av} = 1/3(A_\parallel + 2A_\perp)$ and it is 60 x10^{-4} cm^{-1}.
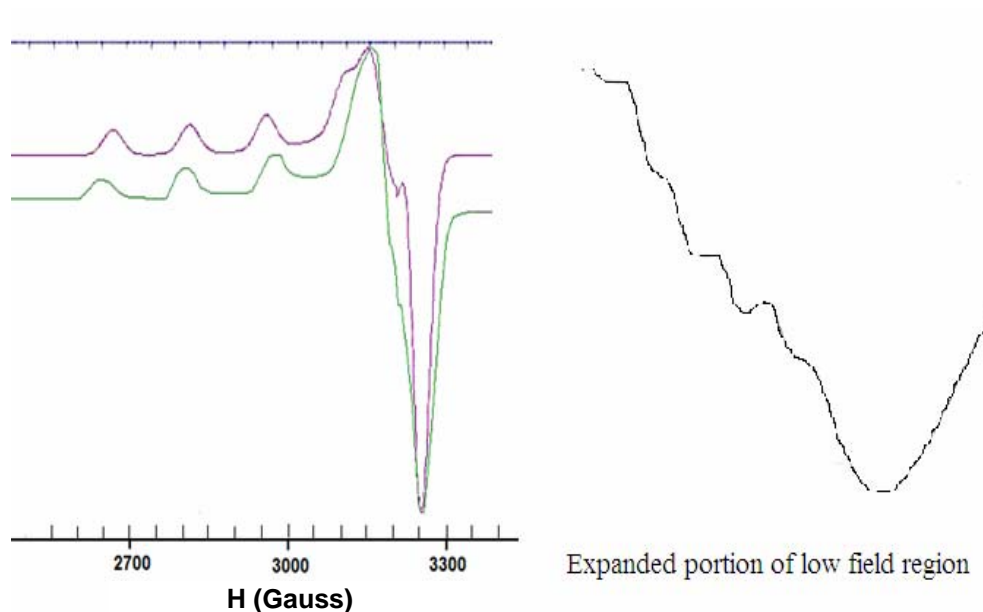

Expanded portion of low field region

H (Gauss)

Figure 5.29. EPR spectrum of the compound [CuL^{1}OAc] (**16**) in DMF at 77 K (Experimental (green) and simulated best fit (purple) of the EPR spectra).

For the nitrato complex **17,** in the parallel region three of the copper hyperfine lines are moderately resolved (Figure 5.30) while perpendicular features overlap the fourth one. Appearance of seven lines in the perpendicular region is due to nitrogen superhyperfine splitting. Here the $g_\parallel =$ 2.240, $g_\perp =2.051$ and $A_\parallel =159$ x10^{-4} cm^{-1}. The presence of half field signal indicates a dimeric structure for this complex ($g = 4.332$).
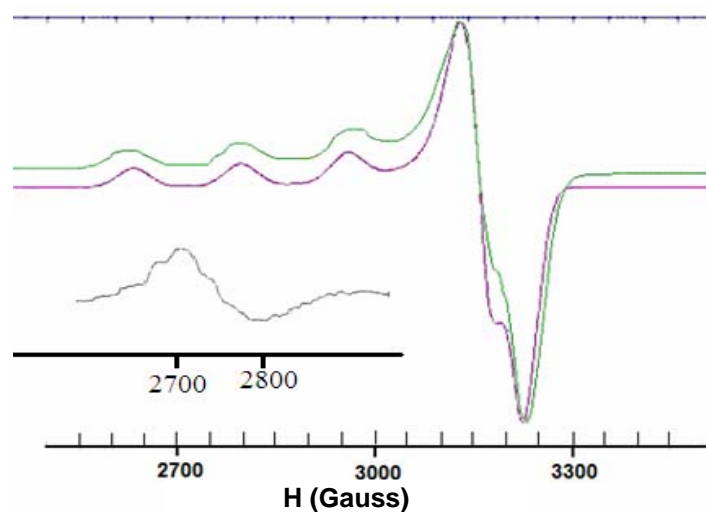
Figure 5.30. EPR spectrum of the compound $[CuL^1NO_3]_2$ **(17)** in DMF at 77 K (Experimental (green) and simulated best fit (purple) of the EPR spectra).

For the azido complex **18** also we got an axial spectrum (Figure 5.31) with $g_{\parallel} = 2.233$, $g_{\perp} = 2.047$ and $A_{\parallel} = 152$ $x10^{-4}$ cm^{-1} values. The spectrum shows well resolved four hyperfine lines in the parallel region corresponding to monomeric Cu(II) complex.

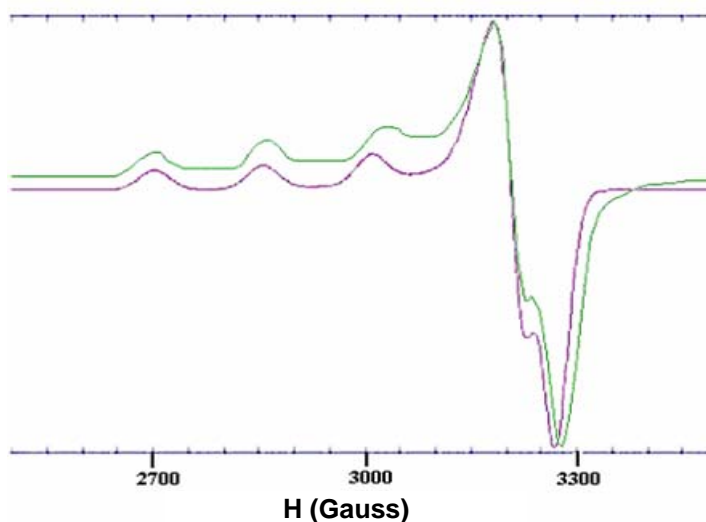**Figure 5.31.** EPR spectrum of the compound $[CuL^1N_3\,]$ **(18)** in DMF at 77 K (Experimental (green) and simulated best fit (purple) of the EPR spectra).

In thiocyanato complex **19,** an axial spectrum (Figure 5.32) is obtained with four hyperfine lines having $g_{\parallel}$= 2.223, $g_{\perp}$ =2.066 and $A_{\parallel}$ =195 x10^{-4} cm^{-1} values.
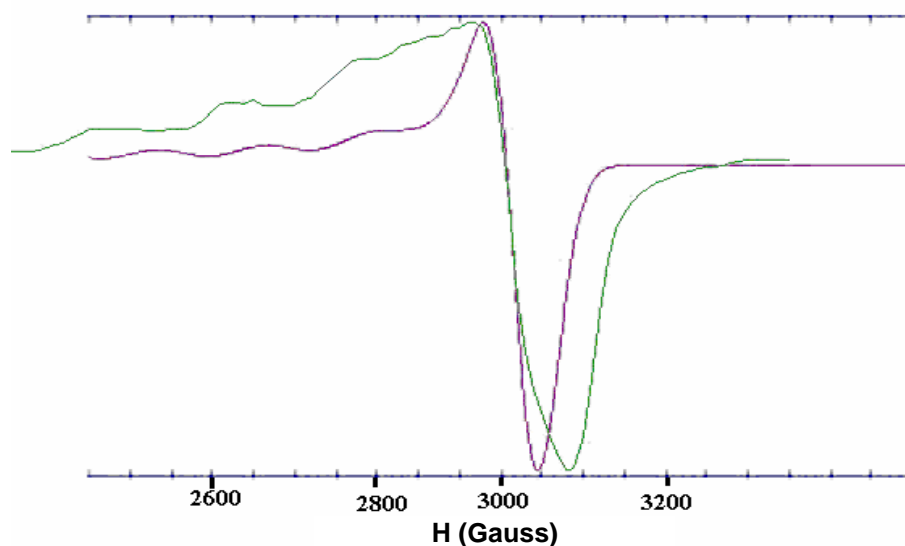

Figure 5.32. EPR spectrum of the compound [CuL^{1}SCN]·$^3/_2$H$_2$O (**19**)in DMF at 77 K (Experimental (green) and simulated best fit (purple) of the EPR spectra).

In the EPR spectrum of five coordinate copper(II) complex [Cu(HL^1)L^1]$_2$ (ClO$_4$)$_2$·6H$_2$O (**20**), the four hyperfine lines are observed in the parallel region and an axial spectrum is obtained with $g_{\parallel}$ = 2.265, $g_{\perp}$ =2.077 and $A_{\parallel}$ =150 x10^{-4} cm^{-1} values. The EPR spectrum of the complex **21** is also axial. For compounds, **22** and **23** EPR spectra are also axial with four hyperfine lines characteristic of monomeric copper(II) complexes, which arise from coupling of the odd electron with Cu nuclei (^{65}Cu, I = 3/2). The $g_{\parallel} > g_{\perp}$ values accounts to the distorted square based pyramid structure in five coordinated complexes **15** and **21** and rules out the possibility of a trigonal bipyramidal structure, which would be expected to have $g_{\parallel} < g_{\perp}$. Here for the four coordinated complexes **16, 17, 18, 19, 22** and **23,** $g_{\parallel} > g_{\perp}$ which suggest a square planar geometry.

Table 5.4. EPR spectral assignments of Cu(II) complexes in polycrystalline state at 298 K and solution at 77 K

Compound	Polycrystalline state (298 K)						DMF solution (77 K)			
	g_{iso}	$g_{\parallel}/g_3$	$g_{\perp}/g_1, g_2$	G	$g_{\parallel}$	$g_{\perp}$	g_{av}	$A_{\parallel}{}^a$	$A_{\perp}{}^a$	$A_{av}{}^a$
$[Cu_3L^1{}_2Cl_3]Cl\cdot4H_2O$ (**15**)	2.089	-	-	-	2.250	2.061	2.124	178.33	-	-
$[CuL^1OAc]$ (**16**)	-	2.262	2.082	3.258	2.250	2.045	2.113	150	16	60.666
$[CuL^1NO_3]_2$ (**17**)	2.129	-	-	-	2.240	2.051	2.114	159	-	-
$[CuL^1N_3]$ (**18**)	-	2.315	2.130	2.448	2.233	2.047	2.109	152	-	-
$[CuL^1SCN]\cdot^3/_2H_2O$ (**19**)	-	2.306	2.104 2.028	-	2.223	2.066	2.118	195	-	-
$[Cu(HL^1)L^1]_2(ClO_4)_2\cdot6H_2O$ (**20**)	-	2.297	2.123	2.441	2.265	2.077	2.139	150	-	-
$[Cu(HL^2)Cl_2]_2\cdot H_2O$ (**21**)	2.150	-	-	-	2.297	2.200	2.232	150.55	-	-
$[CuL^2OAc]\cdot^6/_5 H_2O$ (**22**)	2.150	-	-	-	2.219	2.079	2.125	181.66	-	-
$[CuL^2N_3]\cdot CH_3OH$ (**23**)	-	2.045	2.130	-	2.248	2.053	2.118	150.33	-	-

[a]A values in 10^{-4} cm^{-1}

For the six coordinated compound **20** as the $g_\parallel > g_\perp$ distorted octahedral geometry is suggested. For all the compounds g_{av} is also calculated using the equation, $g_{av} = 1/3 \ (g_\parallel + 2g_\perp)$ and it is in the range 2.109 - 2.232. According to Kivelson and Neiman considerable covalent character is suggested for M–L bond for the complexes when the $g_\parallel < 2.3$ [35]. The $g_\parallel$ values in all these complexes are less than 2.3 is an indication of covalent bonding in these complexes. The $g_\parallel$ values are nearly the same for all the complexes indicating that the bonding is dominated by the semicarbazone moiety. The EPR spectral assignments are given in Table 5.4.

The EPR bonding parameters are given in Table 5.5. The EPR parameters $g_\parallel$, $g_\perp$, $A_\parallel$(Cu) and the energies of *d-d* transitions were used to evaluate the bonding parameters α^2, β^2 and γ^2 which may be regarded as measures of covalency of the in-plane σ bonds, in-plane π-bonds and out-of-plane π-bonds respectively. The value of in-plane σ-bonding parameter α^2 was estimated from the expression,

$$\alpha^2 = - A_\parallel/0.036 + (g_\parallel - 2.00277) + 3/7 \ (g_\perp - 2.00277) + 0.04 \ [36,37]$$

The orbital reduction factors, $K_\parallel^2 = \alpha^2\beta^2$ and $K_\perp^2 = \alpha^2\gamma^2$ were calculated using the following expressions [38].

$$K_\parallel^2 = (g_\parallel - 2.00277) \ E_{d\text{-}d}/8\lambda_0$$
$$K_\perp^2 = (g_\perp - 2.00277) \ E_{d\text{-}d}/2\lambda_0$$

Where λ_0 is the spin orbit coupling constant with a value of -828 cm^{-1} for Cu(II) d^9 system.

According to Hathaway [34], for pure σ bonding $K_\parallel \approx K_\perp \approx 0.77$, and for in-plane π-bonding, $K_\parallel < K_\perp$; while for out-of-plane π-bonding, $K_\perp < K_\parallel$. In

the complexes, except **19, 20, 21** and **22,** it is observed that $K_\perp < K_\parallel$ which indicates the presence of significant out-of-plane π-bonding. In the complexes **19, 20, 21** and **22,** $K_\parallel < K_\perp$ indicate in-plane π-bonding. Furthermore, α^2, β^2 and γ^2 have values less than 1 which is expected for 100% ionic character of bonds; suggest the covalency of the bonds. But in complex **21**, the value of γ^2 is unexpected and is greater than 1. The empirical factor f = $g_\parallel$ /$A_\parallel$ (cm^{-1}) is an index of tetragonal distortion and depends on the nature of the coordinated atom. In all the compounds, *f* falls in the range 114-151 cm^{-1} corresponding to a Cu(II) center with medium to extreme distortion [39].

Table 5.5. EPR bonding parameters of Cu(II) complexes

Compound	α^2	β^2	γ^2	K	$K_\parallel$	$K_\perp$	f [a]
[Cu$_3$L$_2^1$Cl$_4$]·4H$_2$O (**15**)	0.807	0.674	0.635	-	0.738	0.716	126.17
[CuL^{1}OAc] (**16**)	0.721	0.785	0.536	-	0.753	0.622	150.00
[CuL^{1}NO$_3$]$_2$ (**17**)	0.739	0.774	0.630	-	0.756	0.682	140.88
[CuL^{1}N$_3$] (**18**)	0.711	0.718	0.551	-	0.714	0.626	146.90
[CuL^{1}SCN]·^{3}/$_2$H$_2$O (**19**)	0.829	0.614	0.704	-	0.713	0.764	114.01
[Cu(HL^1)L^1]$_2$(ClO$_4$)$_2$·6H$_2$O (**20**)	0.750	0.806	0.913	-	0.778	0.828	151.00
[Cu(HL^2)Cl$_2$]$_2$·H$_2$O (**21**)	0.794	0.671	2.078	-	0.730	1.288	149.78
[CuL^{2}OAc]·^{6}/$_5$ H$_2$O (**22**)	0.788	0.646	0.911	-	0.714	0.847	122.15
[CuL^{2}N$_3$]CH$_3$OH (**23**)	0.723	0.793	0.649	-	0.757	0.685	149.53

[a] Expressed in units of cm.

References

[1] T.S. Lobana, R. Sharma, G. Bawa, S. Khanna, Coord. Chem. Rev. 253 (2009) 977.

[2] B.S. Garg, M.R.P. Kurup, S.K. Jain, Y.K. Bhoon, Trans. Met. Chem. 13 (1988) 309.

[3] H. Beraldo, D. Gaminob, Mini. Rev. Med. Chem. 4 (2004) 31.

[4] D.X. West, P.B. Sonawane, A.S. Kumbhar, R.G.Yerande, Coord. Chem. Rev. 123 (1993) 49.

[5] T.A. Reena, E.B. Seena, M.R.P. Kurup, Polyhedron 27 (2008) 1825.

[6] M. Akkurt, S. Ozfuric, S. Ide, Anal. Sci. 16 (2000) 667.

[7] L.A. Saryan, E. Ankel, C. Krishnamurthi, D.H. Petering, H. Elford, J. Med. Chem. 22 (1979) 1218.

[8] J.E. Huheey, E.A. Keiter, R.L. Keiter, Inorganic Chemistry, Principles of Structure and Reactivity, fourth ed., Harpercollins College Publishers, 1993.

[9] W.J. Geary, Coord. Chem. Rev. 7 (1971) 81.

[10] V.M. Kolb, J.W. Stupar, T.E. Janota, W.L. Duax, J. Org. Chem. 54 (1989) 2341.

[11] E.B. Seena, M.R.P. Kurup, Polyhedron 26 (2007) 829.

[12] R.C. Chikate, A.R. Belapure, S.B. Padhye, D.X. West, Polyhedron 24 (2005) 889.

[13] V.D. Khanolkar, D.D. Khanolkar, Indian J. Chem. 18A (1979) 315.

[14] J. Jezierska, B. Jezowska-Trzebiatowska, G. Petrova, Inorg. Chim. Acta 50 (1981) 153.

[15] A. Sreekanth, H.-K. Fun, M.R.P. Kurup, Inorg. Chem. Commun. 7 (2004) 324.

[16] B.S. Garg, M.R.P. Kurup, S.K. Jain, Y.K. Bhoon, Trans. Met. Chem. 13 (1988) 92.

[17] B.S. Garg, M.R.P. Kurup, S.K. Jain, Y.K. Bhoon, Trans. Met. Chem. 13 (1988) 247.

[18] P.B. Sreeja, M.R.P. Kurup, Spectrochim. Acta 61A (2005) 331.

[19] V. Philip, V. Suni, M.R.P. Kurup, Polyhedron 25 (2006) 1931.

[20] V. Philip, V. Suni, M.R.P. Kurup, M. Nethaji, Spectrochim. Acta 64A (2006) 171.

[21] A. Sreekanth, U.L. Kala, C.R. Nayar, M.R.P. Kurup, Polyhedron 23 (2004) 41.

[22] P.F. Rapheal, E. Manoj, M.R.P. Kurup, Polyhedron 26 (2007) 818.

[23] A.B.P. Lever, Inorg. Chem. 4 (1964) 1042.

[24] A.B.P. Lever, E. Mantovani, B.S. Ramaswami, Can. J. Chem. 49 (1971) 1957.

[25] R.A. Bailey, S.L. Kozak, T.W. Michelsen, W.N. Mills, Coord. Chem. Rev. 6 (1971) 407.

[26] A.M. Bond, R.L. Martin, Coord. Chem. Rev. 54 (1984) 23.

[27] C.R.K. Rao, P.S. Zacharias, Polyhedron 16 (1997) 1201.

[28] M.J.M. Campbell, Coord. Chem. Rev. 15 (1975) 279.

[29] R.P. John, A. Sreekanth, V. Rajakannan, T.A. Ajith, M.R.P. Kurup, Polyhedron 23 (2004) 2549.

[30] M. Joseph, M. Kuriakose, M.R.P. Kurup, E. Suresh, A. Kishore, G. Bhat, Polyhedron 25 (2006) 61.

[31] U.L. Kala, S. Suma, M.R.P. Kurup, Suja Krishnan, R.P. John, Polyhedron 26 (2007) 1427.

[32] I.M. Proctor, B.J. Hathaway, P. Nicholis, J. Chem. Soc. A (1968) 1678.

[33] S. K. Jain, B.S. Garg, Y.K. Bhoon, Spectrochim. Acta 42A (1986) 959.

[34] B.J. Hathaway, D.E. Billing, Coord. Chem. Rev. 5 (1970) 1949.

[35] D. Kivelson, R. Neiman, J. Chem. Phys. 35 (1961) 149.

[36] A.H. Maki, B.R. McGarvey, J. Chem. Phys. 29 (1958) 35.

[37] B.J. Hathaway, in: G. Wilkinson, R.D. Gillard, J. A. McCleverty (Eds.), Comprehensive Coordination Chemistry, vol. 5, Pergamon, Oxford, (1987) 533.

[38]   B.N. Figgis, Introduction to Ligand Fields, Interscience, New York, (1996) 295.

[39]   L. Latheef, M.R.P. Kurup, Spectrochim. Acta A 70 (2008) 86.

…..⧉⧉…..

SPECTRAL STUDIES ON Ni(II), Co(II) AND Mn(II) COMPLEXES OF N^4-SUBSTITUTED SEMICARBAZONES

6.1. Introduction

Nickel occurs as Ni(I), Ni(II) or Ni(III) in biological systems such as the active sites of certain hydrogenases and dehydrogenases [1]. Hence the nickel species in various coordination environments are of interest to inorganic biochemists. It is predominantly divalent and ionic in simple compounds. Nickel forms four, five and six coordinate complexes *viz.* square planar, tetrahedral, trigonal bipyramidal, square pyramidal and octahedral geometries. The coordination compounds of nickel are also studied for their magnetic behavior. In last few years, nickel(II) complexes containing sulfur donors have received considerable attention due to the identification of a sulfur rich coordination environment in biological nickel centers such as at the active sites of certain ureases, methyl-S-coenzyme-M-methyl reductase, hydrogenases and may play a role in the supposed mutagenicity of nickel compounds. According to the reports labile four coordinated nickel(II) complexes with tridentate thiosemicarbazone and semicarbazone ligands exhibit antibacterial activities, where as six coordinated nickel(II) complexes with thiosemicarbazone and semicarbazone ligands show no activities against the test microorganisms [2].

The synthesis and reactivity of cobalt complexes of Schiff base ligands have played an important part in the development of coordination chemistry [3,4]. Cobalt exhibits two important oxidation states as +2 and +3, and salts of Co(II) are more stable, as they are not easily oxidized to Co(III) state. However, in basic solutions, oxidation of Co(II) to Co(III) takes place relatively easily. The overall formation constant is greater for higher oxidation state and thus the complexation makes it difficult to be reduced. In spite of stabilization of Co(III) by complexation, high spin six coordinate, high/low spin five coordinate and four coordinate complexes of Co(II) are widely reported. It is observed that Co(II) forms more tetrahedral complexes than any other transition metal ion except Zn(II) due to its d^7 configuration. The cobalt complexes of tetradentate Schiff base ligands have been extensively used to mimic cobalamin (B_{12}) coenzymes [5-8], dioxygen carriers and oxygen activators [9-11] and enantioselective reduction [12]. ^{60}Co is the radioactive isotope of cobalt which is using in radiotherapy. Cobalt compounds are used in the production of pigments, inks and varnishes. Cobalt is ferromagnetic. The Curie temperature is 1388 K with 1.6~1.7 Bohr Magneton per atom. Cobalt oxides, CoO and Co_3O_4 are antiferromagnetic at low temperature.

Manganese is a naturally occurring metal that is found in many rocks. Manganese is used principally in steel production to improve hardness, stiffness and strength. It may also be used as an additive in gasoline to improve the octane rating of the gas. Manganese is naturally ubiquitous in the environment. Manganese is essential for normal physiologic functioning in humans and animals, and exposure to low levels of manganese in the diet is considered to be nutritionally essential in humans. Chronic (long-term) exposure to high levels of manganese by inhalation in humans may result in central nervous system (CNS) effects. Visual reaction time, hand steadiness,

and eye-hand coordination were affected in chronically-exposed workers. A syndrome named manganism may result from chronic exposure to higher levels; manganism is characterized by feelings of weakness and lethargy, tremors, a mask-like face, and psychological disturbances. Respiratory effects have also been noted in workers chronically exposed by inhalation. Impotence and loss of libido have been noted in male workers afflicted with manganism.

Manganese is an essential trace element, forming the active sites of a number of metalloprotiens. In these metalloprotiens, manganese can exist in any of the five oxidation states or in mixed valence states [13]. Potential importance of manganese complexes is evidenced by the realization that the active system in photosystem II (PSII) is a tetranuclear manganese complex [14]. Manganese coordination compounds are also of growing importance as homogeneous catalysts in oxidation reactions. Manganese has a vital role in many enzymatic systems such as peroxide dimutase, peroxidase, dioxygenase and catalase in which mononuclear manganese active sites are present [15]. Metal complexes of manganese play important roles ranging from bioinorganic chemistry to solid state physics. Manganese coordination compounds are also of growing importance as homogeneous catalysts in oxidation reactions [16-19]. Manganese complexes are also studied for their magnetic behavior. The chemistry of manganese, in various oxidation states of the metal and in various combination of nitrogen and oxygen donor environment, is presently witnessing intense activity [20-22]. The common oxidation states of manganese are +2, +3, +4, +6 and +7, though oxidation states from +1 to +7 are observed. The most common and stable oxidation state of manganese is +2. Majority of manganese complexes are high spin paramagnetic d^5 systems and are colored.

This chapter describes the syntheses and characterization of five nickel(II), three cobalt(II) and two manganese(II) complexes of N^4-substituted semicarbazones, HL^1 and HL^2.

6.2. Experimental
6.2.1. Materials

The syntheses of the semicarbazones, HL^1 and HL^2 have been described already in Chapter 2. Nickel(II) acetate tetrahydrate, nickel(II) chloride hexahydrate, potassium thiocyanate, nickel(II) sulfate, cobalt(II) bromide, cobalt(II) acetate tetrahydrate, cobalt(II) perchlorate hexahydrate, manganese(II) chloride tetrahydrate and manganese(II) perchlorate hexahydrate were commercial products of higher grade (Aldrich) and reagents used were of Analar grade and used without further purification.

6.2.2. Synthesis of complexes
[NiL^1$_2$]·H$_2$O (24)

Ni(OAc)$_2$·4H$_2$O (0.124 g, 0.5 mmol) in 20 ml of methanol was added to methanolic solution of HL^1 (0.317 g, 1 mmol) and refluxed for 3 h. The compound formed was filtered, washed with ether and dried over P$_4$O$_{10}$ *in vacuo.*

Yield ~0.45 g.

[NiL^{1}SCN]·H$_2$O (25)

A solution of the semicarbazone, HL^1 (0.317 g, 1 mmol) in 20 ml was refluxed with solution of Ni(OAc)$_2$·4H$_2$O (0.248 g, 1 mmol) in the same solvent for 1 h. Methanolic solution of KSCN (0.097 g, 1 mmol) was then added to the solution followed by a further refluxing for 3 h. The compound formed was filtered, washed with ether and dried over P$_4$O$_{10}$ *in vacuo.*

Yield ~0.35 g.

[Ni(HL^1)Cl$_2$]·4H$_2$O (26)

Methanolic solutions of HL^1 (0.317 g, 1 mmol) and NiCl$_2$·2H$_2$O (0.166 g, 1 mmol) were refluxed for 4 h. The compound formed was filtered, washed with ether and dried over P$_4$O$_{10}$ *in vacuo*.

Yield ~0.30 g.

[NiL^2$_2$] (27)

Ni(OAc)$_2$·4H$_2$O (0.124 g, 0.5 mmol) in 20 ml of methanol was added to solution of HL^2 (0.290 g, 1 mmol) in DMF and refluxed for 3 h. The compound formed was filtered, washed with ether and dried over P$_4$O$_{10}$ *in vacuo*.

Yield ~0.40 g.

[Ni(HL^2)(SO$_4$)]·4H$_2$O (28)

HL^2 (0.290 g, 1 mmol) was dissolved in DMF and refluxed with a solution of NiSO$_4$ (0.223 g, 1 mmol) in 20 ml of methanol. The compound formed was filtered, washed with ether and dried over P$_4$O$_{10}$ *in vacuo*.

Yield ~0.45 g.

[CoL^{1}Br]·H$_2$O (29)

Methanolic solutions of HL^1 (0.317 g, 1 mmol) and CoBr$_2$ (0.218 g, 1 mmol) were refluxed for 4 h. The compound formed was filtered, washed with ether and dried over P$_4$O$_{10}$ *in vacuo*.

Yield ~0.30 g.

[CoL^{2}OAc] (30)

Co(OAc)$_2$·4H$_2$O (0.249 g, 1 mmol) in 20 ml of methanol was added to solution of HL^2 (0.290 g, 1 mmol) in DMF and refluxed for 4 h. The compound formed was filtered, washed with ether and dried over P$_4$O$_{10}$ *in vacuo*.

Yield ~0.45 g.

[CoL^{2}ClO$_4$]·DMF (31)

Co(ClO$_4$)$_2$·6H$_2$O (0.365 g, 1 mmol) in 20 ml of methanol was added to solution of HL^2 (0.290 g, 1 mmol) in DMF and refluxed for 4 h. The compound formed was filtered, washed with ether and dried over P$_4$O$_{10}$ *in vacuo*.

Yield ~0.45 g.

[MnL^1(HL^1)]ClO$_4$ ·4H$_2$O (32)

A solution of semicarbazone, HL^1 (0.317 g, 1 mmol) in 20 ml of methanol was treated with a methanolic solution of manganese(II) perchlorate hexahydrate (0.361 g, 1 mmol). The solution was heated under reflux for 4 h after adding three drops of triethyl amine. The resulting solution was allowed to stand at room temperature and upon slow evaporation complex is separated out, which was collected, washed with ether and dried over P$_4$O$_{10}$ *in vacuo*.

Yield ~0.30 g.

[Mn(HL^2)Cl]Cl·2H$_2$O (33)

A solution of the semicarbazone, HL^2 (0.317 g, 1 mmol) in DMF is mixed with a methanolic solution of manganese(II) chloride tetrahydrate (0.290 g, 1 mmol) and the mixture was heated under reflux for 4 h after adding three drops of triethyl amine. The resulting solution was allowed to stand at room temperature and the complex was formed upon slow evaporation. The complex separated out was collected, washed with ether and dried over P$_4$O$_{10}$ *in vacuo*.

Yield ~0.40 g.

6.2.3. Analytical methods

Elemental analyses were carried out using a Vario EL III CHNS analyzer at the SAIF, Kochi, India. Infrared spectra were recorded on a Thermo Nicolet AVATAR 370 DTGS model FT-IR Spectrophotometer with

KBr pellets at the SAIF, Kochi, India. Electronic spectra were recorded on a Cary 5000 version 1.09 UV-VIS- NIR Spectrophotometer using solutions in DMF. EPR spectra of manganese(II) complexes were recorded in polycrystalline state at 298 K and in DMF at 77 K.

6.3. Results and discussion

The analytical data of all the complexes are listed in Table 6.1. Semicarbazones, HL^1/HL^2 react with corresponding metal(II) salts in the molar ratio 2:1 to form compounds **24** and **27**, whereas in all other compounds this molar ratio is 1:1. Semicarbazones coordinated in the keto form in complexes **26**, **28** and **33** but in complex **32** one molecule of HL^1 undergoes deprotonation which is evident from spectral studies. The molar conductivities of the complexes in DMF (10^{-3} M) solutions were measured at 298 K with a Systronic model 303 direct-reading conductivity bridge, which show that all Ni(II) and Co(II) complexes, **24**-**31** are non-conductive so that the anions are present inside the coordination sphere and get coordinated with metal ion. But in Mn(II) complexes **32** and **33** anions are present outside the coordination sphere which is supported by the conductivity measurement study. The magnetic moments of the complexes were calculated from the magnetic susceptibility measurements at room temperature. All Ni(II) complexes, **24**-**28** are paramagnetic and the effective magnetic moments are found to be in the range 2.59-2.99 B.M. Square planar complexes $[CoL^1Br]\cdot H_2O$ (**29**) and $[CoL^2ClO_4]$ (**31**) have magnetic moments 2.79 and 2.86 B.M. respectively. This may be arising from one unpaired electron plus an apparently large orbital contribution. Tetrahedral complex $[CoL^2OAc]$ (**30**) has magnetic moment 5.41 B.M. which is due to the presence of three unpaired electrons. Mn(II) complexes **32** and **33** are paramagnetic.

Table 6.1. Colors, elemental analyses, magnetic susceptibilities and molar conductivities of Ni(II), Co(II) and Mn(II) complexes of HL^1 and HL^2.

Compound	Color	Found (Calculated) %			μ (B.M.)	Λ_M[a]
		C	H	N		
$[NiL^1_2] \cdot H_2O$ (**24**)	Brown	60.33 (60.95)	3.80 (4.26)	20.17 (19.74)	2.94	1
$[NiL^1SCN] \cdot H_2O$ (**25**)	Green	50.10 (50.58)	3.70 (3.57)	17.95 (18.63)	2.59	30
$[Ni(HL)^1Cl_2] \cdot 4H_2O$ (**26**)	Green	41.88 (41.66)	4.19 (4.47)	13.58 (13.49)	2.68	33
$[NiL^2_2]$ (**27**)	Brown	63.75 (63.67)	4.15 (4.71)	17.59 (17.47)	2.99	1
$[Ni(HL^2)(SO_4)] \cdot 4H_2O$ (**28**)	Orange	38.98 (39.33)	4.43 (4.66)	10.42 (10.79)	2.60	20
$[CoL^1Br] \cdot H_2O$ (**29**)	Brown	45.70 (45.69)	4.10 (3.41)	14.91 (14.80)	2.79	5
$[CoL^2OAc]$ (**30**)	brown	55.03 (55.48),	4.62 (4.90)	13.84 (13.62)	5.41	2
$[CoL^2ClO_4] \cdot DMF$ (**31**)	Black	46.06 (45.95)	3.91 (4.24)	12.91 (13.40)	2.86	10
$[MnL^1(HL^1)]ClO_4 \cdot 4H_2O$(**32**)	Brown	50.08 (50.27)	3.68 (4.34)	16.16 (16.28)	5.6	84
$[Mn(HL^2)Cl]Cl \cdot 2H_2O$ (**33**)	Brown	54.54 (55.00)	3.80 (4.34)	14.87 (15.09)	5.5	88

a = ohm^{-1} cm^2 mol^{-1}

6.3.1. Infrared spectra

The significant bands observed in the IR spectra of complexes of HL^1 and HL^2 with the tentative assignments are presented in Table 6.2. IR spectra

of complexes are presented in Figures 6.1-6.10. The comparison of the IR spectra of the semicarbazones and the complexes revealed significant variations in the characteristic bands due to coordination with the central metal ion. It is found that the azomethine $v(C=N)$ band suffered a negative shift in the region 1528-1568 cm^{-1} in the complexes **24**-**28**. The shifting of the azomethine band to lower frequency is attributed to the conjugation of the *p* orbitals on the double bond with the *d* orbital on the metal ion with reduction of the force constant. The bands observed in the region 1583-1599 cm^{-1} in the IR spectra of complexes **24**, **25** and **27** are assigned to the newly formed C=N as a result of enolization of the semicarbazones on coordination. These bands are absent in the compounds **26** and **28**, which suggest the coordination of the semicarbazones in these complexes in the neutral keto form. This is again supported by the presence of bands at 1610 and 1701 cm^{-1} respectively for the complexes **26** and **28**, attributed to $v(C=O)$. The presence of bands at 3245 and 3379 cm^{-1} in the spectra of the complexes **26** and **28** is assigned to $v_a(NH)$ vibrations of the imino group. The coordination through the azomethine nitrogen is further evidenced by the $v(Ni–N_{azo})$ bands in the region 502-509 cm^{-1} for the complexes **24**-**28**. In the complexes **24**-**28**, the $v(N–N)$ frequency shifts to 1136-1153 cm^{-1} which also support coordination through azomethine nitrogen in all the complexes.

[NiL^{1}SCN]·H$_2$O (**25**) exhibits a sharp band at 2065 cm^{-1} and a medium band at 697 cm^{-1} correspond to $v(CN)$ and $v(CS)$ of SCN group respectively. This shows monodentate S bonded thiocyanate group. We can distinguish the nature of the linkage of the sulfate anion in the complex depending upon the mode of coordination of the sulfate anion [23]. The presence of bands at 1117, 1228 and 1032 cm^{-1} indicates bidentate chelating nature of the sulfato anion in the complex [Ni(HL^2)(SO$_4$)]·4H$_2$O (**28**).

Table 6.2. IR spectral assignments for Ni(II), Co(II) and Mn(II) complexes

Compound	$\nu(NH)$	$\nu(C=N_{azo})$	$\nu(CO)$	$\nu(C=N)^a$	$\nu(N-N)$	$\nu(M-O)$	$\nu(M-N_{azo})$
$[NiL^1_2]\cdot H_2O$ (**24**)	-	1564	-	1594	1136	507	509
$[NiL^1SCN]\cdot H_2O$ (**25**)	-	1568	-	1599	1139	420	509
$[Ni(HL)^1Cl_2]\cdot 4H_2O$ (**26**)	3245	1564	1610	-	1149	421	502
$[NiL^2_2]$ (**27**)	-	1557	-	1583	1137	433	505
$[Ni(HL^2)(SO_4)]\cdot 4H_2O$ (**28**)	3379	1528	1701	-	1153	478	508
$[CoL^1Br]\cdot H_2O$ (**29**)	-	1567	-	1597	1148	471	505
$[CoL^2OAc]$ (**30**)	-	1561	-	1602	1136	485	508
$[CoL^2ClO_4]\cdot DMF$ (**31**)	-	1559	-	1604	1141	440	509
$[MnL^1(HL^1)]ClO_4\cdot 4H_2O$ (**32**)	3365	1540	1669	1570	1148	503	591
$[Mn(HL^2)Cl]Cl\cdot 2H_2O$ (**33**)	3380	1529	1702	-	1153	508	609

^{a} Newly formed C=N
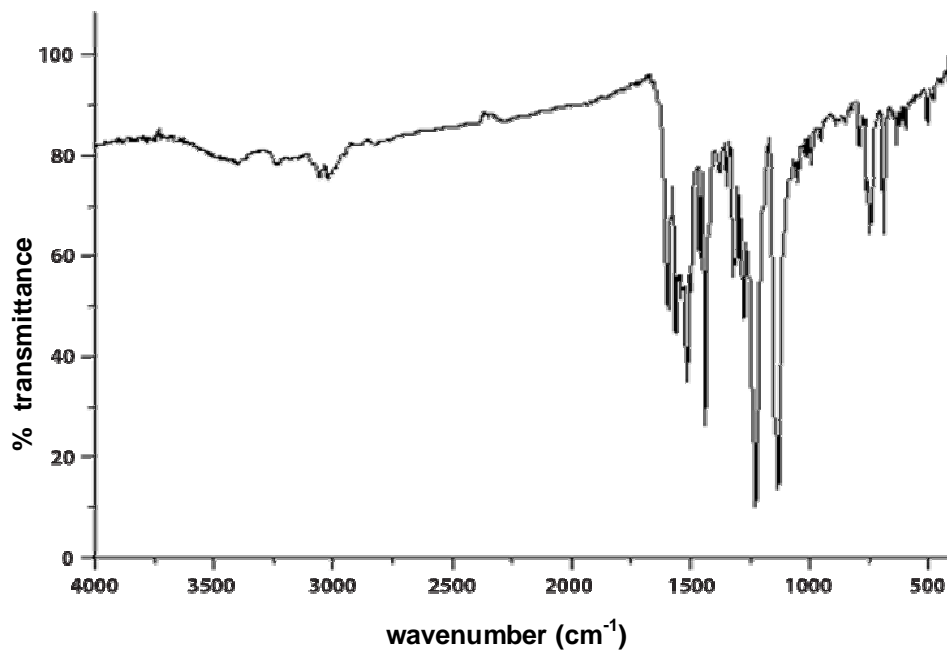
Figure 6.1. IR spectrum of the compound [NiL$^1_2$]·H$_2$O (**24**).
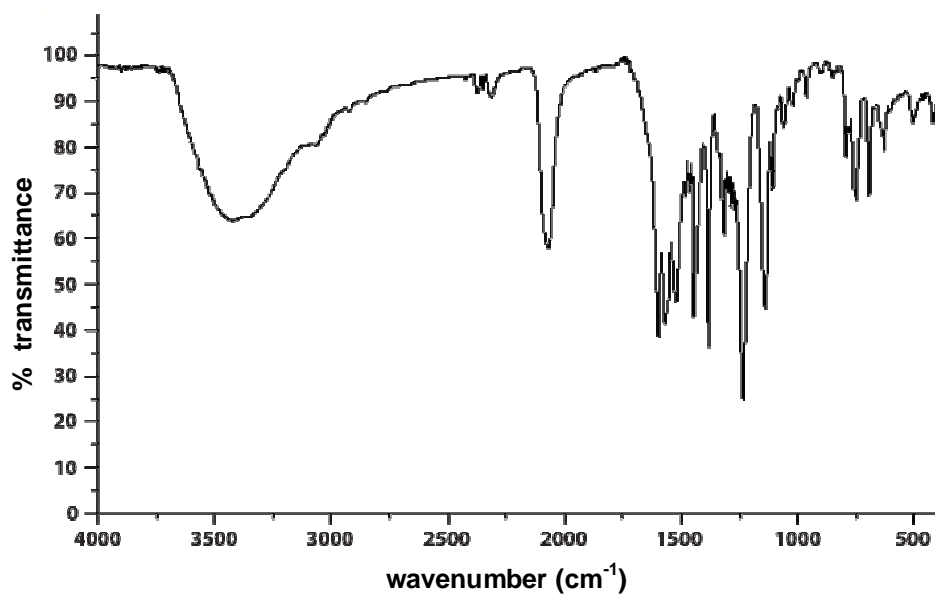
Figure 6.2. IR spectrum of the compound [NiL^{1}SCN]·H$_2$O (**25**).
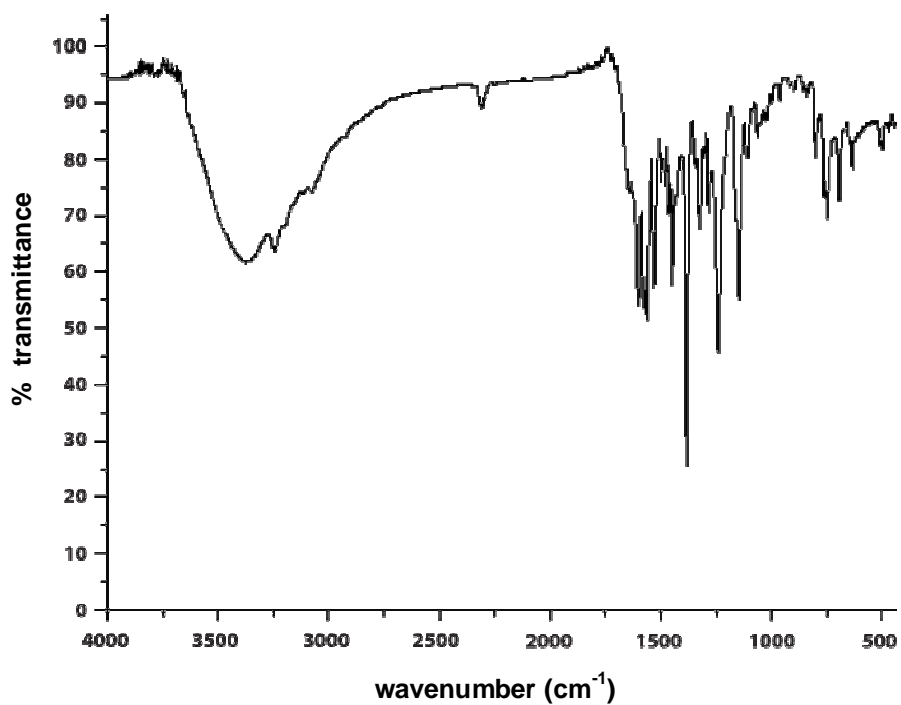
Figure 6.3. IR spectrum of the compound [Ni(HL)^{1}Cl$_2$]·4H$_2$O (**26**).
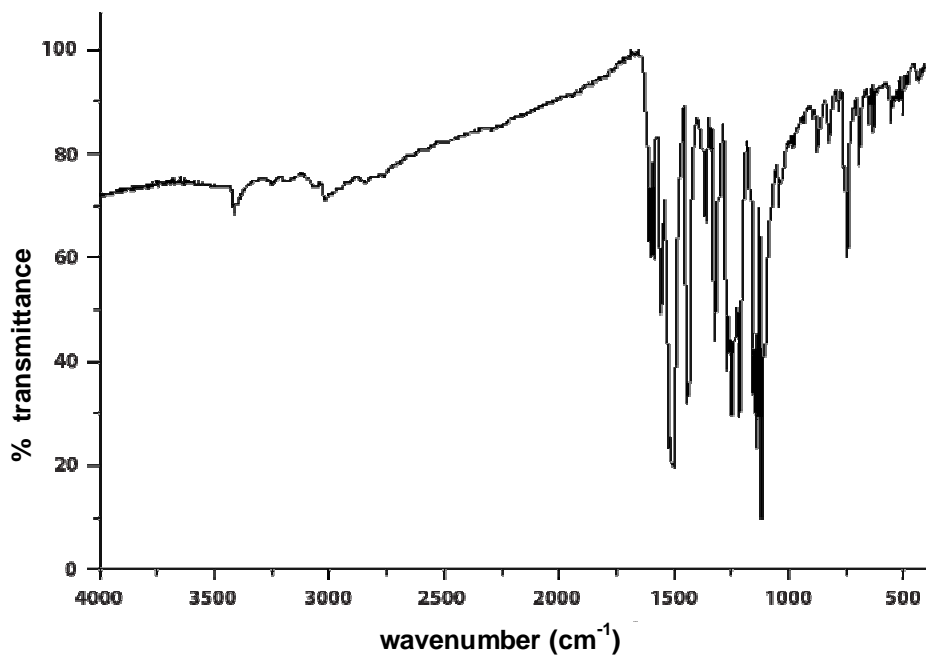
Figure 6.4. IR spectrum of the compound [NiL$^2_2$] (**27**).
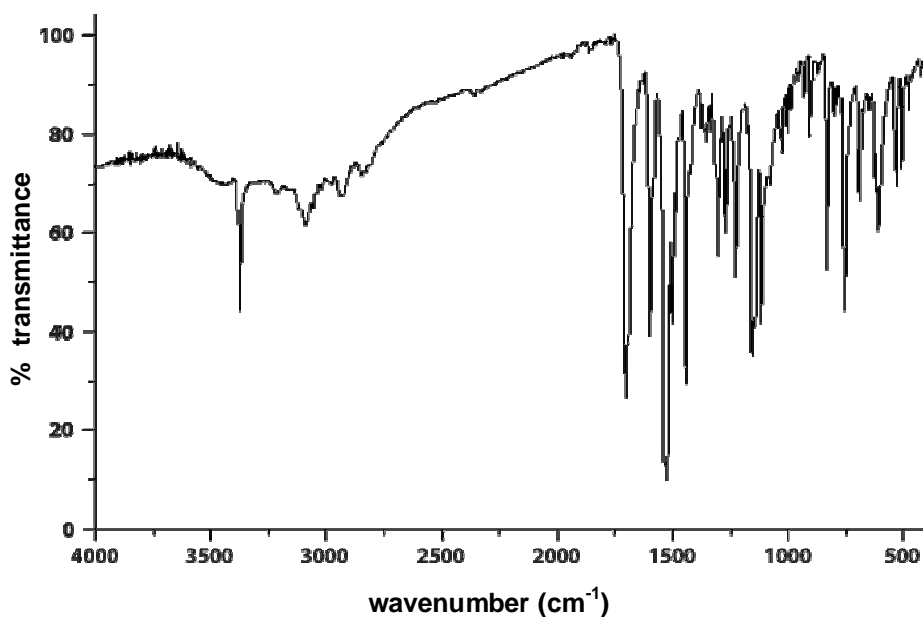
Figure 6.5. IR spectrum of the compound $[Ni(HL^2)(SO_4)]\cdot 4H_2O$ (**28**).

In the Co(II) complexes **29**-**31** semicarbazones coordinated in the enolate form, which is evident from the absence of v_a(NH) vibration band. The enolization of the semicarbazones in these complexes is further supported by the presence of newly formed bands in the range 1597-1604 cm^{-1} which is assigned to the newly formed C=N. The coordination of azomethine nitrogen to the metal center causes the azomethine band, v(C=N) to be shifted to lower wavenumbers. This red shift is observed in the range 1559-1567 cm^{-1} for the complexes **29**-**31**. The presence of v(Co–N$_{azo}$) bands at 505, 508 and 509 cm^{-1} in complexes **29**-**31** respectively confirm the coordination through azomethine nitrogen atom. The change in v(N–N) value in the spectra of the complexes **29**-**31** is observed in the range 1136-1148 cm^{-1}. In the complex [CoL^{2}OAc] (**30**), symmetric and asymmetric stretching modes of acetate group are observed at 1371 and 1534 cm^{-1} respectively. The compound [CoL^{2}ClO$_4$]. DMF (**31**) displays two bands at 1164 and 1122 cm^{-1} and a strong band at 624 cm^{-1} and a weak band at 870 cm^{-1} indicating the presence of coordinated

perchlorate. The band at 1164 cm^{-1} is assignable to v_3(ClO$_4$) and bands at 624 and 870 cm^{-1} are assignable to v_4(ClO$_4$) and v_1(ClO$_4$) respectively.
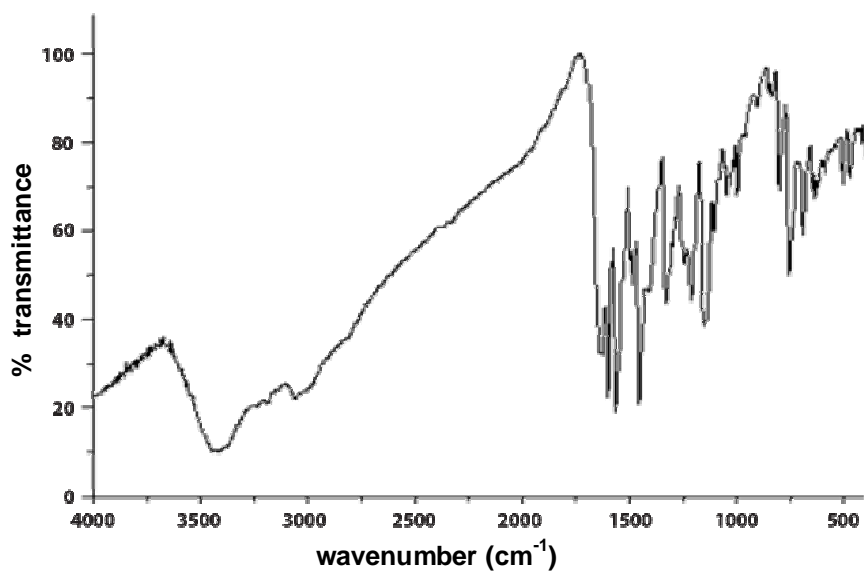
Figure 6.6. IR spectrum of the compound [CoL^{1}Br]·H$_2$O (**29**).
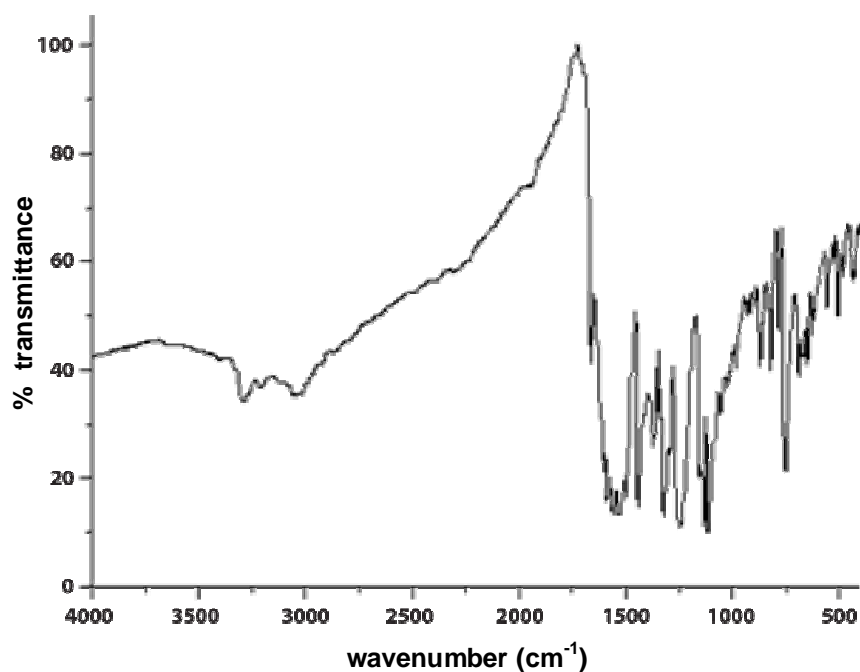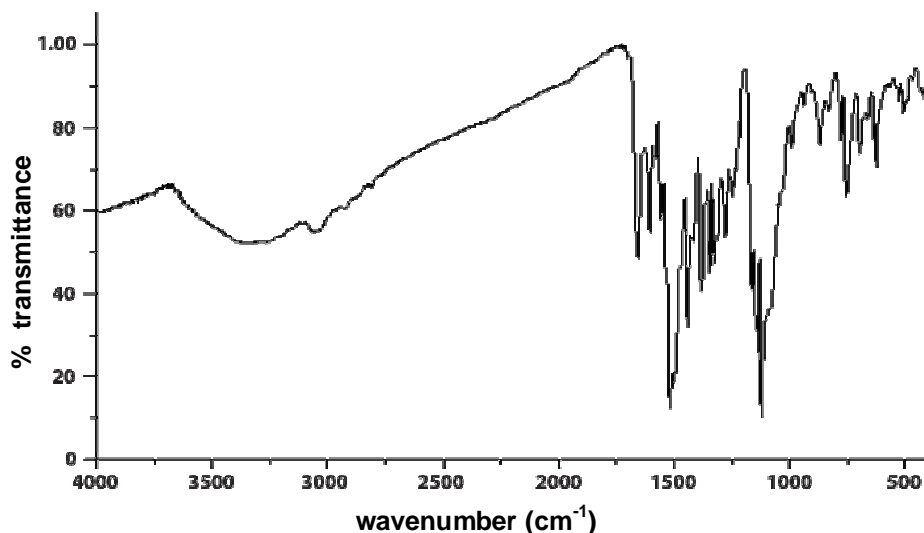

Figure 6.7. IR spectrum of the compound [CoL^{2}OAc] (**30**).

Figure 6.8. IR spectrum of the compound [CoL^{2}ClO$_4$]·DMF (**31**).

The new band seen at 1570 cm^{-1} for **32** is assigned to the newly formed C=N due to the deprotonation of the semicarbazone, HL^1. The coordination through the azomethine nitrogen is further evidenced by the v(Mn–N$_{azo}$) peaks in the region 503-508 cm^{-1} for the complexes **32** and **33**. In the complex **32** the v(N–N) frequency shifts to 1148 cm^{-1} and in the complex **33** to 1153 cm^{-1}. These shifts in the v(N–N) frequencies also support coordination through azomethine nitrogen in all the complexes. In the complexes **32** and **33** the presence of bands at 1669 and 1702 cm^{-1} respectively indicates the existence of keto form of the semicarbazones and small shift in the frequencies suggest the coordination through keto oxygen atom. The bands at 3365 and 3380 cm^{-1} for the complexes **32** and **33** respectively are assigned to v_a(NH) vibrations of the imino group, indicate that the semicarbazones are coordinated in the neutral form. In these complexes the bands at 503 and 508 cm^{-1} are assignable to v(Mn–O), consistent with keto oxygen coordination. The perchlorate complex **32** shows a band at 1098 cm^{-1} which can be assigned to v_3(ClO$_4$) and the presence of a band at 623 cm^{-1}, assignable to v_4(ClO$_4$), suggests the presence of free perchlorate anion [24].
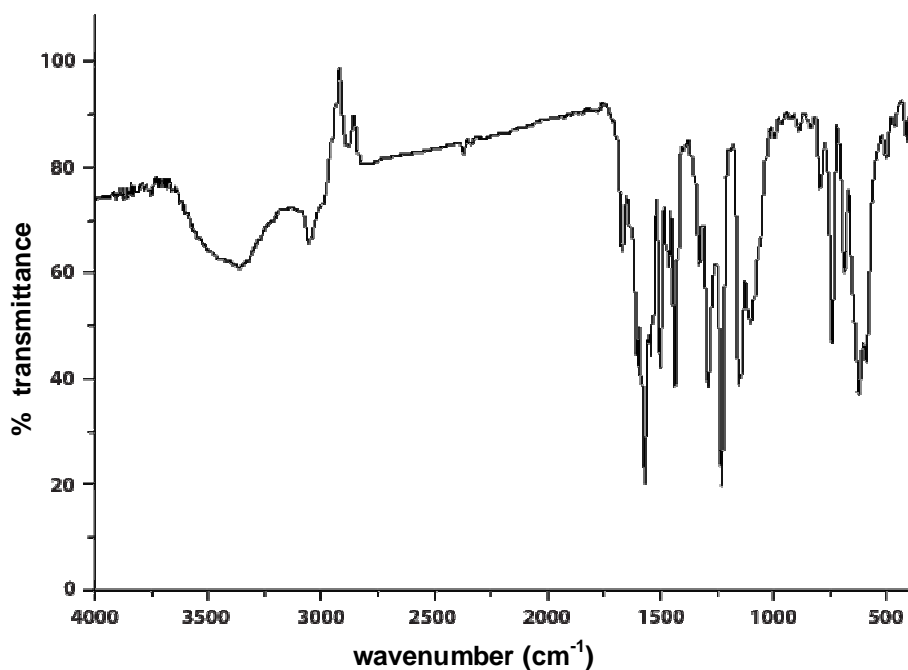
Figure 6.9. IR spectrum of the compound [MnL^1(HL^1)]ClO$_4$·4H$_2$O (**32**).
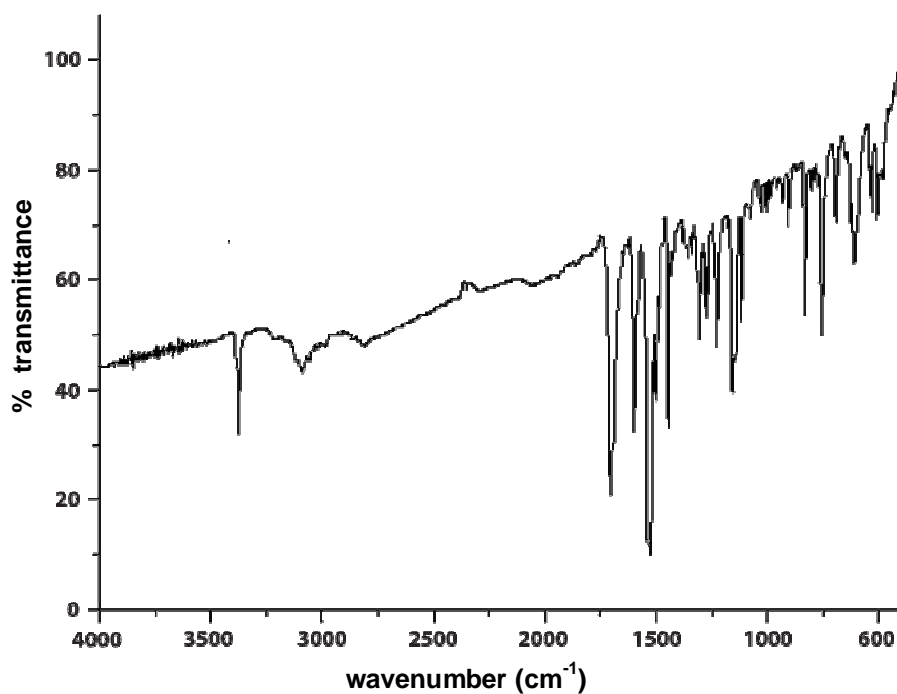
Figure 6.10. IR spectrum of the compound [Mn(HL^2)Cl]Cl·2H$_2$O (**33**).

6.3.2. Electronic spectra

The electronic spectral data of the complexes in DMF are summarized in Table 6.3 and the electronic spectra are shown in Figures 6.11-6.19. The intraligand electronic transitions of semicarbazones, HL^1 and HL^2 suffered considerable shift on coordination. The shift of the intraligand bands to longer wavelength region in the complexes is the result of weakening of C–O bond and the conjugation system being enhanced upon complexation [25]. In the electronic spectra of compounds **24-28** bands in the region 30680-32790 cm^{-1} are assigned as intraligand transitions. The intense bands observed in the range 23260-24630 cm^{-1} are assigned as O→Ni LMCT transitions. The ground state of Ni(II) in an octahedral coordination is $^3A_{2g}$ and expects three spin allowed transitions $^3T_{2g}(F)←^3A_{2g}(F)(v_1)$, $^3T_{1g}(F)←^3A_{2g}(F)(v_2)$ and $^3T_{1g}(P)←^3A_{2g}(F)(v_3)$ in an increasing order of energy. However we could not isolate these bands, probably due to the presence of high-intensity charge transfer bands. The *d-d* bands are appearing as weak shoulders in the region 15650-16450 cm^{-1}.

In the electronic spectra of Co(II) complexes **29-31** the intraligand transitions were observed in the range 28820-30300 cm^{-1}, which shows a red shift. Charge transfer bands were observed in the range 21660-25060 cm^{-1}, which are intense and due to the combination of O→Co and N→Co LMCT transitions. The ground state in a Co(II) tetrahedral is $^4A_2$ and the possible transitions are $^4T_2←^4A_2$, $^4T_1(F)←^4A_2$ and $^4T_1(P)←^4A_2$. Usually, $^4T_1(F)←^4A_2$ and $^4T_1(P)←^4A_2$ transitions appear as multiple absorption in the near infrared and visible regions respectively. The electronic spectra of four coordinate square planar complexes of Co(II) is similar to that of the low spin five coordinate Co(II) complexes. This gives rise to mainly two absorption bands corresponding to $^2E←^2A_1$ at higher and $^2B_1←^2A_1$ at lower energy regions. However, in the electronic spectra of the complexes, **29-31,** *d-d* transitions appear as shoulders in the region 13000-13700 cm^{-1}.

The ground state of high spin octahedral Mn(II) complex is $^6A_{1g}$. As there are no other terms of sextet spin multiplicity, spin allowed *d-d* transitions are not expected. However, some forbidden transitions occur such as $^4E_g(G) \leftarrow ^6A_{1g}$, $^4E_g(D) \leftarrow ^6A_{1g}$, $^4T_{1g}(G) \leftarrow ^6A_{1g}$, $^4T_{2g}(G) \leftarrow ^6A_{1g}$. Also for octahedral complexes, transitions are Laporte forbidden. Thus doubly forbidden transitions are extremely weak. In the present compounds *d-d* bands are very weak due to their low intensity. These broad bands are at *ca.* 12000 cm^{-1} (Figures 6.20-6.22). In the Mn(II) complexes **32** and **33** high intense transitions are observed at *ca.* 24000 cm^{-1} which are assumed to be due to the ligand to metal charge transfer transitions.

Table 6.3. Electronic spectral assignments of Ni(II), Co(II) and Mn(II) complexes

Compound	Absorbance λ_{max} (cm^{-1})
[NiL$^1_2$]·H$_2$O (**24**)	32150, 25190, 16260
[NiL^{1}NCS]·H$_2$O (**25**)	32150, 24630, 16160
[Ni(HL^1)Cl$_2$]·4H$_2$O (**26**)	32790, 24330, 16450
[NiL$^2_2$] (**27**)	31450, 23310, 15650
[Ni(HL^2)(SO$_4$)]·4H$_2$O (**28**)	30680, 23260, 16260
[CoL^{1}Br]·H$_2$O (**29**)	30300, 24040, 13700
[CoL^{2}OAc] (**30**)	30120, 25060, 13180
[CoL^{2}ClO$_4$]·DMF (**31**)	28820, 216450, 13000
[MnL^1(HL^1)]ClO$_4$·4H$_2$O (**32**)	32260, 24040, 13290
[Mn(HL^2)Cl]Cl·2H$_2$O (**33**)	31450, 28650, 13250
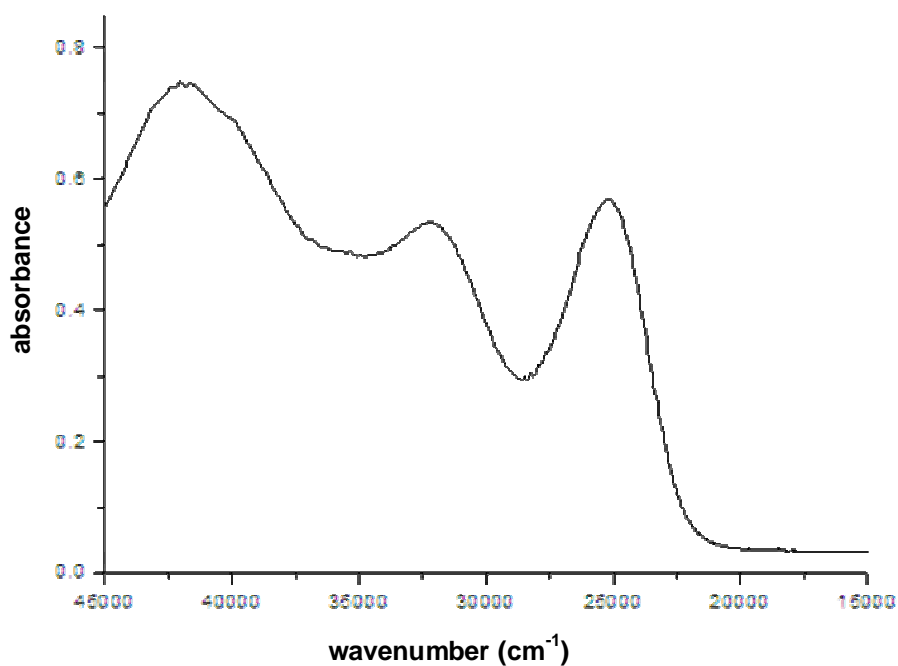
Figure 6.11. Electronic spectrum of the compound $[NiL^1_2] \cdot H_2O$ (**24**).
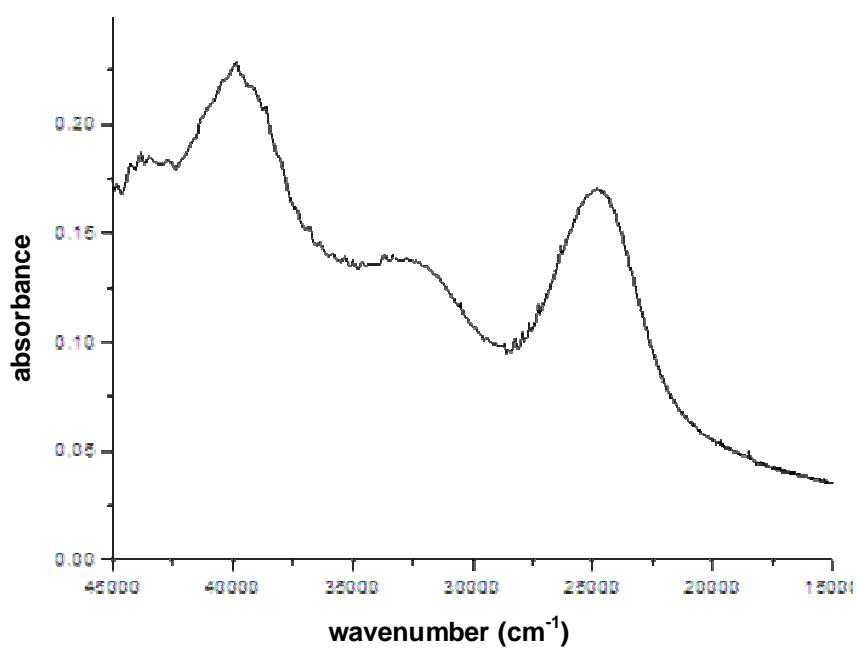
Figure 6.12. Electronic spectrum of the compound $[NiL^1SCN] \cdot H_2O$ (**25**).
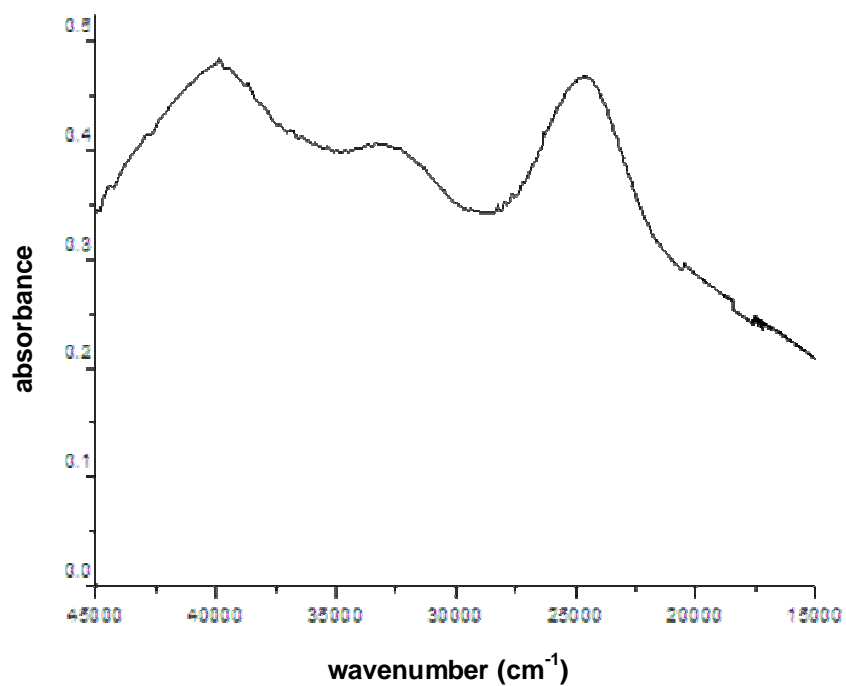
Figure 6.13. Electronic spectrum of the compound $[Ni(HL)^1Cl_2]\cdot 4H_2O$ (**26**).
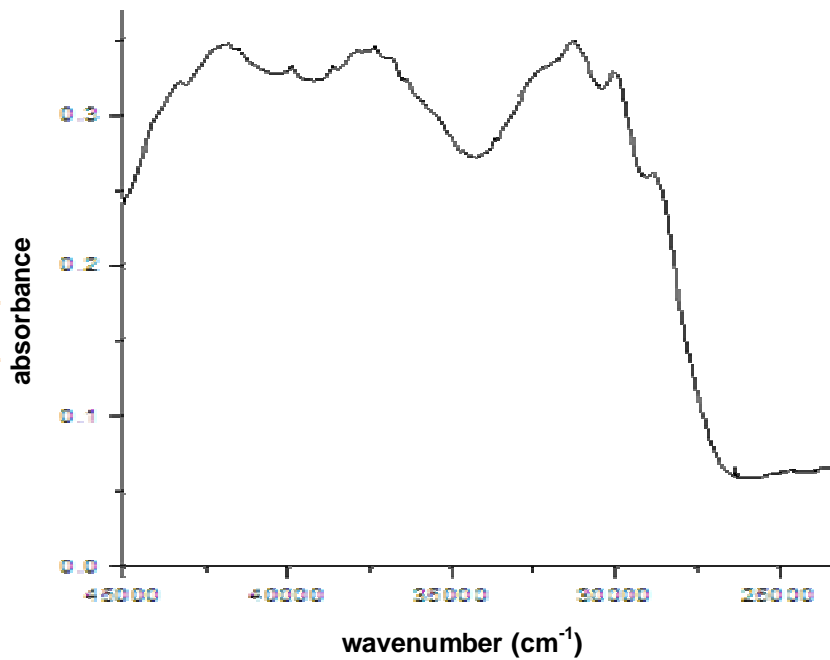
Figure 6.14. Electronic spectrum of the compound $[NiL^2_2]$ (**27**).
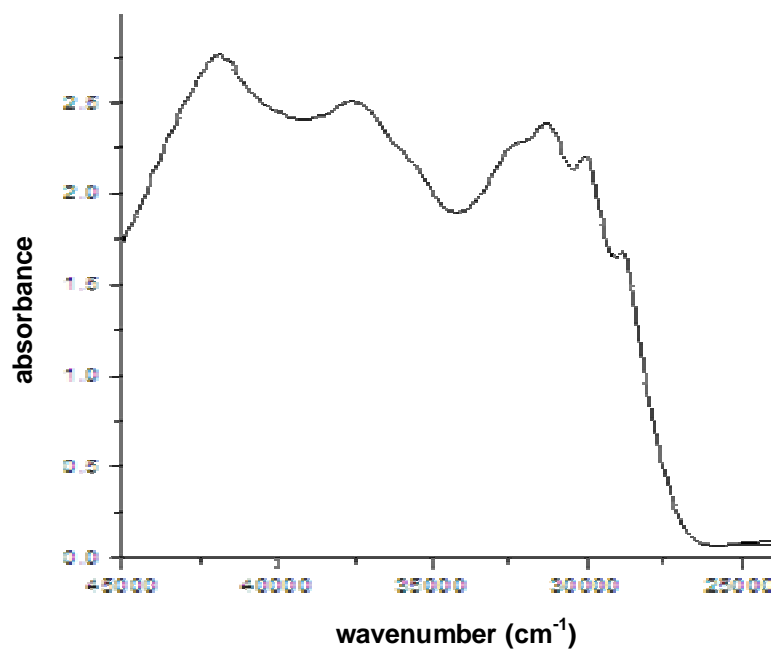
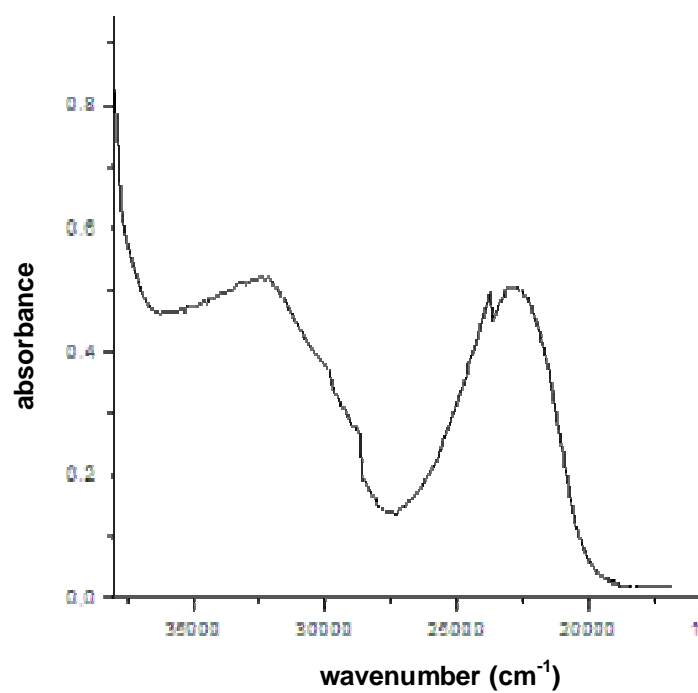**Figure 6.15.** Electronic spectrum of the compound [Ni(HL^2)(SO$_4$)]·4H$_2$O (**28**).

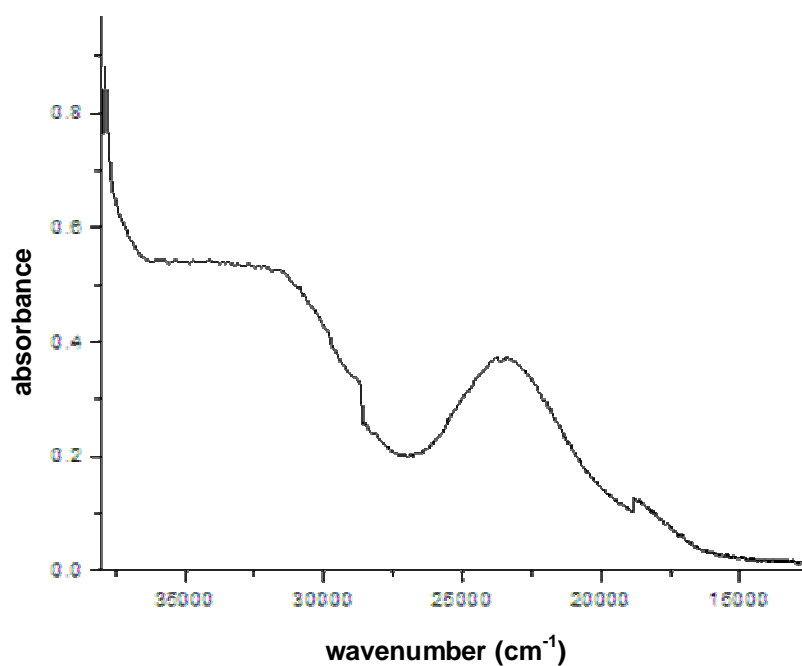**Figure 6.16.** Electronic spectrum of the compound [CoL^{2}OAc] (**30**).

Figure 6.17. Electronic spectrum of the compound [CoL²ClO₄]·DMF (**31**).
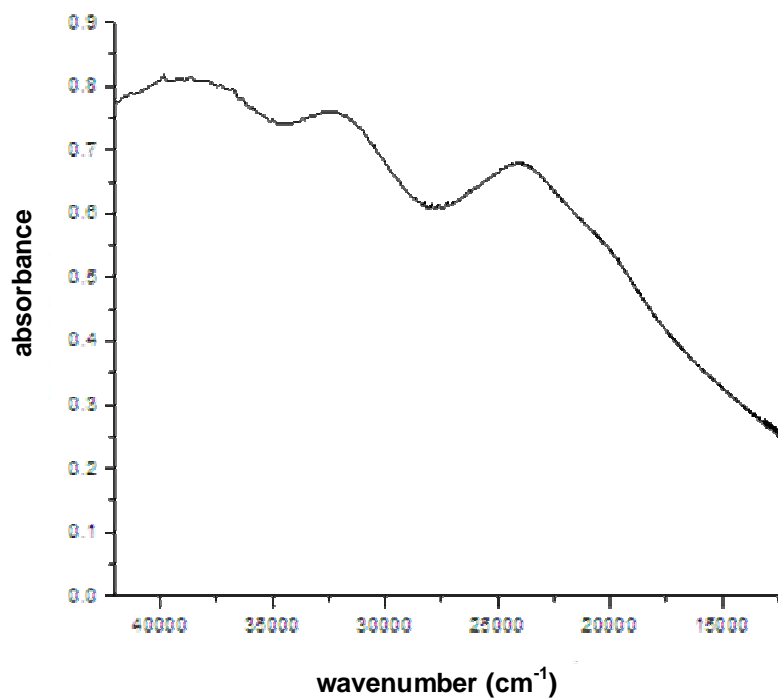

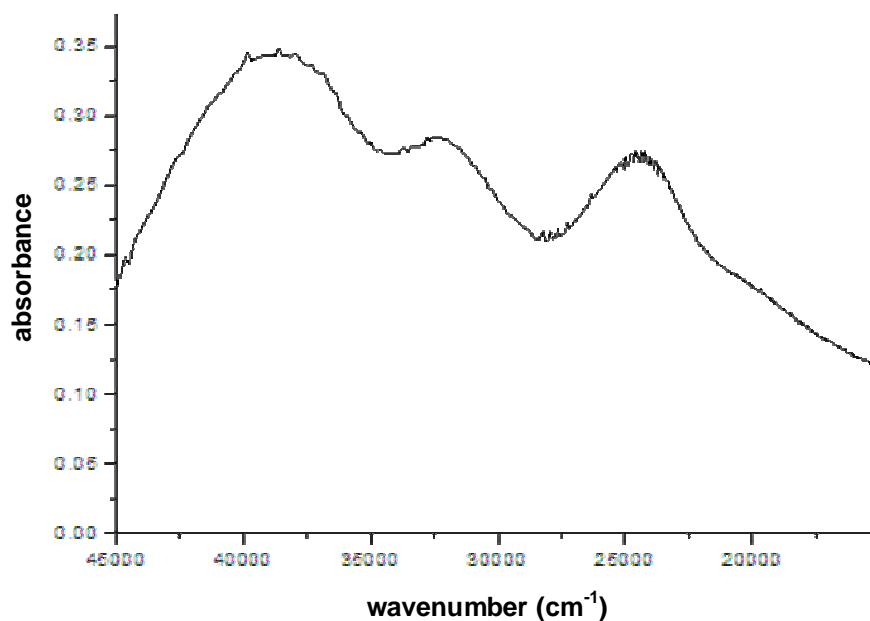**Figure 6.18.** Electronic spectrum of the compound [MnL¹(HL¹)]ClO₄·4H₂O (**32**).

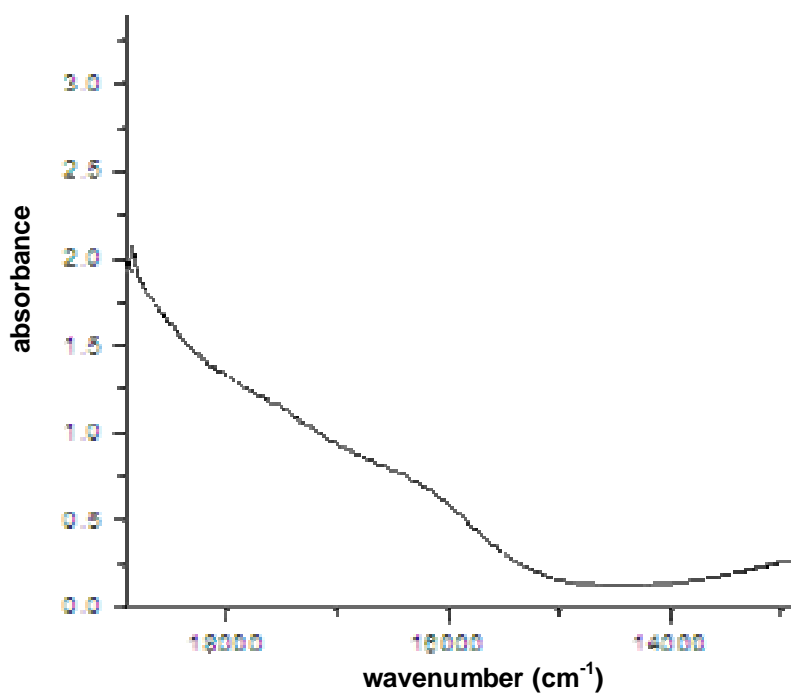**Figure 6.19**. Electronic spectrum of the compound $[Mn(HL^2)_2]Cl_2 \cdot 2H_2O$ (**33**).

Figure 6.20. Electronic spectrum of the compound $[NiL^1_2] \cdot H_2O$ (**24**) in the visible region.
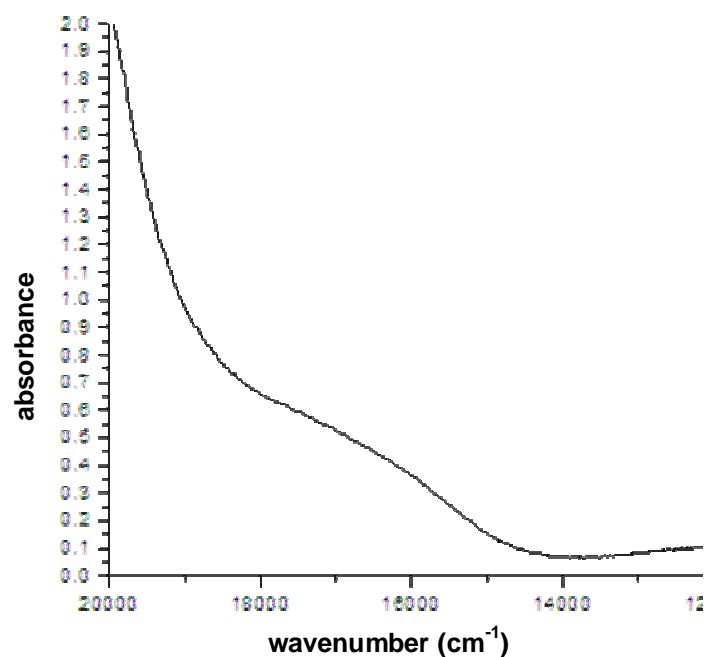
Figure 6.21. Electronic spectrum of the compound [NiL^{1}SCN]·H$_2$O (**25**) in the visible region.
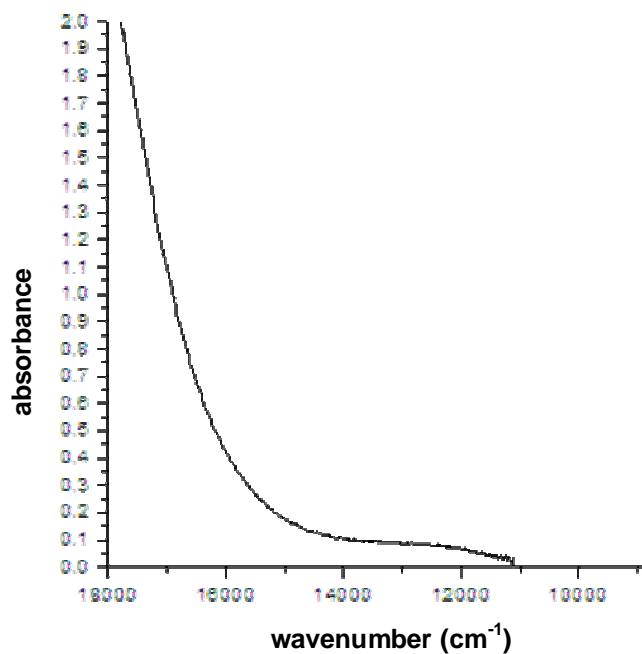

Figure 6.22. Electronic spectrum of the compound [CoL^{2}ClO$_4$]·DMF (**31**) in the visible region.

6.3.3. Electron paramagnetic resonance spectra

The spin Hamiltonian for the high spin Mn(II) is expressed as

$$\hat{H} = g\beta BS + D[S_z^2 - S(S+l)/3] + E(S_x^2 - S_y^2)$$

Where, B is the magnetic field vector, g is the spectroscopic splitting factor, β is the Bohr magneton, D is the axial zero field splitting parameter, E is the rhombic zero field splitting parameter and S is the electron spin vector [26]. If D and E are both zero, then the only contributor to the spectrum is the first-order Zeeman term and the result for Mn^{2+} is an isotropic spectrum, with a single six line signal with g_{eff} near 2.0. In weak fields, Mn(II) centers give a single transition at $g=2$, which is split into six hyperfine lines by the ^{55}Mn nuclear spin ($I=5/2$). However, simple spectra of this type are indicative of a cubic ligand field where the zero field splitting parameter D is negligible and all of the $\Delta M_s = \pm 1$ transitions are degenerate, as a result. For a small but finite value for D and E, the degeneracy is removed and the spectrum exhibits fivefold fine structure.

If D is very large only one transition is expected. However, for the case where D or E is very large, the lowest doublet has effective g values of $g_{\parallel} = 2$, $g_{\perp} = 6$ for $D \neq 0$ and $E=0$ but for $D=0$ and $E \neq 0$, the middle Kramer's doublet has an isotropic g value of 4.29.

For the compound $[MnL^1(HL^1)]ClO_4 \cdot 4H_2O$ (**32**) and $[Mn(HL^2)Cl]Cl \cdot 2H_2O$ (**33**) the X-band EPR spectra were recorded in polycrystalline state at 298 K and in frozen DMF at 77 K. The EPR spectrum of compound **32**, in polycrystalline state at 298 K has two signals with g values 2.011 and 2.514, whereas compound **33** has g value 2.070 (Figures 6.23 and 6.24).
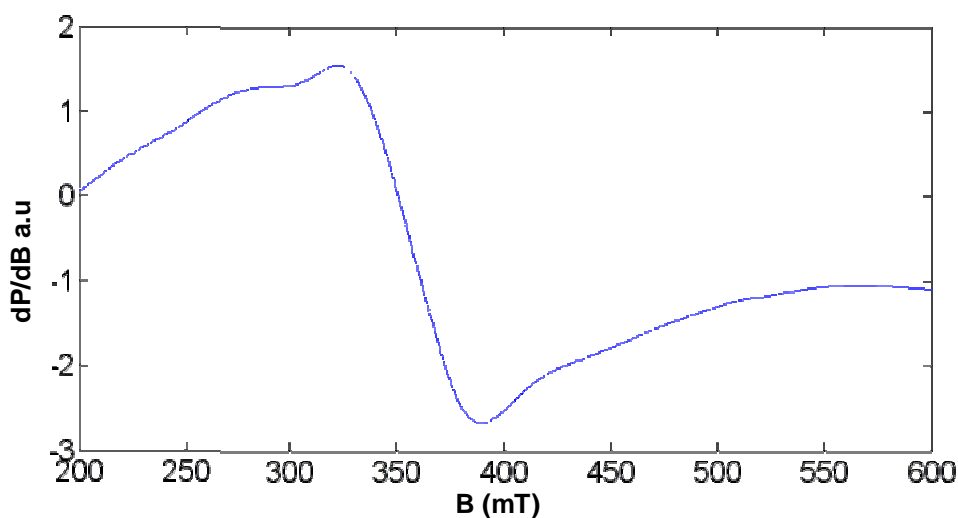
Figure 6.23. EPR spectrum of the compound [MnL^1(HL^1)]ClO$_4$·4H$_2$O (**32**) in polycrystalline state at 298 K.
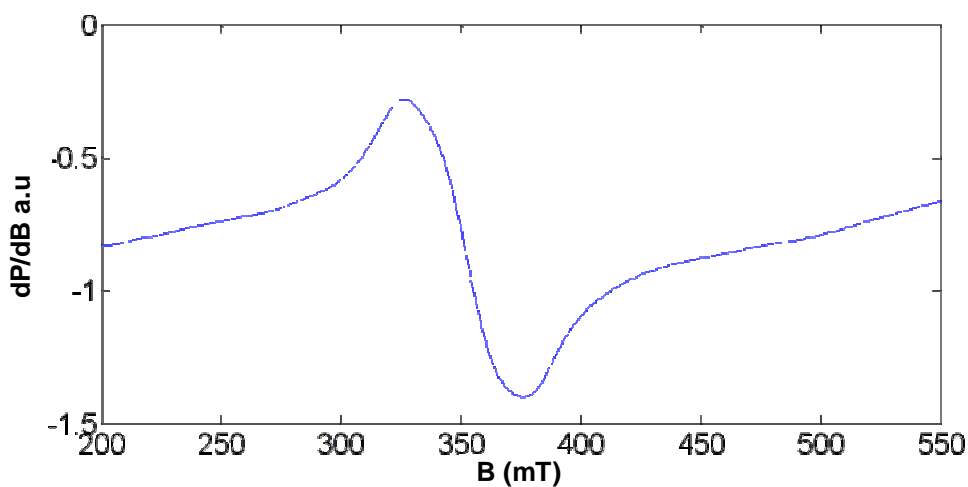
Figure 6.24. EPR spectrum of the compound [Mn(HL^2)$_2$]Cl$_2$·2H$_2$O (**33**) in polycrystalline state at 298 K.

In the spectra from DMF solutions at 77 K, a hyperfine sextet is observed with *g* values 2.005 and 2.004 respectively for compounds **32** and **33** (Figures 6.25 and 6.26). *A* values are 94.50 and 94.47 *G* respectively for **32** and **33**. The six hyperfine lines are due to the interaction of the electron spin with nuclear spin (^{55}Mn, *I*=5/2). The observed *g* values are very close to the

free electron spin value of 2.0023 which is consistent with the typical manganese(II) system and also suggestive of the absence of spin orbit coupling in the ground state $^6A_{1g}$ without another sextet term of higher energy. The D and E values for compound **32** are 350 and 120 mHz respectively.
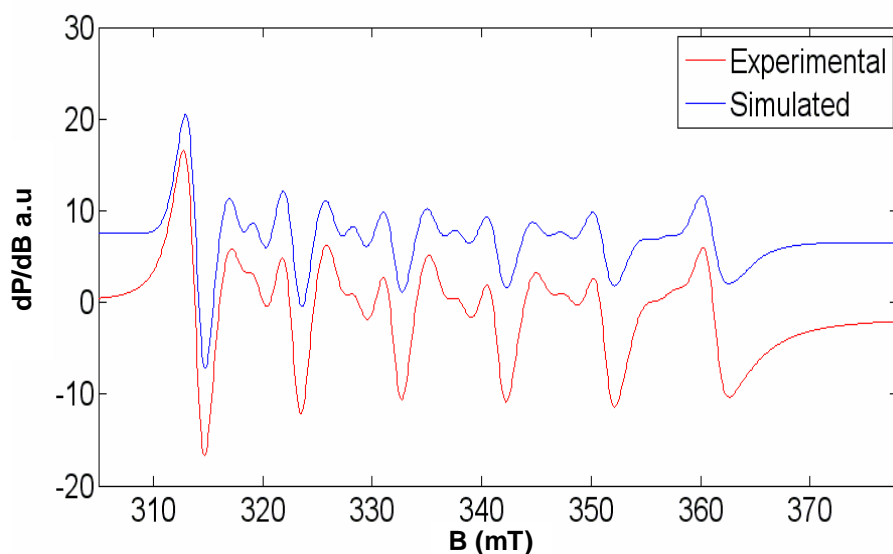

Figure 6.25. EPR spectrum of the compound [MnL^1(HL^1)]ClO$_4$·4H$_2$O (**32**) at 77 K (Experimental (red) and simulated best fit (blue) of the EPR spectra).
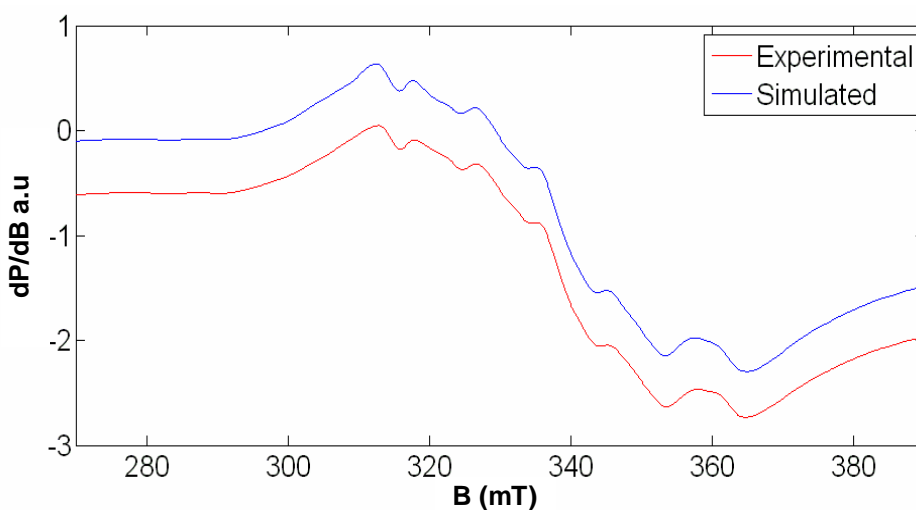

Figure 6.26. EPR spectrum of the compound [Mn(HL^2)$_2$]Cl$_2$·2H$_2$O (**33**) at 77 K (Experimental (red) and simulated best fit (blue) of the EPR spectra).

References

[1]   V.V. Pavlishchuk, S.V. Kolotilov, A.W. Addison, R.J. Butcher, E. Sinn, J. Chem. Soc., Dalton Trans. 3 (2000) 335.

[2]   N.C. Kasuga, K. Sekino, M. Ishikawa, A. Honda, M. Yokoyama, S. Nakano, N. Shimada, C. Koumo, K. Nomiya, J. Inorg. Biochem. 96 (2003) 298.

[3]   S. Yamada, Coord. Chem. Rev. 190 (1999) 537.

[4]   M. Amirnasr, K.J. Schenk, A. Gorji, R. Vafazadeh, Polyhedron 20 (2001) 695.

[5]   M.M. Aly, J. Coord. Chem. 43 (1998) 89.

[6]   R. Cini, S.J. Moore, L.G. Marzilli, Inorg. Chem. 37 (1998) 6890.

[7]   S.M. Polson, R. Cini, C. Pifferi, L.G. Marzilli, Inorg. Chem. 36 (1997) 314.

[8]   S. Hirota, E. Kosugi, L.G. Marzilli, O. Yamauchi, Inorg. Chim. Acta 275 (1998) 90.

[9]   A.E. Martell, D.T. Sawyer, Oxygen Complexes and Oxygen Activation by Transition Metals, Plenum Press, New York, 1988.

[10]   N.J. Henson, P.J. Hay, A. Redondo, Inorg. Chem. 38 (1999) 1618.

[11]   C. Benchini, R.W. Zoeliner, Adv. Inorg. Chem. 44 (1997) 263.

[12]   T. Nagata, K. Yoruzu, T. Yamada, T. Mukaiyama, Angew. Chem. Int. Ed. Engl. 34 (1995) 2145.

[13]   A. Sreekanth, M. Joseph, H.-K. Fun, M.R.P. Kurup, Polyhedron 25 (2006) 1408.

[14]   M. Maneiro, M.R. Bermejo, M. Fondo, A.M. Gonzalez, J. Sanmartin, J.C. Garcia-Monteagudo, R.G. Pritchard, A.M. Tyryshkin, Polyhedron 20 (2001) 711.

[15]   D. Huang, X. Zhang, C. Chen, F. Chen, Q. Liu, D. Liao, L. Li, L. Sun, Inorg. Chim. Acta 353 (2003) 284.

[16]   J. Brinksma, R. Hage, J. Kerschner, B.L. Feringa, Chem. Commun. (2000) 537.

[17]   K.B. Jensen, E. Johansen, F.B. Larsen, C.J. McKenzie, Inorg. Chem. 43 (2004) 3801.

[18]   W. Zhang, J.L. Loebach, S.B. Wilson, E.N. Jacobsen, J. Am. Chem. Soc. 112 (1990) 2801.

[19]   R. Hage, Recl. Trav. Chim. Pays-Bays 115 (1996) 385.

[20]   K. Weighardt, Angew. Chem., Int. Ed. Engl. 28 (1989) 1153.

[21]   M. Yagi, M. Kaneko, Chem. Rev. 101 (2001) 21.

[22]   G.C. Dismukes, Chem. Rev. 96 (1996) 2909.

[23]   K. Nakamoto *in* Infrared and Raman Spectra of Inorganic and Coordination Compounds, fourth ed., John Wiley & Sons, New York, 1986.

[24]   B.S. Garg, M.R.P. Kurup, S.K. Jain, Y.K. Bhoon, Trans. Met. Chem. 13 (1988) 309.

[25]   L. Latheef, M.R.P. Kurup, Polyhedron 27 (2008) 35.

[26]   D.J.E. Ingram, Spectroscopy at Radio and Microwave Frequencies, second ed., Buttorworth, London (1967).

…..ഇൽ…..

SUMMARY AND CONCLUSION

The work presented in this thesis describes the synthesis, structural and spectral characterization of two novel N^4-substituted semicarbazones of di-2-pyridyl ketone and quinoline-2-carboxaldehyde and their metal complexes. The thesis is divided into six chapters.

Chapter 1

This chapter includes a brief prologue on semicarbazones and their transition metal complexes with an extensive literature survey relating the history, applications and recent developments. This gives a detailed idea about bonding and stereochemistry of the semicarbazones. The different analytical and spectroscopic techniques used for the analysis of the semicarbazones and metal complexes are discussed.

Chapter 2

This chapter deals with the syntheses and characterization of two NNO donor semicarbazones. The semicarbazones synthesized are di-2-pyridyl ketone-N^4-phenyl-3-semicarbazone (HL^1) and quinoline-2-carboxaldehyde -N^4-phenylsemicarbazone (HL^2). These semicarbazones are characterized by CHN analysis, IR, UV, ^{1}H and ^{13}C NMR techniques. Single crystal X-ray diffraction is also used for structural elucidation of quinoline-2-carboxaldehyde-N^4-phenylsemicarbazone (HL^2). HL^2 crystallizes into an orthorhombic lattice space group $P2_12_12_1$. The molecule is almost planar and exists in the keto form in the solid state. Spectral studies also reveal the existence of these semicarbazones in the keto form in solid state.

Chapter 3

This chapter describes the syntheses and characterization of eight zinc(II) complexes of N^4-substituted semicarbazones, HL^1 and HL^2. For the characterization of these complexes we have used CHN analysis, IR, UV spectral studies and single crystal X-ray diffraction studies. In the complexes $[Zn(HL^1)Br_2]$ (**1**) and $[Zn(HL^1)Cl_2]$ (**2**) the semicarbazone coordinates as neutral keto form whereas in all other complexes semicarbazones coordinate in monoanionic enolate form. IR spectral data indicates that in zinc(II) complexes semicarbazones are tridentate, coordinated through keto/enol oxygen, azomethine nitrogen and pyridyl/quinolyl nitrogen atoms. All the complexes are found to be diamagnetic as expected for a d^{10} Zn(II) system. We isolated single crystals for X-ray diffraction studies for $[Zn(HL^1)Br_2]$ (**1**), $[ZnL^1_2]$ (**5**) and $[ZnL^1_2] \cdot 0.3H_2O$ (**6**). The compound **1** crystallizes in monoclinic space group $P2_1/n$, compound **5** crystallizes in monoclinic space group $P2_1/n$ whereas compound **6** crystallizes in orthorhombic space group $P2_12_12_1$. In compound **1** semicarbazone coordinates in keto form and in compounds **5** and **6** it undergoes deprotonation. The compound **1** has distortion from square pyramidal geometry whereas compounds **5** and **6** show distortion from octahedral geometry. $[ZnL^1_2]$ (**5**) and $[ZnL^1_2] \cdot 0.3H_2O$ (**6**) are polymorphic. *d-d* transitions are not found for zinc(II) complexes because of d^{10} electronic configuration.

Chapter 4

This chapter describes the syntheses and characterization of six cadmium complexes of N^4-substituted semicarbazones using CHN analysis, infrared, electronic spectra and X-ray diffraction studies. We isolated single crystals of three cadmium(II) complexes for X-ray diffraction studies. $[CdL^1(OAc)]_2 \cdot 2CH_3OH$ (**9**) crystallized in

orthorhombic space group p_{bca}. In this compound semicarbazone undergoes deprotonation and cadmium(II) is hexacoordinated through enol oxygen, azomethine nitrogen, pyridyl nitrogens and oxygen atoms from acetate group. The compound is centrosymmetric and due to the coordinating way of pyridyl nitrogen atoms a cyclic architecture is observed. $[Cd(HL^2)Cl_2]$ (**13**) crystallized in triclinic space group *P*-1. $[Cd(HL^2)Br_2] \cdot DMF$ (**14**) crystallized in monoclinic space group $P2_1/c$. In these two compounds semicarbazone exists in keto form and cadmium(II) is pentacoordinated. Both compounds have distortion from square pyramidal geometry.

Chapter 5

This chapter deals with the syntheses and characterization of mononuclear and binuclear copper(II) complexes with potential NNO donor ligands. The methods used to characterize the complexes are CHN analyses, conductivity measurements, magnetic susceptibility measurements, IR, UV and EPR studies. Mononuclear copper(II) complexes exhibit magnetic moments in the range 1.51-2.04 B.M., which are close to their spin-only value. Magnetic moment of binuclear copper(II) complexes lie in the range 1.12-1.40 B.M. The EPR spectra of all copper(II) complexes were recorded both in polycrystalline state at 298 K and in DMF at 77 K. The *g* values and various EPR spectral parameters were calculated. In the complexes other than $[CuL^2N_3] \cdot CH_3OH$ (**22**), the unpaired electron is present in the $d_{x^2-y^2}$ orbital. The $g_{\parallel} > g_{\perp}$ values accounts to the distorted square based pyramid structure in five coordinated complexes. For the four coordinated complexes $g_{\parallel} > g_{\perp}$ suggest a square planar geometry. The $g_{\parallel}$ values in all these complexes are less than 2.3 which is an indication of covalent character for M–L bond in these complexes.

Chapter 6

This chapter deals with the syntheses and characterization of nickel(II), cobalt(II) and manganese(II) compounds. The methods used to characterize the complexes are CHN analyses, conductivity measurements, magnetic susceptibility measurements, IR, UV and EPR studies. Five nickel(II) complexes were synthesized and in these complexes semicarbazones act as tridentate ligands. Spectral studies support the tricoordination of the semicarbazone. Three cobalt(II) complexes and two manganese(II) complexes were also synthesized and characterized.

…..ജ്ഞ…..

CURRICULUM VITAE

REENA T.A.
Rose House
Thamarakulam P.O.
Alappuzha (DIST)
Kerala-690530

E mail: reena_fasaludeen@yahoo.com
reenafaisal@cusat.ac.in

ACADEMIC PROFILE

Pursuing Ph.D (2006 – present)

Topic of work: Spectral studies and crystal structures of some transition metal complexes of N^4-substituted semicarbazones

Supervising Guide: Dr. M.R. Prathapachandra Kurup
                              Professor of Inorganic Chemistry
                              Department of Applied Chemistry
                              Cochin University of Science & Technology, Kochi

Master of Science (Chemistry)
Score: 73% (1996-1998)
M.E.S. College, Mampad
University of Calicut

B.Ed (Physical Science)
Score: 58% (1998-1999)
Farooq college
University of Calicut

Bachelor of Science (Chemistry)
Score: 83% (1993-1996)
M.E.S. College, Mampad
University of Calicut

Pre-Degree (Science)
Score: 61% (1991-1993)
M.E.S. College, Mampad
University of Calicut

SSLC
Score: 74% (1991)
NSS High School, Nilambur

ADDITIONAL QUALIFICATIONS

- CSIR-UGC (NET) for Lectureship qualified
- SET qualified

RESEARCH EXPERIENCE

- Three years and nine months of research experience in the field of coordination complexes of semicarbazones.

TEACHING EXPERIENCE

- Science teacher, Al-Asrar Al-Quabandi School, Kuwait (2004-2006)
- Science teacher, International Bangladeshi School, Saudi Arabia (2002-2004)
- Junior lecturer, Govt. Higher secondary school, Mavelikkara, Kerala (2001-2002)
- Science teacher, International Eritrean school, Saudi Arabia (1999-2001)

COMPUTING SKILLS

- Expertise in Windows Operating systems, MS-Office
- Skiled in common chemistry tools like ACD Labs, Origin50 etc
- Familiar with crystallographic softwares
- Proficient in EPR simulation package

PERSONAL PROFILE

Father's name	T. S. Abdul Rahman
Husband's name	Fasaludeen. K. M
Date of Birth	02-05-1976
Gender	Female
Marital Status	Married
Nationality	Indian
Languages Known	English, Hindi, Malayalam and Arabic
Permanent address	Rose House, Thamarakulam (P.O) Alappuzha (dist), Kerala *reena_fasaludeen@yahoo.com*

RESEARCH PUBLICATIONS

- Synthesis and spectral studies of cadmium(II) complexes derived from di-2-pyridyl ketone and N(4)-phenylsemicarbazide: First structural report of a cadmium(II) complex of semicarbazone, T.A. Reena, E.B. Seena, M.R.P. Kurup, Polyhedron 27 (2008) 1825.

- Zinc(II) complexes derived from di-2-pyridyl ketone-N^4-phenyl-3-semicarbazone: Crystal structure and Spectral studies, T.A. Reena, E.B. Seena, M.R.P. Kurup, Polyhedron 27 (2008) 3461.

- Synthesis, spectral and structural studies of a novel semicarbazone synthesized from quinoline-2-carboxaldehyde and N^4-phenyl-3-semicarbazide, T.A. Reena, M.R.P. Kurup, J. Chem. Cryst. 40 (2010) 927.

- Copper(II) complexes derived from di-2-pyridyl ketone-N^4-phenyl-3-semicarbazone: Synthesis and spectral studies, T.A. Reena, M.R.P. Kurup, Spectrochim. Acta. 76 (2010) 322.

PRESENTATIONS

- Participated as a delegate in the National Seminar on Applications of Radioisotopes and Radiation Technology (January, 2007).

- Presented a paper entitled Synthesis, characterization and X-ray crystal studies of cadmium(II) complex of semicarbazone in the International conference on Material for the millennium at CUSAT (March, 2007).

- Presented a poster in the 12th Biennial symposium on Modern Trends in Inorganic Chemistry at IIT, Madras (December, 2007).

- Presented a poster in the International conference on Coordination and Organometallic Chemistry (ICCOC 2009), Department of Chemistry, Bharathiar University, Coimbatore, India.

…..৪৩…..